

# **Drug induced degradation of driver proteins: A novel approach to target MLL-fusions**

Sandra Cantilena

Developmental Biology and Cancer Section

Institute of Child Health

University College London

A thesis submitted for the Degree of Doctor of Philosophy

## DECLARATION

I, Sandra Cantilena, confirm that the work presented in this thesis is my own. Where information has been derived from other sources, I confirm that this has been indicated in the thesis.

Signature.....

## ABSTRACT

Acute leukaemias in infants are associated with inferior outcomes. The majority of infant acute leukaemia is characterized by balanced chromosomal translocations involving the mixed lineage leukaemia (*MLL*) gene. Previous work in the department established that the novel formed *MLL* fusions are the proto-oncoproteins responsible for leukaemia initiation and maintenance so that inhibition of *MLL*-fusions, in conditional mouse models, resulted in complete disease remission. Therefore, a therapy that inactivates the *MLL* fusion protein, by protein degradation for example, would offer new hope to these patients. The aim of this study is to identify clinically approved drugs that are capable of inducing degradation of *MLL* leukaemic fusion proteins. An indicator cell line consisting of a THP1 cell clone expressing firefly luciferase fused to the *MLL*-AF9 protein, combined with renilla luciferase, was used to screen a collection of 1,280 approved drugs for their ability to induce proteolysis of *MLL* fusion proteins. 25 drugs lowered the luciferase to renilla ratio, of which 3 were confirmed by western blotting to decrease *MLL*-fusion protein levels. One drug was taken forward for further analysis. This drug was able to induce the proteolysis of various *MLL* fusion proteins in human *MLL* rearranged cell lines and primary patient material. Transcriptome profiling showed shut down of the *MLL*-fusion signature within 16hrs of addition of the drug. Proteolysis of *MLL* fusion proteins should also result in a block in self-renewal, as was previously shown in the conditional mouse model. While the drug had no significant impact on the colony formation of normal haematopoietic progenitor cells, it was able to block the colony formation ability of *MLL* rearranged cell lines. Finally, global

alterations in the epigenetic landscape following drug treatment were analysed. This study highlights a new approach to identifying drugs that block driver oncogenes and has identified a potential novel treatment for a major subtype of acute leukaemias in infants.

# TABLE OF CONTENTS

DECLARATION .....	2
ABSTRACT .....	3
TABLE OF CONTENTS .....	5
LIST OF FIGURES .....	10
LIST OF TABLES.....	14
ABBREVIATIONS .....	15
ACKNOWLEDGEMENTS .....	21
1 CHAPTER I: INTRODUCTION .....	22
1.1 Haematopoiesis .....	22
1.2 Molecular control of haematopoiesis .....	27
1.3 Acute leukaemia in infants .....	30
1.4 Acute leukaemia aetiology .....	35
1.5 Leukaemic stem cells.....	37
1.6 MLL structure .....	40
1.7 Normal function of MLL.....	44
1.8 Transcriptional regulation by MLL.....	46
1.9 MLL rearranged leukaemia and MLL rearrangements .....	50
1.10 MLL fusion genes .....	53
1.11 Transcriptional Regulation by MLL-fusions.....	56

1.12	Models of MLL fusion leukaemia .....	58
1.13	MLL target genes.....	62
1.14	Models of oncoprotein degradation .....	66
1.15	Drug discovery versus drug repositioning.....	69
1.16	High/Medium throughput screening.....	73
	PROJECT AIM.....	74
2	CHAPTER II: MATERIALS & METHODS .....	75
2.1	Molecular Biology .....	75
2.1.1	DNA constructs .....	75
2.1.2	Preparation of total protein lysate for western blot analysis .....	76
2.1.3	Western Blot analysis.....	76
2.1.4	RNA isolation .....	80
2.1.5	cDNA preparation.....	80
2.1.6	Quantitative real-time PCR.....	81
2.2	Cell Biology.....	83
2.2.1	Cell culture and cell lines.....	83
2.2.2	Flow cytometry .....	85
2.2.3	Apoptosis .....	85
2.2.4	Colony forming assays .....	86
2.2.5	Isolation of human CD34 <sup>+</sup> CB cells .....	86
2.2.6	Luciferase assays and dual luciferase assays .....	87

2.3	Animal work .....	88
2.4	RNA-sequencing.....	88
2.5	ChIP-sequencing .....	89
3	CHAPTER III: Generation of cell lines expressing fusion genes, their validation and use in medium throughput screening.....	96
3.1	Introduction .....	96
3.2	Results.....	99
3.2.1	Radicicol, a potential destabiliser of leukaemic fusion proteins .....	99
3.2.2	MLL-AF9-luciferase reporter construction and cell lines production 103	
3.2.3	Indicator leukaemic fusion gene cell line validation.....	105
3.2.4	Medium throughput screening.....	107
3.2.5	Drug hit validation.....	112
3.3	Discussion .....	119
4	CHAPTER IV: Studying the effect of DSF in human acute myeloid leukaemia .....	121
4.1	Introduction .....	121
4.2	Results.....	125
4.2.1	Copper enhances the effect of disulfiram .....	125
4.2.2	Copper-disulfiram complexes target both wild type MLL and MLL-fusions to the same degree.....	130

4.2.3	Disulfiram metabolite diethyldithiocarbamate also degrade MLL fusion proteins .....	132
4.3	Discussion .....	134
5	CHAPTER V: INVESTIGATING THE EFFECT OF DISULFIRAM ON GENE EXPRESSION.....	137
5.1	Introduction .....	137
5.2	Results.....	139
5.2.1	Effect of disulfiram and diethyldithiocarbamate on gene expression	139
5.2.2	Examining gene expression changes after short exposures to DSF.	146
5.2.3	Discussion.....	151
6	CHAPTER VI: Studying disulfiram mechanism of action .....	155
6.1	Introduction .....	155
6.2	Results.....	158
6.2.1	Disulfiram impairs the DNA binding domain of MLL fusions.....	158
6.3	Discussion .....	175
7	CHAPTER VII: Investigating the effect of DSF <i>in vivo</i> and <i>in vitro</i> functional assays.....	181
7.1	Introduction .....	181
7.2	Results.....	183
7.2.1	Studying consequences of drugs administration on cell viability .	183

7.2.2	Disulfiram inhibit cell self-renewal ability .....	189
7.2.3	Investigating the effect of disulfiram on primary ALL .....	193
7.2.4	Studying the consequences of disulfiram <i>in vivo</i> .....	196
7.2.5	Discussion.....	200
8	CHAPTER VII: CONCLUSIONS.....	201
	REFERENCES .....	207
	APPENDIX.....	220

## LIST OF FIGURES

Figure 1 Classical model of murine haematopoiesis .....	24
Figure 2 Alternative, composite and bypass models of haematopoiesis .....	26
Figure 3 Domains of the MLL protein and their interactions.....	41
Figure 4 The normal function of the MLL complex .....	48
Figure 5 MLL and MLL fusion proteins.....	52
Figure 6 Aberrant transcriptional elongation by MLL-fusions .....	57
Figure 7 Retroviral transduction in vivo model .....	61
Figure 8 Mammalian <i>HOX</i> cluster genes .....	63
Figure 9 <i>De novo</i> drug discovery versus drug repositioning .....	72
Figure 10 Retroviral vectors.....	75
Figure 11 Optimisation of HoxA10 primers used in ChIP assay.....	94
Figure 12 Melting curves of primers used in ChIP assay .....	95
Figure 13 Effect of Radicicol on MLL-AF6 protein expression in SHI-1 .....	100
Figure 14 HOXA10 and MEIS1 gene expression levels upon Radicicol treatment.....	102
Figure 15 Effect of radicicol on luciferase activity in THP-1 MA9-Luc-Ren .....	106
Figure 16 Scheme of the screening .....	108
Figure 17 Decision tree for drug redeployment screening .....	109
Figure 18 Second step of the screening: western blot analysis in SHI-1 .....	114
Figure 19 Third step of the screening: western blot analysis in MV4-11 .....	115

Figure 20 MLL fusion protein expression in human <i>MLL-r</i> cell lines after drug treatment.....	117
Figure 21 Mechanism of ALDH inhibition by disulfiram.....	124
Figure 22 Disulfiram metabolism.....	124
Figure 23 Effect of Disulfiram on human leukaemic cell lines .....	126
Figure 24 Effect of copper-disulfiram mix on human leukaemic cell lines .....	128
Figure 25 Detection of MLL-AF4 protein expression over a time course with disulfiram and copper.....	129
Figure 26 Disulfiram-copper complexes target WT MLL and MLL fusions .....	131
Figure 27 Effect of the copper-diethyldithiocarbamate mixture on MLL-AF6 protein expression.....	133
Figure 28 Formation of the DSF-copper complex in vivo .....	136
Figure 29 Differential gene expression after 16 hours of DSF treatment .....	143
Figure 30 Gene Set Enrichment Analysis (GSEA) results after 16H.....	144
Figure 31 Effect of DSF and DDC on gene expression at 16 hours.....	145
Figure 32 Time-course of <i>HOXA10</i> expression after DSF treatment .....	147
Figure 33 Effect of DSF and DDC on gene expression at 4 hours.....	148
Figure 34 Effect of short period exposures to disulfiram on protein levels .....	150
Figure 35 Similarities between MLL and DNMT1 .....	154
Figure 36 ChIP and library preparation with MLL-N antibody from Bethyl Laboratories and Diagenode.....	160

Figure 37 ChIP and library preparation with H3K4me3 and H3K27Ac antibody .....	163
Figure 38 Overview of MLL, H3K4me3 and H3K27ac binding at the HOXA locus .....	165
Figure 39 Disulfiram and copper administration results in a decreased binding of MLL-AF9 to promoter regions of HOXA10 .....	166
Figure 40 Peaks distribution in <i>c-MYB</i> and <i>MEF2C</i> loci.....	168
Figure 41 Peaks with dynamic MLL binding.....	169
Figure 42 Peaks with dynamic MLL binding and dynamic acetylation .....	170
Figure 43 Changes in H3K27Ac at the TSS correlates with gene expression changes. ....	172
Figure 44 Correlation of epigenetic changes with leukaemic and/or with oncogene-regulated transcriptional programs.....	173
Figure 45 Disulfiram mechanism of action .....	179
Figure 46 Potential mechanism of MLL-fusion detachment from DNA.....	180
Figure 47 Disulfiram and diethyldithiocarbamate complexes with copper do not affect cell viability after 16 hours of treatment.....	184
Figure 48 Disulfiram and diethyldithiocarbamate complexes with copper reduce cell proliferation rates in a time dependent manner .....	186
Figure 49 Disulfiram and diethyldithiocarbamate induced cells death after 48h of treatment.....	188
Figure 50 GSEA plot showing negative correlation with published leukaemic stem cell signature .....	190
Figure 51 Disulfiram inhibit leukaemic self-renewal .....	192

Figure 52 DSF effect on patient-derived ALL <i>MLL</i> rearranged cells .....	194
Figure 53 Bioluminescent ALL-MSC assay.....	195
Figure 54 Disulfiram increase CD11b expression in vivo.....	197
Figure 55 Disulfiram treatment reduces spleen size of leukaemic mice.....	199

## LIST OF TABLES

Table 1 The French-American-British (FAB) classification of human AML .....	32
Table 2 The World Health Organisation (WHO) classification of human AML ..	33
Table 3 MLL fusion partner genes .....	55
Table 4 Components of a 4% Stacking and 7% Resolving gels .....	77
Table 5 List of primary and secondary antibodies used in western blot analysis .....	79
Table 6 List of all TaqMan probes used .....	81
Table 7 List of all primer sets .....	82
Table 8 List of all Human Leukaemic cell lines used in this study .....	84
Table 9 List of antibodies tested in ChIP assay .....	92
Table 10 List of all primers tested in this study for ChIP assays .....	93
Table 11 Drugs passing the first step of the screening .....	111
Table 12 Compounds passing the screening .....	116
Table 13 Concentration, purity and integrity of RNA samples used in RNA-seq analysis at 16 hours .....	140

## ABBREVIATIONS

ADH	Alcohol dehydrogenase
AF10	ALL1 fused gene from chromosome 10
AF4	ALL1 fused gene from chromosome 4
AF6	ALL1 fused gene from chromosome 6
AF9	ALL1 fused gene from chromosome 9
ALDH	Aldehyde dehydrogenase
ALL	Acute lymphoblastic leukaemia
AMG	Aorta-gonad-mesonephros
AML	Acute myeloid leukaemia
AML1	Acute myeloid leukaemia 1 protein
ANT-C	Antennapedia complex
APC	Allophycocyanine
APL	Acute promyelocytic leukaemia
APS	Ammonium persulfate
BCR	Breakpoint cluster region
BD	Bromodomain
BMP	Bone morphogenetic protein
BX-C	Bithorax complex
CB	Cord blood

CBP	cAMP binding protein
cDNA	Complementary deoxyribonucleic acid
CFU	Colony-forming unit
ChIP	Chromatin immunoprecipitation
ChIP-seq	Chromatin immunoprecipitation sequencing
CLP	Common lymphoid progenitor
CML-CP	Chronic myeloid leukaemia in chronic phase
CML-BP	Chronic myeloid leukaemia in blast phase
c-MYB	Avian myeloblastosis viral oncogene homologue
CMP	Common myeloid progenitor
CREB	cAMP responsive element binding protein
CuCl <sub>2</sub>	Copper chloride
CYP33	Cyclophilin 33
DDC	Diethyldithiocarbamate
DMEM	Dulbecco's modified eagle's Medium
DMSO	Dimethyl sulphoxide
DNMT1	DNA methyltransferase 1
DOT1L	Disruptor of telomeric silencing 1
DSB	Double strand breaks
DSF	Disulfiram
DSG	Disuccinimidyl glutarate

EDTA	Ethylenediaminetetraacetic acid
EGTA	Ethylene glycol tetraacetic acid
EMA	European medicine agency
ENL	Eleven-nineteen leukaemia
FAB	French-American-British
FACS	Fluorescence activated cell sorting
FcγRII/III	Fcγ receptor-II/III
FCS	Foetal calf serum
FDA	American food and drug administration
FDR	False discovery rate
FNB	Fenbendazole
GATA-1	GATA binding factor 1
GD21	Gene Desert region on chromosome 21
GFP	Green Fluorescent Protein
GMP	Granulocyte/ Monocyte Progenitors
GSEA	Gene set enrichment analysis
HCT	Haematopoietic cell transplant
HDAC1	Histone deacetylase 1
HDAC2	Histone deacetylase 2
H3K4	Histone H3 lysine 4
H3K27ac	Acetylated Histone H3 lysine 27

HOM-C	Homeotic complex
HOX-A	Homeobox A cluster
HPC	Haematopoietic progenitor cells
HSC	Haematopoietic stem cells
HTS	High Throughput Screening
IMDM	Iscove's modified dulbecco's medium
IP	Intraperitoneal
LEDGF	Lens epithelium derived growth factor
Lin	Lineage-associated surface markers
LUC	Luciferase
LMPP	Lymphoid-primed multipotent progenitors
LT-HSC	Long term haematopoietic stem cells
LTR	Long terminal repeats
MeDDC	Methyl diethyldithiocarbamate
MEIS1	Myeloid ectropic viral integration site 1
MEP	Megakaryocytes/erythroid progenitors
MFI	Mean fluorescence intensity
MLL	Mixed lineage leukaemia
<i>MLL</i> <sup>-/-</sup>	MLL deficient mice
MLL <sup>C</sup>	C terminal fragment of MLL
MLL <sup>N</sup>	N terminal fragment of MLL

MLP	Multi lymphoid progenitors
MPP	Multipotent progenitors
MTS	Medium throughput screening
MXT	Mitoxantrone
NaCl	Sodium chloride
NELF	Negative elongation factor
NES	Normalised enriched score
NGS	Next generation sequencing
NK cells	Natural killer cells
NSG	NOD.Cg-Prkdc <sup>scid</sup> Il2rg <sup>tm1Wjl</sup> / SzJ mice
PBS	Phosphate-buffered saline
PBS-T	PBS-Tween
PCR	Polymerase chain reaction
PHD finger	Plant homology domain
PI	Propidium Iodide
PML	Promyelocytic leukaemia protein
PRO-B	B-cell progenitors
PRO-T	T-cell progenitor
pTEFb	Positive transcription elongation factor
PU.1	Haematopoietic transcription factor PU.1
PVDF	Polivinylidene Fluoride

qRT-PCR	Quantitative real-time PCR
RAR $\alpha$	Retinoic acid receptor alpha
RbBP5	Retinoblastoma binding protein 5
RNA	Ribonucleic acid
RNA-seq	RNA sequencing
RPMI	Roswell Park Memorial Institute
SNL1	Speckled nuclear localization signal 1
SNL2	Speckled nuclear localization signal 2
STAT	Signal transducer and activator of transcription
ST-HSC	Short term haematopoietic stem cells
TAD	Transcriptional activation domain
TEL	Translocation-ETS-leukaemia
TEMED	Tetramethylenediamine
TF	Transcription factor
TO-PRO3	Monomeric cyanine nucleic acid stain
WDR5	WD-repeat protein 5
WHO	World Health Organisation
WNT	Wingless type mouse mammary tumour virus integration site

## ACKNOWLEDGEMENTS

First of all I would like to thank my principal supervisor, Dr. Jasper de Boer for his terrific guidance. The constant support, encouragement and scientific advice he has provided during these years were invaluable. The optimism and enthusiasm for his research motivated me throughout the most stressful times of my PhD. I would like to express my deepest gratitude also to my secondary supervisor, Dr. Owen Williams for his continuous support, guidance and the innumerable scientific discussions and suggestions.

I am grateful to all the members of our team and of the Cancer Section I had the privilege to work with during the past years. They have all been an amazing source of friendship and advice. I would especially like to thank Dr. Luca Gasparoli and Dr. Clemence Virely for their help and friendship. I would like to thank Dr. Mark Kristiansen, Tony Brooks and Dr. Paola Niola at UCL Genomics for running the RNA-seq and ChIP-seq experiments; and Dr. Joost Marteens at Radboud University for his help with data analysis.

I also thank all my friends scattered around UK and Italy. Their friendship was irreplaceable to get through the toughest times. My special gratitude goes to Alessandro for his endless love, support and patience during this time. You always believed in me and you helped me to keep things in perspective.

Finally, I would like to thank all my family from the bottom of my heart for their love and for being a constant source of encouragement for me.

I would like to dedicate this thesis to my family

# 1 CHAPTER I: INTRODUCTION

## 1.1 Haematopoiesis

Haematopoiesis is the highly organised process of development of blood cells. Extensive xenotransplantation studies using different mouse models allowed a better understanding of human haematopoiesis (Doulatov et al., 2012). This process occurs in two waves. The initial wave, also known as primitive haematopoiesis, consists in the production of red blood cells necessary to oxygenate the growing embryo and it take place in the yolk sac, before circulation is initiated. Once circulation is initiated, haematopoiesis proceeds to intra embryonic sites: the aorta-gonad-mesonephros (AMG) region and in umbilical arteries and vitelline arteries. In a second wave (definitive haematopoiesis) haematopoiesis moves to the foetal liver which is the main haematopoietic organ until birth. After birth the bone marrow becomes the main haematopoietic site through the whole adult life (Orkin, 2000, Orkin and Zon, 2008).

Haematopoiesis is organised in a hierarchical order with haematopoietic stem cells (HSC) at the apex of this hierarchy. HSCs are defined by two characteristics; they have the potential to self-renew and to differentiate into various haematopoietic progenitor cells (HPC). HPCs will give rise to specific precursors which will then differentiate into mature blood cells (Orkin, 2000). The haematopoietic lineages can be identified by the expression of lineage specific surface markers. The murine and human HSCs express different

surface markers. Murine HSCs are found within a subpopulation of bone marrow cells called LSK which do not express the lineage-associated cell surface markers ( $\text{Lin}^-$ ) but express the stem cell antigen ( $\text{Sca-1}^+$ ) and c-kit (LSK population:  $\text{Lin}^- \text{Sca-1}^+ \text{c-kit}^+$ ). Within this LSK subset the cells exhibiting long-term self-renewing capacity (LT-HSC) reside in the  $\text{CD34}^- \text{CD38}^+$  compartment. Cells showing short-term self-renewal (ST-HSC) express the cell surface marker CD34 but not the CD38 ( $\text{CD34}^+ \text{CD38}^-$ ). Human HSCs are found in the subset  $\text{CD34}^+ \text{CD38}^- \text{Thy1}^+ \text{CD45RA}^-$  [reviewed in (Doulatov *et al.*, 2012)], although recent studies described the existence of rare  $\text{CD34}^-$  cells expressing stem cell features. These cells seem to be more primitive than  $\text{CD34}^+$  cells; therefore should be placed higher up in the haematopoietic hierarchy (Anjos-Afonso *et al.*, 2013). HSCs are extremely important for the treatment of various blood disorders due to their ability to regenerate the entire adult haematopoietic system after transplantation.

The classical model of haematopoiesis proposed that myeloid and lymphoid development results from generation of lineage restricted multipotent progenitors: a common lymphoid progenitor (CLP) and a common myeloid progenitor (CMP) (Figure 1). The lymphoid lineage consists of T, B and NK cells which are responsible for the adaptive and innate immune responses whereas, the myeloid lineage produces granulocytes (neutrophils, eosinophils and basophils), monocytes, erythrocytes and megakaryocytes. CLPs are characterised by the expression of interleukin 7 $\alpha$  receptor (IL-7R $\alpha$ ) and reside in the compartment  $\text{Lin}^- \text{Sca}^{\text{lo}} \text{IL-7R}\alpha^+$ . This fraction will generate all lymphoid cell types (T, B and NK cells). The cells do not expressing IL-7R $\alpha$  ( $\text{IL-7R}\alpha^-$ ) are

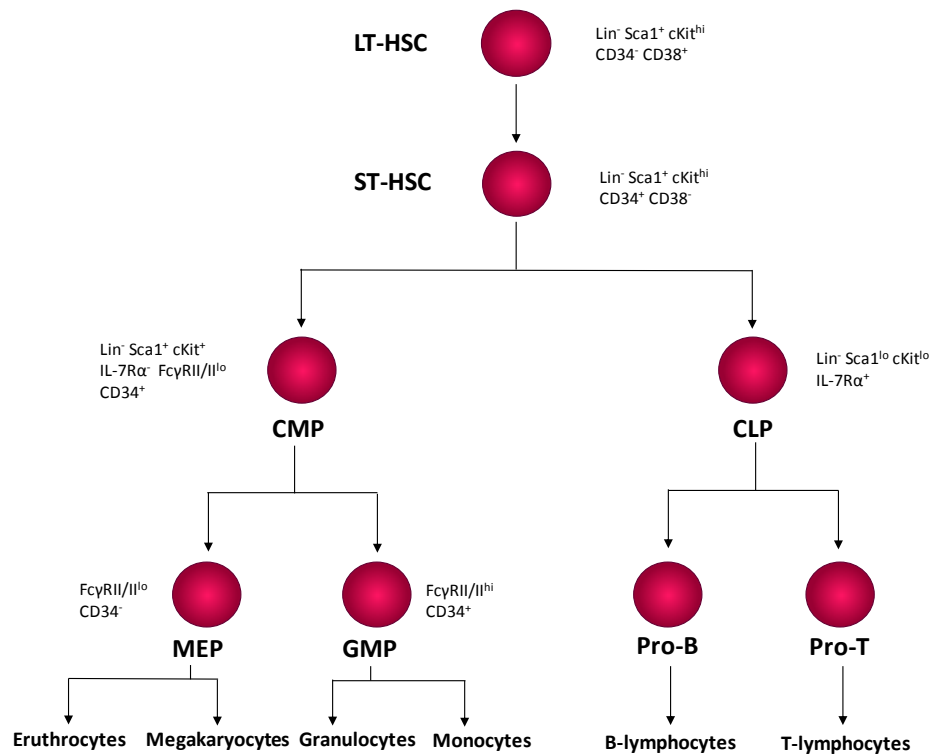


**Figure 1 Classical model of murine haematopoiesis**

According to the Long term haematopoietic stem cells (LT-HSC) have the potential to self-renew and to give rise to short term haematopoietic stem cells (ST-HSC) with reduced self-renewal capacity. Subsequently the ST-HSC can then differentiate into common myeloid progenitors (CMP) and common lymphoid progenitors (CLP). CMP generates megakaryocyte-erythrocyte progenitors (MEP) and granulocyte-macrophage progenitors (GMP) which will give rise to mature myeloid cells. CLP give rise to B-cell progenitors (Pro-B) and T-cell progenitors (Pro-T) which will give rise to cells belonging to the mature lymphoid lineage (B lymphocytes, T lymphocytes and NK cells) [adapted from (Iwasaki and Akashi, 2007)].

CMP and reside in the Lin<sup>-</sup>Sca<sup>+</sup>c-kit<sup>+</sup>IL-7αR<sup>+</sup> subset. The CMPs will give rise to megakaryocyte-erythrocyte progenitors (MEP) and to granulocyte-macrophage progenitors (GMP). MEPs and GMPs can be distinguished by the expression of the myeloid differentiation marker FCγ receptor II/III (FCγRII/III) [reviewed in (Doulatov *et al.*, 2012)].

Adolfsson *et al* proposed an alternative model of haematopoiesis. They identified a population of cells (lymphoid multipotent progenitors, LMPP) exhibiting myeloid and lymphoid differentiation potential but unable to give rise to megakaryocyte and erythroid progenitors. These two subsets were distinguished by the expression of FMS-like tyrosine kinase 3 (Flt3). The LSK Flt3<sup>+</sup> cells were able to generate B lymphocytes, T-lymphocytes, granulocytes and macrophages while cells lacking Flt3 expression (LSK Flt3<sup>-</sup>) produced megakaryocytes and erythrocytes (figure 2A) (Adolfsson *et al.*, 2005). A third model, named the composite model, combined both the classical and alternative model. The model proposes that ST-HSC give rise to CMP and LMPP which can both produce granulocytes and macrophages (figure 2B) (Adolfsson *et al.*, 2005). Yamamoto *et al* proposed a fourth model of haematopoiesis named the myeloid bypass model (figure 2C). The model proposed the existence of myeloid-restricted progenitors with long term repopulating activity (MyRP) giving rise to megakaryocytes (MkRP), to megakaryocyte-erythroid (MERP) and to common myeloid cells (CMRP) without passing through a multipotent progenitor (MPP) stage (Yamamoto *et al.*, 2013). It is challenging to combine all these murine studies into a unique model of human haematopoiesis due to the complexity of the commitment steps

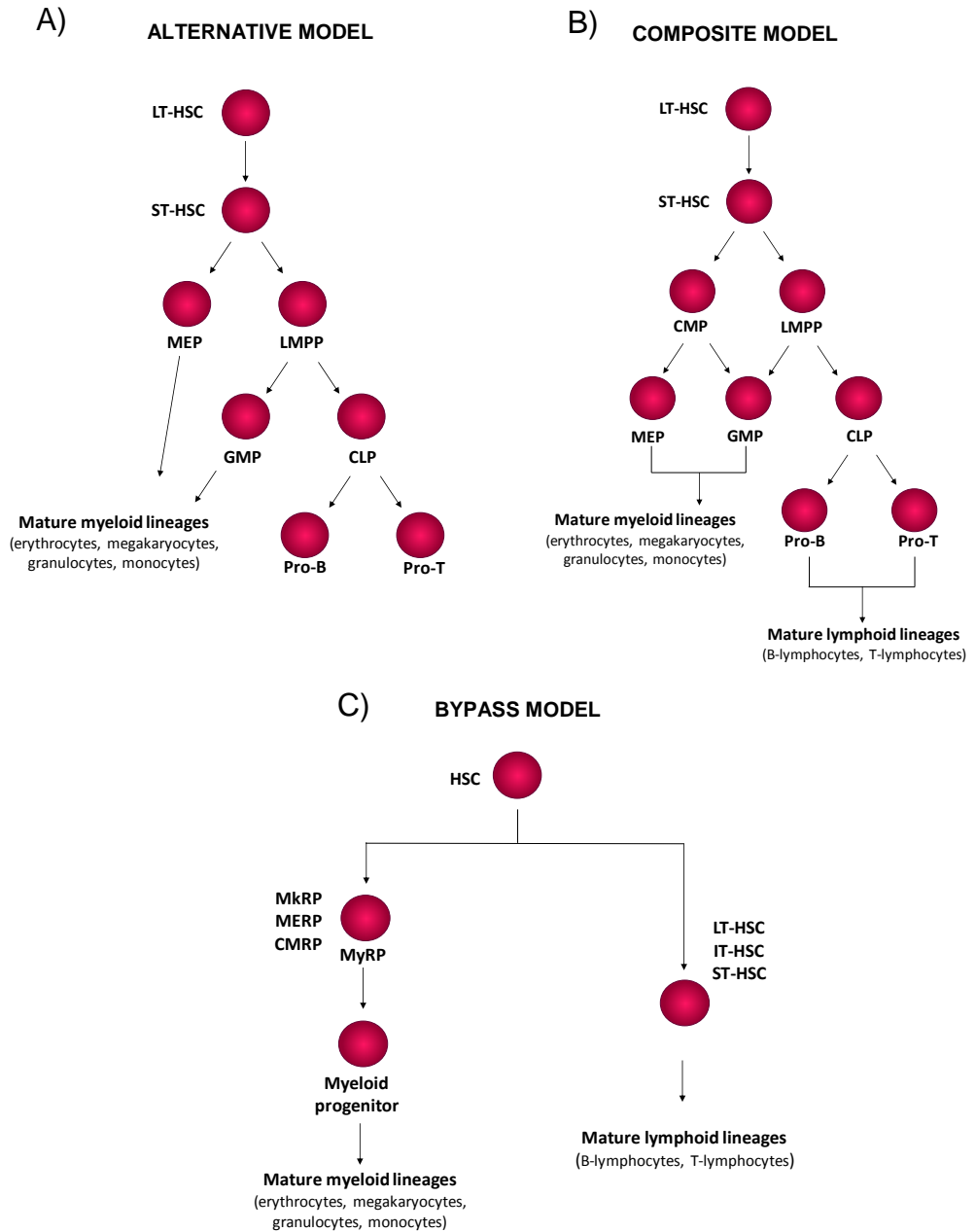


**Figure 2 Alternative, composite and bypass models of haematopoiesis**

The alternative model (A) proposes the coexistence of a subset of lymphoid primed multipotent progenitors (LMPP) with lymphoid and myeloid potential. The composite model (B) combined the classical and the alternative models showing the coexistence of CMP and LMPP. The myeloid bypass model (C) suggests the presence of a subset of myeloid restricted progenitor cells (MyRP).

## 1.2 Molecular control of haematopoiesis

Transcription factors (TF) play an essential role in HSCs generation and regulation. TF controls stem cell development during embryogenesis, their maintenance and their lineage commitment and differentiation (Orkin, 2000). Some transcription factors, like HOXA9, are required to control HSC self-renewal while others like MLL (KMT2), AML1 (RUNX1), and TEL (ETV6) are required for HSC generation. All these factors are involved in chromosomal translocations in human haematopoietic malignancies. Other transcription factors, such as PU.1 and GFI1 are required for lineage differentiation. However, this distinction is not clear cut. HSC transcription factors can also have a lineage specification role and vice versa factors involved in lineage differentiation programs can act within HSCs [reviewed in (Orkin and Zon, 2008)].

Loss of function and overexpression studies in transgenic mice allowed the identification of some important transcription factors essentials for haematopoiesis. Through homologous recombination experiments in embryonic stem (ES) cells Yagi et al generated mixed lineage leukaemia MLL (KMT2) deficient mice ( $MLL^{-/-}$ ) and studied their haematopoiesis.  $MLL^{-/-}$  mice were embryonic lethal at E10.5 and E11.5-E14.5 (Yagi et al., 1998) and showed severe developmental defects (Hess et al., 1997). The clonogenic potential of haematopoietic precursors was tested in foetal liver and yolk sac from  $MLL^{-/-}$ ,  $MLL^{+/+}$  and  $MLL^{+/-}$  embryos. Although  $MLL^{-/-}$  cultures developed all cell types the number of colonies was reduced compared to  $MLL^{+/+}$  and  $MLL^{+/-}$  cultures (Hess et

al., 1997, Yagi et al., 1998). These studies proved the importance of MLL in growth of haematopoietic precursors. Although *Mll* is important for proper establishment of haematopoiesis in embryos a conditional knockout model showed that *Mll* is not required to maintain haematopoiesis postnatally (McMahon et al., 2007).

Another gene involved in control of HSC self-renewal is Homeobox A9 (*Hoxa9*). Knockout studies from Lawrence et al showed that *Hoxa9*<sup>-/-</sup> bone marrow cells have reduced repopulation ability and proliferation capacity (Lawrence et al., 2005). Two transcription factors that are frequent targets of chromosome translocations are AML1 (RUNX1) and TEL (ETV6). Generation of AML1 deficient mice (*Aml1*<sup>-/-</sup>) resulted in block of foetal liver haematopoiesis at E11.5 and in consequent embryonic lethality at E12.5, suggesting the importance of AML1 in definitive haematopoiesis in all lineages (Okuda et al., 1996). Embryonic lethality at E11.5 due to yolk sac vascular defects was observed also in *Tel* knockout mice (*Tel*<sup>-/-</sup>). To study TEL function in adult haematopoiesis mouse chimeras were generated with *Tel*<sup>-/-</sup> and *Tel*<sup>+/-</sup> ES cells. Experiments proved that *Tel* is required for haematopoiesis only in the bone marrow (Wang et al., 1998).

Two transcription factors playing a major role in HSC lineage commitment are PU.1 and GATA1. The transcription factor PU.1 is an ETS family member expressed in HSCs which controls monocyte/macrophage and B-lymphoid commitment. Conditional knock out model showed that HSCs express PU.1 and that PU.1 constitutive expression maintains the HSC population in foetal liver

and bone marrow. Furthermore, knockout studies showed that lack of PU.1 inhibits HSC maturation (Iwasaki *et al.*, 2005). GATA1 is a zinc finger protein regulating erythroid differentiation. GATA1 deficiency is embryonically lethal at approximately E11.5. Conditional knockout studies resulted in the depletion of the erythroid compartment in spleen and in bone marrow (Gutierrez *et al.*, 2008, Iwasaki *et al.*, 2005).

The role of HSC during development is clearly crucial and so is the role of cell signalling pathways controlling HSC generation and maintenance. For example, the bone morphogenetic protein pathway (BMP pathway) is required during embryogenesis and promotes HSC emergence and survival but this pathway is not essential after HSC lineage commitment. The wingless-type MMTV (mouse mammary tumour virus) integration site (Wnt) and the Janus kinase (JAK) signal transducer and activator of transcription (STAT) (JAK-STAT) are two other pathways controlling HSCs self-renewal [reviewed in (Kim *et al.*, 2014)].

### 1.3 Acute leukaemia in infants

Myeloid and lymphoid progenitors are often called blasts (myeloblasts and lymphoblasts). In a healthy bone marrow only 5% of the cells are blasts while leukaemic bone marrow is characterised by the presence of 20% of blasts (Harris et al., 1999). Leukaemia is a malignant disease characterised by the clonal expansion of haematopoietic progenitors (lymphoid or myeloid) which are no longer able to differentiate into the different blood cell types. This differentiation block can manifest itself at different stages: more immature in acute leukaemia and more mature in chronic leukaemia. Different types of leukaemia can be categorised as acute or chronic according to how fast the disease develops. It is possible to further classify leukaemia into subgroups according to which lineage is affected: myeloid leukaemia or lymphoblastic leukaemia (Harris et al., 1999).

Acute lymphoblastic leukaemia (ALL) is one of the most common paediatric cancers and represents 75% of all acute leukaemias in children. The disease affects both adults and children with a peak of incidence at 2 to 5 years of age. The survival rates are almost 90% for leukaemia patients in general, however the outcome for patients with *MLL* rearrangements is still poor (Pui et al., 2011). Acute myeloid leukaemia (AML) is less frequent in children than ALL and is defined by the clonal expansion of myeloblasts in bone marrow and peripheral blood. Chromosomal abnormalities are found in cases of both ALL and AML; the most recurrent cytogenetic abnormalities are balanced chromosomal translocations. One of the most frequent targets of chromosomal translocation

is the mixed lineage leukaemia (*MLL*) gene. The *MLL* gene is found translocated in both ALL, AML and in biphenotypic leukaemia [reviewed in (Krivtsov and Armstrong, 2007)]. These translocations occur in more than 70% of infant acute leukaemia while in older children the *MLL* rearrangements are less frequent. Approximately 80% of infant ALL and 50% of infant AML are characterised by *MLL* translocations (Felix and Lange, 1999). *MLL* translocations also characterise 10% of cases of adult AML and in therapy related leukaemia [(Biondi et al., 2000, Krivtsov and Armstrong, 2007)].

The first diagnosis of AML is based on morphological analysis of myeloblasts, which are characterised by round and irregular nuclei and by a small cytoplasmic area. AML is a heterogeneous disease consisting of different biological and morphological subtypes. The French-British-American (FAB) group categorised the AML subtypes into nine groups on the basis of blast morphology (table 1) [reviewed in (Lowenberg et al., 1999)]. The FAB group classified also ALL into three subtypes (L1, L2, and L3) according to cell morphology. However, given the limited morphological heterogeneity of lymphoblast, the FAB classification did not provide any advantage in terms of clinical management. Another classification system was proposed by the World Health Organisation (WHO). The WHO classification is not based only on blast morphology but takes in account several characteristics of biological and clinical relevance (table 2).

Despite treatment improvements that have increased AML survival rates from < 20% in 1970 to about 50% in 2008, the cure rates are still low in comparison to

FAB SUBTYPE	NAME	ASSOCIATED TRANSLOCATION/GENE
Mo	Undifferentiated AML	Inv(3q26), EVI1
M1	Myeloblastic leukaemia with minimal maturation	n.a.
M2	Myeloblastic leukaemia with maturation	t(8;21), AML1-ETO
M3	Promyelocytic leukaemia	t(15;17), PML-RAR $\alpha$
M4	Myelomonocytic leukaemia	11q23, MLL
M4eos	Myelomonocytic leukaemia with eosinophilia	Inv(16), CBF $\beta$ -MYH11
M5	Monocytic leukaemia	11q23, MLL
M6	Erythroid leukaemia	unknown
M7	Megakaryoblastic leukaemia	unknown

**Table 1 The French-American-British (FAB) classification of human AML**

List of the subtypes of AML according to FAB classification and corresponding chromosomal translocation and genes involved (adapted from Lowenberg et al, 1999).

NAME	DESCRIPTION
<b>AML WITH RECURRENT GENETIC ABNORMALITIES</b>	<ul style="list-style-type: none"> <li>• AML with translocation between Chr 8 and 21 t(8;21); AML-ETO</li> <li>• AML with inversions in Chr 16 inv(16); CBFβ-MYH11</li> <li>• AML with translocations between Chr 15 and 17 t(15;17); PML-RARα</li> <li>• AML with translocation between Chr 9 and 11 t(9;11); MLLT3-MLL</li> <li>• AML with translocation between Chr 6 and 9 t(6;9); DEK-NUP214</li> <li>• AML with inversions in Chr 3 inv(3); RPN1-EVI1</li> <li>• AML megakaryoblastic with translocation between Chr 1 and 22 t(1;22); RBM15-MKL1</li> <li>• Provisional entity: AML with mutated NPM1</li> <li>• Provisional entity: AML with mutated CEBPA</li> </ul>
<b>AML WITH MULTILINEAGE DYSPLASIA</b>	<ul style="list-style-type: none"> <li>• Patients with prior MDS or with MPD that transforms in AML</li> </ul>
<b>AML AND MDS THERAPY RELATED</b>	<ul style="list-style-type: none"> <li>• Patients who have had previous chemotherapy and/or radiation and subsequently develop AML or MDS</li> <li>• Leukaemias may be characterised by specific chromosome abnormalities</li> </ul>
<b>AML NOT OTHERWISE CATEGORISED</b>	<ul style="list-style-type: none"> <li>• Subtypes of AML that do not fall in the above categories</li> </ul>
<b>MYELOID PROLIFERATIONS RELATED TO DOWN SYNDROME</b>	<ul style="list-style-type: none"> <li>• Transient abnormal myelopoiesis</li> <li>• AML associated with Down syndrome</li> </ul>

**Table 2 The World Health Organisation (WHO) classification of human AML**

List of the subtypes of AML according to WHO classification and corresponding chromosomal translocations and genes involved

childhood leukaemia in general (Rubnitz and Inaba, 2012). The standard AML treatment, which has not changed in the past 4 decades, is based on cytotoxic drugs inhibiting cell proliferation. The first line treatment consist of an intensive induction therapy of 7 days of cytarabine followed by 3 days of an anthracycline (7+3) in order to induce remission of leukaemic blasts (<5% in the bone marrow). The induction therapy is followed by consolidation chemotherapy or by haematopoietic cell transplant (HCT) (Saygin and Carraway, 2017). Despite the fact that “7+3” therapy remains the AML standard treatment, new cytotoxic agents (CPX-351 and vosaroxin), epigenetic modifiers (DNMT inhibitors, HDAC inhibitors) and monoclonal antibodies demonstrated clinical activity and are under investigation (Saygin and Carraway, 2017). An alternative therapeutic approach could be the use of differentiation therapy which, instead of killing the proliferating cells, would induce their maturation and/or senescence (Sell, 2005).

## 1.4 Acute leukaemia aetiology

In 1950 childhood leukaemia was incurable while nowadays more effective treatments improved the cure rates which are around 85%. However, treatments are still not adequate in high risks groups (for example in patients with fusion genes such as *MLL-AF4* or *BCR-ABL*) and often childhood leukaemia survivors have high risk of developing secondary neoplasms.

To explain leukaemia onset, Greaves proposed a two-step model, also known as a two-hit model, based on which the leukaemia onset would be the consequence of two independent genetic mutations [reviewed in (Greaves, 2006)]. Chromosomal rearrangements in both ALL and AML are not sufficient to induce malignant transformation but instead they would generate a pre-leukaemic clone *in utero*. Overt disease would require post-natal acquisition of secondary genetic mutations [reviewed in (Greaves, 2006)]. This model is supported by studies in identical twins concordant for infant leukaemia (ALL). Monozygotic twins share genetic identity and for this reason they were used in biomedical research to study several medical conditions. Studies in identical twins with concordant leukaemia proposed that *MLL* rearrangements may originate *in utero* (Ford *et al.*, 1993). Each leukaemic patient, with *MLL* fusion genes, has a unique clonotypic breakpoint. Studies on DNA breakpoint regions in three pairs of identical twins, with ALL and *MLL* gene fusion, showed that twins share a common breakpoint region and also that the *MLL* rearrangements were not inherited but acquired. This data suggested that *MLL* rearrangements occurred in one foetus only, where the pre-leukaemic cell clone was generated,

then through intraplacental vascular anastomoses spread to the other twin (Ford et al., 1993). The retrospective analysis of neonatal blood spots (Guthrie cards) of leukaemic patients, based on PCR detection of *MLL-AF4* fusion sequences, revealed that the *MLL* rearrangements were detectable already at birth (Gale et al., 1997). These studies provided the evidence that for children with acute leukaemias and *MLL* fusion genes the disease initiated *in utero*.

The high concordance rates in infants ALL expressing *MLL*-fusions ( $\cong 100\%$  in identical twins) in combination with the very short latencies ( $\cong 18$  months) suggest that the *MLL*-fusions are sufficient to induce leukaemia. The hypothesis that a single driver mutation (or single hit) might be sufficient for the transformation of a normal cell into a malignant one it is in contrast with the idea that cancers are the result of the acquisition of multiple mutations. More recently it has been shown that in many cases of infant ALL with *MLL* rearrangements, *MLL*-fusions were the only detectable clonal mutations suggesting that they are sufficient to induce leukaemia (Andersson et al., 2015). Greaves proposed that during embryonic/foetal development there must be a short time frame in which micro-environmental conditions support proliferation and expansion of stem cells characterised by a constitutive expression of self-renewal signatures (Greaves, 2015). Under these circumstances a mutation in a single driver oncogene is sufficient to cause the malignant phenotype.

## 1.5 Leukaemic stem cells

Haematopoiesis is a hierarchical process with haematopoietic stem cells (HSC) at the apex of this hierarchy. HSCs are defined by their ability of self-renew and to differentiate in more mature progenitors. Malignant stem cells are considered the origin of many malignancies and in leukaemia these cells are called leukaemic stem cells (LSC). Very similarly to normal haematopoiesis, leukaemogenesis is also organised as a hierarchy with LSC at its origin. LSCs are rare cells that share features with normal HSCs, such as the indefinite self-renewal potential that is able to initiate and maintain leukaemogenesis [reviewed in (Bonnet, 2005)]. However, while normal HSCs differentiate into mature haematopoietic lineages, the progeny of LSC remain in a more undifferentiated status.

Data supporting the hierarchical organisation of AML and providing also the evidence for the existence of LSCs were generated by the studies of Dick and colleagues. LSCs from AML patients were first identified on the basis of surface marker expression, such as CD34 and CD38, using flow cytometry techniques. Bonnet and Dick demonstrated that the CD34<sup>+</sup>CD38<sup>-</sup> compartment, from AML patient samples, was the only cell subset able to engraft non-obese diabetic (NOD)/SCID mice (Bonnet and Dick, 1997). These cells were initially defined as SCID leukaemia-initiating cells (SL-IC). Moreover, the CD34<sup>+</sup>CD38<sup>-</sup> cell subset when serially transplanted into secondary recipients was able to recapitulate the disease [reviewed in (Bonnet and Dick, 1997, Huntly and Gilliland, 2005)]. This proved that AML has a hierarchical organisation but also that LCSs might

originate from normal HSCs. In normal HSCs the self-renewal machinery is already activated so through accumulation of few pre-leukaemic mutations the HSCs may become LSCs. However, other studies showed that leukaemia can be initiated also in more committed progenitors. One of the first studies showing this alternative origin of leukaemia came from Weissman group (Cozzio et al., 2003). In this study HSC, CMP, GMP, MEP and CLP were purified from C57BL/6 mice, and then those cells were transduced with a vector encoding MLL-ENL. The immortalised cells generated were transplanted into congenic recipients and all the transduced cells, with the exception of MEP and CLP, induced leukaemia (Cozzio et al., 2003). Committed progenitors do not normally possess self-renewal activity; this property must be reactivated before these cells acquire additional tumorigenic mutations. Moreover, committed progenitors persist for a short period of time throughout life and therefore have less chance than HSCs to accumulate the necessary mutations [reviewed in (Huntly and Gilliland, 2005)]. The establishment of new immunodeficient mouse models and the development of new transplantation techniques (intrabone marrow injections) showed that LSCs could originate also from more mature CD34<sup>+</sup>CD38<sup>+</sup> AML (Taussig et al., 2008). This subset of mature progenitors, CD34<sup>+</sup>CD38<sup>+</sup>, was able to engraft primary but not secondary recipients [reviewed in (Horton and Huntly, 2012)]. Also in mature CD34<sup>+</sup>CD38<sup>-</sup> cells the frequency of LSC was higher than the frequency in CD34<sup>+</sup>CD38<sup>+</sup> cells [reviewed in (Horton and Huntly, 2012)].

LSC express also other surface markers, besides CD34 and CD38, like the myeloid antigens CD33 and CD123 or other novel markers like TIM3, CD47 and

CD96. However, the expression of these other cell surface markers is more often patient specific [reviewed in (Horton and Huntly, 2012)]. Flow cytometry based methods allow the identification and isolation of LSCs, however, limiting dilution transplantations are the gold standard assay to detect LSCs.

## 1.6 MLL structure

The *MLL* gene is located on chromosome 11, band q23. The size of the gene is roughly 90 Kb and it contains 37 exons and coding sequences for about 12 Kb [reviewed in (Eguchi et al., 2003) (Winters and Bernt, 2017)]. The *MLL* gene encodes a protein containing 3968 amino acids and with molecular weight of about 430 kDa which, in the cytoplasm, undergoes post-translational cleavage. The threonine protease taspase1 cleaves MLL into two fragments: an N-terminal fragment of 320kDa ( $MLL^N$ ) and a C-terminal fragment of 180kDa ( $MLL^C$ ). The proteolytic cleavage site sequences are conserved in Trx, the *Drosophila* homologue of MLL, suggesting that the cleavage is essential for MLL function (Yokoyama et al., 2002). After cleavage, both  $MLL^N$  and  $MLL^C$  peptides remain noncovalently associated through the FYRN and FYRC domains. This interaction increases the protein stability (reviewed in (Daser and Rabbitts, 2005, Eguchi et al., 2003, Hess, 2004).

The MLL N-terminus is composed of the following domains: three AT-hooks, two small SNL1 and SNL2 (speckled nuclear localisation domains), a repression domain, plant homology domain (PHD finger) and a bromo domain (figure 3). The **AT hooks** are located near the N-terminus, their function is to recognise and bind the minor groove of DNA. These AT-hooks may stabilize protein-DNA complexes or mediate protein-protein interactions through binding to DNA [reviewed in (Daser and Rabbitts, 2005)]. Two highly conserved sub-nuclear localisation domains, **SNL1** and **SNL2**, mediate the nuclear localisation of MLL proteins [reviewed in (Ayton and Cleary, 2001)]. The region following

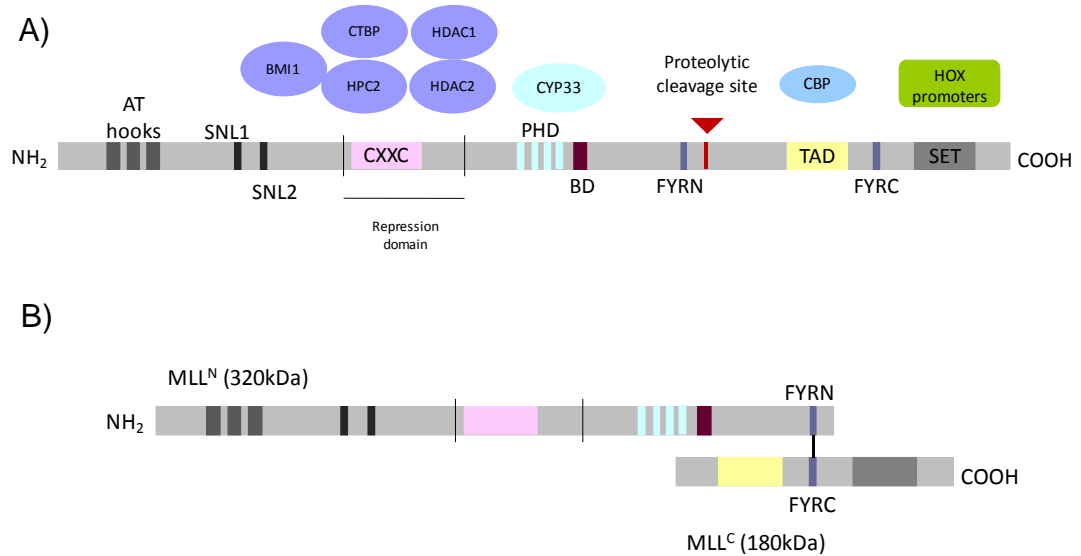


**Figure 3 Domains of the MLL protein and their interactions**

The MLL gene is located on the chromosome 11q23 and it encodes a protein of about 4000 amino acids. (A) The structure of the wild-type MLL protein and binding proteins. The MLL N-terminal portion contains three AT hooks, which are responsible to bind the minor groove of DNA; two sub-nuclear localisation domains (SNL1 and SNL2) that promote MLL nuclear localisation; a repressor domain, containing a CXXC zinc finger motif. The CXXC domain binds the promoter region of MLL target genes and interacts with histone deacetylases (HDAC1 and HDAC2) and polycomb group proteins HPC2 and BMI1. The middle portion of MLL contains a PHD zinc finger domain and a bromodomain, both responsible for protein-protein interactions. The C-terminal portion contains a transcriptional activation domain (TAD) that promotes activation of MLL and a SET domain with H3K4 methyltransferase activity. (B) The mature MLL protein cleaved by taspase1. The protease divides the MLL in an N-terminus domain of 320kDa and a C-terminus domain of 180kDa. The two fragments remains non-covalently associated through the regions FYRN and FYRC. Adapted from (Eguchi et al., 2003) and from (Daser and Rabbits, 2005).

SNL1 and SNL2 has transcriptional repression activity. The repression domain recruits histone deacetylases HDAC1, HDAC2, co-repressor proteins CTBP and the polycomb proteins HPC2 and BMI-1 [reviewed in (Daser and Rabbits, 2005)]. Contained within the repression domain there is a domain showing homology with two proteins: DNA methyltransferase1 (DNMT1) and with methyl binding domain protein 1 (MBD1), both regulating transcription through methylation. This region is a cysteine-rich zinc finger **CXXC domain**, responsible for MLL binding to unmethylated DNA regions [reviewed in (Ayton and Cleary, 2001, Eguchi et al., 2003)]. The last two domains in the MLL N-terminus are PHD fingers and a bromodomain. The four plant homodomain (**PHD**) zinc fingers are responsible for protein-protein interactions. The third PHD zinc finger binds the nuclear cyclophilin (CYP33). CYP33 has a RNA recognition motif (RRM) and when overexpressed the expression of MLL target genes *HOXC8* and *HOXC9* is downregulated. The bromodomain (**BD**) also allows protein-protein interactions [reviewed in (Daser and Rabbits, 2005)]. Moving towards the MLL C-terminus there is the proteolytic cleavage site of taspase1 followed by a transcriptional activation domain (**TAD**). TAD promotes transcriptional activation by interacting directly with the cAMP responsive-element (CREB) binding protein (CBP) [reviewed in (Eguchi et al., 2003)]. The closest region to the MLL C-terminus is the **SET domain**. It is a highly conserved region with histone-lysine methyltransferase activity. By methylation of histone 3 at lysin 4 (H3K4) SET affects chromatin structure and expression of *HOX* target genes [reviewed in (Eguchi et al., 2003)]. Trimethylation of H3K4 correlates with transcriptional activation. The two MLL fragments (MLL<sup>N</sup> and

MLL<sup>C</sup>) display opposite transcriptional properties. The MLL<sup>N</sup> represses transcription of target genes, probably through recruitment of HDAC and polycomb proteins. When MLL<sup>N</sup> dimerises with MLL<sup>C</sup>, the complex activates transcription. Transcriptional activation is promoted by the interaction of TAD with the CREB binding protein. This protein has histone acetyltransferase (HAT) activity which results in acetylation of histone H3 and H4 at promoter sites of target genes [reviewed in (Hess, 2004, Yokoyama et al., 2002)].

## 1.7 Normal function of MLL

MLL is expressed during embryonic development and in most adult tissues, including myeloid and lymphoid cells. The *MLL* gene is the mammalian homologue of the *Drosophila Trithorax* gene (*Trx*). *Trx* belongs to the Trithorax group (TrxG) of transcription factors positively regulating the expression of the *homeotic (HOM-C)* genes (Bithorax and Antennapedia complexes) during development in *Drosophila* [reviewed in (Hess, 2004)]. *HOM-C* gene expression, during development, is repressed by genes belonging to the Polycomb group (PcG).

Knock-out studies provided relevant information regarding the normal function of MLL. *Mll*<sup>-/-</sup> mice were embryonic lethal at E10.5. Embryos showed several developmental defects and dysregulation of *Hox* gene expression. Furthermore, in *Mll*<sup>-/-</sup> mice *Hox* gene expression was initiated but not maintained, suggesting that MLL is important in maintaining rather than initiating expression of *Hox* genes. *Mll* heterozygous mice (*Mll*<sup>+/-</sup>) showed retarded growth at birth, axial skeletal and haematopoietic abnormalities (Hess et al., 1997, Yagi et al., 1998). MLL is a positive regulator of *Hox* genes, which are required during embryonic development and haematopoietic differentiation. Therefore, a deficiency of *Mll* would reflect in developmental defects and in disordered haematopoiesis.

The excision of *Mll* exons 3 and 4, in an inducible MLL knock out model (Mx-Cre), resulted in bone marrow failure in adult mice (Jude et al., 2007). This study showed that MLL is essential during adult haematopoiesis. However, a

simultaneous *Mll* conditional knock out (*MllcKO*) study from McMahon and colleagues, used a Vav-Cre transgene to conditionally delete *Mll* exons 8 and 9 in the embryo. The resulting mice had normal haematopoiesis, suggesting that *Mll* is not required to maintain adult steady state haematopoiesis. However, *Mll* was found to be required for reconstitution of irradiated recipient mice and therefore is likely to be necessary for adult haematopoiesis under conditions of replicative stress (McMahon et al., 2007). MLL has a crucial role in regulating *HOX* gene expression (Krivtsov and Armstrong, 2007). Indeed, *HOX* genes are some of the best characterised MLL target genes. These genes are transcription factors regulating embryonic development and differentiation of haematopoietic cells [reviewed in (Thorsteinsdottir et al., 1997)]. The 39 *HOX* genes identified in vertebrates are grouped in four clusters (*HOXA*, *HOXB*, *HOXC*, *HOXD*) on four human chromosomes: 7, 17, 12 and 2. The *HOX* genes occupying the 3' end of each cluster are expressed in the most immature haematopoietic cells. While, genes located towards the 5' end of each cluster are expressed in early stages of differentiation [reviewed in (Thorsteinsdottir et al., 1997)]. In human haematopoiesis *HOX* gene expression is restricted to early haematopoietic progenitors while their expression is down-regulated in mature cells [reviewed in (Slany, 2009)].

## 1.8 Transcriptional regulation by MLL

MLL is a histone methyltransferase recruited to the promoters of genes occupied by RNA pol II (Bannister and Kouzarides, 2011, Linggi et al., 2005). The balanced chromosomal translocation giving rise to leukaemic fusion proteins like MLL-fusions alter the epigenetic landscape.

Nakamura et al discovered that MLL is part of a multiprotein supercomplex associated with the promoter of MLL target genes. The role of these macromolecular complexes is to mediate methyltransferase activity during transcriptional initiation and elongation (Nakamura et al., 2002). The proteins associated with MLL<sup>N</sup> are important to target the MLL complex to specific loci [reviewed in (Crawford and Hess, 2006, Slany, 2009)]. Menin is a DNA binding protein of 67kDa and a tumour suppressor encoded by the gene *Men1*. Menin physically interacts with MLL through a consensus sequence [RXRFP, known as high-affinity menin binding motif (hMBM)] located near the amino terminus of MLL (Yokoyama et al., 2005). MLL-menin association on *HOX* gene promoters is essential to maintain *HOX* genes expression and menin presence is also necessary for initiation and maintenance of leukemogenic transformation mediated by MLL (Yokoyama et al., 2005). MLL and menin create a surface of interaction for the lens epithelium derived growth factor (LEDGF) to promote interaction of MLL complex with chromatin (Yokoyama and Cleary, 2008). The MLL<sup>C</sup> binds four different proteins: MOF, WDR5, RbBP5 and ASH2L. MOF is a H4K16 acetyltransferase neutralising histone charges and unwinding chromatin. The WD-repeat protein 5 (WDR5) presents the H3K4 tail for its consecutive

methylation and together with retinoblastoma binding protein 5 (RbBP5) interacts directly with the SET domain of MLL. ASH2L does not bind directly MLL<sup>C</sup> but interacts with RbBP5 and together they stabilise the MLL complex [reviewed in (Crawford and Hess, 2006, Slany, 2009)].

The MLL complex is recruited, at the promoter of genes with stalled transcriptional machinery, to methylate H3K4 and to activate transcription of target genes. At genes with stalled transcriptional machinery the RNA Pol II is associated with negative elongation factor (NELF) and to DRB sensitivity-inducible factor (DSIF) which also acts as negative elongation factor (figure 4) [reviewed in (Smith et al., 2011)]. Following the methylation of H3K4, a complex formed by the positive transcription elongation factor b (pTEFb), AF4 and ENL/AF9 is recruited by the transcriptional machinery. To release the paused RNA polymerase, the complex pTEFb-AF4-ENL/AF9 phosphorylates the RNA Pol II C-terminal repeat domain (CTD) and the negative elongation factors (NELF and DSIF), AF4 and ENL/AF9 (figure 4) (reviewed in Smith et al, 2011). Then the complex pTEFb-AF4-ENL/AF9 dissociates and the MLL complex detaches from DNA. At this stage another complex formed by AF4, AF10, AF9/ENL and disruptor of telomeric silencing-1 (DOT1L) binds the DNA and methylates H3K79 to promote transcriptional elongation (Yokoyama et al., 2010). As soon as elongation starts, the MLL complex dissociates from RNA pol II [reviewed in (Krivtsov and Armstrong, 2007, Smith et al., 2011)].



with menin that together with LEDGF facilitates the MLL complex interaction with chromatin. The proteins interacting with the MLL<sup>C</sup> (ASH2L, RbBP5, WDR5) are required for H3K4 methylation. Following the H3K4 methylation, a complex formed by pTEFb, AF4 and AF9/ENL induces phosphorylation of RNA Pol II C-terminal repeat domain (CTD) and of the negative elongation factors (NELF and DSIF). The complex AF4-ENL/AF9 dissociates from pTEFb and another complex formed by DOT1L, AF10, AF4, AF9/ENL binds DNA. DOT1L methylate H3K79, the transcriptional elongation can start and the MLL complex detach from DNA. MLL<sup>N</sup>, MLL N-Terminal region; MLLC, MLL<sup>C</sup> C-terminal region; NELF, negative elongation factor; DSIF, DRB sensitivity-inducing factor; DOT1L, disruptor of telomeric silencing-1; pTEFb, positive transcription elongation factor (adapted from (Slany, 2009, Smith et al., 2011, Dou and Hess, 2008)).

## 1.9 MLL rearranged leukaemia and MLL rearrangements

Acute leukaemias are characterised by a large variety of genetic aberrations: point mutations, deletions, duplications, translocations. The most frequent cytogenetic aberrations are balanced chromosomal translocations.

The genomic regions in which recombination occur are known as breakpoint cluster regions (BCR). BCRs are localised in introns and each patient has a unique and specific DNA breakpoint [reviewed in (Greaves and Wiemels, 2003)]. In *MLL* rearranged leukaemia, the breakpoint region falls within an 8.3kb intronic region located between exon 8 and 14 (figure 5) [reviewed in (Eguchi et al., 2003)]. The BCR region contains repetitive Alu sequences and consensus binding sites for topoisomerase II which can make the DNA more vulnerable to double-strand breaks (DSB) [reviewed in (Greaves and Wiemels, 2003)]. DSBs could also be generated by apoptotic endonucleases in cells recovering from the induction of the apoptotic programme [reviewed in (Greaves and Wiemels, 2003)].

In *MLL* rearranged leukaemia, the balanced chromosomal translocations results in the deletion of the *MLL* C-terminal region and in the consequent in frame fusion of the N-terminal *MLL* region with the C-terminal portion of the translocation partner gene. The translocation results in the generation of chimeric proteins with novel properties (Eguchi et al., 2003). Whereas, many studies indicate that the *MLL*-fusion proteins containing the N-terminal *MLL* portion are able to induce leukaemia, in some cases the reciprocal fusion product, containing the N-terminal portion of the translocation partner fused to

the MLL<sup>C</sup> region, can also be detected. However the role of reciprocal fusions in transformation is still controversial [reviewed in (Hess, 2004) (Sanders et al., 2011)].

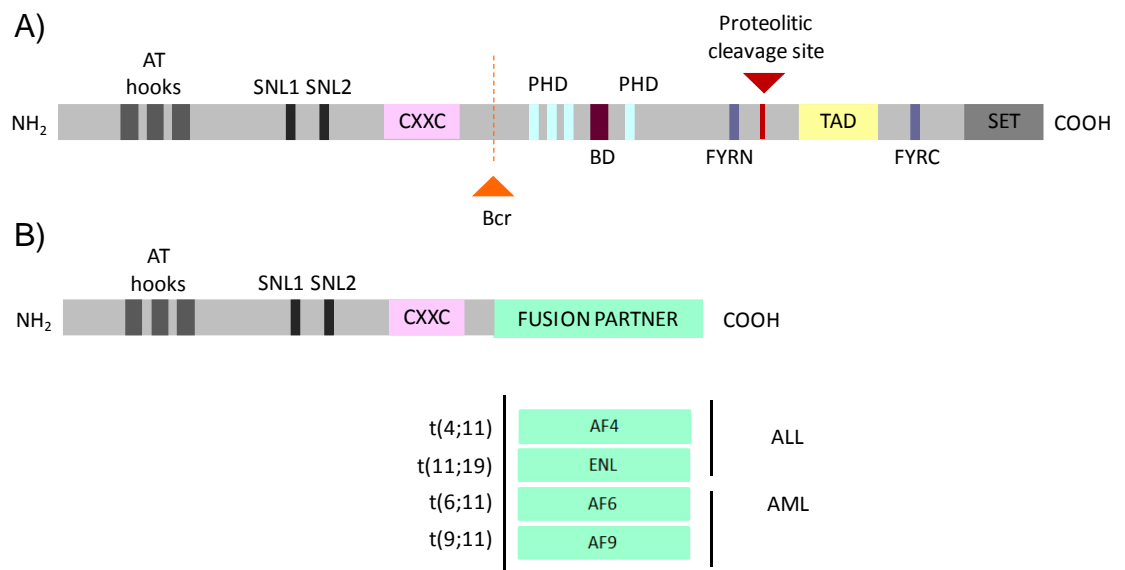


**Figure 5 MLL and MLL fusion proteins**

Schematic diagram illustrates wild type MLL and MLL fusion proteins. In the upper diagram (A), the breakpoint cluster region (BCR) is indicated in orange. The lower diagram (B) shows a chimeric fusion protein generated as consequence of the chromosomal translocation and some of the most common translocation partners.

## 1.10 MLL fusion genes

To date, over 100 (~135) MLL fusion partner genes have been identified, characterised by fusion of 5' MLL sequences to numerous different partner genes. Most of the MLL partner genes are expressed in haematopoietic cells and in adult tissues [reviewed in (Ayton and Cleary, 2001)].

MLL fusion partners can be classified into several categories. The most frequent fusion partners are nuclear proteins: AF4, AF9, AF10, ENL and ELL [reviewed in (Dou and Hess, 2008)]. These factors regulate the transcription of target genes. The nuclear proteins ENL and AF9, respectively on chromosome 19p13 and chromosome 9p22, share a highly conserved region at their C-terminal domain which has been shown to induce transformation when fused to MLL (Slany et al., 1998). The N-termini of both proteins is characterised by the presence of the YEATS domain binding acetylated histone lysine residues [reviewed in (Schulze et al., 2009)]. It has been shown that these translocation partners together with AF4, AF10 and ELL are all components of the multiprotein supercomplex promoting transcriptional activation (Smith et al., 2011).

A second group of MLL partner genes includes cytoplasmic signalling proteins, such as AF6, GAS7, EEN or septins (SEPT2, 5, 6, 9, and 11) which regulate cell cycle and vesicle trafficking. The dimerization of cytoplasmic proteins contribute to myeloid leukaemia however, the mechanism of leukaemogenesis is not entirely defined. The last group of fusion partners includes the histone acetyltransferases p300 and CBP. Both proteins usually interact with wild-type

MLL through the transcriptional activation domain (TAD), which is most frequently deleted in MLL fusions [reviewed in (Krivtsov and Armstrong, 2007)]. Table 3 summarise some of the partners gene so far identified. The cytoplasmic fusion partners are very rare with the exception of AF6 which together with the nuclear translocation partners accounts for more than 50% of leukaemia cases characterised by MLL translocations (Meyer et al., 2006).

The mechanism of leukaemic transformation in these two groups is different. As described in the paragraph 1.8 the wild type MLL is part of a multiprotein supercomplex responsible for regulating the transcription of MLL target genes. The fusion of MLL<sup>N</sup> with nuclear partner genes results in an abnormal transcription complex which causes the constitutive activation of MLL target genes (Dou and Hess, 2008). When MLL<sup>N</sup> is fused to cytoplasmic partner genes the target genes regulation is activated by dimerization of MLL fusions (Eguchi et al., 2003).

<b>Fusion partner</b>	<b>Chromosome location</b>	<b>Function</b>	<b>Localisation</b>
AF4	4q21	Transcriptional activator	N
AF9	9p23	Transcriptional activator	N
ENL	19p13.3	Transcriptional activator	N
AF10	10p12	Transcriptional activator	N
ELL	19p13.1	RNApol II transcription elongation	N
CBP	16q13	Histone acetyltransferase	N
P300	22q13	Histone acetyltransferase	N
EPS15	1q32	?	C
GAS7	17p13	Actin assembly	C
EEN	19p13	Regulation of endocytosis	C
AF6	6q27	Maintenance of cell-cell junctions	C
AFX	Xq13	Forkhead transcription factor	C
SEPT2	Xq22	Septin family	C
SEPT5	22q11	Septin family	C
SEPT6	Xq24	Septin family	C
SEPT9	17q25	Septin family	C
SEPT11	4q21	Septin family	C
AF1p	1p32	Regulation of endocytosis	C,N
LAF4	2q11	Transcriptional activator	N
GMPS	3q25	Guanosine monophosphate synthetase	C
LPP	3q28	Cell motility and focal adhesion	C,N
AF5q31	5q31	Transcriptional activator (?)	?
GRAF	5q31	Negative regulator of RhoA	C
FKHRL1	6q21	Forkhead transcription factor	N
AF9q34	9q34	RAS GTPase activating protein	C
ABI1	10p11.2	Cell motility	C
CALM	11q14-q21	Regulation of endocytosis	C,N
LARG	11q23.3	Activator of Rho GTPases	C
GPHN	14q24	Gly and GABA receptor assembly	C
AF17	17q21	Transcription factor	N
AF17q25	57q21	Septin family	C
AF22	22q11	Septin family	C

**Table 3 MLL fusion partner genes**

List of the MLL fusion partner genes, their chromosome location and cellular localisation. Known gene functions are indicated. N: indicates nuclear localisation; C, cytoplasmic localisation, (?) not known or not confirmed [adapted from (Eguchi et al., 2003) and from (Krivtsov and Armstrong, 2007)].

## 1.11 Transcriptional Regulation by MLL-fusions

As consequence of chromosomal translocation the MLL C-terminal domain is lost as well as part of the MLL N-terminal domain. The AT hooks, SNL1, SNL2 and CXXC domain are the MLL N-terminal regions retained in the fusion proteins. Given the high number of translocation partners a mechanism of transformation for MLL-fusions it has been proposed exclusively for the most common nuclear translocation partners. As mentioned earlier, the macromolecular complex containing the wtMLL, responsible for the H3K4 methylation, is recruited by RNA pol II at the promoter of MLL target genes [reviewed in (Krivtsov and Armstrong, 2007, Smith et al., 2011)]. Following H3K4 methylation, the complex containing the pTEFb phosphorylates the negative elongation factors and RNA pol II to release the paused RNAPolIII. This event is followed by recruitment of DOT1L complex which is responsible for H3K79 methylation, resulting in transcriptional elongation (figure 5) [reviewed in (Krivtsov and Armstrong, 2007) (Smith et al., 2011) (Yokoyama et al., 2010)].

This highly organised process is clearly disrupted in presence of MLL fusions. In the presence of the MLL-fusions an abnormal transcription elongation complex is assembled. The most common MLL-fusion partners are part of the complexes assembled around RNA pol II (Dou and Hess, 2008). Therefore, in *MLL* rearranged leukaemias the MLL-fusion recruits the pTEFb complex and then the DOT1L complex that constantly methylate H3K79 leading to an abnormal transcription of target genes (Bitoun et al., 2007, Yokoyama et al., 2010). This reflects in a continuous transcription of MLL target genes (figure 6).

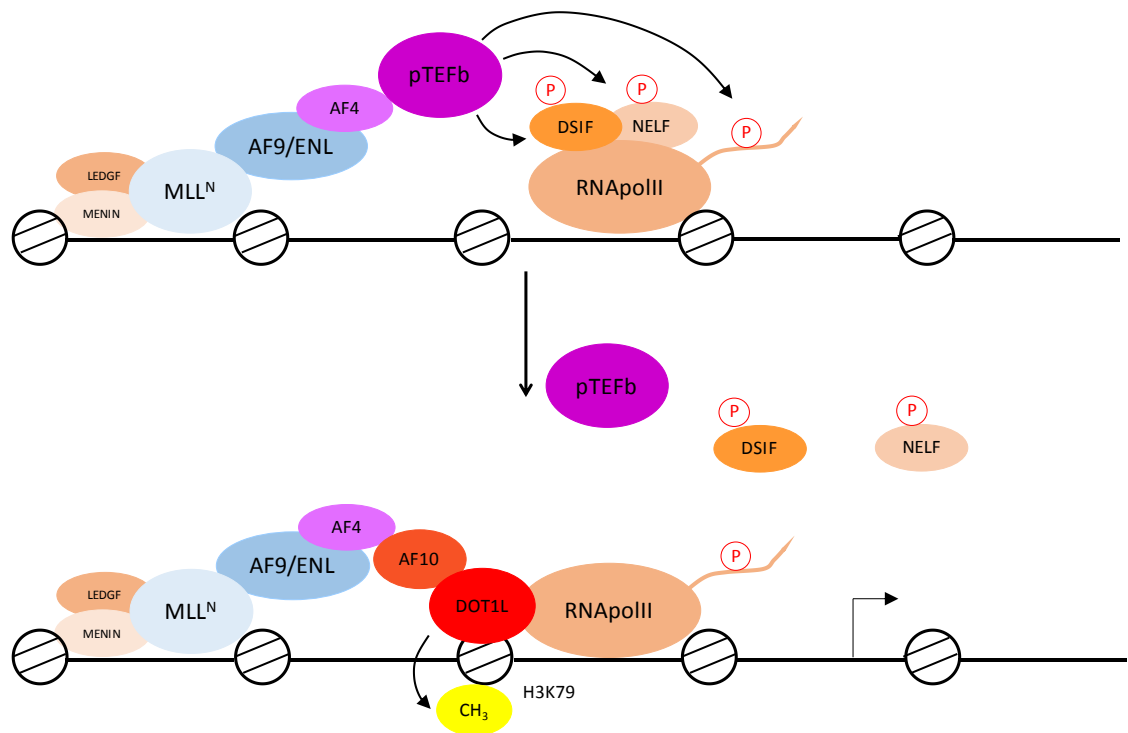


**Figure 6 Aberrant transcriptional elongation by MLL-fusions**

Aberrant transcription elongation caused by the presence of MLL-fusions. The MLL-fusions recruits the pTEFb complex and then the DOT1L complex. This results in continuous H3K79 methylation and constant transcription of target genes. MLL<sup>N</sup>, MLL N-Terminal region; NELF, negative elongation factor; DSIF, DRB sensitivity-inducing factor; DOT1L, disruptor of telomeric silencing-1; pTEFb, positive transcription elongation factor.

## 1.12 Models of MLL fusion leukaemia

In order to investigate the relevance of fusion proteins in the pathogenesis of MLL-fusion associated leukaemia, many research groups developed *in vivo* experimental models mimicking the effect of chromosomal translocations. The first *in vivo* model was an Mll-AF9 knock-in mouse model. Using homologous recombination Corral et al fused the 3' end of the human *AF9* gene with the exon 8 of the endogenous murine *Mll* (Corral et al., 1996). The in frame fusion of *Af9* with *Mll* was introduced in embryonic stem cells (ES). Then, chimeric ES cells were injected into blastocysts to produce chimeric mice. The chimeric mice and their progeny developed AML after six months of age (Corral et al., 1996). Sporadically, chimeric mice developed ALL with longer latency, suggesting that secondary mutations were necessary for leukaemia development (Corral et al., 1996, Dobson et al., 1999). This knock-in model is limited by the fact that the fusion proteins are expressed in all the cells expressing the endogenous *Mll* and not only in the haematopoietic cells.

In order to allow tissue/cell-specific expression, the same group developed the "translocator" mouse model (Collins et al., 2000, Forster et al., 2003). These mice were generated by homologous recombination in ES cells by introducing the loxP sites into introns of *Mll*, *Af9* (Collins et al., 2000) and *Enl* (Forster et al., 2003) in correspondence of the breakpoint regions in human leukaemia. Mice carrying these alterations were crossed with mice expressing the Cre recombinase. The Cre-loxP system guarantees site specific recombination. Tissue specificity was achieved by driving the expression of the Cre

recombinase under the control of *Lmo2* promoter, which is expressed in HSC (Forster et al., 2003). These mice developed AML with a latency of 2-4 months indicating that the recombination event might be sufficient to induce leukaemia without cooperation of secondary mutations (Drynan et al., 2005, Forster et al., 2003).

Another method frequently used to generate *in vivo* mouse models of MLL-fusion leukaemia was by retroviral transduction (figure 7). Haematopoietic progenitor cells (HPC) derived from mouse bone marrow were transduced with a retroviral construct over-expressing MLL-ENL (Lavau et al., 1997). These cells when transplanted into SCID recipients developed AML (Lavau et al., 1997). This kind of approach was used to study leukaemias associated with other MLL fusions like MLL-CBP (Lavau et al., 2000a) and MLL-ELL (Lavau et al., 2000b).

Most of the *in vivo* studies were carried out using murine MLL-fusion models. Barabe et al developed the first *in vivo* model expressing the MLL-fusion in human cells (Barabe et al., 2007). Using the retroviral approach Barabe et al induced leukaemia in immunodeficient mice by transplanting human cord blood cells (CB) transduced with MLL-AF9 or MLL-ENL. Mice transplanted with cells transduced with MLL-ENL developed ALL while MLL-AF9 transductions induced AML and ALL *in vivo* (Barabe et al., 2007). All mice developed leukaemia with short latencies (less than 19 weeks) suggesting one more time that the MLL fusion is sufficient to initiate the disease. The frequency of leukaemia initiating

cells (less than 1:2000) was estimated in secondary transplants by limiting dilutions (Barabe et al., 2007).

Our laboratory also used a modified retroviral approach to generate a mouse model conditionally expressing MLL-ENL. MLL-ENL expression was regulated using a Tet-Off system (Horton et al., 2005). In this model, MLL-ENL expression was under the control of the tetracycline-responsive element (TRE) promoter and it depends on the TRE binding to the tetracycline transactivator (tTA). In presence of doxycycline the tTA is not able to bind TRE, this results in loss of MLL-ENL expression (Horton et al., 2005). Horton et al demonstrated that MLL-ENL continuous expression was essential for survival of leukaemic cells *in vitro and in vivo* (Horton et al., 2005, Horton et al., 2009).

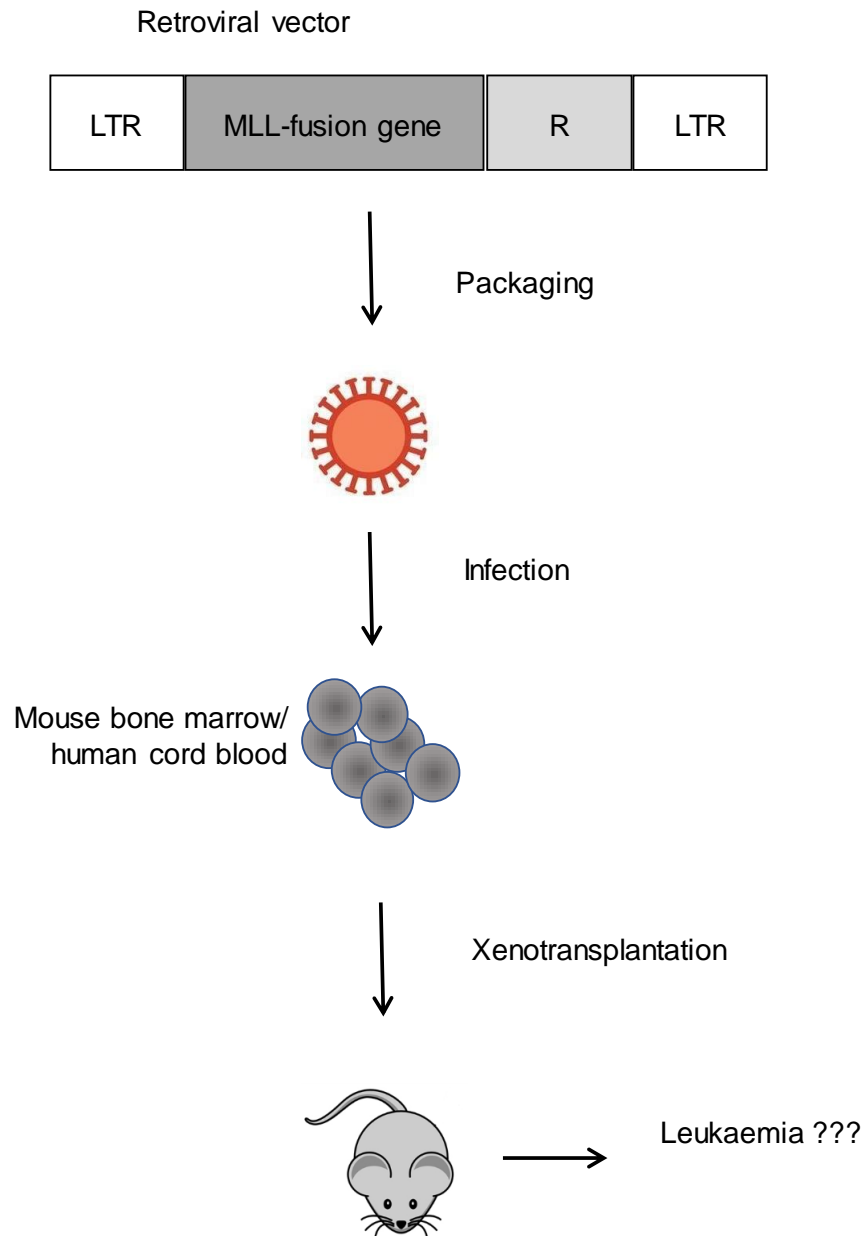


**Figure 7 Retroviral transduction in vivo model**

The diagram illustrates a schematic strategy for transduction of human or murine cells. Retroviral transduction approach can be used to generate constitutive and conditional expression models. Murine bone marrow cells or human cord blood cells are transduced with a retroviral vector. Then transduced cells are transplanted into recipient mice. LTR: long terminal repeat, R: gene providing antibiotic resistance [adapted from (Eguchi et al., 2003)].

### 1.13 MLL target genes

In a chromatin immunoprecipitation (ChIP) experiment followed by microarray analysis (ChIP-on-chip) MLL was found associated with promoters of about 5,000 genes. Also, MLL was localised to about the 90% of transcriptional start sites occupied by RNA pol II and in genomic areas enriched with H3K4 methylation (Guenther et al., 2005). These data suggest that MLL is a global regulator of transcription. In this same study MLL was found to bind the *HOXA* cluster of genes. However, these findings were contradicted by another study showing that MLL was responsible for H3K4 methylation at less than 5% of promoters characterised by H3K4me3, suggesting that MLL regulates a much smaller subset of target genes (Wang et al., 2009).

The *HOX* genes are transcription factors involved in the control of development and haematopoietic differentiation [reviewed in (Slany, 2009)]. *HOX* genes were first identified in *Drosophila melanogaster* where they are required to specify body segmentation. The *homeobox* genes are clustered in the two complexes of *Bithorax* (*BX-C*) and *Antennapedia* (*ANT-C*), which together are part of a larger complex called *homeotic complex* (*HOM-C*) [reviewed in (Hess, 2004)]. In vertebrates, *HOX* genes are grouped in four clusters (*HOXA*, *HOXB*, *HOXC* and *HOXD*) on four human chromosomes: 7, 17, 12 and 2. Each cluster contains 9 to 11 *HOX* genes [reviewed in (Thorsteinsdottir et al., 1997)]. *HOX* gene expression correlates with their chromosome location (figure 8). The genes located at the 3' end of each cluster are activated earlier than genes occupying the 5' end of each cluster, these genes are characterised by later expression

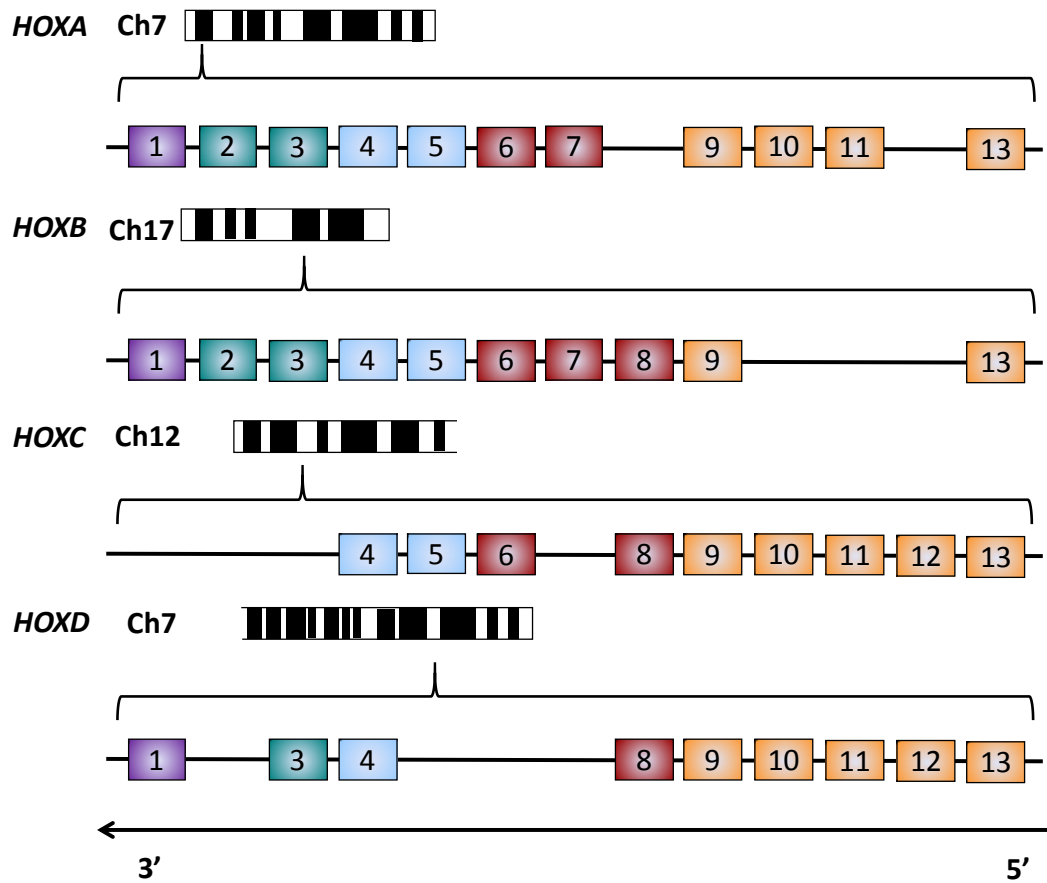


**Figure 8 Mammalian *HOX* cluster genes**

The diagram illustrates the organization of the human *HOX* genes. The *HOX* genes are grouped in four clusters: A, B, C and D on four human chromosomes (Ch7, Ch17, Ch12, Ch2). The *HOX* genes expression correlates with their location on each chromosome, in order from 3' end to the 5' end. (adapted from Shah and Sukumar, 2010).

[reviewed in (Thorsteinsdottir et al., 1997)]. The *HOX* genes are the best characterised MLL target genes. *HOX* genes need to be correctly regulated during normal haematopoiesis to allow normal cell maturation. *HOX* genes dysregulation causes a block in the normal haematopoietic development causing leukaemia onset. *MLL* knockout studies showed that the *MLL* knock-out has an impact on embryos development and a crucial role in regulation of *HOX* gene expression [reviewed in (Krivtsov and Armstrong, 2007)] (Hess et al., 1997, Yagi et al., 1998).

Another well-known MLL target gene is the myeloid ecotropic viral integration site1 (*Meis1*), encoding a homeodomain transcription factor. *MEIS1* is a co-factor of *HOXA* family members and, exactly like for *HOX* genes, its regulation is crucial during normal haematopoiesis. *MEIS1* and *HOX* constitutive overexpression is an essential step in leukaemic transformation. *MLL* fusion genes are not able to transform foetal liver cells derived from *Meis1*<sup>-/-</sup> mice, suggesting that *MEIS1* is essential to induce and maintain transformation mediated by *MLL* (Wong et al., 2007). It has been demonstrated that *Meis1* is essential in vitro and in vivo to maintain growth and survival of leukaemic cells (Kumar et al., 2009).

Further studies showed that *c-MYB* is one of the downstream targets of *HOXA9* and *MEIS1* (Hess et al., 2006). *c-MYB* is a transcription factor playing a key role in haematopoietic proliferation and differentiation (Zhou and Ness, 2013). Hess showed that *c-MYB* is highly expressed in immature haematopoietic cells and its expression needs to be down-regulated during terminal differentiation,

exactly like for *HOXA9* and *MEIS1* (Hess et al., 2006). Although this study suggests that MYB acts downstream of *HOXA9* and *MEIS1*, another study from Lowe's laboratory showed that MLL-AF9 enforces a c-MYB program contributing to leukaemia maintenance (Zuber et al., 2011). This study shows that MLL-AF9 binds the promoter region of canonical targets, such as *HOXA9* and *MEIS1*, but also to promoters of transcription factors like MYB which is required for leukaemia maintenance. Furthermore, the suppression of MYB eradicated AML *in vivo* (Zuber et al., 2011). Few mutations can convert c-MYB into a transforming protein that is able to regulate a completely different set of target genes (Liu et al., 2006). In a subset of paediatric T-cell acute lymphoblastic leukaemia (T-ALL) Mansour *et al.* identified mutations, in non-coding genomic sites, which introduce c-MYB binding sites with consequent generation of a super enhancer activating the *TAL1* oncogene (Mansour et al., 2014). Mutations involving the c-MYB locus are less frequent in AML, however a rare c-MYB-GATA1 fusion oncogene has been described (Belloni et al., 2011) (Quelen et al., 2011) and gain in *MYB* locus in an uncommon AML harbouring the MYST3-translocation (Murati et al., 2009).

## 1.14 Models of oncoprotein degradation

Although recently targeted therapies have brought significant improvements in cancer treatment, only a few such therapies have offered a definitive cure for patients.

An example of targeted therapy is the inhibition of the chromosomal translocation found in patients with chronic myeloid leukaemia (CML). The disease is characterised by the presence of the Philadelphia chromosome which is the result of a balanced chromosome translocation involving chromosomes 9 and 22, t(9;22). The translocation generates the *BCR-ABL* fusion gene, on chromosome 22, which is essential and sufficient for CML [reviewed in (Salesse and Verfaillie, 2002)]. The reciprocal fusion *ABL-BCR* on chromosome 9 is transcriptionally active but it has not been linked to CML [reviewed in (Salesse and Verfaillie, 2002)]. The first line treatment for patient in chronic phase (CML-CP) is inhibition of BCR-ABL tyrosine kinase activity using imatinib [reviewed in (Shami and Deininger, 2012)]. Patients need to continuously inhibit the kinase activity to achieve complete remission. However, some patients are intolerant or resistant to imatinib and therefore they have high risk of disease progression into the acute phase, also known as blast phase (CML-BP) or blast crisis, which resemble acute leukaemia [reviewed in (Shami and Deininger, 2012)]. Although second generation inhibitors have been developed, many patients still develop resistance.

A new and more effective targeted therapy is to target oncoproteins to induce their proteasome dependent degradation, a process which is one of the major

cell regulatory mechanisms. This approach was discovered accidentally by analysing the effects of arsenic trioxide and retinoic acid in acute promyelocytic leukaemia (APL). More than 95% of acute promyelocytic leukaemia cases are the result of the t(15;17) translocation and this is often the only genetic abnormality detected [reviewed in (de The and Chen, 2010)]. The translocation event fuses the promyelocytic leukaemia (*PML*) gene with the retinoic acid receptor (*RAR $\alpha$* ) gene and it generates the PML/*RAR $\alpha$*  fusion protein [reviewed in (Ablain and de The, 2011)]. The fusion retains all functional domains of both PML and *RAR $\alpha$*  proteins. The fusion proteins induce a block in differentiation at the promyelocyte stage and confer self-renewal and growth properties to leukaemic cells [reviewed in (Ablain and de The, 2011)]. Arsenic trioxide and retinoic acid target different moieties of the fusion protein resulting in its complete degradation and in differentiation of APL blasts into granulocytes [reviewed in (Ablain et al., 2011, de The and Chen, 2010)]. PML and *RAR $\alpha$*  degradation is generally proteasome dependent although autophagy and SUMOylation have also been implicated [reviewed in (Lallemant-Breitenbach and de Thé, 2010)]. The PML-*RAR $\alpha$*  degradation is not the consequence of leukaemic blast differentiation but the primary cause of disease eradication [reviewed in (Ablain and de The, 2011)].

A previous study from our lab showed that the inactivation of MLL-fusion proteins, in immortalised myeloid cells with conditional expression of MLL-ENL, resulted in inhibition of cell self-renewal. The ablation of MLL-ENL resulted also in a complete regression of the disease *in vitro* and *in vivo* (Horton et al., 2009). More recently, Mangolini et al showed that TEL-AML1 knock down, via shRNA,

in human leukaemic cell lines impaired the cells ability to form colonies in methylcellulose assays (Mangolini et al., 2013). Fuka and colleagues provided further evidence of the driving role of TEL-AML1 in leukaemia development and maintenance by silencing its expression *in vitro* and *in vivo* (Fuka et al., 2012).

Leukaemic fusion genes, upon translation, generate fusion proteins which play a central role in the initiation and maintenance of acute leukaemias. All these studies proved that the inactivation of driver oncoproteins results in the inhibition of cell self-renewal, in a delayed disease progression or in a complete eradication of leukaemia. Therefore this suggests that targeting the leukaemic fusion proteins would be an effective approach to combat the associated leukaemia.

## 1.15 Drug discovery versus drug repositioning

“Drug research, as we know it today, began its career when chemistry had reached a degree of maturity that allowed its principles and methods to be applied to problems outside of chemistry itself and when pharmacology had become a well-defined scientific discipline in its own right” [reviewed in (Drews, 2000)].

In the early days of pharmaceutical development, the discovery of drugs to treat human diseases was based on the use of natural compounds isolated from plants or micro-organisms. In the following centuries these natural compounds, led to the development of new agents. In 1815 Sertuner isolated morphine from opium extracts [reviewed in (Drews, 2000)]. In most cases, happy coincidences and serendipitous examinations promoted the discovery of treatments. In 1929, Alexander Fleming was studying the properties of staphylococci when luckily in a culture contaminated with a fungus he discovered bactericidal activity. That mould was the well-known penicillium, which produces the antibiotic penicillin. The clarification of penicillin structure paved the way for the discovery of new antibiotics with similar chemical structures [reviewed in (Drews, 2000)]. Only later in the century, with progress in pharmacology and development of new technologies, has the process of drug discovery become more scientific. Advances in genomic engineering facilitated the replacement of natural proteins with their recombinant versions. In 1982, the first product of DNA recombinant technology was described: humulin, recombinant human insulin [reviewed in

(Drews, 2000, Drews and Ryser, 1997)]. Nowadays, all the advances in science and computational biology allowed the development of high-throughput screening (HTS). In automated HTS, large libraries containing a large number of compounds are tested on a large number of targets.

Drug discovery is still a complicated, expensive and time-consuming process with a very low success rate. On average, it takes a minimum of fifteen years to develop a new drug from the early stages of discovery to when it is available for patients (Ashburn and Thor, 2004). One approach that could possibly speed up this process is called “*Drug Repositioning*” or “*Drug Redeployment*”. Drug repositioning is the process of testing existing or abandoned drugs for their efficacy in treating diseases other than the one for which they were originally used (Sardana et al., 2011). This strategy offers the chance to bypass the traditional drug discovery process (figure 9) and also to reduce development risks. In fact, these compounds have already passed through several stages of preclinical testing. Thus, toxicology, pharmacokinetic profiles and safety of the candidates are well known and in most cases the compounds are already FDA-approved (Ashburn and Thor, 2004). Identification of candidate drugs can come from serendipitous observations, from novel insights of human biology or high throughput screening. In the last few years, researchers and pharma industries have been actively attempting to transform the accidental event into a rational research of repositioning opportunities.

An active area in drug repositioning is the identification of drugs for orphan/rare diseases (Ekins et al., 2011). Orphan diseases affect a small percentage of the

population (Sardana et al., 2011). The European Commission on Public Health defined rare the diseases affecting 1 in 2000 people. There are 7,000-8,000 known rare diseases and big pharma companies usually do not invest in research for their treatment due to the high cost of research and limited market (Muthyala, 2011). This makes these diseases especially appropriate for drug repositioning. One of the most common strategies for orphan drug discovery is based on high-throughput screening (Muthyala, 2011).

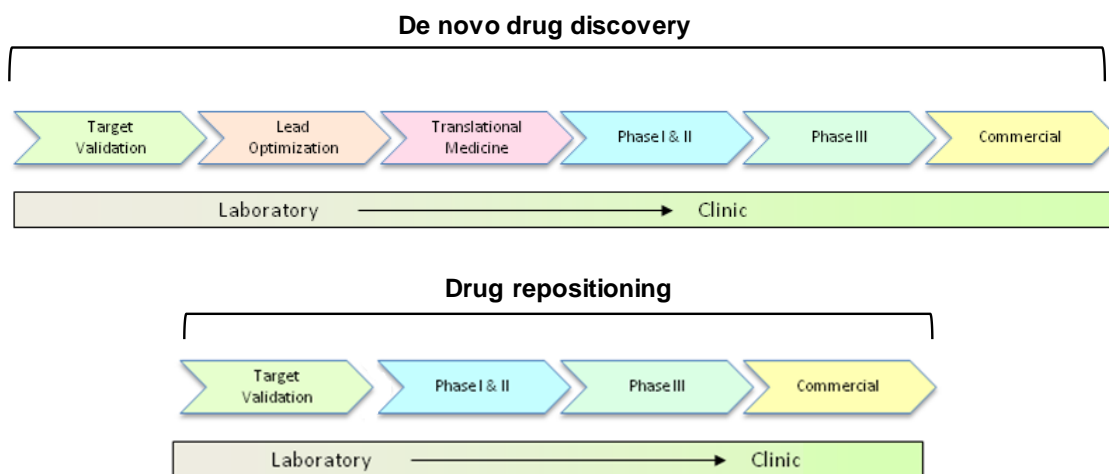


**Figure 9 *De novo* drug discovery versus drug repositioning**

The *de novo* drug discovery timeline (upper panel) is compared to the drug repositioning timeline (lower panel). The first involves in average of 15-20 years while the repositioning approach reduce the developing time (adapted from Ashburn and Thor, 2004).

## 1.16 High/Medium throughput screening

Advances in bioinformatics, genomics, the sequencing of human genome and of various pathogens, increased extremely the number of biological targets of therapeutic interest. The increased number of compounds to test and the optimisation of nanotechnologies led to the adoption of High-Throughput Screenings (HTS). Automated HTS is a well-established process used for years in the discovery process. The technique allows completion of millions of chemical, genetic or pharmacologic tests against biological targets thanks to the help of automated-friendly robots (Broach and Thorner, 1996). HTS provides high quality data and the results are generally a starting point for drug design. It requires testing thousands of natural and synthetic compounds against a biological target using a quantitative bioassay. The aim is to identify high quality “hits”, in other words compounds with activity in that particular bioassay. Early HTS were based on absorbance measurements, while more recently the most common assays are luminescence or fluorescence based (Boisclair et al., 2004). However, it is clear that all HTS need a counter-screen to avoid false positive or negative hits. Also, in order to confirm positive hits, orthogonal methodologies have become necessary for “hit validation”. Hit validation is necessary in order to provide the best possible hit selection (Macarron et al., 2011, Mayr and Bojanic, 2009).

## PROJECT AIM

The MLL-fusion proteins play a central role in initiation and maintenance of *MLL* rearranged acute leukaemia. These fusions are usually associated with very poor clinical outcomes. Recent studies impressively achieved leukaemia eradication by blocking the driver fusion gene (Ablain and de The, 2011) (Horton et al., 2009) (Shami and Deininger, 2012). Therefore, a potential cure for *MLL* rearranged leukaemia patients could be the inactivation of the MLL-fusion proteins. The aim of this PhD project is to develop an approach of medium throughput screening (MTS), based on a dual luciferase assay, in order to identify clinically approved compounds destabilising MLL-fusion proteins. Such screening requires the generation of an indicator MLL-fusion gene cell line, in this case a cell line overexpressing a luciferase tagged MLL-fusion gene. Therefore my objectives were:

- 1) To validate the indicator MLL-fusion gene cell line and perform the medium throughput screening.
- 2) To identify and validate the positive hits on a panel of human MLL rearranged cell lines.
- 3) To investigate the mechanisms of action of the selected compounds.

## 2 CHAPTER II: MATERIALS & METHODS

### 2.1 Molecular Biology

#### 2.1.1 DNA constructs

Dr. Jasper de Boer generated the luciferase reporters used to produce the leukaemic indicator cell line. Using a PCR-based cloning approach, MLL-AF9 was fused to a firefly luciferase. Then the MLL-AF9-firefly luciferase was cloned into a pMSCVneo retroviral vector. Using the same strategy Dr. de Boer generated also the vector carrying the renilla luciferase (figure 10).

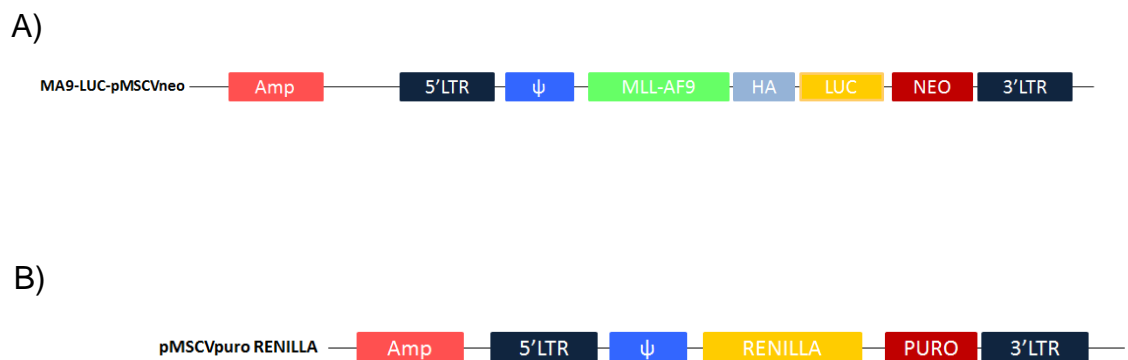


**Figure 10 Retroviral vectors**

Retroviral vectors used to generate the AML indicator leukaemic cell line. (A) Retroviral vector expressing MLL-AF9 fused to the firefly luciferase (MA9-LUC-pMSCVneo). (B) Retroviral vector expressing the renilla luciferase (pMSCVpuro-RENILLA).

### **2.1.2 Preparation of total protein lysate for western blot analysis**

Cells were harvested, washed with PBS and centrifuged at 300g for 5 minutes at 4°C. Cell pellets were lysed using 60µL of 2x Sample Reducing Buffer (200mM DTT, 2% sodium dodecyl sulphate (SDS), 10% v/v Glycerol, 0.02% v/v Bromophenol Blue, 125 mM TrisHCl pH6.8) per  $0.5 \times 10^6$  cells. The lysate was incubated for 5 minutes at 100°C, vortexed for 10 seconds and centrifuged at 13,200rpm for 10 minutes at 4°C. The supernatant containing the protein extract was recovered and frozen at -20°C. In order to denature proteins before loading, samples were incubated newly at 100°C for 5 minutes and kept on ice until loading.

### **2.1.3 Western Blot analysis**

Protein electrophoresis was performed using the SE 400 Vertical Unit (Amersham Biosciences), the OmniPAGE (Clever Scientific) and the Bio-rad Mini- PROTEAN Tetra handcast systems. Protein samples were stacked in a 4% Bis-Tris-polyacrylamide gel and resolved on 7% Bis-Tris-polyacrylamide (Table 4). Page Ruler Protein Ladder plus molecular weight marker and protein samples were subjected to electrophoresis at 120V at room temperature for 2-2.5 hours. SDS-PAGE was performed in presence of 1x Running buffer diluted from the 20x Running Buffer (Tris, MOPS, 0.5M EDTA, 20% SDS). Samples were then transferred onto a nitrocellulose membrane (LI-COR Biosystems) for 3 hours at 400mA at 4°C in transfer buffer (CAPS).

### Components of 4% stacking gel

Reagent	Volume
1.25M Bis-Tris (pH 6.8)	4.3 ml
30% Acrylamide	2 ml
Water	8.9 ml
10%APS	150 $\mu$ l
Temed	20 $\mu$ l

### Components of 7% resolving gel

Reagent	Volume
1.25M Bis-Tris (pH 6.8)	11.4 ml
30% Acrylamide	9.34 ml
Water	19.06 ml
10%APS	400 $\mu$ l
Temed	20 $\mu$ l

**Table 4 Components of a 4% Stacking and 7% Resolving gels**

After, membranes were blocked in PBS with 5% non-fat milk and 0.1% Tween-20 (Sigma) (PBS-T) for 1 hour at room temperature, and incubated over night with one of the primaries antibodies listed in Table 5. Excess of antibody was removed by washing membranes three times with PBS-T for 10 minutes each. Finally, proteins were detected using one of the secondary antibodies listed in Table 5. If secondary antibodies horseradish peroxidase conjugated (GE healthcare) and a chemoluminescence reagent (ECL, Biorad) were used, membranes were exposed to a film (Amersham, GE Healthcare). The film was next developed using the Xograph Compact X4 developer. In this case a densitometer (GS-800, BioRad) was used to scan the developed film and bands were quantified using the Quantity One software (Biorad). Some membranes were instead imaged using Odyssey CLX imaging system (LI-COR Biosystems). The bands were quantified using Image Studio, which is the manufacturer's software. The intensities of the bands were normalised first to the intensity of the housekeeping gene and then to the control sample in the specific experiment. In some experiments membranes were stripped using Restore™ Western Blot Stripping Buffer (ThermoFisher Scientific, Loughborough, UK) for 10 minutes at room temperature and re-probed with different primary and secondary antibodies.

### Primary antibodies

Name of antibodies	Dilution	Supplier
MLL <sup>N</sup> /HRX clone N4.4 mouse monoclonal	1:5000	Millipore
Clathrin HC clone TD.1 mouse monoclonal	1:2000	Santa Cruz
Actin clone I-19	1:2000	Santa Cruz
Vinculin clone EPR8185	1:10000	Abcam

### Secondary antibodies

Name of antibodies	Dilution	Supplier
Anti-mouse IgG HRP-linked whole antibody	1:5000	Biorad
Anti-rat HRP-linked whole antibody	1:5000	GE Healthcare
Anti-rabbit HRP-linked whole antibody	1:5000	Biorad
Anti- goat HRP-linked whole antibody	1:5000	Invitrogen
Anti- mouse IRDye800CW	1:10000	LI-COR
Anti- rabbit IRDye680RD	1:10000	LI-COR

**Table 5 List of primary and secondary antibodies used in western blot analysis**

#### **2.1.4 RNA isolation**

Total RNA was isolated from the cells using the RNeasy Mini Kit (Qiagen) according to the manufacturer's instructions. The cells were disrupted by adding lysis buffer RLT, containing  $\beta$ -mercaptoethanol. To ensure complete homogenization, samples were vortexed for 30 seconds at the highest settings. One volume of 70% ethanol was added to the samples and the mixture transferred into an RNeasy spin column. Columns were centrifuged for 15 seconds at 10,000xg and the flow-through was discarded. 700 $\mu$ l of wash buffer RW1 were added to the column followed by centrifugation. Samples were then washed twice with 500  $\mu$ l of wash buffer RPE. The RNA was eluted with 30 $\mu$ l of nuclease free water and the concentration determined using a spectrophotometer (NanoDrop ND-1000, Lebttech International). The ratio of absorbance at 260 nm to 280 nm was used to assess the purity of RNA. A ratio of  $\sim$ 2.0 is accepted as pure for RNA (NanoDrop user's manual).

#### **2.1.5 cDNA preparation**

RNA was converted into cDNA using the High Capacity RNA-to-cDNA kit (Applied Biosystems) according to the manufacturer's instructions. 1 $\mu$ g or 500ng of RNA was converted using 1 $\mu$ l of 20x enzyme mix, 10 $\mu$ l of 2x RT Buffer Mix in a total volume of 10 $\mu$ l, made up with water.

## 2.1.6 Quantitative real-time PCR

Quantitative Reverse Transcription PCR (qRT-PCR) was performed on isolated mRNA using TaqMan probe based chemistry. SensiFAST™ Probe Hi-Rox mastermix (BIOLINE) was used according to manufacturer's instruction in a StepOnePlus Real-Time PCR System (Applied Biosystems). All probes were from Applied Biosystems (Table 6). In all measurements *18s* was used as housekeeping gene. Quantitative RT-PCR was also performed on immunoprecipitated chromatin using Sybr-green technology, SensiFAST™ SYBR Hi-Rox mastermix (BIOLINE). Various forward and reverse primer concentrations were tested, to determine the optimal primer concentration for measuring MLL enrichment in CHIP experiments. All primer sets and optimal concentrations are listed in Table 7.

### TaqMan Probes

Gene	Product Id	Concentration
<i>HOXA10</i>	Hs_00172012_m1	Optimised by manufacturer
<i>18s</i>	Hs_99999901_s1	Optimised by manufacturer
<i>c-MYB</i>	Hs_00920556_m1	Optimised by manufacturer
<i>MEIS1</i>	Hs_01017441_m1	Optimised by manufacturer

**Table 6** List of all TaqMan probes used

### Sybr-green Primer set

<b>Gene</b>	<b>Sequence</b>	<b>Concentration</b>
<i>HoxA10</i> Fw	5'-ACCGCAGGATGAAACTGAAG-3'	400nM
<i>HoxA10</i> Rw	5'-TTCCCCCAGAAAACAACAAA-3'	400nM
<i>Gene Desert 21</i> Fw	5'-GGGGGATCAGATGACAGTAAA-3'	100nM
<i>Gene Desert 21</i> Rw	5'AATGCCAGCATGGGAAATA-3'	100nM

**Table 7 List of all primer sets**

## **2.2 Cell Biology**

### **2.2.1 Cell culture and cell lines**

Human leukaemic cell lines (Table 8) were obtained from the German Collection of Microorganisms and Cell Cultures (DSMZ, Brunswick, Germany). The identity of human leukaemic cell lines was confirmed by STR profiling in the GOSH Haematology department. All human leukaemic cell lines, with the exception of SHI-1, were cultured in Roswell Park Memorial Institute (RPMI) medium (Sigma-Aldrich), supplemented with 10% or 20% heat-inactivated Foetal Calf Serum (FCS) (Sigma-Aldrich, Dorset, UK), 100U/ml Penicillin (Sigma-Aldrich), 100µg/ml Streptomycin (Sigma-Aldrich) and 2mM L-glutamine (Sigma-Aldrich) (complete RPMI). SHI-1 cells were cultured in Iscove's Modified Dulbecco's Medium (IMDM, Sigma-Aldrich) supplemented with 20% heat-inactivated FCS, 100U/ml Penicillin (Sigma-Aldrich), 100µg/ml Streptomycin (Sigma-Aldrich) and 2mM L-glutamine (Sigma-Aldrich)(complete IMDM). Each cell line was sub-cultured every 3-4 days and plated according to supplier's guidelines (DSMZ).

### Human Leukaemic Cell Line

Cell line	Translocation	Fusion gene
THP-1	t(9;11)	MLL-AF9
SHI-1	t(6;11)	MLL-AF6
MV4-11	t(4;11)	MLL-AF4
OCIAML3	N.A.	NPM1 mutation
KASUMI1	t(8;21)	AML1-ETO

**Table 8 List of all Human Leukaemic cell lines used in this study**

The list shows the panel of human leukaemic cells lines used in the study. Most of the cell lines used were purchased from the DSMZ, the German Resource Centre for Biological Material.

N.A. Not applicable

### **2.2.2 Flow cytometry**

Cells were washed in PBS once and then were stained in FACS buffer (PBS supplemented with 0.05% w/v sodium azide and 1% w/v BSA). Following the staining the cells were washed using FACS buffer and re-suspended in 200µl of FACS buffer prior the analysis. Flow cytometry was performed on LSRII analyser (BD Bioscience), CyAN ADP analyser (Beckman Coulter), FACS Array (SORP) (BD Bioscience).

### **2.2.3 Apoptosis**

Apoptosis was detected using the Annexin V Apoptosis Detection Kit APC (eBioscience) combined with Propidium Iodide (PI) staining. Annexin-V is a protein that binds phosphatidylserine, a cell membrane component. Usually phosphatidylserine face the cytosolic side of cellular membranes but when cells undergo apoptosis it is flipped and exposed on the outer surface of membranes. In this case phosphatidylserine can bind annexin-V which usually is conjugated with fluorochromes detectable in flow cytometry. The phosphatidylserine can be exposed also during necrosis because of the loss of integrity of cell membranes. Propidium iodide (PI) is a red fluorescent DNA intercalating agent. Since PI cannot cross membranes of living cells it is commonly used to detect death cells by flow cytometry. Cells were washed first in PBS and then in 1X Annexin V Binding Buffer. After centrifugation the cell pellet was re-suspended in 95µl of 1X Binding Buffer and 5µl of Annexin V-APC. Cells were incubated for 15minutes in the dark and then were washed with 1X Binding Buffer. The

mixture was re-suspended in 195µl of 1X Binding Buffer and 5µl of Propidium Iodide (PI). Cells were analysed by flow cytometry.

### **2.2.4 Colony forming assays**

For human cells,  $1 \times 10^4$  cells were washed in PBS and re-suspended in 600µl of cell resuspension solution (HSC002, R&D system). The cells were added to 2.7 ml of human methylcellulose (R&D system) in presence of DMSO or different concentrations of Disulfiram. 600µl of this mixture was plated into 24 multi-well plates using blunt end needles. Cells were cultured for two weeks before being cultured for 2 extra days in presence of 180µl of 10mg/ml 2-(P-iodophenyl)-3-(p-nitrophenyl)-5-phenyl tetrazolium chloride (INT) in 75% ethanol, diluted 1:20 with PBS. The plate was finally acquired using a calibrated densitometer (GS-800, BioRad) and the colonies were quantified using ImageQuant TL software (GE Healthcare).

For cord blood cells,  $3 \times 10^4$  CD34<sup>+</sup> cells were re-suspended in 300µl cell resuspension solution (HSC008 R&D systems). The cells were added to 3ml of human methylcellulose in presence of DMSO or Disulfiram. 1.5ml of the mixture was plated into 3cm plates using blunt end needles. Cells were cultured for two weeks before being cultured for 2 extra days in presence of 180µl of INT and acquired using the densitometer.

### **2.2.5 Isolation of human CD34<sup>+</sup>CB cells**

Human cord blood CD34<sup>+</sup> cells were purified by magnetic activated cells sorting (MACS) (Miltenyi Biotec, Surrey, UK) using the human CD34 microbead kit,

according to manufacturer's protocol. Purified CD34<sup>+</sup> cells were cultured in human methylcellulose with or without disulfiram and copper.

## **2.2.6 Luciferase assays and dual luciferase assays**

To measure firefly luciferase signal expressed by the cells, the Luciferase Assay System (Promega) was used according to manufacturer's instructions.  $1 \times 10^3$  cells were plated in a white 96-multiwell plate (Non-TC treated, Greiner Bio One) and washed with PBS. After a centrifugation step, cell pellets were re-suspended in 20 $\mu$ l of 1X Passive Lysis Buffer and incubated for 15 minutes at room temperature on a shaker. Then 100 $\mu$ l of Luciferase Buffer was injected into each well by the injector of the luminometer Infinite 200 PRO plate reader (TECAN). Levels of luciferase signals were recorded in each well.

To measure simultaneously firefly and renilla luciferase signals we used non-commercial reagents.  $1 \times 10^3$  cells were plated in a white 96-multiwell plate (Non-TC treated, Greiner Bio One) and washed with PBS. As previously described, following centrifugation cells were re-suspended in 20 $\mu$ l of 1X Passive Lysis Buffer (Promega) and incubated for 15 minutes at room temperature on a shaker. 100 $\mu$ l of luciferase buffer (20mM Tricine, 2.67mM MgSO<sub>4</sub>, 0.1mM EDTA, 33.3mM DTT, 270 $\mu$ M co-enzyme A, 470 $\mu$ M d-luciferin, 530  $\mu$ M ATP, pH 7.8) were injected into each well and the firefly luciferase activity was measured. Next, 100 $\mu$ l of renilla buffer (220mM K<sub>3</sub>PO<sub>4</sub>, 1.1M NaCl, 2.2mM EDTA, 0.44g/l BSA, 1.3mM NaN<sub>3</sub>, 1.43 $\mu$ M coelenterazine) were dispensed into each well and the renilla luciferase activity was measured. Firefly luciferase

activity was divided by the renilla luciferase activity and the final value was normalised to the control sample.

### **2.3 Animal work**

All mice were maintained in the animal facilities of the UCL Institute of Child Health and the experiments were performed according to United Kingdom Home Office regulations. All xenotransplantations in this study were performed by Dr. Owen Williams on 5-12 week old NOD.Cg-Prkdc<sup>scid</sup>Il2rg<sup>tm1Wjl</sup>/SzJ (NSG) mice. NSG mice lack mature T cells, B cells and natural killer (NK) cells and are deficient in multiple cytokine signalling pathways, they have multiple defects in innate immunity. Mice were intravenously injected in the tail vein with  $1 \times 10^6$  Maha cells [murine AML (MLL-AF9)] or with  $1 \times 10^6$  of primary human AML (MLL-AF9).

### **2.4 RNA-sequencing**

Total RNA was extracted using the RNeasy Plus Mini Kit (Qiagen) according to manufacturer's instructions. For each sample, RNA integrity was verified using the Bioanalyzer 2100 (Agilent Technologies, Santa Clara, CA) prior to proceeding with amplification. All samples were submitted to UCL Genomics for RNA-seq and processed using an Illumina TruSeq RNA sample prep kit Version2 (p/n RS-122-2001) according to manufacturer's instructions (Illumina, Cambridge, UK). mRNA was first selected using paramagnetic dT beads and fragmented by metal hydrolysis to approximately 150bp lengths. Random primed cDNA was generated and ligated to adapters compatible with Illumina

sequencing and then amplified by 14 cycles of PCR. Libraries generated were quantified, normalised and then pooled prior to sequencing on the Illumina NextSeq 500 (Illumina). In order to detect differences in gene expression we sequenced 20 million reads per sample. The sequencing results were analysed by using the RNA express workflow on the Illumina BaseSpace (Illumina) website. The STAR aligner allowed first the alignment of the sequencing reads to the human genome (GRCh38) and then the mapping to genes. Then DESeq2 evaluated the differentially expressed genes between our treated and untreated samples. The list of differentially expressed genes was then compared to MLL-AF9 and MLL-AF4 gene sets (Bernt et al., 2011; Guenther et al., 2008) using the Gene Set Enrichment Analysis (GSEA) software from Broad Institute. RNAseq data were also compared to MLL-AF9 signature (Walf-Vorderwulbecke *et al.*, 2017), and to gene sets obtained from 93 AML patients (Mullighan *et al.*, 2007) and from a leukaemic stem cell signature (Sommerville *et al.*, 2009). A positive enrichment score shows correlation between data sets while negative enrichment score confirm anti-correlation.

## **2.5 CHIP-sequencing**

To improve formation of covalent links between proteins and DNA cells were fixed using two cross-linking agents.  $25 \times 10^6$  THP-1 cells were re-suspended in 20ml PBS and cross-linked with disuccinimidyl glutarate (DSG) to a final concentration of 2mM for 30 minutes at room temperature (RT) on rotating wheel. Cell pellets were washed three times in PBS, cross-linked with 1% formaldehyde for 15 minutes at RT on rotating wheel and quenched with

0.125M glycine for 5 minutes at RT. The MLL chromatin immunoprecipitation required this two-step cross-link. The histones chromatin immunoprecipitation required the one step fixation with formaldehyde. Cell pellet were incubated on rotating wheel at 4°C first in 0.25% Triton X 100, 10mM EDTA, 0.5mMEGTA, 20mM HEPES pH 7.6 (Buffer A) for 10 minutes and then in 150mM NaCl, 10mMEDTA, 0.5mM EGTA, 20mM HEPES pH 7.6 (Buffer B) for 10 minutes. Cells were suspended in ChIP incubation buffer (0.15% SDS, 1% Triton X 100, 150mM NaCl, 10mM EDTA, 0.5mM EGTA, 20mM HEPES pH 7.6) supplemented with protease inhibitors and incubated for 30 minutes on ice before sonication. Double fixed cells were sonicated using a Bioruptor sonicator (Diagenode) for 13 cycles, 30 seconds ON and 30 seconds OFF for each cycle while cells crosslinked with formaldehyde only were sonicated for 6 cycles, 30 seconds ON and 30 seconds OFF for each cycle. Sonicated chromatin was centrifuged at maximum speed for 10 minutes and supernatant was stored at -80°C. In order to check the quality of sonication 30µl of sonicated chromatin were reverse cross-linked over-night (O/N) at 65°C. Chromatin was incubated first at 37°C for 30 minutes with 1µl of RNase A/T mix and then at 55°C for 2hours with 2µl 0.5M EDTA pH 8.0, 4µl Tris HCl pH 6.5, 1µl proteinase K. Reverse cross-linked chromatin was run on a 1.5% agarose gel. Once quality of sonicated chromatin was assessed, three aliquotes of chromatin (900µl) were diluted 1:10 in incubation buffer supplemented with 0.1% BSA, protease inhibitor cocktail (Sigma, Aldrich), 30µl of protein A beads and 3µg of antibody. In table 9 are listed all the antibodies tested. The mixture was incubated overnight at 4°C on rotating wheel. Beads were washed sequentially with four

different buffers at 4°C: twice with a solution 0.1% SDS, 0.1% sodium deoxycholate, 1% Triton X 100, 150mM NaCl, 10 mM Tris pH8, 0.1 mM EDTA, 0.5mM EGTA, one time in 0.1% SDS, 0.1% sodium deoxycholate, 1% Triton X 100, 500mM NaCl, 10 mM Tris pH8.0, 0.1 mM EDTA, 0.5mM EGTA, one time with a solution of 0.25M LiCl, 0.5% sodium deoxycholate, 0.5% NP40, 10mM Tris pH8.0, 0.1mM EDTA, 0.5mM EGTA and one time with 10mM Tris pH8.0, 0.1mM EDTA, 0.5mM EGTA. Chromatin was eluted from the beads with 400µl of elution buffer (1% SDS, 0.1M NaHCO<sub>3</sub>) at room temperature for 20 minutes. Protein-DNA cross-links were reversed at 65°C overnight in the presence of 200mM NaCl, after which the mixture was incubated first with 4µl of RNase A/T mix for 1 hour at 37°C and then with 0.5M EDTA pH8.0, 1M Tris HCl pH6.5, 40µg of proteinase K for 2 hours at 55°C. DNA was purified using the MinElute PCR purification kit (Qiagen) column and specific DNA regions supposed to be engaged with MLL or histons were analysed by quantitative PCR (q-PCR) using the sensiFAST SYBR Hi-ROX kit (Bioline) according to manufacturer instructions in the StepOnePlus™ Real-Time PCR system (Life Technologies). Purified DNA (2µl) was mixed with the sensiFAST SYBR Hi-ROX mastermix, nuclease free water and primers (Table 10). To evaluate primers efficiency, two primers concentrations were tested and a standard curve was generated from serial dilutions of input DNA (figure 11). The slope of the curve estimated the primers efficiency. Moreover, to evaluate PCR specificity and to detect presence of primer-dimers we analysed the melting curves generated. Presence of single peaks suggested specificity of the reaction (figure 12).

<b>Antibody</b>	<b>Manufacturer</b>	<b>Cat. number</b>
MLL-N	Bethyl	A300-086A
<b>MLL-N</b>	Diagenode	Ab1542-Ab1547
<b>H3K4me3</b>	Active Motif	39915
<b>H3K27ac</b>	Millipore	Ab4729

**Table 9 List of antibodies tested in CHIP assay**

In the table the antibodies in bold were the one optimised in CHIP experiments.

Gene	Sequence (5'-3')	Supplier
HoxA9 – 1FW	TGTACCACCACCATCACCAC	Sigma
HoxA9 – 1RW	TCCACCTTTCTCTCGACAGC	Sigma
HoxA9 – 2FW	GCGGTTCCAGGTTTAATGCCA	Sigma
HoxA9 – 2RW	TGTACCACCACCATCACCAC	Sigma
HoxA9 – P1 – FW	GAAGTTGGTGTGGGACGC	Sigma
HoxA9 – P1 – RW	AACGGCCCAAAGTATCTCGG	Sigma
HoxA9 – P2 – FW	TAAACCTGAACCGCTGTCGG	Sigma
HoxA9 – P2 – RW	GCCTTCGCTGGGTTGTTTT	Sigma
HoxA9 – P3 – FW	ACAAACCCCATCGTAGAGCG	Sigma
HoxA9 – P3 – RW	GCCCGTCCAGCAGAACAATA	Sigma
HoxA9 – FW	GGGAGACGGGAGAGTACAGA	Sigma
HoxA9 – RW	GCTCTACGATGGGGTTTGT	Sigma
<b>HoxA10 – FW</b>	<b>ACCGCAGGATGAAACTGAAG</b>	Sigma
<b>HoxA10 – RW</b>	<b>TTCCCCAGAAAACAACAAA</b>	Sigma
<b>GD21 – FW</b>	<b>GGGGGATCAGATGACAGTAAA</b>	Sigma
<b>GD21 – RW</b>	<b>AATGCCAGCATGGGAAATA</b>	Sigma
GD18 – FW	ACTCCCCTTTCATGCTTCTG	Sigma
GD18 – RW	AGGTCCCAGGACATATCCATT	Sigma
MYOG – FW	GGATTGAGTCTGCCAGG	Sigma
MYOG – RW	GATGGAAGGGCAGAGGTG	Sigma

**Table 10 List of all primers tested in this study for ChIP assays**

The primers in bold in the table were those used in the ChIP assay.

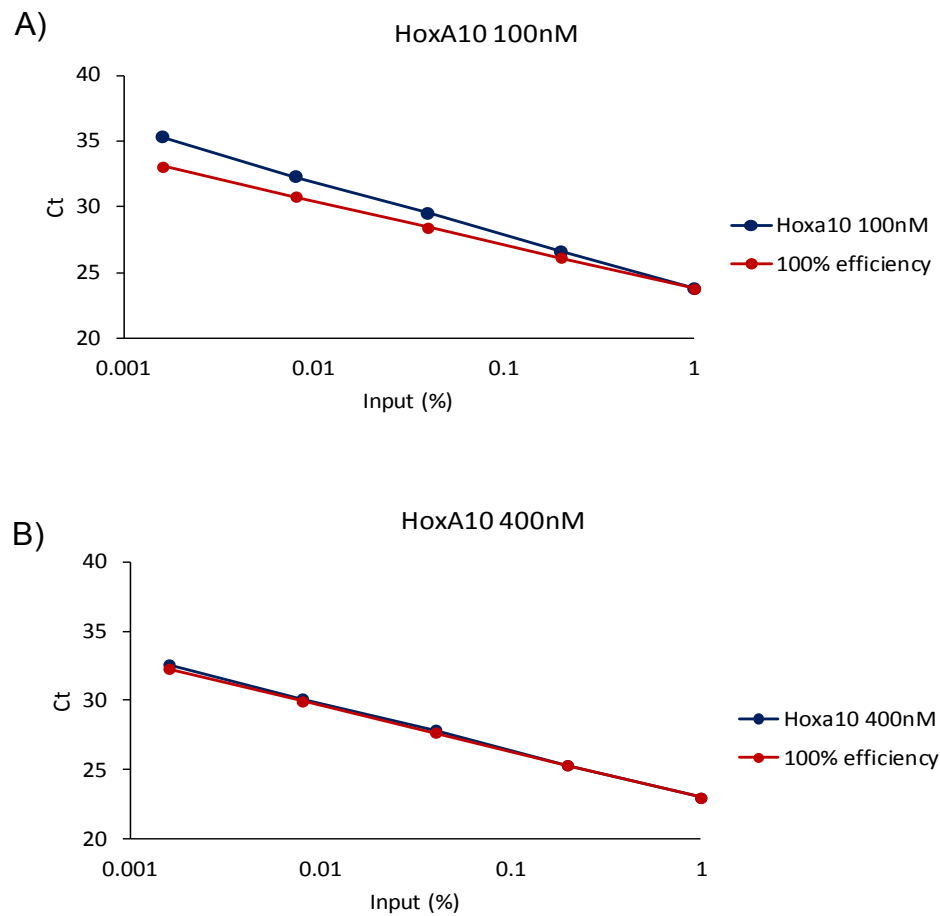


**Figure 11 Optimisation of HoxA10 primers used in ChIP assay**

The graphs are showing the standard curves generated for the optimisation of HoxA10 primers (A) (B). Two primers concentrations (100nM and 400nM) were tested on 5 fold serial dilutions of input DNA. Ct values were plotted against the percentage of input DNA. The slope of the standard curve estimated the efficiency of HoxA10 primers (blue line). The standard curves for both primers concentrations (blue line) were compared to the curve showing the 100% efficiency (red line) we were supposed to obtain in each reaction. Only the curve of the HoxA10 400nM primers was overlapping entirely the curve we could have obtained for a reaction 100% efficient. These data were obtained from a single experiment.

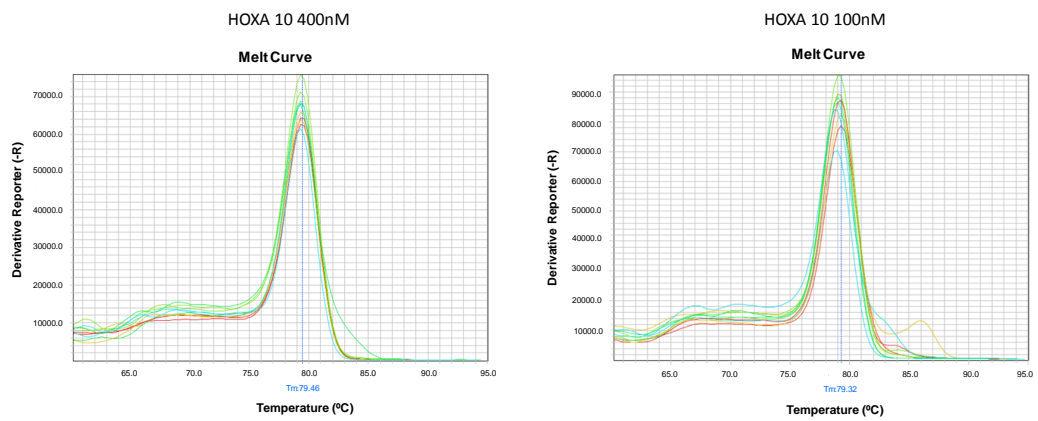


**Figure 12 Melting curves of primers used in ChIP assay**

The figure is showing melting curves generated for HoxA10 primers (400nM and 100nM). Q-PCR was performed on serial dilutions of input DNA. Detection of single peaks proved primers specificity. This experiment was executed only once but the melting curves were analysed after q-PCR in each ChIP assay.

### **3 CHAPTER III: Generation of cell lines expressing fusion genes, their validation and use in medium throughput screening**

#### **3.1 Introduction**

The Mixed Lineage Leukaemia gene (*MLL*) can translocate to a variety of partner genes, resulting in fusion genes which upon translation generate novel onco-proteins. The *MLL* translocations are associated with very poor clinical outcomes (Slany, 2009). The encoded *MLL* fusion proteins play a central role in initiation and maintenance of AML. Therefore, inactivation of the *MLL* fusion proteins represents a potential cure for these patients.

Delayed disease progression and complete eradication of leukaemia has been achieved previously by targeting fusion proteins. Ablain and de Thé discovered that a combination of arsenic trioxide and retinoic acid induced the proteasome dependent degradation of the PML/RAR $\alpha$  fusion (Ablain and de The, 2011). This treatment resulted in the terminal differentiation of acute promyelocytic leukaemia (APL) cells. Indeed, nowadays APL is one of the most curable forms of AML. Furthermore, imatinib and second generation BCR-ABL inhibitors are effective in the treatment of newly diagnosed chronic myelogenous leukaemia (CML) and acute lymphoblastic leukaemia (ALL) expressing this fusion gene (Shami and Deininger, 2012). A previous pre-clinical study from our laboratory showed that the inactivation of *MLL* fusion proteins (*MLL-ENL*) in an animal model resulted in a complete regression of the disease (Horton et al., 2009).

Taken together, all these studies showed that inactivation of the driving fusion gene resulted in a block of leukaemia self-renewal. This suggests that targeting these leukaemic fusion proteins would be an effective approach to combat the associated leukaemias.

Drug discovery is still a long, complicated, expensive and time consuming process. Despite all the advances in computational biology and high throughput screening techniques there is still a very low success rate. Drug redeployment/repositioning is an alternative to *de novo* drug development, which is becoming more widely used as an approach to establishing novel therapies. Drug redeployment/repositioning uses existing or abandoned drugs to treat disorders other than those they were originally prescribed for (Ashburn and Thor, 2004). Whereas introducing a new drug to the market takes approximately 13-15 years, this time is significantly reduced for repositioned drugs. Since the latter have already passed through several stages of preclinical testing, much is known about their safety, toxicology and pharmacokinetic profiles. It is often the case that the American Food and Drug Administration (FDA) and the European Medicine Agency (EMA) have already approved these drugs for use in man. This means that drug repositioning could facilitate the drug discovery process by reducing development risks and by cutting research costs.

The aim of this study is to develop an approach of medium throughput screening for destabilisers of leukaemic fusion proteins based on a dual luciferase assay. The firefly luciferase (*Photinus pyralis*) gene is a reporter gene

encoding an enzyme catalysing an ATP-dependent chemiluminescent reaction. It catalyses the conversion of its substrate D-luciferin in oxyluciferin (oxidative decarboxylation). The measurement of the photons emitted during the reaction allows the quantification of the reporter. Commonly, two reporters are used in this assay: the experimental reporter (firefly luciferase in our study), which is linked to the experimental conditions, and a control reporter (renilla luciferase in our study), which serves as internal control. In these assays, the activities of the two luciferases are detected sequentially in the same tube and/or multi-well plate. A screening based on this kind of assay will facilitate the identification of drugs potentially targeting leukaemic fusion proteins.

## 3.2 Results

### 3.2.1 Radicicol, a potential destabiliser of leukaemic fusion proteins

Radicicol is a natural compound which a previous study has shown to induce degradation of Trithorax, the *Drosophila* MLL homologue (Tariq *et al.*, 2009). Furthermore, Tariq *et al.* showed radicicol specific degradation of N-terminal wild type MLL (wtMLL) but no effect on the C-terminal MLL. Therefore, we reasoned that this drug may also be used to induce specific degradation of MLL fusion proteins since these retain much of the N-terminal MLL moiety.

To investigate whether radicicol could induce the degradation of MLL-fusion proteins, we treated an MLL-AF6 cell line with 30 $\mu$ M radicicol for 6 hours. N-terminal MLL expression levels were quantified by immunoblot. We found that radicicol treatment resulted in depletion of wild type N-terminal MLL, as previously reported. More importantly, the MLL fusion protein was also completely depleted within 6 hours of treatment (figure 13). The reduction in MLL wild type and MLL-fusion protein levels was assessed by normalising the protein levels to the unrelated Clathrin that remained unaffected in treated Shi-1 cells. This indicates that radicicol is able to induce the degradation of MLL fusion proteins.

We hypothesised that degradation of the N-terminal MLL and MLL-AF6 fusion proteins should result in downregulation of their transcriptional target genes. Therefore we measured the gene expression levels of known MLL target genes

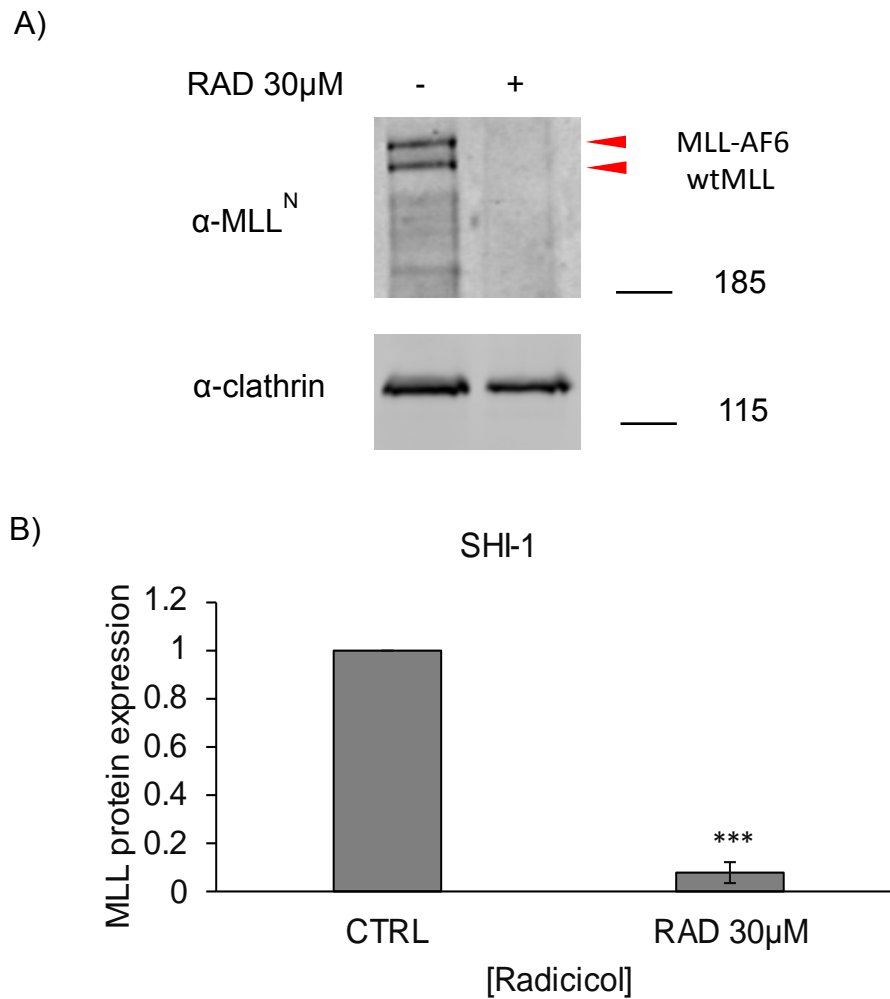


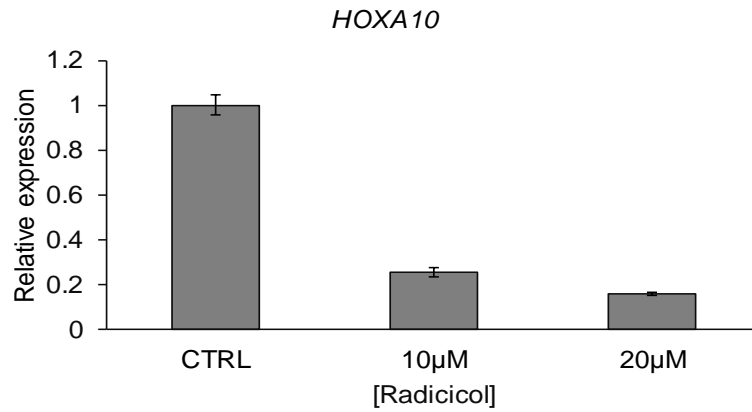
**Figure 13 Effect of Radicicol on MLL-AF6 protein expression in SHI-1**

The western blot (A) shows the MLL protein expression levels in SHI-1 after treatment with radicicol. Cells were treated at 37°C for 6 hours with 30μM radicicol. The western blot was probed with an anti-MLL<sup>N</sup> antibody. An anti-clathrin antibody was used as a loading control for protein loading. Films were scanned and bands quantified using QuantityOne software. (B) The bar chart represents the quantification of MLL-AF6 expression levels normalised to Clathrin ± s.d. for three independent experiments. \*P<0.05, \*\*P<0.01, \*\*\*P<0.005 compared to control (one sample t-test).

after exposure to radicicol. *HOXA10* and *MEIS1* are two of the best characterised downstream target genes. Total RNA was extracted from SHI-1 treated for 6 hours with radicicol (10 $\mu$ M and 20 $\mu$ M) and qRT-PCR was performed. We observed a dose-dependent decrease in both *HOXA10* and *MEIS1* gene expression levels as result of radicicol treatment (figure 14).

In summary, we demonstrated that radicicol, a macrocyclic antifungal antibiotic, induced degradation of both N-terminal MLL and MLL-fusion proteins in AML cells. Furthermore, radicicol inhibits the expression of *HOXA10* and *MEIS1*, two genes associated with the self-renewal program in MLL-rearranged AML cells. Although radicicol exhibits interesting biological activities *in vitro*, the compound was shown to be too toxic and unstable for clinical use (Neckers and Workman, 2012). However, we reasoned that radicicol may be a useful compound for validating the *in vitro* effect of MLL-fusion proteins inhibition.

A)



B)

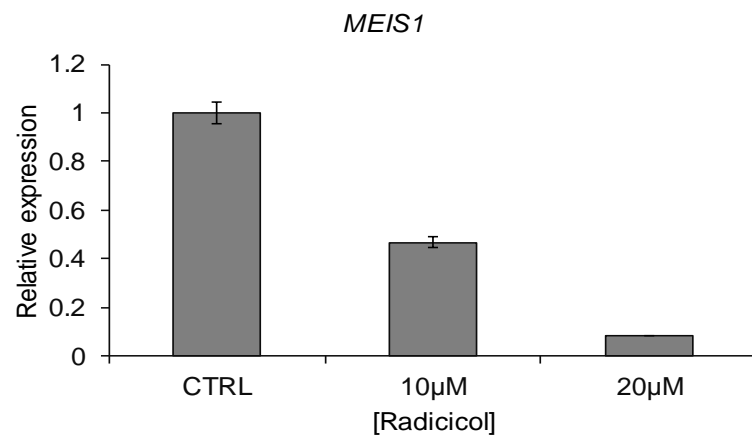


**Figure 14 HOXA10 and MEIS1 gene expression levels upon Radicicol treatment**

Plots represent the analysis of HOXA10 (A) and MEIS1 (B) mRNA levels in SHI-1 cells treated for 6 hours with two concentrations of radicicol (10µM and 20µM). mRNA expression of genes of interest was measured by qRT-PCR. Data are normalised to untreated control cells.

### **3.2.2 MLL-AF9-luciferase reporter construction and cell lines production**

We reported selective destabilisation of MLL wild type and fusion proteins by radicicol. However, it was reported that radicicol was ineffective in vivo, limiting clinical impact of our discovery (Neckers and Workman, 2012). In order to discover clinically approved drugs that have similar activity to radicicol, we designed a novel screening platform that would allow the identification of drugs.

The screening was based on expression of luciferase tagged MLL fusion proteins. The advantage of this approach is that protein degradation can be followed by analysing changes in luciferase activity. Dr. Jasper de Boer generated the luciferase reporter and the leukaemic indicator cell lines. Using a PCR-based cloning approach, MLL-AF9 was fused to a firefly luciferase. The MLL-AF9-Luciferase (MA9-Luc from now on) was then cloned into a pMSCVneo retroviral vector (pMSCVneo-MA9-LUC). This vector was then used to generate the indicator fusion gene cell line (THP-1 MA9-Luc-Ren). Firefly and renilla activities in THP-1 MA9-Luc-Ren can be estimated performing a dual luciferase assay which allows the simultaneous detection of both primary reporter gene (firefly luciferase) and internal control (renilla reporter). In this configuration a positive hit, causing specific degradation of the MLL-AF9-Luciferase fusion reporter would be expected to affect only the firefly luciferase activity while leaving the renilla activity unchanged.

In summary, we established a screening platform that could be used to measure the relative quantity of MLL-fusion proteins allowing the identification of drugs with anti MLL fusion activity similar to Radicicol.

### 3.2.3 Indicator leukaemic fusion gene cell line validation

To validate that the assay based on the indicator leukaemic cell line (THP-1-MA9-Luc-Ren) reflected correctly the protein levels of MLL-AF9 we tested the response of the cells to treatment with radicicol.

Thp-1-MA9-Luc-Ren cells were incubated for 6 hours with radicicol (10 $\mu$ M and 20 $\mu$ M). Firefly and renilla luciferase activities were measured using the Infinite200Pro luminometer (Tecan) and a dual luciferase reporter assay system. Reporter inactivation was calculated as the ratio of firefly and renilla luciferase activities. After 6 hours of treatment both concentrations of radicicol reduced luciferase activity (firefly luciferase/renilla luciferase) (figure 15B). Radicicol considerably reduced activity levels of the firefly luciferase while the renilla luciferase was affected to a far lesser degree (figure 15A).

These results demonstrated that radicicol is able to induce degradation of the MLL-AF9-Luciferase fusion protein in the THP-1-MA9-Luc-Ren indicator cell line. More importantly, we established that the THP-1-MA9-Luc-Ren system correctly reports MLL fusion protein levels in cell culture in response to experimental perturbations of MLL protein stability. We concluded that the THP-1-MA9-Luc-Ren leukaemic indicator cell line can indeed be used in the planned medium throughput screening.

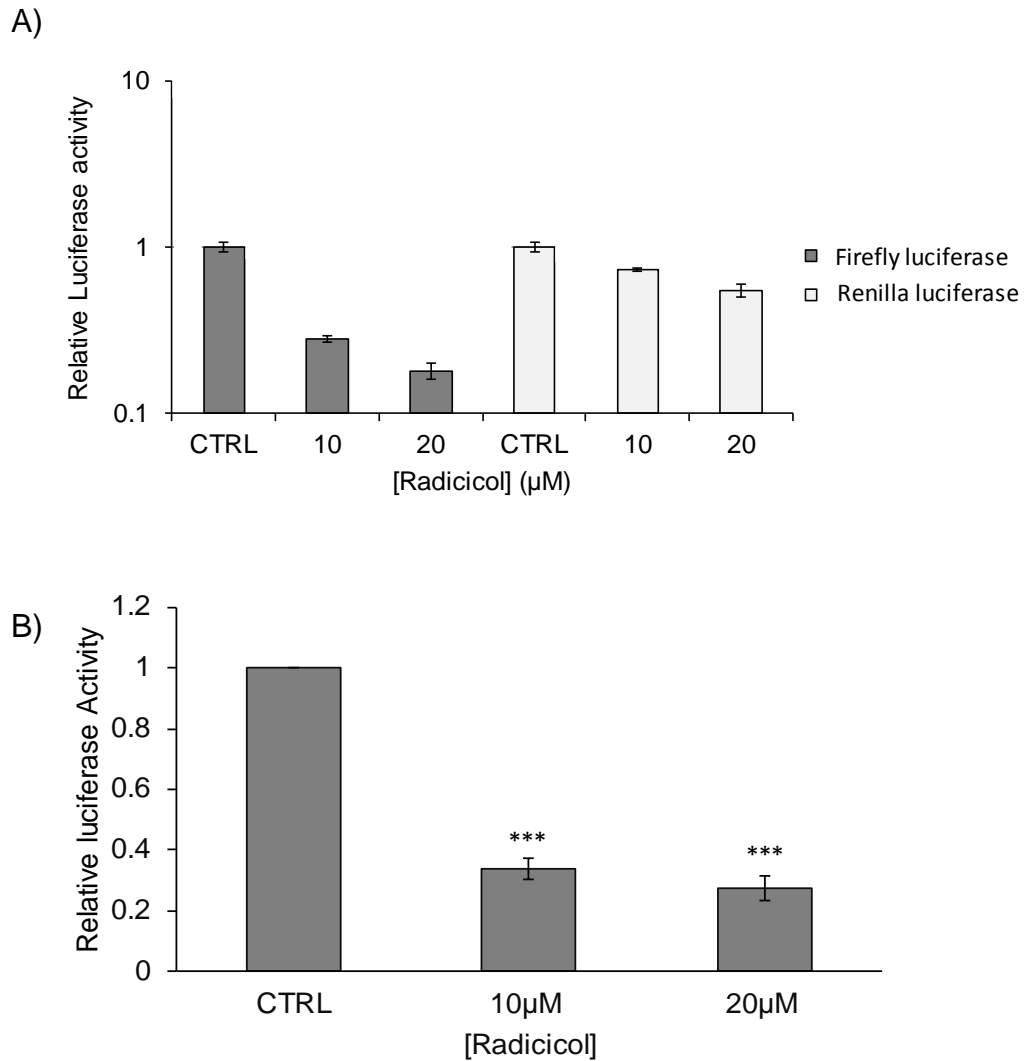


**Figure 15 Effect of radicicol on luciferase activity in THP-1 MA9-Luc-Ren**

The upper histogram (A) shows that the two concentrations of radicicol greatly decreased the firefly luciferase activity with minimal changes to the renilla luciferase. The lower histogram (B) shows the relative luciferase activity in THP-1-MA9-Luc-Ren treated with radicicol 10 $\mu\text{M}$  and 20 $\mu\text{M}$  and in control cells treated with DMSO. Firefly luciferase values were divided by the renilla luciferase ones, then this value was normalised to the control sample. The luciferase signal was measured, with the Infinite200Pro luminometer which dispensed sequentially luciferase reaction buffer and renilla reaction buffer into each well. Bars represent the mean of three experiments and the error bars represent standard deviations. \* $P < 0.05$ , \*\* $P < 0.01$ , \*\*\* $P < 0.001$  compared to control (One-sample t-test).

### 3.2.4 Medium throughput screening

We developed our reporter assay in order to perform high throughput experiments. All the experiments were performed in a 96 multi-well plate format to minimise screening time, a typical problem of luminescence based assays, and to increase throughput. The luminescence reader detects luminescence signals and immediately provides quantitative data. Changes of MLL fusion protein levels were monitored by analysing changes in firefly luciferase-renilla luciferase ratio. This ratio was then normalised to the negative control sample. Compounds inducing more than 50% decrease in the renilla luciferase signal were excluded from the analysis. This approach would eliminate drugs that caused decrease in the firefly luciferase due to induction of cell death, since this would cause a decrease also in renilla activity. A potential positive hit was defined as a drug causing 30% decrease or more in the firefly-renilla ratio (figure 16 and figure 17). As shown in our decision tree in figure 17, these positive hits required further validation which in our screening was based on evaluation of MLL fusion protein levels by western blot analysis. Compounds inducing  $\geq 30\%$  decrease of MLL fusion protein levels in two human MLL-r cell lines passed the whole screening.

To identify drugs able to induce MLL fusion degradation, we tested the Prestwick chemical library on the THP-1-MA9-Luc-Ren indicator cell line. This library contains 1280 small molecules, all FDA (Food and Drug Administration) and EMA (European Medicine Agency) approved. The Prestwick chemical library is designed to reduce the risks of low quality hits, the costs of the

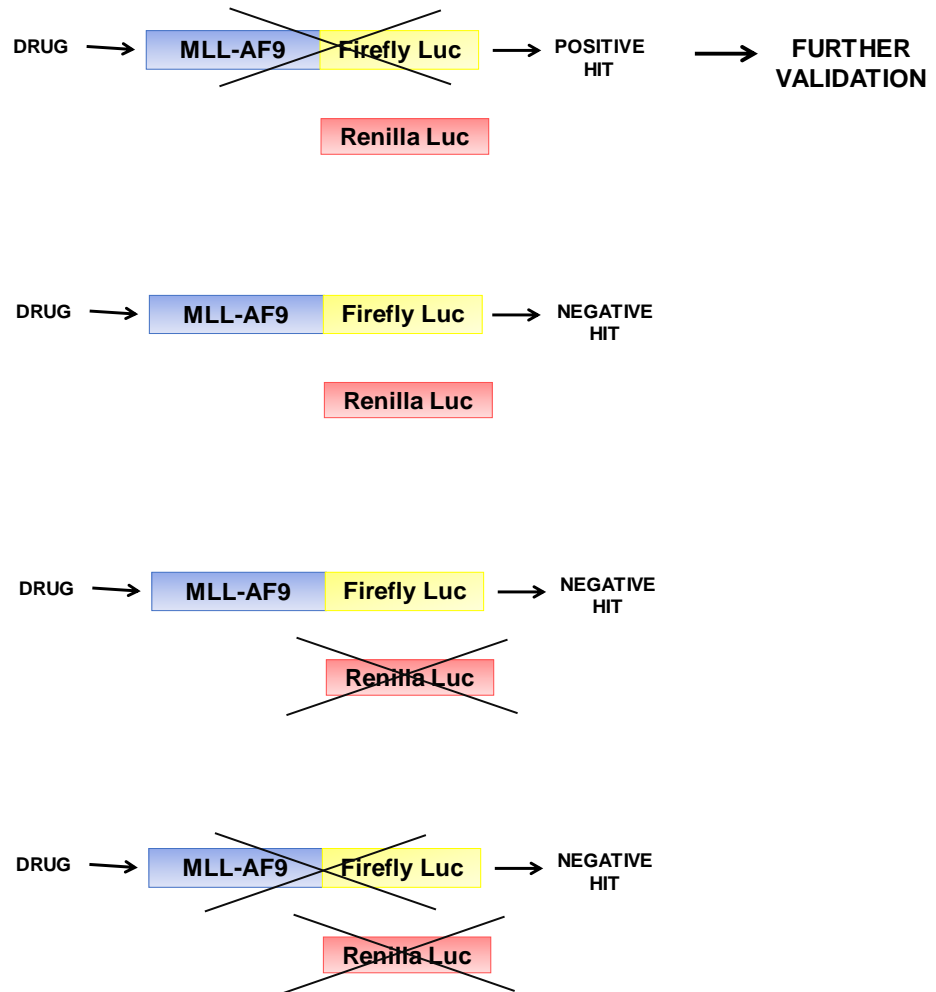


**Figure 16 Scheme of the screening**

The leukaemic fusion gene (MLL-AF9) is linked to firefly luciferase and the indicator cells co-express renilla luciferase. Candidate positive hits would cause a decrease only in the firefly luciferase activity.

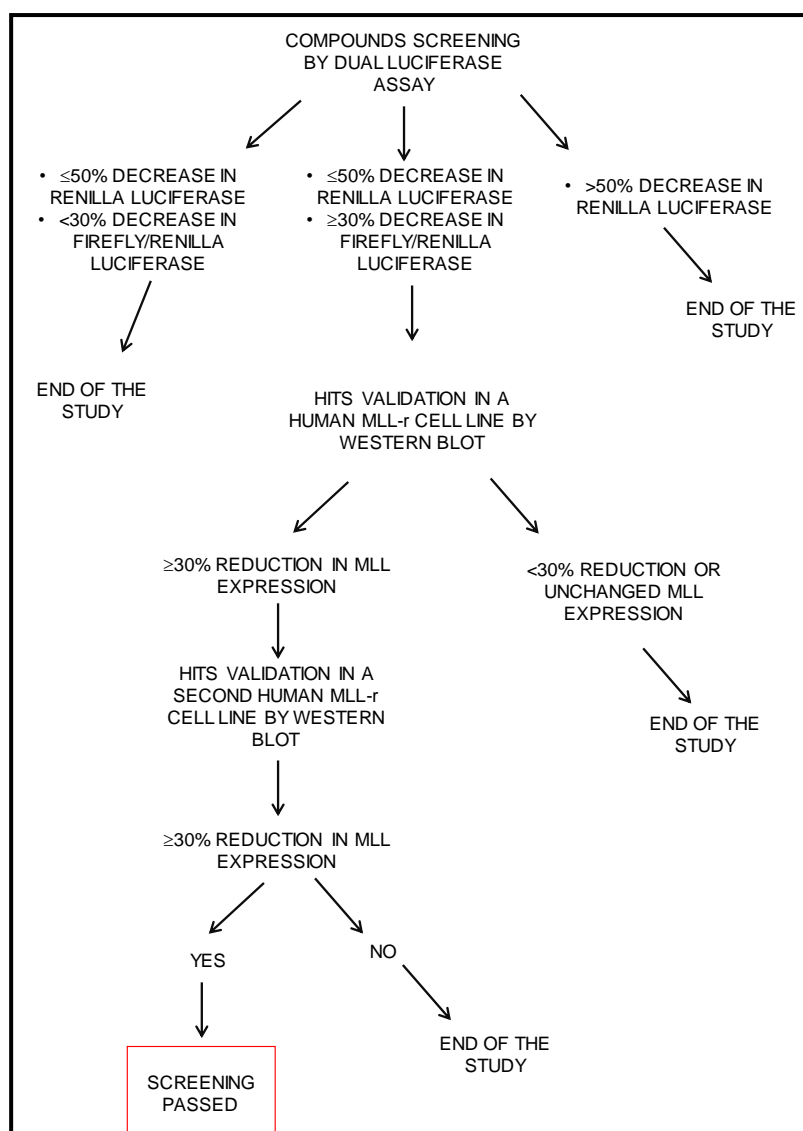


**Figure 17 Decision tree for drug redeployment screening**

Candidate compounds potentially targeting MLL fusion proteins after the first screening based on a dual luciferase assay needs to be further validated. Drugs inducing more than 50% decrease in the renilla luciferase signal will be excluded from the analysis. Drugs causing  $\geq 30\%$  decrease in firefly luciferase-renilla ratio were considered a positive hit and proceeded to the next step of validation by western blot. Drugs causing  $\geq 30\%$  reduction in MLL protein expression, in a human MLL-r cell line, continued to the third step of validation. Drugs passed the screening only if they produced again  $\geq 30\%$  reduction in MLL expression in a second human MLL-r cell line.

screening, and to speed up the discovery process. Compounds are all characterised by high chemical and pharmacological diversity as well as for their bioavailability and safety in humans.

THP-1-MA9-Luc-Ren cells were treated for 6 hours with 10 $\mu$ M of each compound. Each 96 multi-well plate also contained cells treated with DMSO and radicicol as negative and positive controls. Detection of luminescence signals was followed by the analysis of normalised firefly-renilla ratio (Appendix 1). This analysis led to identification of the 24 compounds which caused decrease of 30% or more in the firefly: renilla ratio. These 24 drugs passed our initial screen (table 11). In conclusion, our screening platform allowed identification of 24 drugs with potential anti-MLL fusion activity.

Drug	Relative luciferase activity (%)
Fenbendazole	70%
Vinpocetine	50%
Disulfiram	70%
Clotrimazole	50%
Mitoxantrone	70%
Clomipramine	50%
lobenguane	70%
Nabumetone	60%
Pantoprazole	60%
Felbamate	60%
Indoprofen	40%
Leflunomide	50%
Doxorubicin	60%
Rifabutin	70%
Hydralazine	50%
Niclosamide	10%
Imatinib	70%
Phenazopyridine	50%
Parbendazole	70%
Rizatriptan	60%
Tegafur	60%
lpriflavone	10%
Altrenogest	60%
Dimenhydrinate	60%

**Table 11 Drugs passing the first step of the screening**

The table shows the 24 drugs which caused a decrease of 30% or more in the luciferase activity and that then passed the dual luciferase assay screening

### 3.2.5 Drug hit validation

Multistep cross-validation, based on a different technique, is a prerequisite to reduce the number of false positive hits and to increase the robustness of the initial screening. As shown in our decision tree (figure 18) the next two steps of validation were based on assessing the relative MLL fusion levels by western blot analysis.

Human *MLL* rearranged cell lines were exposed to candidate drugs. We used SHI-1 and MV4-11 expressing respectively the MLL-AF6 and MLL-AF4 fusion. SHI-1 and MV4-11 cells were treated for 6 hours with the 24 selected drugs and the lysates were analysed by western blot (figure 18 and figure 19). Drugs generating a reduction of 30% or more in MLL fusion protein levels in both MLL-r cell lines passed our screening (table 12). Seven drugs passed the screening: fenbendazole, disulfiram, mitoxantrone, leflunomide, doxorubicin, rifabutin and phenazopyridine.

To check reproducibility of data obtained in MLL-AF6 and MLL-AF4 expressing cell lines we tested the first three drugs that passed the screening on MLL-AF9 cells. SHI-1, MV4-11 and THP-1 cells were treated for 6 hours with fenbendazole, disulfiram and mitoxantrone. Western blot analysis confirmed that fenbendazole, an anthelmintic drug used against gastrointestinal parasites, targeted MLL-AF6 and MLL-AF4 fusion proteins while western blot analysis were not consistent for MLL-AF9 fusion protein (figure 20). Therefore, we excluded this drug from further analysis. Instead, after 6 hours of treatment disulfiram and mitoxantrone reduced MLL-AF9, MLL-AF6 and MLL-AF4 protein

levels. Mitoxantrone is an inhibitor of DNA topoisomerase II which intercalates between DNA bases and induces DNA double strand breaks. Unfortunately the wide range of serious side effects (bone marrow suppression, neutropenia, cardiac toxicity) led us to exclude mitoxantrone from further analysis. Disulfiram is a compound used, for about 60 years, in treatment of chronic alcoholism. The low toxicity levels of disulfiram combined with its high tolerability in patients, led us to study in more detail the effects of this drug on MLL proteins.

In conclusion, out of the 1280 drugs contained in the Prestwick chemical library seven passed the screening. Western blot analysis on three different MLL rearranged cell lines confirmed that disulfiram was able to reduce MLL protein levels in all the lines.

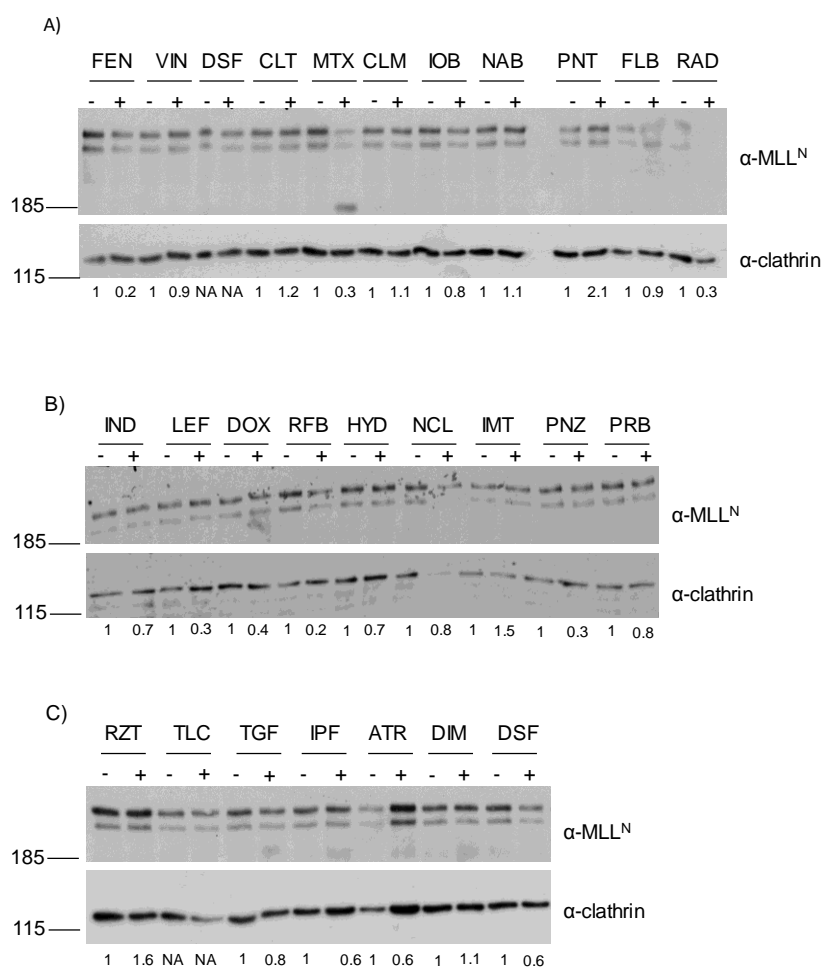


**Figure 18 Second step of the screening: western blot analysis in SHI-1**

SHI-1 cells were seeded in a 24 multi-well plate at the density of  $1 \times 10^6$  cells/ml. Cells were treated for 6 hours at 37°C with 10µM of the following drugs: (A) Fenbendazole (FEN), Vinpocetine (VIN), Disulfiram (DSF), Clotrimazole (CLT), Mitoxantrone (MTX), Clomipramine (CLM), lobenguane (IOB), Nabumetone (NAB), Pantoprazole (PNT), Felbamate (FLB), Radicol (RAD), (B) Indoprofen (IND), Leflunomide (LEF), Doxorubicin (DOX), Rifabutin (RFB), Hydralazine (HYD), Niclosamide (NCL), Imatinib (IMT), Phenazopyridine (PNZ), Parbendazole (PRB), (C) Rizatriptan (RZT), Tolcapone (TLC), Tegafur (TFG), Ipriflavone (IPF), Altrenogest (ATR), Dimenhydrinate (DIM), Disulfiram (DSF). Lysates from treated and untreated cells were analysed by western blot. Films were scanned, bands were quantified using Quantity One software and normalised to Clathrin control. Numbers underneath each lane represent densitometric quantification. All experiments were performed once.

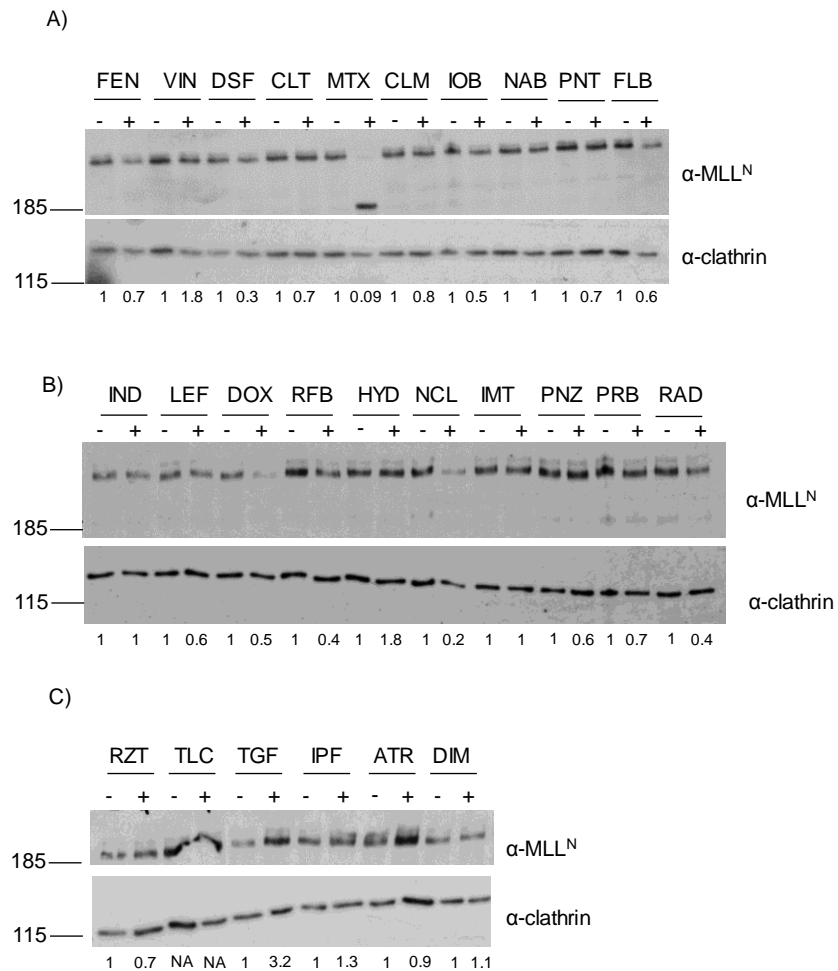


**Figure 19 Third step of the screening: western blot analysis in MV4-11**

MV4-11 cells were seeded in a 24 multi-well plate at the density of  $1 \times 10^6$  cells/ml. Cells were treated for 6 hours at  $37^\circ\text{C}$  with  $10\mu\text{M}$  of the following drugs: (A) Fenbendazole (FEN), Vinpocetine (VIN), Disulfiram (DSF), Clotrimazole (CLT), Mitoxantrone (MTX), Clomipramine (CLM), Iobenguane (IOB), Nabumetone (NAB), Pantoprazole (PNT), Felbamate (FLB), Radicol (RAD), (B) Indoprofen (IND), Leflunomide (LEF), Doxorubicin (DOX), Rifabutin (RFB), Hydralazine (HYD), Niclosamide (NCL), Imatinib (IMT), Phenazopyridine (PNZ), Parbendazole (PRB), (C) Rizatriptan (RZT), Tolcapone (TLC), Tegafur (TFG), Ipriflavone (IPF), Altrenogest (ATR), Dimenhydrinate (DIM), Disulfiram (DSF). Lysates from treated and untreated cells were analysed by western blot. Films were scanned, bands were quantified using Quantity One software and normalised to Clathrin control. Numbers underneath each lane represent densitometric quantification. All experiments were performed once.

Drug	Relative luciferase activity (%)	MLL expression detected in SHI-1 (%)	MLL expression detected in MV4-11 (%)	Passing Screening
Fenbendazole	70%	20%	70%	YES
Vinpocetine	50%	90%	180%	NO
Disulfiram	70%	60%	30%	YES
Clotrimazole	50%	120%	70%	NO
Mitoxantrone	70%	35%	9%	YES
Clomipramine	50%	100%	80%	NO
lobenguane	70%	80%	50%	NO
Nabumetone	60%	100%	100%	NO
Pantoprazole	60%	200%	70%	NO
Felbamate	60%	90%	60%	NO
Indoprofen	40%	70%	100%	NO
Leflunomide	50%	30%	60%	YES
Doxorubicin	60%	40%	50%	YES
Rifabutin	70%	20%	40%	YES
Hydralazine	50%	70%	180%	NO
Niclosamide	10%	80%	20%	NO
Imatinib	70%	150%	101%	NO
Phenazopyridine	50%	30%	60%	YES
Parbendazole	70%	80%	70%	NO
Rizatriptan	60%	160%	70%	NO
Tegafur	60%	80%	320%	NO
Ipriflavone	10%	60%	130%	NO
Altrenogest	60%	60%	90%	NO
Dimenhydrinate	60%	110%	110%	NO

**Table 12 Compounds passing the screening**

The table shows the 24 drugs that passed the dual luciferase assay screening and those that passed the second and third screening by western blot analysis. Only 7 drugs passed the whole screening: Fenbendazole, Disulfiram, Mitoxantrone, Leflunomide, Doxorubicin, Rifabutin and Phenazopyridine.

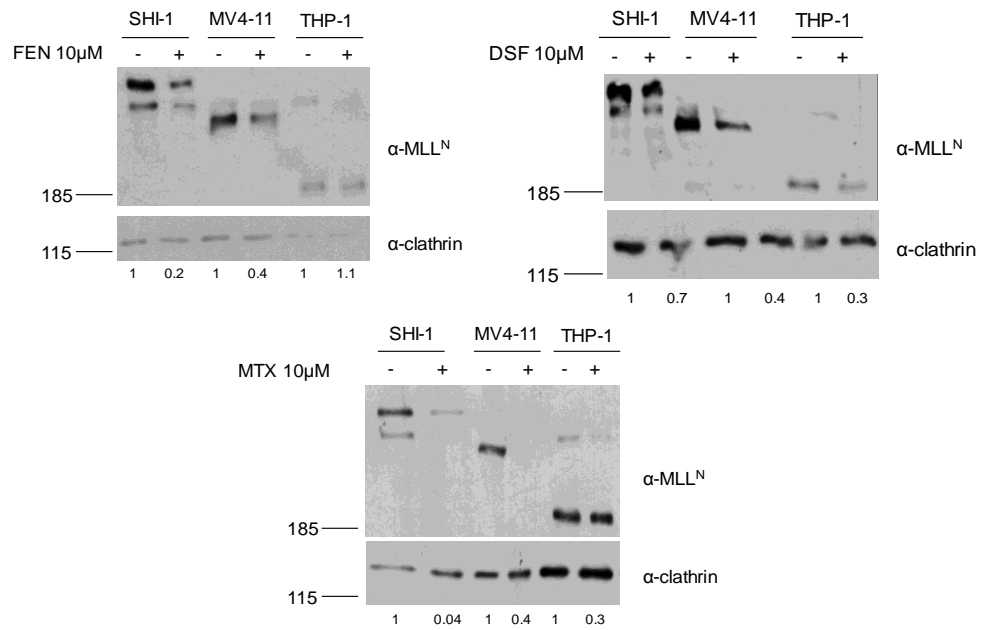


**Figure 20 MLL fusion protein expression in human *MLL-r* cell lines after drug treatment**

The western blot analysis shows expression levels of both wild type MLL and MLL fusion protein in SHI-1, MV4-11 and THP-1 treated for 6 hours with 10μM of each compound (fenbendazole, disulfiram and mitoxantrone). The western blot was probed with a mouse anti-human MLL<sup>N</sup>/HRX (clone N4.4) and an anti-clathrin antibody was used as control for protein loading. Numbers represents densitometric quantification of total MLL bands normalised to Clathrin. Disulfiram and mitoxantrone reduced MLL-fusion protein expression in all the three cell lines, while after fenbendazole treatment the MLL-fusion protein expression reduction was detectable only in SHI-1 and MV4-11. All experiments were performed once.

levels. Mitoxantrone is an inhibitor of DNA topoisomerase II which intercalates between DNA bases and induces DNA double strand breaks. Unfortunately the wide range of serious side effects (bone marrow suppression, neutropenia, cardiac toxicity) led us to exclude mitoxantrone from further analysis. Disulfiram is a compound used, for about 60 years, in treatment of chronic alcoholism. The low toxicity levels of disulfiram combined with its high tolerability in patients, led us to study in more detail the effects of this drug on MLL proteins.

In conclusion, out of the 1280 drugs contained in the Prestwick chemical library seven passed the screening. Western blot analysis on three different MLL rearranged cell lines confirmed that disulfiram was able to reduce MLL protein levels in all the lines.

### 3.3 Discussion

The aim of this project was to identify compounds capable of degrading MLL-fusion proteins. We identified radicicol as a potential candidate. Results from our experiments showed specific degradation of wild type MLL and the MLL fusion protein. As a consequence of MLL protein depletion, expression of MLL target genes was downregulated. The crucial drawback is that radicicol is too unstable and toxic to be used in patients (Neckers and Workman, 2012). Therefore, we developed an approach of medium throughput screening to identify drugs with similar activity to radicicol.

This approach required the expression of luciferase tagged MLL-fusion proteins. Dr. de Boer generated an MLL-AF9 firefly luciferase reporter and then he established a cell line (THP-1) co-expressing the firefly luciferase reporter (experimental reporter) and the renilla luciferase (control reporter) (THP-1-MA9-Luc-Ren). To validate the use of the indicator cell line (THP-1-MA9-Luc-Ren) for the medium throughput screening, we exposed cells to radicicol. Radicicol induced degradation of the experimental reporter protein suggesting that the indicator line is suited for the dual luciferase assay screening and also that radicicol itself could be used as positive control during the screening.

The screening was carried out using Prestwick chemical library. Degradation of the MLL-fusion was monitored by analysing changes in the firefly luciferase-renilla luciferase ratio (Appendix 1). Potential positive hits decreased only firefly luciferase activity leaving the renilla luciferase unchanged. Only drugs causing 30% decrease or more in luciferase activity were considered as potential

positive hits and passed to the next step of validation. 24 compounds, out of the 1280 contained in the Prestwick library, passed this first step of the screening.

The following two steps of the screen validation were based on western blot approach. We tested the 24 drugs on two human *MLL* rearranged cell lines, SHI-1 and MV4-11, expressing the MLL-AF6 and MLL-AF4 fusion proteins. Compounds producing a 30% reduction or more in MLL-fusion protein expression in both cell lines passed our screening. The positive hits were: fenbendazole, disulfiram, mitoxantrone, leflunomide, doxorubicin, rifabutin and phenazopyridine. We decided to confirm the effect of the first three drugs on the table 11 on a third *MLL-r* cell line. The anthelmintic fenbendazole did not affect consistently MLL protein levels in MLL-AF9 cells. In contrast, disulfiram and mitoxantrone decreased MLL protein levels in all *MLL-r* cell lines analysed. We continued to study the effect of disulfiram on MLL fusion proteins given its low toxicity profile and the high tolerability in patients.

## 4 CHAPTER IV: Studying the effect of DSF in human acute myeloid leukaemia

### 4.1 Introduction

Disulfiram was one of the 8 candidate drugs that passed the medium throughput screening. Dual luciferase assays and western blot experiments showed that disulfiram induced a decrease in MLL fusion protein expression. Disulfiram (DSF) is an FDA approved drug used for treatment of alcohol abuse. It is relatively non-toxic and well tolerated in patients. Furthermore, some studies suggested a potential anti-tumour effect (Chen *et al.*, 2006, Liu *et al.*, 2012). Therefore, we decided to study this compound in greater detail.

Disulfiram was discovered by chance as a treatment for chronic alcoholism. In the early years of the twentieth century disulfiram was used in the rubber industry in order to speed up the vulcanization of rubber. Workers from rubber industries from around the world (from America to Sweden) developed severe reactions after drinking alcohol: severe nausea, vomiting, headache, blurred vision, chest pain [reviewed in (Kragh, 2008)]. At that time, disulfiram was already used in the clinic to treat scabies (Gordon and Seaton, 1942). In 1948 two Swedish researchers, studying anthelmintic drugs and copper metabolism of intestinal worms came across disulfiram by chance. Disulfiram has been described as chelator of metal ions, copper in particular. In invertebrates copper is responsible for the transport of oxygen molecules and Hald and Jacobsen hypothesised that disulfiram could also be used as an anthelmintic. The two

researchers decided to test low doses of disulfiram on themselves, certainly it did not take too long before they started to experience the side effects described above, after alcohol consumption (Hald and Jacobsen, 1948). This resulted in the establishment of DSF as a drug used to support the treatment of chronic alcoholism.

Disulfiram works by inhibiting the enzyme acetaldehyde dehydrogenase. After ingestion alcohol is rapidly metabolised in the liver where it is promptly converted in acetaldehyde by alcohol dehydrogenase (ADH). Acetaldehyde is extremely toxic for the human body. Aldehyde dehydrogenase (ALDH) is the enzyme involved in the immediate metabolisation of acetaldehyde into less toxic acetate [reviewed in (Jacobsen, 1952, Zakhari, 2006)]. Jacobsen discovered that disulfiram inhibits the enzyme responsible for metabolising acetaldehyde. Disulfiram, by inhibiting ALDH, causes a rise in acetaldehyde levels in the bloodstream. The mechanism of inhibition of ALDH is based on the oxidation of cysteine residues located at the active site of the enzyme (figure 21). This oxidative event induces a conformational change in the ALDH catalytic site which inhibits its function (Veverka *et al.*, 1997). Once ingested, disulfiram is rapidly converted in diethyldithiocarbamate (DDC) (figure 22). Studies in human promyelocytic cells (Kimoto-Kinoshita *et al.*, 2004) and in pancreatic cancer (Han *et al.*, 2013) suggest that DDC has a pro-apoptotic and anti-tumour effect.

To study the effect of disulfiram and diethyldithiocarbamate on MLL protein levels we performed dose-response experiments in a panel of human *MLL* rearranged cell lines. To further characterise responses to disulfiram exposure

we planned a time course. Results of these experiments provided further insights regarding the effect of disulfiram on MLL proteins.

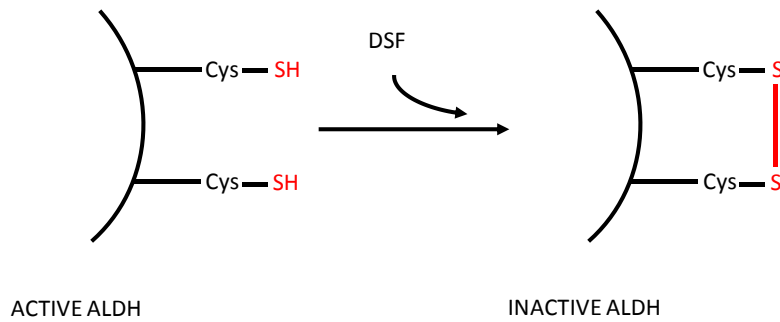


**Figure 21 Mechanism of ALDH inhibition by disulfiram**

Disulfiram oxidise cysteines in the active site of ALDH inducing formation of disulphide bridges. Inhibition of the enzyme activity, due to conformational changes at the active site, lead to unpleasant symptoms following alcohol consumption: flushing, hypotension, nausea, tachycardia.

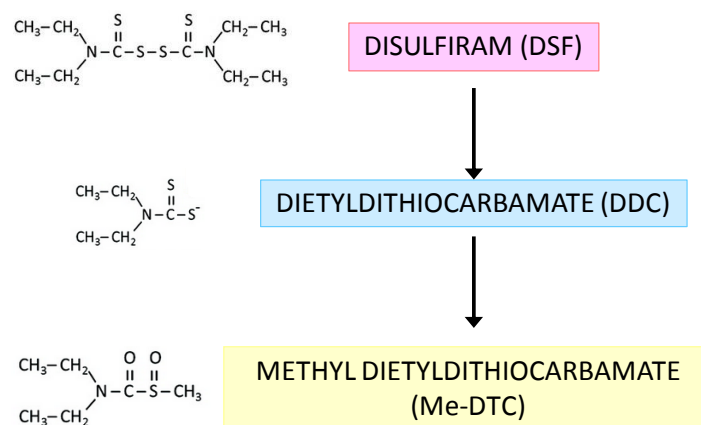


**Figure 22 Disulfiram metabolism**

After consumption disulfiram is rapidly converted in diethyldithiocarbamate which is further metabolised in methyl diethyldithiocarbamate.

## 4.2 Results

### 4.2.1 Copper enhances the effect of disulfiram

We conducted dose-response studies to determine the minimum effective dose of disulfiram required to decrease MLL protein levels. Each dose of disulfiram was tested in three different MLL rearranged cell lines to ensure the reproducibility of the results over a wide variety of MLL fusion proteins. The data from these studies are summarised in figure 23. The dose-response studies revealed that a single dose of 10 $\mu$ M of DSF reduced MLL proteins by about 40% relative to untreated cells after overnight treatment. It is unlikely that a 40% decrease in MLL fusion protein levels would result in a block of leukaemic activity.

However, independent studies in glioblastoma (Liu *et al.*, 2012), breast cancer (Chen *et al.*, 2006) and melanoma (Cen *et al.*, 2004) showed an enhanced cytotoxic and anti-tumour effect of disulfiram in presence of copper ions. Therefore, we reasoned that the copper-disulfiram combination could enhance the effect of DSF on the degradation of MLL fusion proteins. Then we repeated the DSF titration experiment with addition of copper. The dose of copper chloride chosen was 1 $\mu$ M (Cen *et al.*, 2004, Liu *et al.*, 2012) well below the concentration of copper in human serum (14 $\mu$ M). Although cell culture media formulation attempts to reproduce an environment as similar as possible to the *in vivo* environment, there are clear differences between cell medium and human serum. Common cell culture media, even when supplemented with FBS, do not contain copper (Arigony *et al.*, 2013). Protein lysates from cells treated

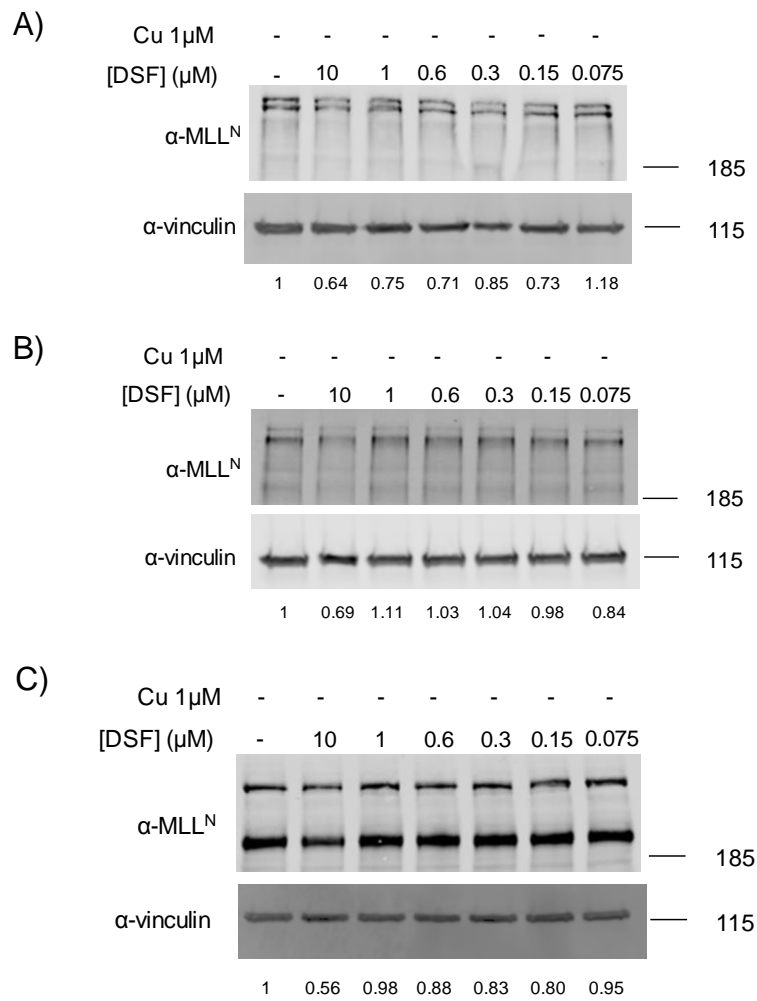


**Figure 23 Effect of Disulfiram on human leukaemic cell lines**

Western blot analysis of protein extracts from SHI-1 (A), MV4-11 (B) and THP-1 (C).  $0.5 \times 10^6$  cells were plated in a 24 multi-well plate and treated for 16 hours with different concentrations of DSF. Protein lysates from untreated cells were used as negative control. Anti-MLL<sup>N</sup>/HRX (clone N4.4) antibody was used to detect the endogenous MLL N-terminus in MLL wild type and fusion proteins. Anti- $\alpha$ -vinculin antibody was used to control protein loading. Proteins were resolved on a 7% bis-acrylamide gel. Numbers underneath each lane represent densitometric quantification.

with the disulfiram-copper combination were analysed by western blot (figure 24). Strikingly the co-administration of copper at 1 $\mu$ M and disulfiram at 0.3 $\mu$ M completely ablated MLL proteins in all the cell lines analysed.

To estimate the minimum time needed by disulfiram to induce degradation of MLL proteins, we performed time course experiments. The experiment was conducted in MLL-AF4 expressing cells (figure 25). Our results clearly demonstrate that the disulfiram-copper combination reduced MLL protein levels after 12 hours of treatment. Changes in proteins levels after 1.5, 3 and 6 hours of treatment were not significant (figure 25B).

Taken together, these results led us to the conclusion that co-administration of disulfiram and copper downregulated levels of MLL proteins. This reduction was achieved with disulfiram at the concentration of 0.3 $\mu$ M and CuCl<sub>2</sub> at 1 $\mu$ M after a minimum treatment of 12 hours.

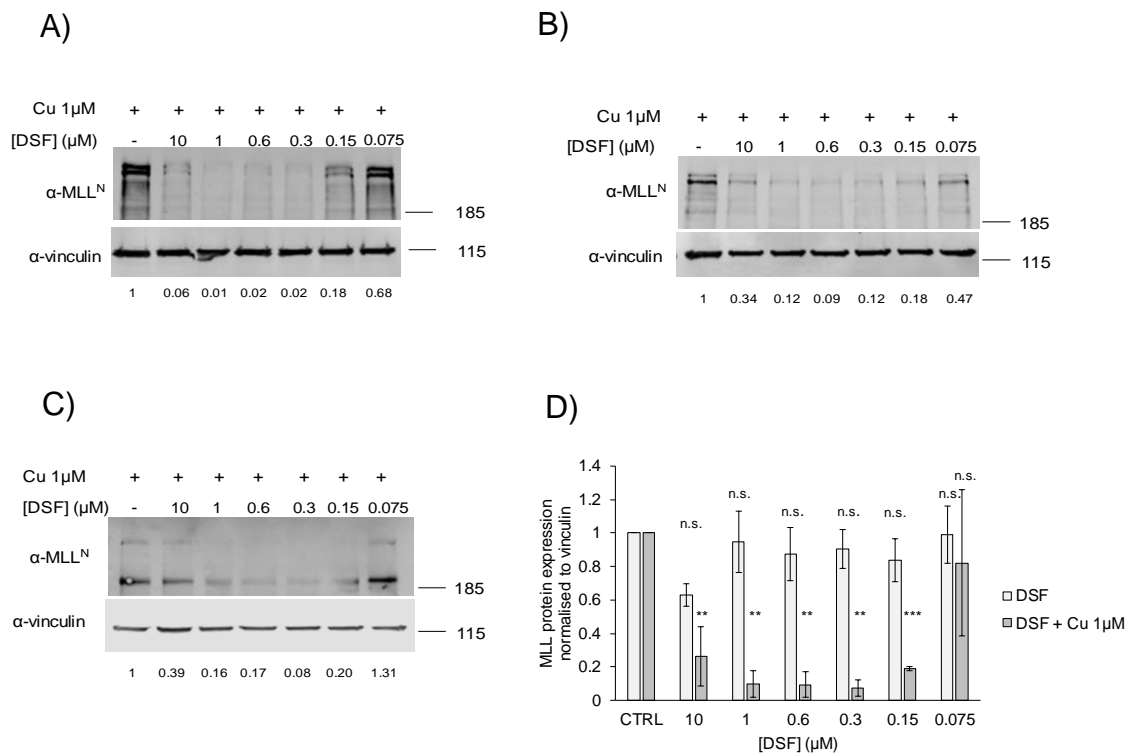


**Figure 24 Effect of copper-disulfiram mix on human leukaemic cell lines**

The western blot analysis shows the titration of disulfiram in SHI-1 (A), MV4-11 (B) and THP-1 (C) in presence of 1μM CuCl<sub>2</sub>. 0.5x10<sup>6</sup> cells were treated with the mixture DSF-CuCl<sub>2</sub>. Protein lysates were collected after 16 hours of treatment and resolved in a 7% bis-acrylamide gel. Membranes were probed with an anti-MLL<sup>N</sup>/ HRX (clone N4.4) antibody and with an anti-vinculin antibody, as protein loading control. Membranes were imaged using Odyssey CLX imaging system. Bands were quantified using the software Image Studio, provided by the manufacturer. The intensities of each band was normalised to the intensity of the housekeeping gene. Numbers represent densitometric quantification. (D) The bar chart represents the quantification of total MLL (MLL fusions and wild type MLL) protein normalised to the loading control vinculin in samples treated with copper-disulfiram complexes or with disulfiram alone. Bars represent the mean of three experiments and the error bars represent standard deviations. \*P<0.05, \*\*P<0.01, \*\*\*P<0.001 and n.s. P>0.05 compared to control (One-sample t-test).

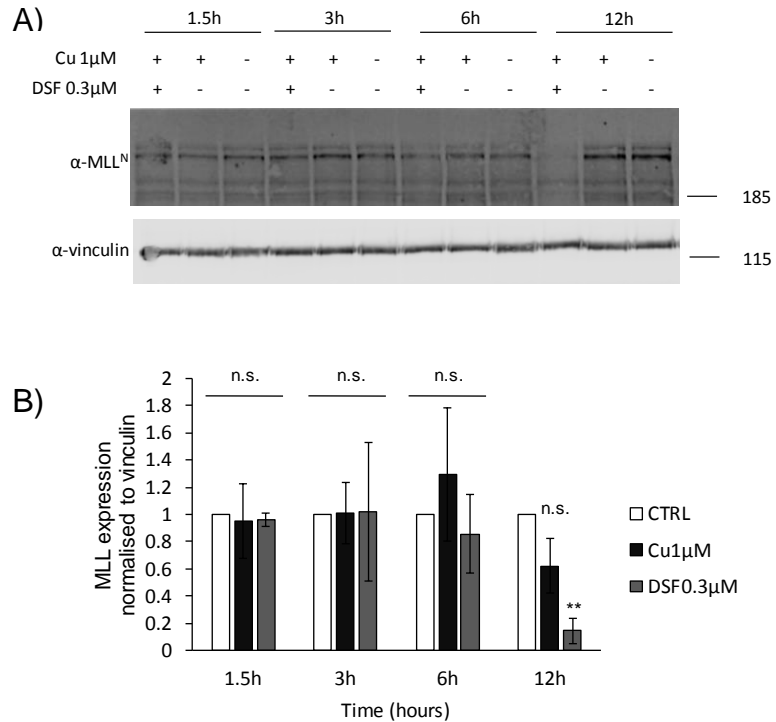


**Figure 25 Detection of MLL-AF4 protein expression over a time course with disulfiram and copper**

Western blot analysis (A) of MV4-11 cells treated with disulfiram (0.3 $\mu$ M) and CuCl<sub>2</sub> (1 $\mu$ M) for 1.5, 3, 6 and 12 hours. Lysates of treated and untreated cells were collected and loaded into a 7% bis-acrylamide gel. After transfer membranes were incubated O/N at +4C° with a mouse anti human MLL<sup>N</sup>/HRX (clone N4.4). An anti-vinculin antibody was used as protein loading control. Membranes were imaged using Odyssey CLX imaging system. The bands were quantified using the software Image Studio, provided by the manufacturer. The intensities of the bands were normalised to the intensity of the loading control. (B) The graph represents the quantification of the total MLL (MLL-AF4 fusion and wild type MLL) protein levels normalised to vinculin. The bars represent the average of three independent experiments and the error bars represent standard deviations. \*P<0.05, \*\*P<0.01, \*\*\*P<0.001 and n.s. P>0.05 compared to control (One-sample t-test).

#### **4.2.2 Copper-disulfiram mixtures target both wild type MLL and MLL-fusions to the same degree**

We carried out further studies to evaluate whether DSF downregulated both MLL wild type (MLLwt) and MLL fusion proteins to the same extent. We treated three different *MLL* rearranged cell lines with the disulfiram-copper mixture for 16 hours. Protein lysates were analysed by western blot. The co-treatment decreased significantly protein levels of wild type MLL and respectively of MLL-AF6, MLL-AF4 and MLL-AF9, compared to untreated cells (figure 26). The treatment with copper alone did not significantly affect fusion protein levels.

This experiment clearly demonstrated that disulfiram, in combination with copper, targets simultaneously and to the same degree MLL wild type and MLL fusion proteins.

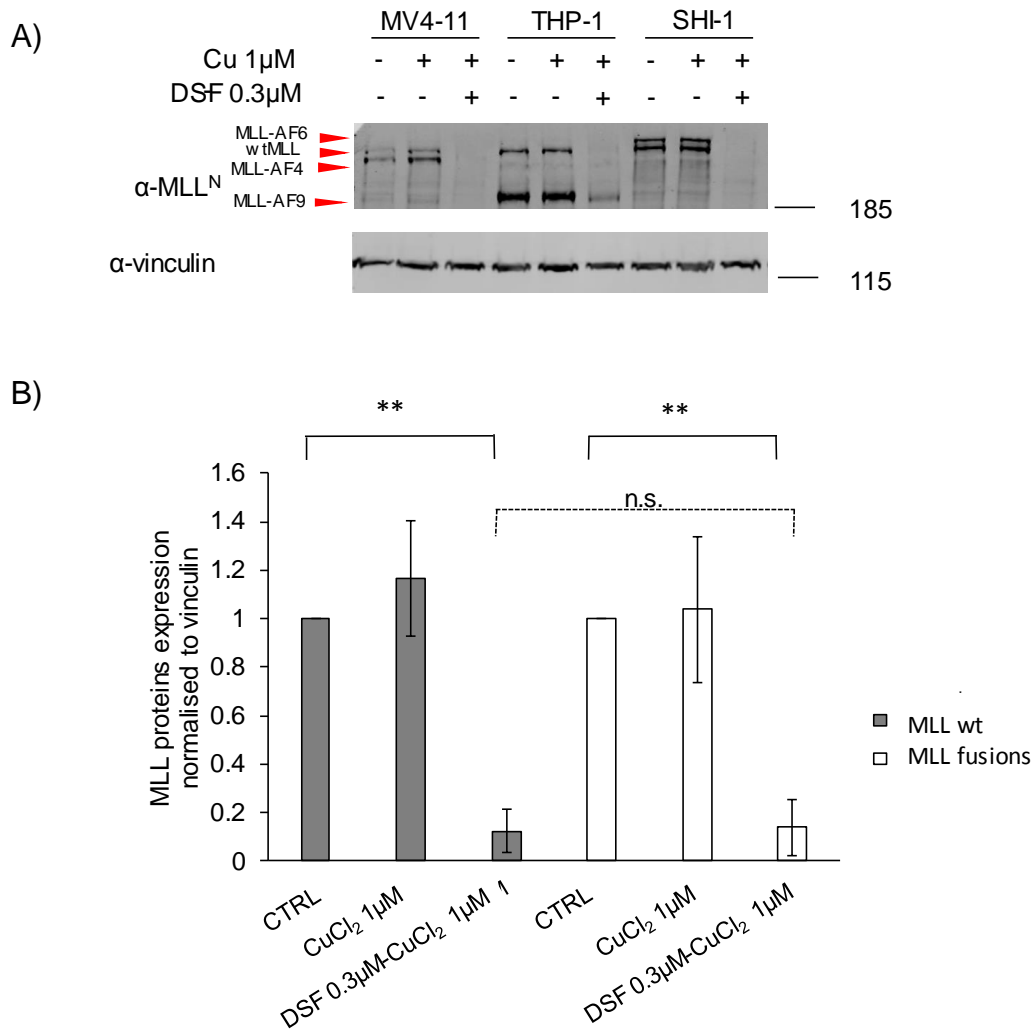


**Figure 26 Disulfiram-copper complexes target WT MLL and MLL fusions**

The western blot shows MLL fusion protein expression in three MLL rearranged cell lines. Lysates from untreated cells and from those treated with copper only or with the combination of the two compounds, were loaded in three consecutive lanes on a 7% Bis-acrilamide gel. Antibodies against MLL<sup>N</sup>/HRX (clone N4.4) and vinculin were incubated O/N and then membranes were developed with the Odyssey CLX imaging system. The graph (B) represents the quantification of MLL-fusions and of wild type MLL normalised to vinculin. The bars represent the average of three independent experiments and the error bars represent standard deviations. \*P<0.05, \*\*P<0.01, \*\*\*P<0.001 and n.s. P>0.05 compared to control (One-sample t-test).

### **4.2.3 Disulfiram metabolite diethyldithiocarbamate also degrade MLL fusion proteins**

After ingestion disulfiram is immediately metabolised in its reduced metabolite, diethyldithiocarbamate (DDC) (figure 22). Similarly to DSF, DDC is a potent copper chelator and it is able to complex with copper. A pro-apoptotic and anti-tumour effect of DDC was illustrated in studies in human promyelocytic cell lines (Kimoto-Kinoshita *et al.*, 2004) and in pancreatic cancer cells (Han *et al.*, 2013).

We investigated the possibility that DDC had the same effect of its precursor DSF on MLL protein levels. In order to examine this, we titrated DDC in presence of copper to estimate the minimum drug dose required to downregulate MLL proteins. This study was performed on MLL-AF6 rearranged cell lines after 16 hours of treatment. Independent experiments showed that DDC induced significant reduction in both MLLwt and MLL-AF6 proteins at concentrations of 0.3 $\mu$ M and above (figure 27).

In conclusion, here we demonstrated that the disulfiram metabolite diethyldithiocarbamate targets MLL proteins to the same extent as disulfiram.

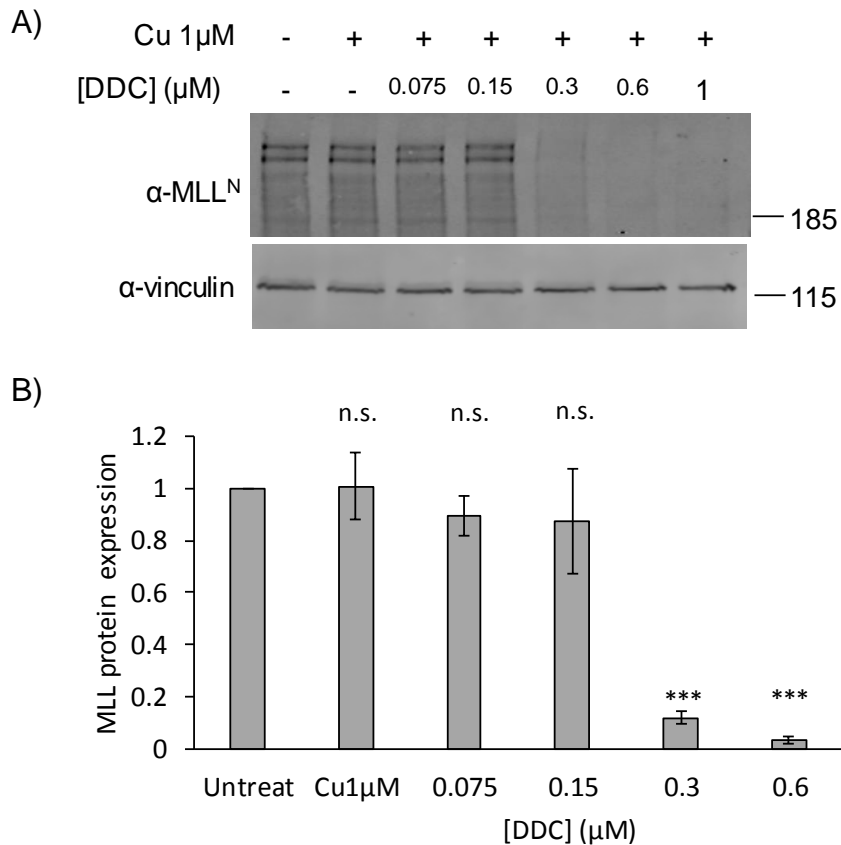


**Figure 27 Effect of the copper-diethyldithiocarbamate mixture on MLL-AF6 protein expression**

The western blot shows the titration of diethyldithiocarbamate in SHI-1 cells. (A) Cells were treated for 16h with 1 $\mu$ M CuCl<sub>2</sub> and a range of different concentrations of diethyldithiocarbamate. Lysates were resolved on a 7% bis-acrylamide gel. MLL proteins were detected using a mouse anti-human MLL<sup>N</sup>/HRX (clone N4.4) antibody. Vinculin was used as protein loading control. Membranes were imaged using Odyssey CLX imaging system. The bands were quantified using the software Image Studio, provided by the manufacturer. (B) The graph represents the quantification of MLL proteins (MLL-fusions and wild type MLL) normalised to vinculin. The bars represent the average of three independent experiments and the error bars represent standard deviations. \*P<0.05, \*\*P<0.01, \*\*\*P<0.001 and n.s. P>0.05 compared to control (One-sample t-test).

### 4.3 Discussion

Disulfiram was one of the 7 compounds passing all the steps of the medium throughput screening. We first examined the effect of disulfiram on MLL protein levels in a panel of human *MLL* rearranged cell lines. We treated cells for 16 hours with a range of DSF concentrations to verify the minimum dose necessary to decrease MLL protein levels. MLL proteins were downregulated by approximately 40% using disulfiram at a concentration of 10 $\mu$ M.

Further experiments established that copper enhances the effect of disulfiram on MLL degradation. Studies in glioblastoma (Liu *et al.*, 2012) and in breast cancers (Chen *et al.*, 2006) showed an enhanced anti-tumour effect of disulfiram in the presence of copper. We reasoned that the co-administration of copper could enhance degradation of MLL proteins promoted by disulfiram. Our experiments clearly showed that 16 hours of co-treatment with copper and disulfiram completely ablated MLL wild type and MLL fusion proteins, while the treatment with copper alone did not affect MLL proteins levels. The lowest concentration of disulfiram inducing MLL degradation, when in combination with copper at 1 $\mu$ M, was 0.3 $\mu$ M. This concentration is much lower than the serum peak concentrations detected in body of alcoholic patients on disulfiram therapy. Copper is a micronutrient essential for several biological processes and it plays a role in redox reactions triggering the generation of reactive oxygen species (ROS). Therefore in the human body the copper levels need to be tightly regulated. To reduce the amount of unbound (free) copper from participating in redox reactions, the majority of copper is associated to enzyme

prosthetic groups or bound to chaperone proteins. The 90-95% of copper present in the human body is bound to ceruloplasmin. Ceruloplasmin is a serum glycoprotein and the major copper carrier [reviewed in (Kono, 2013) (Manto, 2014) (Uauy et al., 1998)]. Next, to identify the shortest length of treatment inducing MLL degradation we performed a time course. Our experiments demonstrated that disulfiram required a minimum of 12 hours to deplete MLLwt and MLL fusion proteins.

*In vivo* DSF is rapidly reduced in its metabolite diethyldithiocarbamate (DDC), which in presence of copper ions is able to form complexes with them (figure 28). Evidence in the literature (Han *et al.*, 2013, Kimoto-Kinoshita *et al.*, 2004) suggests that DDC-copper mixtures had the same pro-apoptotic and anti-tumour effect as DSF-copper mixtures. We studied consequences of co-treatment of copper and DDC on MLL-AF6 rearranged cells. Data from this study confirmed that, as expected, DDC decreased MLL protein levels to the same extent as DSF.

On the basis of our results we can conclude that both disulfiram and its metabolite diethyldithiocarbamate in combination with copper were able to target both MLL wild type and MLL fusion proteins. Ablain and de Thé (Ablain and de The, 2011) showed that by targeting leukaemic fusion proteins it is possible to promote leukaemic cell differentiation and improve cure rates of patients. Here we achieved complete degradation of MLL fusion proteins which may results in a block of leukaemic activity.

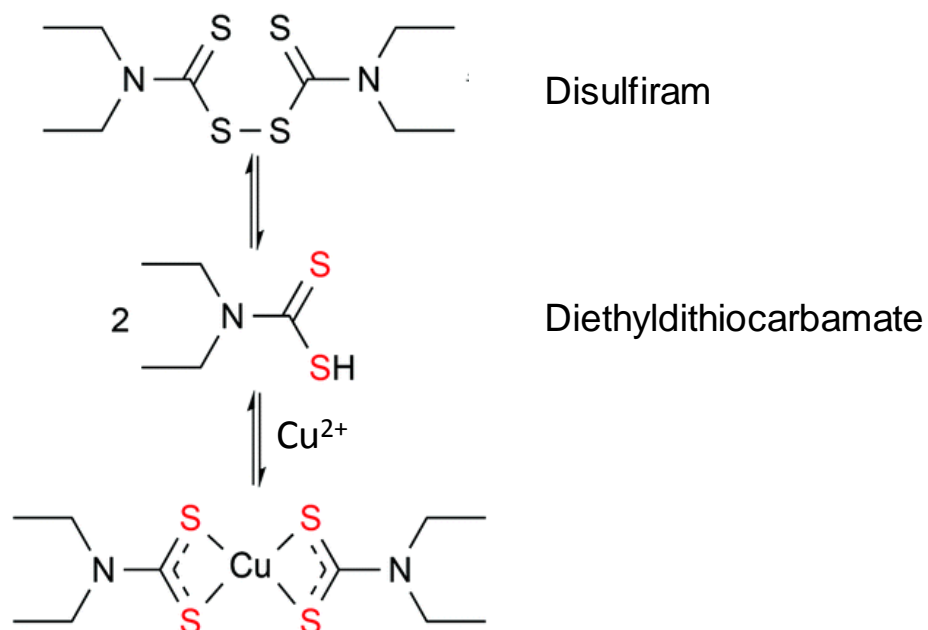


**Figure 28 Formation of the DSF-copper complex in vivo**

In the human body DSF is immediately reduced, in the acidic stomach environment or in the bloodstream, by the glutathione reductase system in its first metabolite diethyldithiocarbamate (DDC). DDC is a chelator of metal ions like copper and in presence of copper ions is able to form complexes with them.

## 5 CHAPTER V: INVESTIGATING THE EFFECT OF DISULFIRAM ON GENE EXPRESSION

### 5.1 Introduction

Independent groups studying normal haematopoiesis and leukaemogenesis examined the role of *HOXA* genes and *MEIS1* in the induction of AML. *HOXA* proteins are a family of transcription factors controlling development and cell fate in *Drosophila melanogaster*. In vertebrates the *HOXA* genes encode for transcription factors that regulating several biological processes and among those they regulates also differentiation and proliferation of haematopoietic cells. *MEIS1* or myeloid ecotropic viral integration site 1 is a *HOXA* co-factor associated with *MLL* rearranged leukaemia [reviewed in (Collins and Hess, 2016)] which, together with *HOXA*, plays a crucial role in embryonic development and haematopoiesis. Tight transcriptional regulation of these two genes is ensured by *MLL*. A key transcription factor downstream of these two factors is *c-MYB* that is required during normal haematopoiesis as well as to maintain leukaemia (Hess *et al.*, 2006). During normal haematopoiesis *HOXA*, *MEIS1* and *c-MYB* expression is restricted to haematopoietic stem cells (HSC) and to early progenitors. Upon further differentiation, their expression decreases. A common feature in *MLL* leukaemias is the constitutive and extremely high expression of *HOXA*, *MEIS1* and *c-MYB*. Their increased expression by *MLL*-fusion proteins is considered to be responsible for the block of normal haematopoietic development and for onset of leukaemia [reviewed in (Collins and Hess, 2016)].

Our previous experiments showed that disulfiram, in combination with copper, degraded wtMLL and MLL fusion proteins. This event is expected to result in downregulation of MLL-fusion target genes. Here we evaluated the effect of DSF on gene expression. With this purpose we performed RNA sequencing in cells expressing the MLL-AF6 fusion, treated with DSF and copper for 16 hours. The generated DSF signature was compared to published MLL fusion gene sets using a Gene Set Enrichment Analysis (GSEA) from the Broad Institute. GSEA is a powerful method to identify pathways of gene expression in predefined groups of genes or gene sets. Gene sets are groups of genes sharing chromosomal location or common biological features. The software algorithm uses statistical approaches to determine whether gene sets are either positively or negatively correlated. The benefit of this method is that it analyses sets of genes collectively, rather than arbitrarily focusing on individual differentially expressed genes. The main advantage of this approach is in the statistical power of the method, which means that a set of differentially expressed genes is more likely to stand out from the background noise than individual genes (Subramanian *et al.*, 2005). In this chapter we will investigate the effect of DSF on the gene expression in MLL rearranged cells.

## **5.2 Results**

### **5.2.1 Effect of disulfiram and diethyldithiocarbamate on gene expression**

The western blot studies described in the chapter 4 of this thesis showed that disulfiram and its first metabolite diethyldithiocarbamate, in combination with copper, were able to induce proteolysis of wtMLL and MLL fusion proteins. Degradation of MLL fusion proteins is expected to have an effect on expression of downstream target genes.

To identify genes affected by disulfiram we treated cells expressing the MLL-AF6 fusion with the DSF-copper mixture. After 16 hours of incubation total RNA was extracted. RNA integrity was assessed by analysing the RNA integrity number (RIN) on TapeStation reports. The high RIN score indicated that the integrity of all RNA samples was sufficient for downstream analyses. RNA purity was assessed analysing the ratio of absorbance at 260nm to 280nm. In all samples this ratio was between 1.9 and 2, indicating the high purity of our samples. Table 13 summarise concentration, purity and integrity of all RNA samples. RNA samples were then submitted to UCL Genomics for sequencing. Sequencing results were analysed using software Galaxy. The pipeline generated by Tony Brooks from UCL Genomics included the Trimmomatic quality control tool to remove poor quality reads from the analysis. Sequences were aligned to the human genome (GRCh38) using the STAR aligner, and aligned reads were then assigned to genes. The SARTools, a DESeq2 R

Samples	RNA (ng/ $\mu$ l)	A260/280	RIN
DSF-Copper-1	81.0	2.0	8.3
DSF-Copper-2	35.5	1.9	7.3
DSF-Copper-3	35.2	2.0	7.40
CTRL-1	403.7	1.9	10
CTRL-2	349.7	2.0	10
CTRL-3	362.6	2.0	10

**Table 13 Concentration, purity and integrity of RNA samples used in RNA-seq analysis at 16 hours**

The table summarise concentration, purity and integrity of RNA samples submitted for sequencing. RIN: RNA integrity number.

software, allowed the quality control of raw data and the analysis of differentially expressed genes in controls versus disulfiram treated cells (figure 29).

In order to evaluate the effect of DSF on gene expression we analysed RNA-seq results using the Gene Set Enrichment Analysis (GSEA) software. Since an MLL-AF6 gene expression profile was not published before we decided to compare our DSF expression profiles with the published MLL-AF9 and MLL-AF4 gene sets (Bernt *et al.*, 2011, Guenther *et al.*, 2008). The GSEA showed a negative enrichment for both these gene sets (figure 30). Negative enrichment indicates an anti-correlation between gene sets. Thus, genes upregulated by MLL-AF9 or MLL-AF4 were downregulated in the DSF treated cells. This result indicates that DSF interfered with the leukaemic transcription programme set up by the MLL fusion proteins.

To validate RNA-seq data and to expand our data to multiple MLL fusion proteins, we measured the expression levels of known MLL fusion downstream target genes in presence or absence of DSF or of its metabolite, DDC. Well studied MLL fusion target genes are *HOXA10*, *MEIS1* and their target *c-MYB*. We treated three human MLL rearranged cell lines (THP-1, SHI-1 and MV4-11) for 16h with DSF and copper or with DDC and copper. Total RNA was extracted and expression of *HOXA10*, *MEIS1* and *c-MYB* was quantified by qRT-PCR. Treatment with the DSF-copper and DDC-copper mixtures resulted in a very significant downregulation of all three MLL fusion target genes in THP-1, SH-1 and MV4-11 cells (figure 31).

Taken all together these results demonstrate that 16 hours of treatment with DSF-copper and DDC-copper mixtures is sufficient to induce downregulation in the expression of downstream MLL fusion target genes, besides inducing MLL fusion protein degradation.

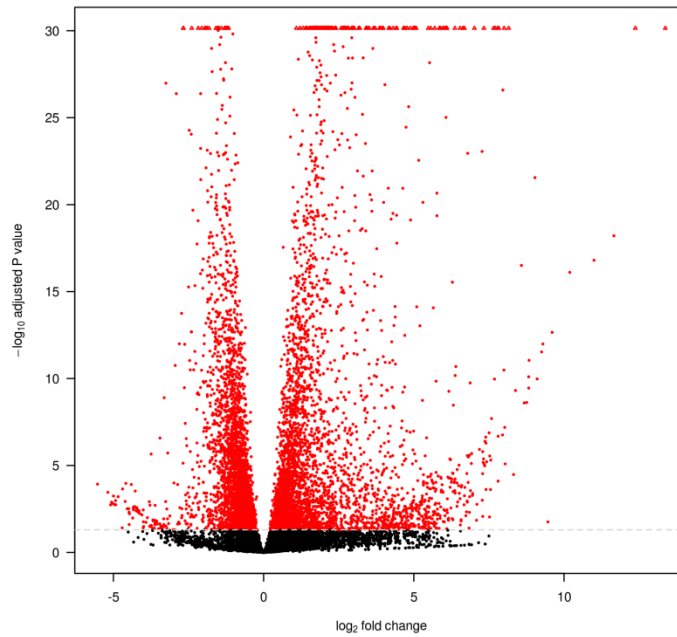


**Figure 29 Differential gene expression after 16 hours of DSF treatment**

The volcano plot shows the total number of differentially expressed genes in control versus disulfiram treated cells after 16 hours of treatment. The log of the adjusted P-value is plotted against the log2 ratio of differential expression. Each dot represents a gene. Red dots represent genes whose expression was significantly changed after disulfiram treatment while black dots indicate genes not affected by treatment, or not significantly expressed in SHI-1 cells.

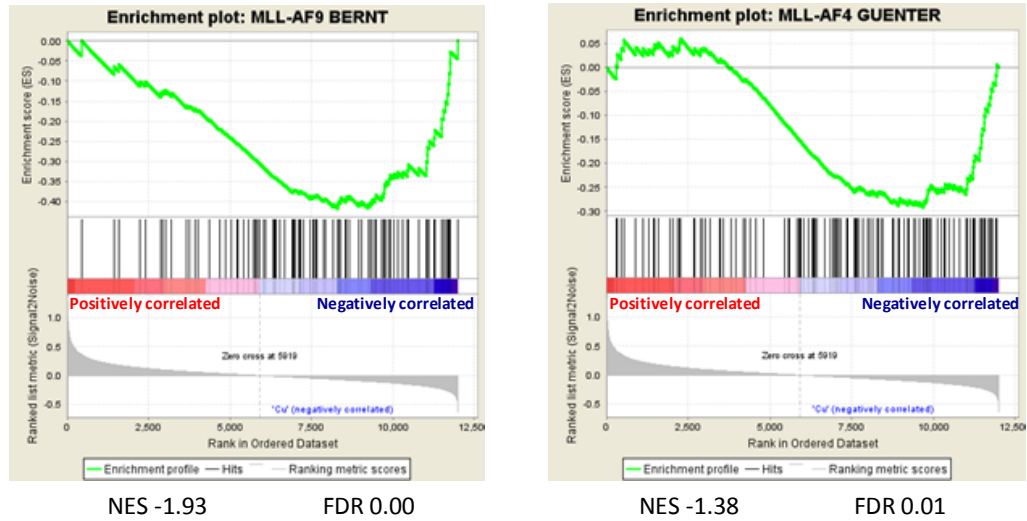


**Figure 30 Gene Set Enrichment Analysis (GSEA) results after 16H**

GSEA of the RNA-seq data from DSF treated SHI-1 cells, examining enrichment of MLL-AF9 and MLL-AF4 gene sets, as published by Bernt et al., 2011, and Guenther et al., 2008. The plots show significant negative enrichment for both MLL-AF9 and MLL-AF4 gene sets in disulfiram treated samples. NES: normalised enriched score; FDR: false discovery rate.

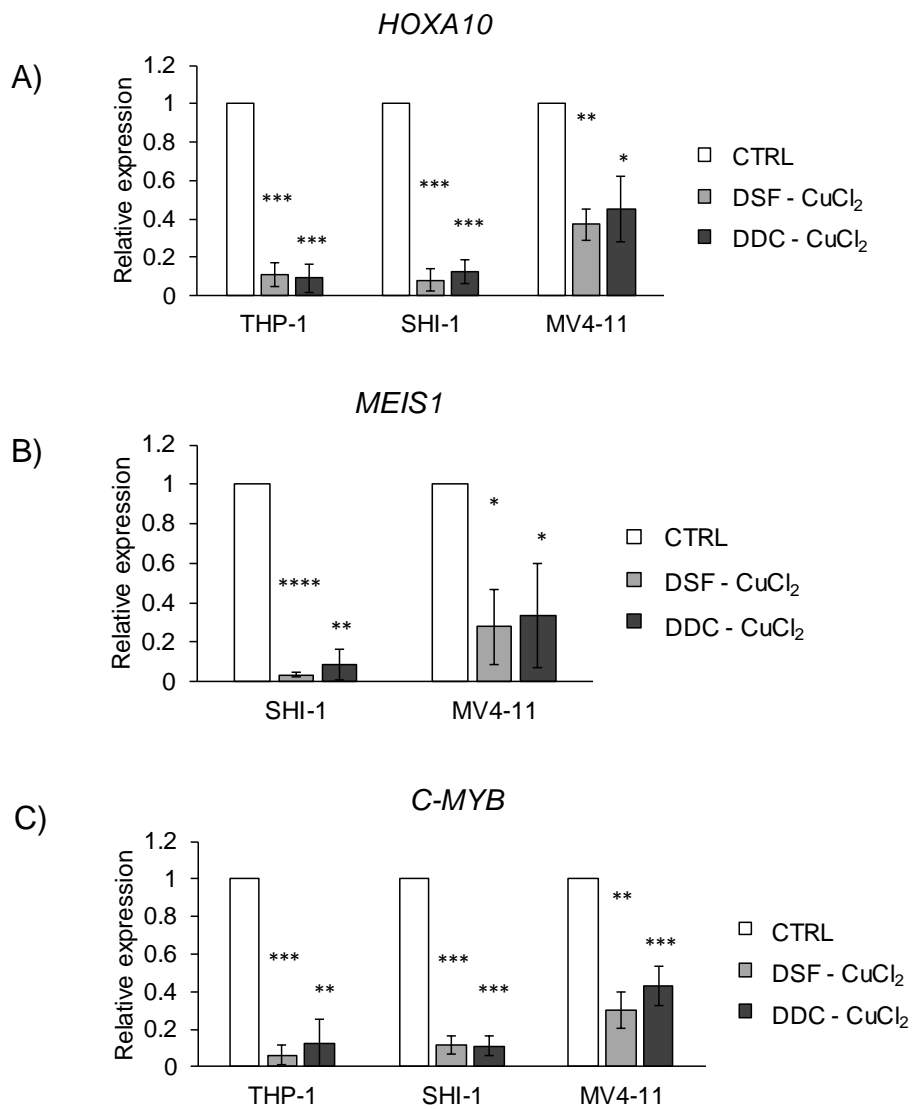


**Figure 31 Effect of DSF and DDC on gene expression at 16 hours**

(A)(B)(C) The bar charts show the relative mRNA expression of *HOXA10*, *MEIS1* and *c-MYB* in THP-1, SHI-1 and MV4-11 cells after 16 hours treatment with 0.3μM DSF- 1μM CuCl<sub>2</sub> (light grey bars), 0.6μM DDC-1μM CuCl<sub>2</sub> (dark grey bars) or vehicle control (white bars). Total RNA was extracted using the QIAGEN extraction kit, its concentration and quality was determined using NanoDrop ND-100 (data not shown). mRNA expression of genes of interest was measured by qRT-PCR. Columns represent mean of three independent experiments and the error bars represent S.D. P-values comparing treated samples to untreated controls were calculated using one-sample t-test. \*P<0.05, \*\*P<0.01, \*\*\*P<0.001.

### 5.2.2 Examining gene expression changes after short exposures to DSF.

Our previous studies showed that the mixtures DSF-copper and DDC-copper induced degradation of wtMLL and MLL fusions proteins after 12 hours. By following a time course of MLL fusion target gene expression we aimed to establish the earliest time-point at which DSF treatment affected the MLL leukaemic gene signature.

We evaluated the expression of MLL target genes after administration of DSF and copper over different periods of time. We exposed SHI-1 cells to the mixture DSF-copper, we extracted total RNA at each time point and we measured *HOXA10* expression by qRT-PCR. RNA after 16 hours of treatment was used as control. The graph in figure 32 showed that downregulation of *HOXA10* expression was detected as early as 4 hours after addition of DSF-copper. This result was surprising as it suggests that disulfiram affects expression of MLL target genes before any MLL degradation becomes detectable.

To validate this result and to expand our analysis to multiple fusion proteins we measured the expression of the major MLL fusion target genes in the panel of AML cell lines used in this study. Total RNA was extracted from THP-1, SHI-1 and MV4-11 treated for 4 hours with the DSF-copper or DDC-copper mixtures. Results of the qRT-PCR are summarised in figure 34. *HOXA10*, *MEIS1* and *c-MYB* expression was significantly downregulated in all the cell lines (figure 33). To further validate these findings we performed western blot analysis of MLL

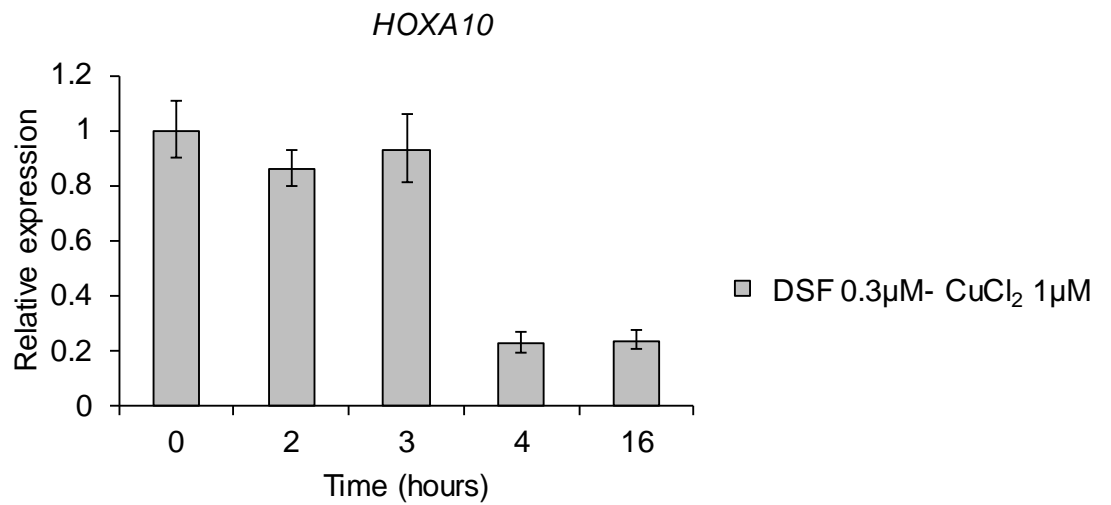


**Figure 32 Time-course of *HOXA10* expression after DSF treatment**

The graph shows the relative mRNA expression of *HOXA10* in SHI-1 cells treated for 0, 2, 3, 4 and 16 hours with 0.3μM DSF and 1μM CuCl<sub>2</sub>. Total RNA was extracted and its concentration and quality was determined using NanoDrop ND-100 (data not shown). mRNA expression of genes of interest was measured by qRT-PCR. Columns represent the mean of triplicates measurements. The error bars represent S.D. These data were obtained from a single experiment.

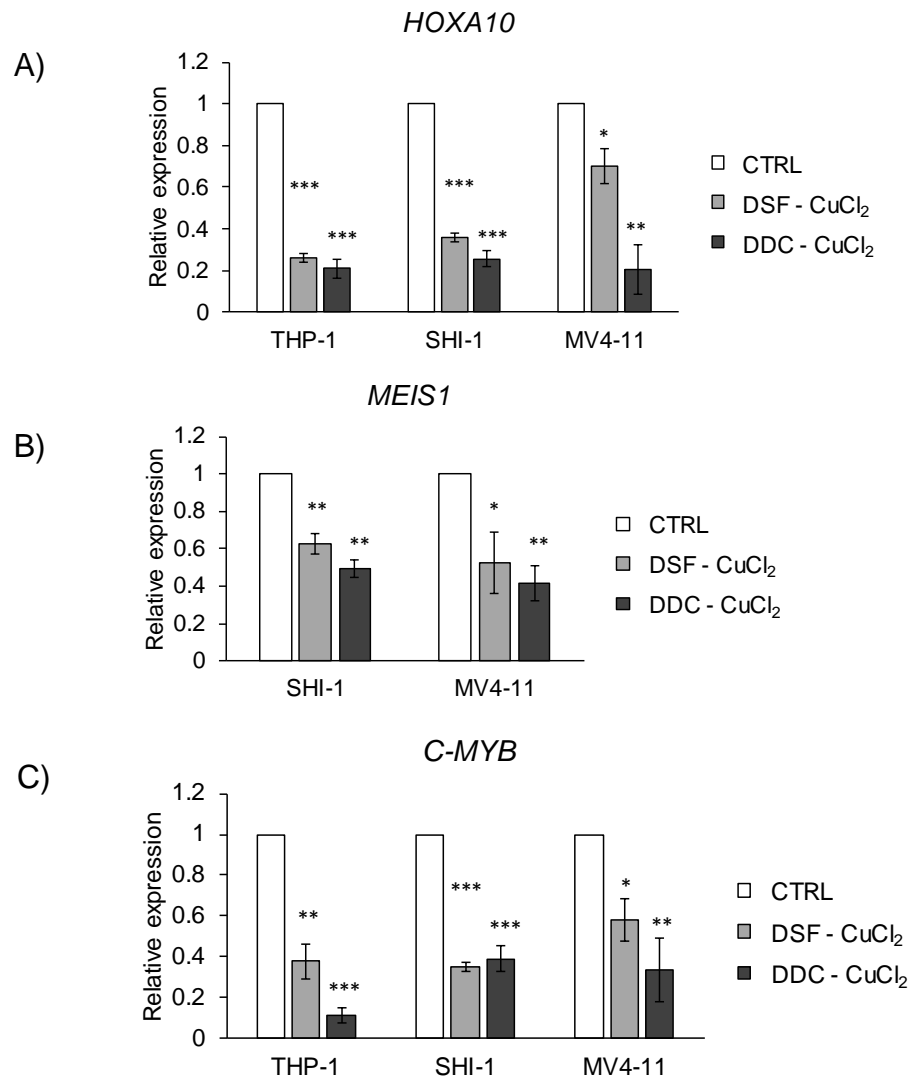


**Figure 33 Effect of DSF and DDC on gene expression at 4 hours**

(A)(B)(C) The graphs show the relative mRNA expression of *HOXA10*, *MEIS1* and *c-MYB* in THP-1, SHI-1 and MV4-11 cells after 4 hours of treatment with 0.3 $\mu$ M DSF-1 $\mu$ M CuCl<sub>2</sub> (light grey bars), 0.6 $\mu$ M DDC-1 $\mu$ M CuCl<sub>2</sub> (dark grey bars) or vehicle control (white bars). Columns represent mean of three independent experiments and the error bars represent S.D. P-values comparing treated samples to untreated controls were calculated using one-sample t-test.

\*P<0.05, \*\*P<0.01, \*\*\*P<0.001

protein levels in MLL-AF6, MLL-AF4 and MLL-AF9 cell lines after 4 hours stimulation with the DSF-copper mixture (figure 34). After disulfiram administration wild type MLL and MLL fusion protein levels were comparable to levels detected in untreated control samples.

All together these surprising data revealed that the MLL leukaemic program was already affected after only 4 hours of treatment with disulfiram and copper. After 4 hours of treatment DSF downregulated the expression of MLL target genes but degradation of wild type MLL and MLL fusion proteins was detectable only after longer exposures to the drug (12-16 hours).

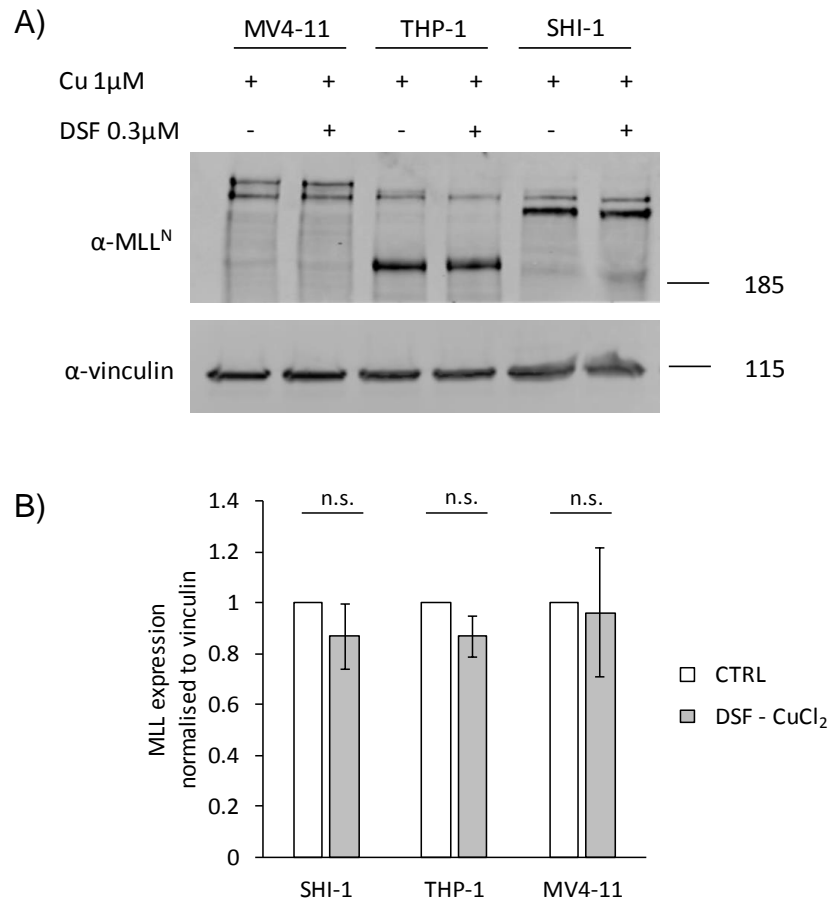


**Figure 34 Effect of short period exposures to disulfiram on protein levels**

The western blot analysis shows MLL protein expression in three MLL rearranged cell lines (A). Lysates from untreated and treated cells were loaded into a 7% bis-acrylamide gel. After transfer membranes were incubated O/N at 4°C with a mouse anti-human MLL<sup>N</sup>/HRX (clone N4.4). Anti-vinculin antibody was used as protein loading control. Membranes were imaged using Odyssey CLX imaging system. The bands obtained were quantified using the software Image Studio provided by the manufacturer. The intensities of the bands were normalised to the intensity of the loading control. (B) The graph represents the quantification of the MLL-fusion protein levels normalised to vinculin. The bars represent the average of three independent experiments and the error bars represent standard deviations. The P-value was obtained comparing treated samples to untreated using the One-sample t-test, n.s. P $\geq$ 0.05.

### 5.2.3 Discussion

To investigate the effects of DSF on transcription of MLL target genes, we generated a DSF gene expression profile by sequencing RNA from cells, expressing the MLL-AF6 fusion, treated with the DSF-copper mixture for 16 hours. Since a MLL-AF6 gene expression profile has not been published before, we compared the DSF gene expression changes to MLL-AF9 and MLL-AF4 gene sets already published (Bernt *et al.*, 2011, Guenther *et al.*, 2008) using the GSEA software. Analysis showed a negative enrichment of the published MLL fusion gene sets in the DSF gene expression profile. This indicates that the expression of target genes, usually upregulated in cells expressing MLL-AF9 or MLL-AF4 fusion, was downregulated in disulfiram treated samples. These results were then validated by qRT-PCR. Downregulation of MLL-fusion target genes (*HOXA10*, *MEIS1* and *c-MYB*) was confirmed in THP-1, SHI-1 and MV4-11 cells. Data from RNA-seq and qRT-PCR performed at 16 hours, combined with western blot at the same time point (showed in chapter 4) suggested that gene expression changes were a consequence of the degradation of MLL-fusion proteins.

By analysing changes in gene expression over different periods of time we found that *HOXA10* mRNA was unexpectedly downregulated already after 4 hours of treatment. To validate this result we measured, by qRT-PCR, the expression of MLL-fusion target genes in SHI-1, THP-1 and MV4-11 cells, untreated or treated for 4 hours with DSF-copper or DDC-copper mixtures. The qRT-PCR analysis confirmed that MLL-fusion target genes were significantly downregulated in all the cell lines after only 4 hours of treatment. Western blot

experiments confirmed that MLL proteins degradation was not detectable after short exposures to the drug (4 hours) but required longer exposures (16 hours).

In conclusion, our exciting findings indicated that 4 hours of treatment with DSF and copper were sufficient to induce downregulation of MLL fusion target genes but were not sufficient to degrade MLL-fusion proteins. MLLwt and MLL-fusion protein degradation was detectable after a minimum treatment of 12 hours. We hypothesised that this difference between proteins degradation and downregulation of their target genes (*HOXA10*, *MEIS1*, *c-MYB*) could be a consequence of a loss of MLL-fusion transcriptional regulation due to a reduced ability of MLL-fusions proteins to bind the promoters of target genes. In wtMLL and in MLL-fusion proteins the region responsible to recognise and bind the DNA is the CXXC domain. This domain is characterised by a Zn finger like motif containing two zinc atoms connected each to four cysteine residues, through disulphide bonds. Point mutations in MLL CXXC domain abrogate the myeloid transformation mediated by MLL fusion proteins and abolished recognition and DNA binding (Ayton *et al.*, 2004). Allen et al demonstrated that point mutations involving cysteine residues caused a zinc release from CXXC domain, resulting in unfolding of the CXXC domain itself (Allen *et al.*, 2006). These studies assessed how the integrity of connections between cysteine residues and zinc ions was essential to maintain the fold of MLL CXXC domain and consequently the DNA binding ability. A recent study in prostate cancer showed that disulfiram inhibits the activity of DNA methyltransferase 1 (DNMT1), an enzyme responsible to methylate CpG at genes promoter (Lin *et al.*, 2011), by oxidising cysteine residues located in the DNMT1 CXXC motif. Mutations involving the

cysteine residues located in DNMT1 CXXC region impair DNA binding of DNMT1 (Pradhan *et al.*, 2008). Other similarities between these two CXXC domains (figure 36) were highlighted in a study published by Riesner (Risner *et al.*, 2013) where the CXXC domain belonging to DNMT1 functionally replaced the MLL-AF9 CXXC domain causing leukaemia in vivo. Given the structural similarities across DNMT1 and MLL we hypothesised that the metal ions chelator DSF could interfere with MLL-fusion CXXC domain. Disulfiram could abrogate the DNA binding ability of MLL-fusions by targeting the cysteine residues of the MLL CXXC domain. This event would consecutively result in the detachment of MLL fusions from the DNA and in a block of the MLL fusion target genes transcription.

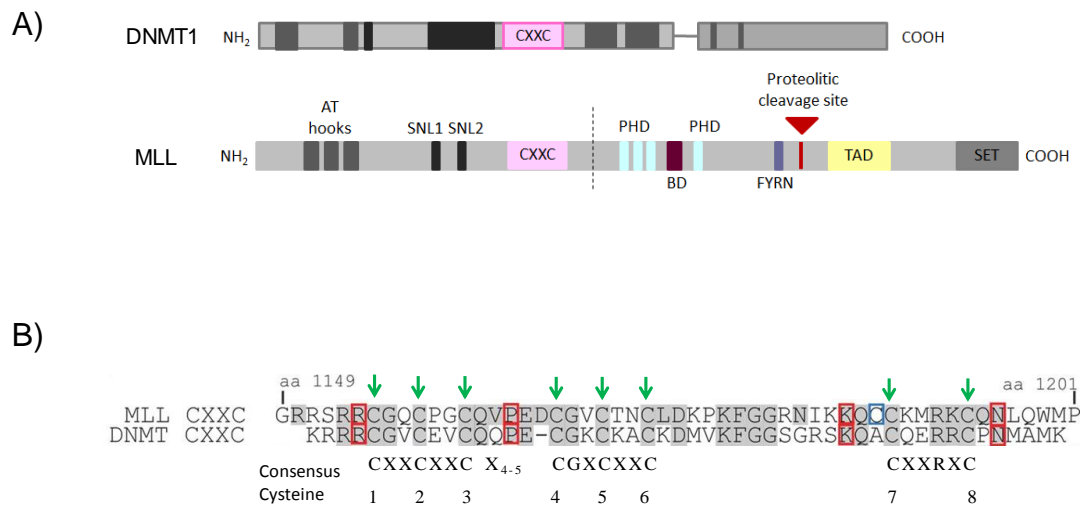


**Figure 35 Similarities between MLL and DNMT1**

DNMT1 and MLL share a conserved CXXC zinc finger motif (A). Alignment of amino acid sequences showing the conservation of the CXXC domain between DNMT1 and MLL. The identical residues in both sequences are highlighted in grey boxes, the red boxes indicate residues identical in MLL and DNMT1 but non identical in CXXC motif of other methyl binding proteins. The residue 1188 in the blue box indicates a cysteine residue conserved in vertebrate MLL paralogs but in DNMT this position is occupied by an alanine. The green arrows indicate the 8 highly conserved cysteine residues (B).

## **6 CHAPTER VI: Studying disulfiram mechanism of action**

### **6.1 Introduction**

The data discussed in chapter 5 of this thesis revealed that co-administration of disulfiram and copper for 4 hours was sufficient to induce downregulation of MLL fusion target genes. However, western blot analysis showed that MLL and MLL fusion proteins were not degraded at the same time point (4h) in fact MLL protein degradation was only detected after prolonged incubations (12-16h). We reasoned that reduced gene expression may be due to a reduced ability of MLL fusions to bind the promoter regions of target genes, and that this may precede fusion degradation. The portion of wtMLL and MLL-fusion proteins able to bind the DNA is the CXXC domain. This domain shows a high degree of homology to the CXXC domain of DNMT1 (Risner et al., 2013). It has been shown that DSF is able to inhibit the activity of DNMT1 by oxidising cysteine residues located in the DNMT1 CXXC motif (Lin et al., 2011). We theorised that DSF could inhibit the MLL-fusion binding to the promoter of their target genes by oxidising the cysteine residues located in the CXXC domain of MLL-fusions. Consequently, the detachment of MLL-fusion proteins from the DNA would cause a block of target gene transcription, fusion protein degradation being a secondary event.

In order to understand the underlying mechanism at the base of this dysregulation we immunoprecipitated and sequenced the chromatin regions interacting with wtMLL and MLL-fusions. A study from Martens' Laboratory

showed that the shared and the specific MLL-AF9 and MLL-AF4 target genes are marked by H3K4me3 and are enriched in H3K27ac (Prange et al., 2017). Therefore, considering that the drug treatment might affect the epigenetic signature of target loci, we immunoprecipitated and sequenced also chromatin regions marked by H3K4me3 and H3K27ac. ChIP-seq is a powerful technique combining chromatin immunoprecipitation (ChIP) with next-generation sequencing (NGS). This methodology allows genome-wide identification of DNA binding sites of transcription factors or co-factors. The procedure requires first the cross linking of protein/transcription factors to the DNA to preserve the regions of interaction for further analysis. Thus it is usually achieved by using one or two fixatives. The most common cross-linker is formaldehyde, which is not very effective at studying transcription factors or in general proteins that do not directly bind to DNA. In these cases, two-step crosslinking is more appropriate. The advantage of double fixation is that the first fixative promotes covalent links between proteins not directly linked to DNA and the second allows reversible protein-DNA fixation. The following steps are sonication, a step necessary to shear the DNA in small fragments (usually 200-400 bp), and co-immunoprecipitation of DNA fragments, using antibodies directed against the protein of interest. The study of the regions of interaction between proteins and DNA requires the reversal of protein-DNA cross-links. Finally the DNA is purified and sequenced.

If our hypothesis is correct in absence of disulfiram the ChIP-seq assay is expected to show binding of MLL and MLL-fusions to the co-immunoprecipitated regions of target loci while in presence of disulfiram we

expect to find a decreased binding of wtMLL/MLL-fusion to co-immunoprecipitated chromatin.

## 6.2 Results

### 6.2.1 Disulfiram impairs the DNA binding domain of MLL fusions

We performed MLL chromatin immunoprecipitation (ChIP) in THP-1 cells, which express the wtMLL and the MLL-AF9 fusion protein, treated with disulfiram and copper for 4 hours and in untreated control cells. We reasoned that drug treatment could alter the epigenetic signature so we immunoprecipitated also H3K4me3 and H3K27ac, marks of active transcription sites and open chromatin, respectively.

In order to immunoprecipitate chromatin regions interacting with MLL and/or MLL-AF9 we used a protocol based on a two-step crosslinking. In the first step the disuccinimidyl glutarate (DSG) promoted covalent links between proteins that, in a second step, were reversibly linked to the DNA using formaldehyde. To immunoprecipitate DNA regions marked by H3K4me3 and H3K27ac we used a protocol in which crosslinking is achieved by using a single cross linker agent: formaldehyde. The immunoprecipitation of fragments interacting with wtMLL and MLL-AF9 required testing of different antibodies directed against MLL N-terminal domain. To amplify promoter regions of MLL/MLL-AF9 target genes we had to test also several primers. All antibodies and primers tested are listed in Table 6 and Table 7 in the Materials and Methods section (Chapter II).

The fragments of DNA immunoprecipitated using the MLL-N antibody from Bethyl Labs were analysed by q-PCR, using primers amplifying the *HOXA10*

target gene region and as a control the gene desert region on chromosome 21 (*GD21*). Gene desert regions are areas of the genome lacking protein coding genes and can be used as negative controls. The q-PCR showed wtMLL/MLL-AF9 enrichment in the *HOXA10* locus (Figure 36A). We submitted these DNA samples to UCL Genomics for sequencing. In the facility, DNA fragments were prepared for sequencing by constructing ChIP libraries. Library construction is essential to make DNA fragments compatible for the Illumina sequencing system. The 5' ends of DNA fragments required phosphorylation while the 3' ends a dA-tailing. Barcode adapters were ligated to the DNA to be amplified prior to start the sequencing. Unfortunately, the library preparation failed for DNA fragments immunoprecipitated using the MLL-N antibody from Bethyl Laboratories. The TapeStation traces after the library preparation, shown in figure 36B, revealed a poor DNA yield. The amount and the quality of the DNA immunoprecipitated using the Bethyl Laboratories antibody was not sufficient to guarantee an efficient library preparation and to generate robust and high quality sequencing.

In order to immunoprecipitate larger amounts of DNA we decided to test another ChIP grade MLL-N antibody. When we immunoprecipitated DNA fragments using the MLL-N antibody from Diagenode we found MLL enrichment in *HOXA10* (figure 36C). When we submitted these DNA samples to UCL Genomics we generated a high resolution library, and the TapeStation traces after library preparation showed that the yield of DNA preparation was much higher (Figure 36D). To immunoprecipitate DNA regions marked by H3K4me3 and H3K27ac we used a protocol in which crosslinking is achieved by using a

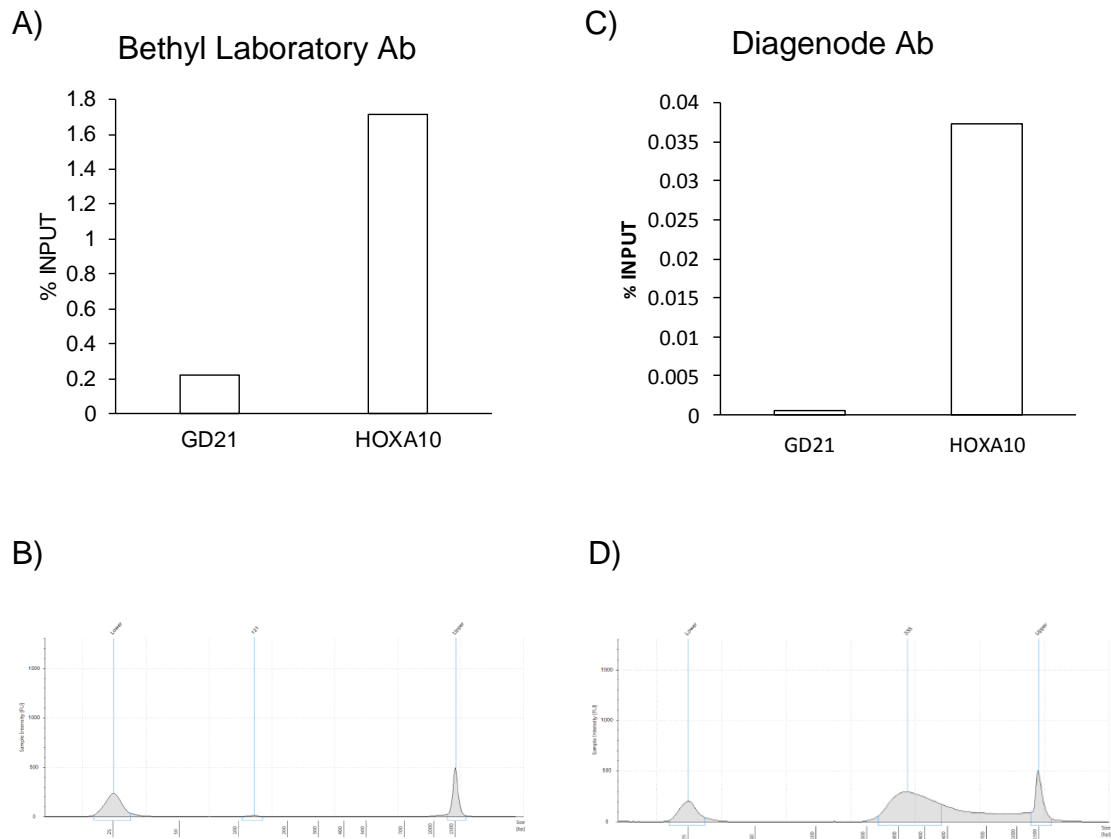


**Figure 36 ChIP and library preparation with MLL-N antibody from Bethyl Laboratories and Diagenode**

The ChIP assay was performed using the MLL-N antibody from Bethyl Laboratories or the antibody from Diagenode. The graph (A) shows the q-PCR analysis of the MLL ChIP using the Bethyl Laboratory antibody. MLL-AF9 and wtMLL were enriched in the *HOXA10* region in untreated cells. The samples were normalised to input DNA and enrichment was relative to the control gene desert region (*GD21*). Bars represent data from a single experiment. The graph (B) shows the TapeStation trace after library preparation of samples immunoprecipitated with the Bethyl antibody. The TapeStation profile shows the upper and lower ladders used for the analysis and an almost inexistent peak for the DNA immunoprecipitated using the Bethyl Laboratories antibody. The absence of a distinct peak indicated the poor DNA yield after the library preparation. The graph (C) shows the q-PCR analysis of the MLL ChIP using the Diagenode antibody. MLL-AF9 and wtMLL were enriched in the *HOXA10* region in untreated

cells. The samples were normalised to input DNA and enrichment was relative to the control gene desert region (*GD21*). Bars represent data from a single experiment. The graph (D) shows the TapeStation profile after library preparation of samples immunoprecipitated using the Diagenode antibody. The presence of a distinct peak between the two ladders (upper and lower) peaks indicated the higher yield obtained when performing CHIP assay using the MLL antibody from Diagenode.

single cross linker agent: formaldehyde. The success of the ChIP experiment was confirmed by measuring substantial enrichment of H3K4me3 or H3K27Ac at the *HOXA10* locus compared to negative control region (figure 37).

Dr Joost Martens, from Radboud University in Netherland, helped us with analysis, interpretation and correlation of sequencing data obtained in MLL, H3K4me3 and H3K27ac ChIP assays. Chromatin fragments were aligned to the human genome using the Burrows-Wheeler Alignment Tool (BWA) and peaks were called using the MACS2 software. The best characterised binding targets of wtMLL and MLL-fusions are the *HOXA* cluster genes. We detected strong binding to *HOXA* locus with the MLL-N antibody from Diagenode (figure 38A). Furthermore, we confirmed that MLL peaks were marked by H3K4me3 and enriched in H2K27ac (Prange et al., 2017). Upon 4 hours DSF-copper treatment, we noted a complete ablation of the MLL specific peaks in the *HOXA* cluster (figure 38A) indicating that DSF evicts MLL (wt and fusion) from the chromatin. We did not note quantitative changes in H3K4me3, while we observed significant overall reduction of H3K27ac (figure 38A). We confirmed the ablation of the MLL peaks (wt and fusion) in the *HOXA* locus by q-PCR analysis. We amplified the *HOXA10* target region and the gene desert region on chromosome 21 (GD21). Independent experiments showed wtMLL/MLL-AF9 enrichment in the *HOXA10* region in untreated control samples but not in DSF-copper treated (figure 39). We then analysed global changes in gene expression by RNA-seq in THP-1 cells after 4 hours of DSF-copper treatment. Sequencing results were analysed as for the previous RNA-seq and the analysis showed that the *HOXA* genes that were dynamically bound by MLL

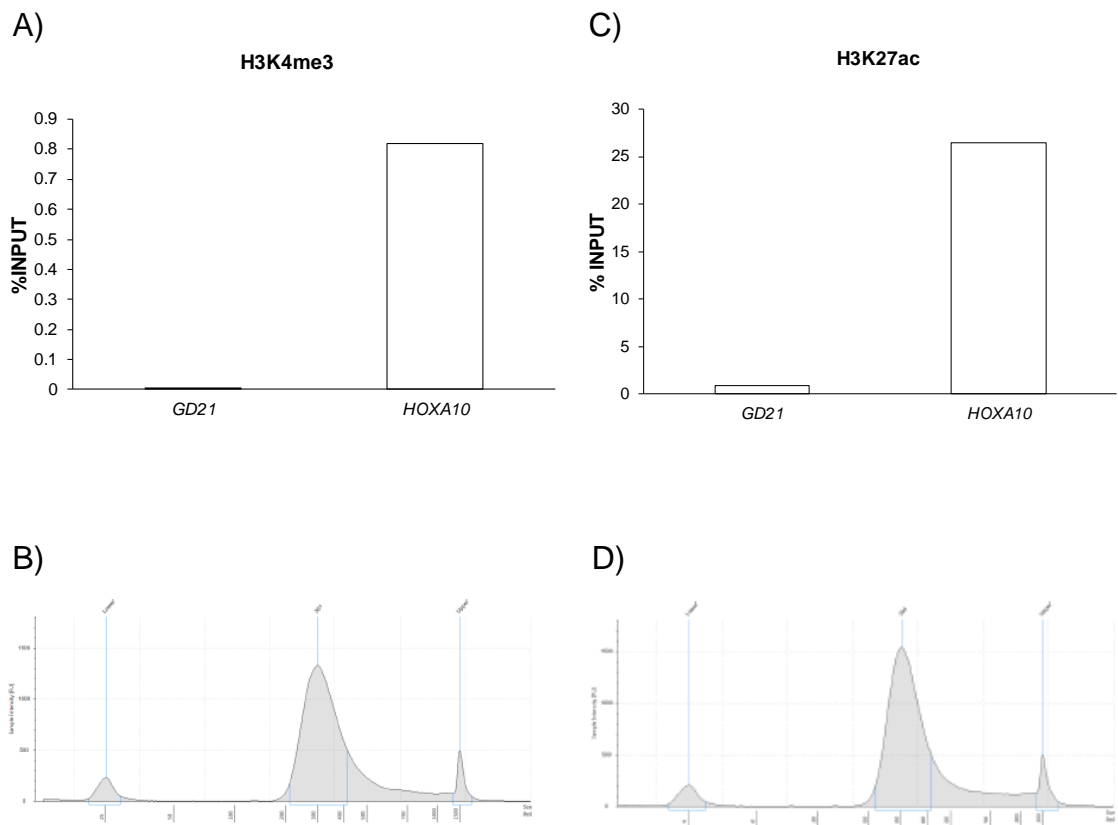


**Figure 37 ChIP and library preparation with H3K4me3 and H3K27Ac antibody**

The ChIP assay was performed using H3K4me3 and H3K27Ac antibodies. The graph (A) shows the q-PCR analysis of the H3K4me3 ChIP using. MLL-AF9 and wtMLL were enriched in the *HOXA10* region. The samples were normalised to input DNA and enrichment was relative to the control gene desert region (*GD21*). Bars represent data from a single experiment. The graph (B) shows the TapeStation trace after library preparation of samples immunoprecipitated with the H3K4me3 antibody. The TapeStation profile shows the upper and lower ladders used for the analysis and the presence of a distinct peak between the two ladders indicated the higher yield obtained in this ChIP. The graph (C) shows the q-PCR analysis of the H3K27Ac ChIP. MLL-AF9 and wtMLL were enriched in the *HOXA10* region. The samples were normalised to input DNA and enrichment was relative to the control gene desert region (*GD21*). Bars represent data from a single experiment. The graph (D) shows the TapeStation profile

after library preparation of samples immunoprecipitated using the H3K27Ac antibody. The presence of a distinct peak between the two ladders (upper and lower) peaks indicated the higher yield obtained when performing ChIP assay using the MLL antibody from Diagenode.

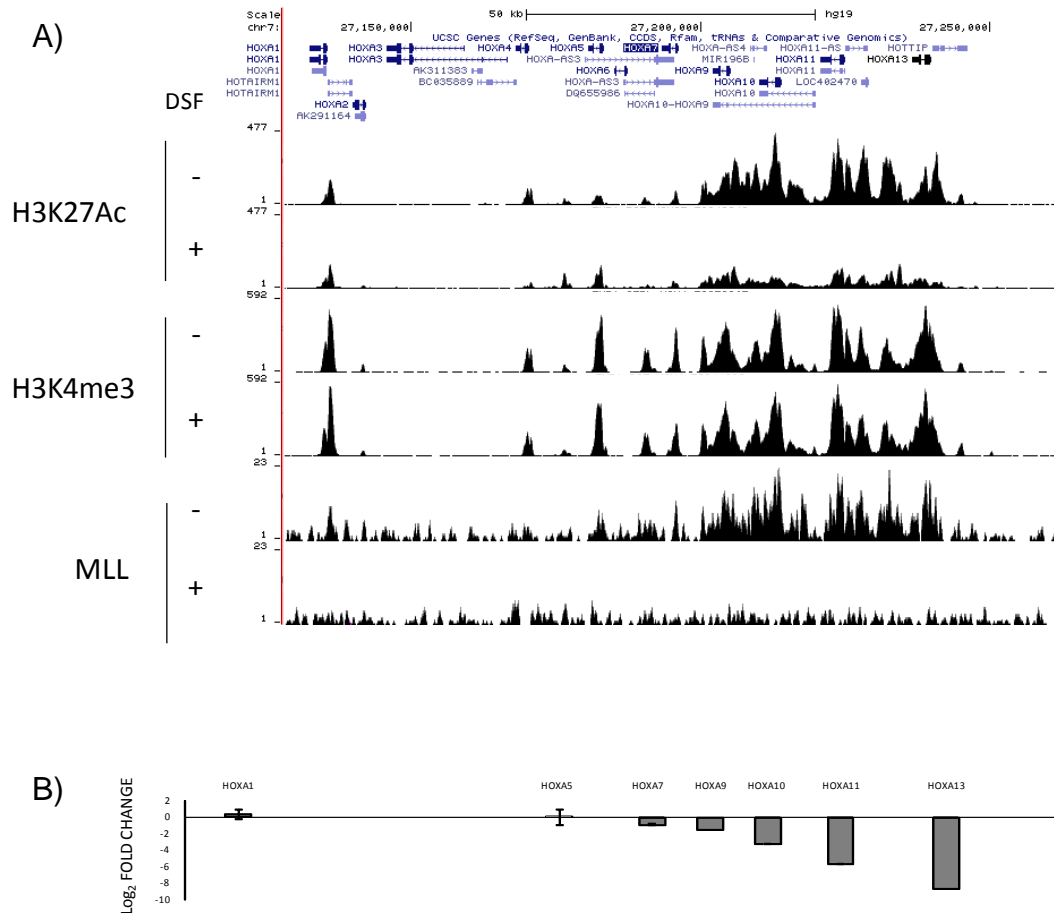


**Figure 38 Overview of MLL, H3K4me3 and H3K27ac binding at the HOXA locus**

Peaks distribution within the *HOXA* locus in THP-1 cells with or without DSF and copper treatment (A). Representative ChIP-seq tracks showing reads per million (y axis) in each sample. Chromatin regions became more or less peak reach upon treatment. Disulfiram and copper did not affect H3K4me3 status, while it caused a decreased acetylation. The absence of MLL peaks in DSF-copper treated samples indicates that wtMLL and MLL-AF9 are not able to bind anymore the immunoprecipitated chromatin regions. *HOXA* genes expression analysed by RNA-seq in THP-1 cells after 4 hours of treatment with DSF and copper (B). The bar charts represent the log<sub>2</sub> fold change and error bars the p-values.

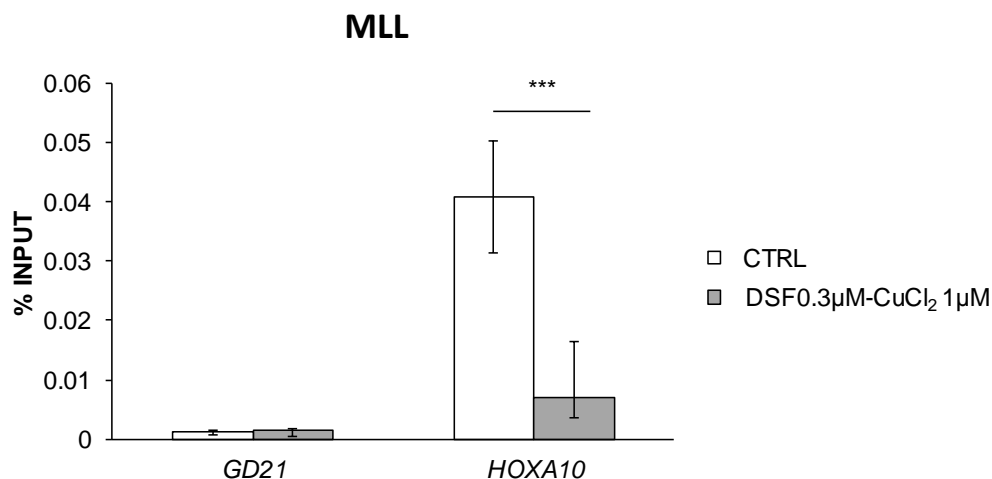


**Figure 39 Disulfiram and copper administration results in a decreased binding of MLL-AF9 to promoter regions of *HOXA10***

THP-1 cells were treated with 0.3µM disulfiram and 1µM CuCl<sub>2</sub> for 4 hours. ChIP assay was performed using the MLL-N antibody from Diagenode. The graph shows the ChIP assay validation by q-PCR. In absence of disulfiram and copper the assay showed wtMLL and MLL-AF9 enrichment in *HOXA10* target regions. In presence of the drug wtMLL and MLL-AF9 were not enriched. The samples were normalised to input DNA and enrichment was relative to the control gene desert region (*GD21*). Bar charts represent the mean of three independent experiments and the error bars represent the standard deviation. The p-value was obtained comparing enrichment in untreated cells versus enrichment in drug treated cells using an unpaired t-test; (\*\*\*) P≤0.001.

and/or MLL-AF9 fusion proteins, were strongly downregulated (figure 38B). This result correlated with the data showing reduction of H3K27ac. Figure 40 shows examples of peaks distribution in the well-characterised MLL target genes, *c-MYB* and *MEF2C*. In both cases the MLL peaks were always marked by H3K4me3, enriched in H2K27ac. After 4 hours of DSF and copper treatment, while we did not detect changes in H3K4me3, we saw a reduction in H3K27ac and MLL peaks.

Next we assessed the epigenetic changes in the whole genome. The normalised global ChIP-seq densities showed 5,703 dynamic MLL peaks (with differences greater than 3 fold change in the levels of wtMLL and/or MLL-AF9 binding) marked by H3K4me3 (figure 41A). To determine the genomic location of the binding sites we analysed the data using the Genomic Regions Enrichment of Annotation Tools (GREAT). According to the Human genome (GRCh37) GREAT localised most of the dynamic peaks (4,230 peaks) around the consensus transcriptional start sites (figure 41B). All the 5,703 dynamic MLL peaks showed co-localisation with H3K27ac. Upon DSF treatment 873 peaks showed a reduced acetylation status (greater than 3 fold change) while 18 peaks showed an increased acetylation (greater than 3 fold change) (figure 42A). 516 peaks out of the 873 peaks were localised within 1Kb of consensus transcriptional start sites (figure 42B). Next we sought to determine whether the changes in H3K27Ac at the TSS upon MLL (wt and fusion) eviction caused by DSF were correlated with gene expression changes. Therefore we compared the gene set consisting of the genes with decreased H3K27Ac (516 peaks) with RNA-seq data derived from THP-1 cells treated with DSF and copper for 4 and

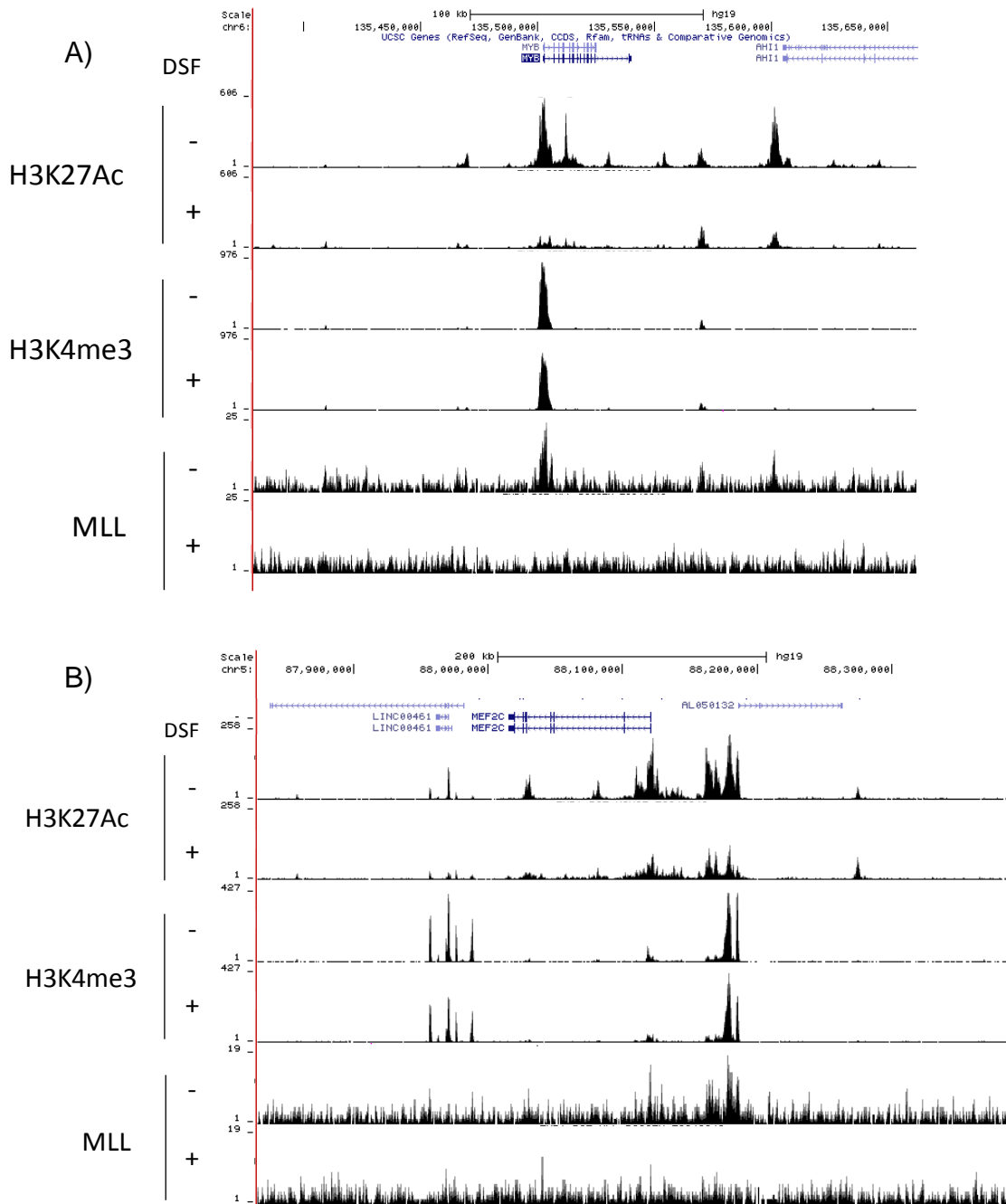


**Figure 40 Peaks distribution in *c-MYB* and *MEF2C* loci**

Overview of MLL, H3K4me3 and H3K4ac binding in *c-MYB* and *MEF2C* loci in THP-1 cells with or without DSF and copper treatment (A) (B). Representative ChIP-seq tracks showing reads per million (y axis) in each sample. Disulfiram and copper did not affect H3K4me3 status, while it caused a decreased acetylation. The absence of MLL peaks in treated samples indicates that wtMLL and MLL-AF9 are not able to bind *c-MYB* and *MEF2C* chromatin regions.

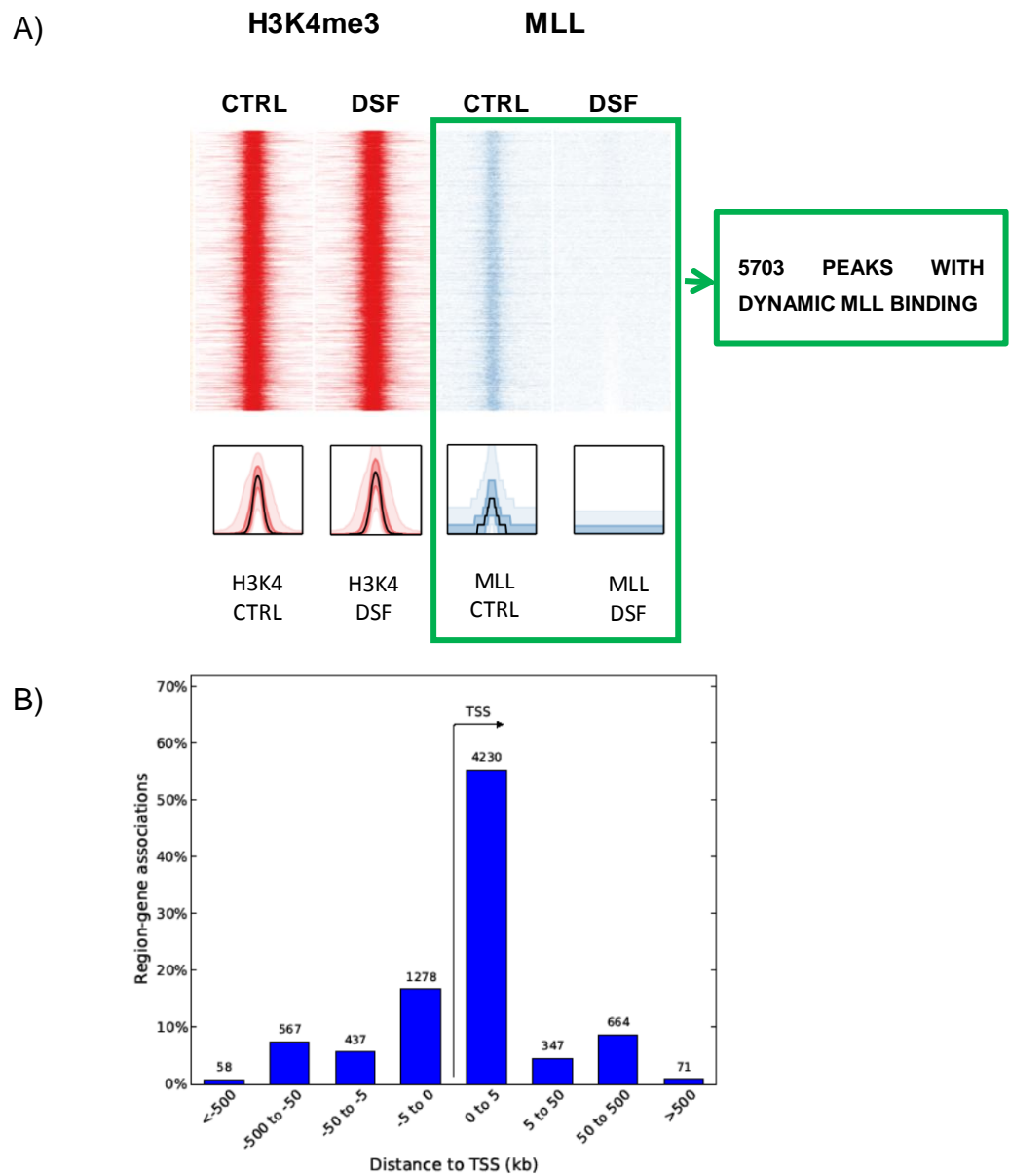


**Figure 41 Peaks with dynamic MLL binding**

The heatmap (A) shows the H3K4me3 peak distribution in red and the MLL peak distribution in blue, in treated and untreated samples. In green are highlighted the 5,703 H3K4me3 peaks that showed changes in wtMLL and MLL-AF9 binding. The graph (B) shows that 4,230 peaks out of the 5,703 were localised at the transcriptional start sites.

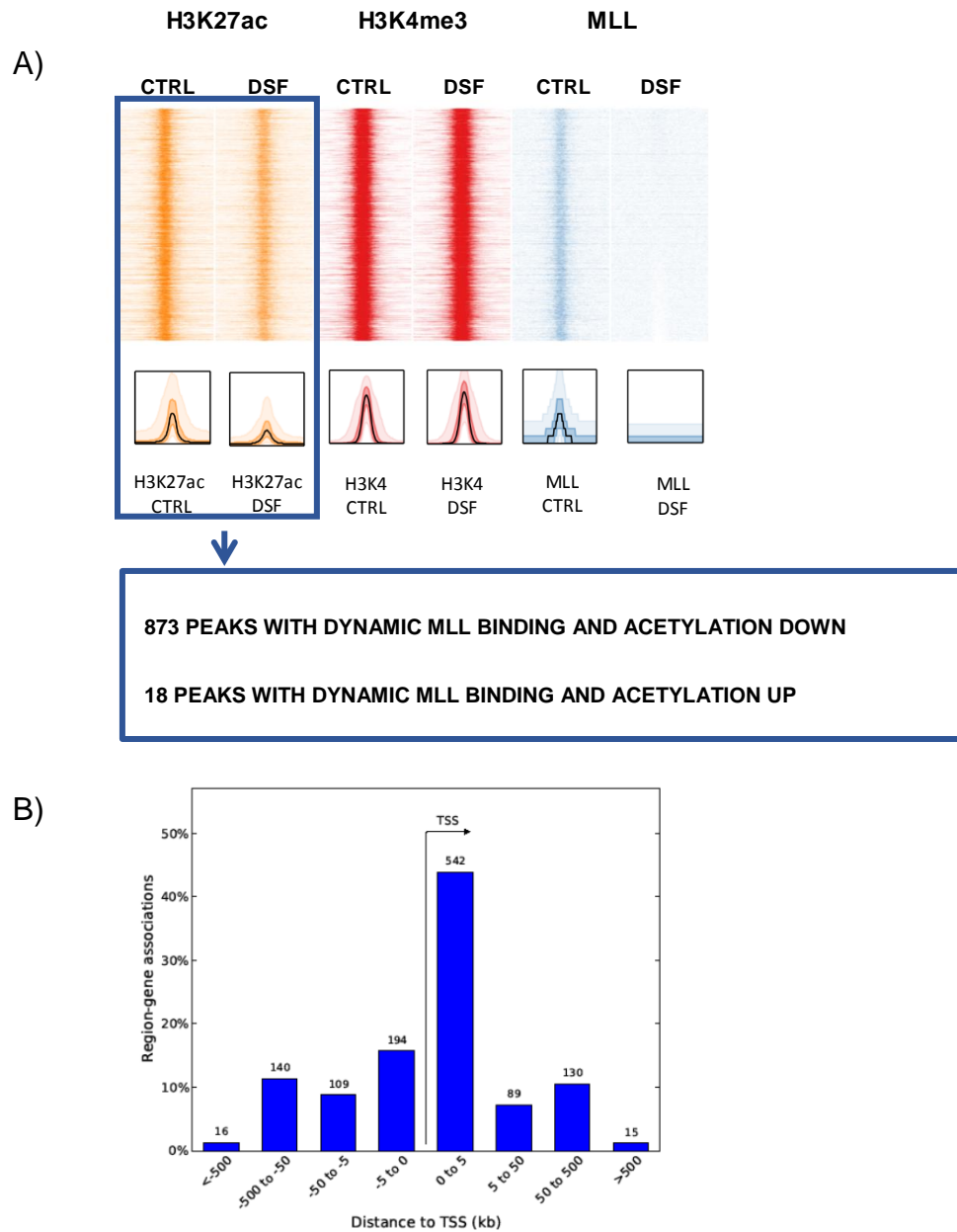


**Figure 42 Peaks with dynamic MLL binding and dynamic acetylation**

The heatmap shows H3K4me3 peak distribution (in red), MLL (in blue) and H3K27Ac (in yellow) in treated and untreated samples (A). In blue are highlighted the peaks that showed reduced wtMLL and MLL-AF9 binding and changes in acetylation, 18 peaks showed increased acetylation and 873 peaks reduced acetylation. The graph (B) shows that 542 peaks out of 873 were localised at the transcriptional start sites.

16 hours. Consistent with prior observations we found that, upon MLL (wt and fusion) eviction by DSF and copper, the genes that had decreased H3K27Ac were downregulated by 4 hours (figure 43A) and fully suppressed by 16 hours of treatment (figure 43B). These results prompted us to consider whether the epigenetic changes seen were reflective of leukaemic specific transcriptional programs and/or oncogene-regulated transcriptional program. We found that the epigenetic changes seen were highly correlated with leukaemic specific transcriptional programmes (figure 44A). Furthermore, these epigenetic changes overlapped with the oncogene-regulated transcriptional signatures of both PML-RARA and MLL-fusions (figure 44B) (Krige et al., 2008, Mullighan et al., 2007, Xu et al., 2005). The GSEA analysis revealed that the genes up-regulated in AML with MLL rearrangements were negatively enriched in our RNA-seq data (at 4 and 16 hours with 16 hours being significantly enriched) (figure 44C). Finally we show that our epigenetic gene expression changes (genes with H3K27Ac suppressed at the TSS upon MLL eviction) is negatively enriched in THP-1 cells in which the endogenous MLL-AF9 fusion protein was specifically silenced via siRNA (figure 44D) (Suzuki et al., 2009).

All together, these data indicates that DSF and copper treatment evicts MLL (wt and fusion) from the chromatin causing changes in H3K27Ac levels and this attenuates the MLL-fusion oncogenic programme

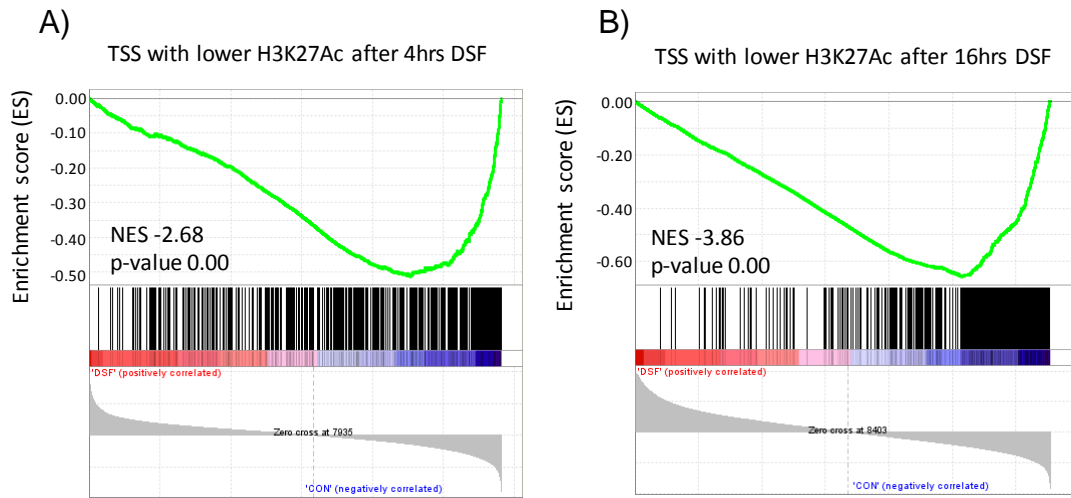


**Figure 43 Changes in H3K27Ac at the TSS correlates with gene expression changes.**

The 516 MLL peaks (wt and fusion) that in ChIP-seq analysis showed a reduced H3K27Ac were compared to RNA-seq data derived from THP-1 cells treated with DSF and copper for 4 (A) and 16 hours (B). The GSEA showed that genes with reduced H3K27Ac were downregulated after 4 hours of treatment with DSF and copper and completely suppressed by 16 hours of drug treatment.

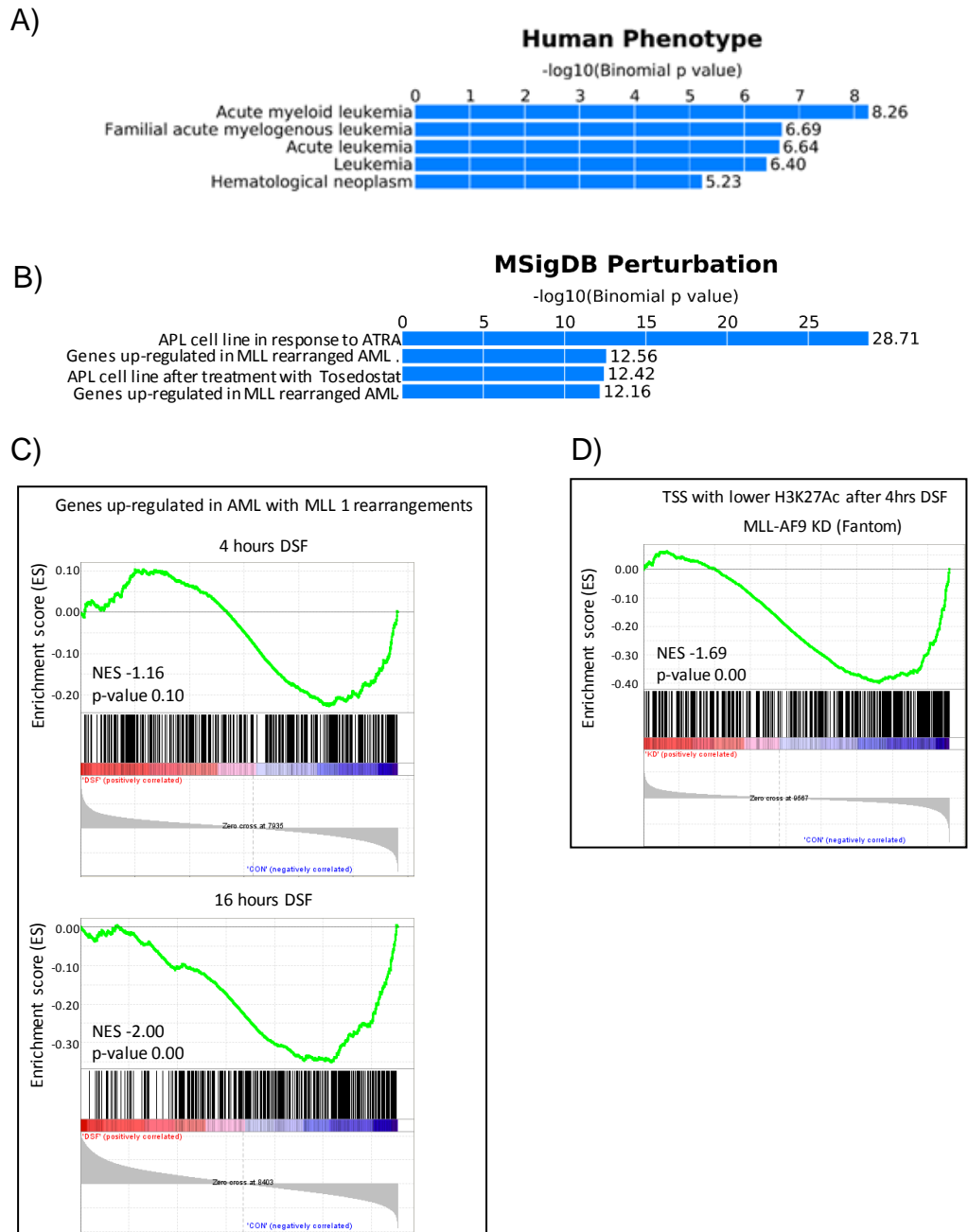


**Figure 44 Correlation of epigenetic changes with leukaemic and/or with oncogene-regulated transcriptional programs**

Phenotype analysis showed enrichment of the 873 peaks with dynamic MLL and dynamic acetylation in acute myeloid leukaemia, acute leukaemia and in haematological malignancies gene sets (A). The perturbation analysis showed enrichment of the 873 genes in APL and in

MLL rearranged AML gene sets (Krige et al., 2008, Mullighan et al., 2007, Xu et al., 2005) (B). GSEA analysis showing that genes up-regulated in MLL-rearranged AML were downregulated in our RNA-seq at 4 hours and significantly at 16 hours (C). GSEA analysis showing that genes with suppressed H3K27Ac at TSS upon MLL eviction were negatively enriched in THP-1 cells in which the MLL-AF9 expression was silenced via siRNA (Kawaji et al., 2009) (D).

### 6.3 Discussion

In the previous chapter of this thesis we showed downregulation of MLL-fusion target genes in *MLL* rearranged cells treated with DSF and copper for 4 hours. Degradation of wild type MLL and MLL fusion proteins was detected in contrast after a minimum drug incubation of 12 hours. We hypothesised that this dysregulation reflected a loss of MLL transcriptional regulation due to a reduced DNA binding ability of MLL/MLL-fusions.

To demonstrate this loss of DNA binding, we immunoprecipitated and sequenced chromatin regions interacting with wtMLL and MLL-AF9 in THP-1 cells with and without DSF treatment for 4 hours. Since the common and specific MLL-AF9 and MLL-AF4 target genes are marked by H3K4me3 and enriched in H3K27ac (Prange et al., 2017) and since disulfiram might alter the epigenetic status of treated cells we decided to use the same approach to study the effect of DSF also on chromatin regions marked by H3K4me3 and H3K27ac. While the antibodies used to immunoprecipitate H3K4me3 and H3K27ac have been previously tested in our laboratory, to obtain a positive outcome in the MLL ChIP we tested two ChIP grade antibodies directed against the MLL N- terminal domain. We successfully prepared a high quality ChIP library for sequencing when ChIP was performed using the MLL-N antibody from Diagenode.

Dr Martens from Radboud University in Netherland helped us to analyse and correlate to each other sequencing data from MLL, H3K4me3 and H3K27ac ChIP assays. We analysed exclusively chromatin regions actively transcribed,

or marked by H3K4me3. ChIP-seq data showed that wtMLL and MLL-AF9 peaks were marked by H3K4me3 and enriched in H3K27ac. Upon DSF and copper treatment we noted a complete ablation of the MLL (wt and fusion) specific peaks and a significant reduction of H3K27Ac, while we did not note quantitative changes in H3K4me3. The transcription mark H3K27Ac turnover far more rapidly than H3K4me3, with half-lives of 1.1 hours and 6.8 hours (Zheng et al., 2013, Zheng et al., 2014). These differences in stability might explain the absence of changes in H3K4me3 and the reduction in H3K27Ac detected after 4 hours of treatment with DSF and copper. We validated MLL ChIP-seq by q-PCR analysis using primers amplifying *HOXA10* and *GD21* target region. The q-PCR data confirmed significant wtMLL/MLL-AF9 enrichment in the *HOXA10* locus, in untreated control but not in cells treated for 4 hours with the DSF-copper mixture. *HOXA* gene expression changes after 4 hours of drug treatment were confirmed also by RNA-seq. The sequencing data showed that the *HOXA* genes, which were bound by MLL and/or MLL-AF9, were strongly downregulated. This downregulation correlated with the epigenetic changes (reduced acetylation) caused by drug treatment. The ChIP-seq data did not allow a clear discrimination between wtMLL and MLL-AF9 peaks. The wtMLL has H3K4me3 activity which has been shown to be redundant in supporting leukaemogenesis (Mishra et al., 2014). Our data support this hypothesis as no changes in H3K4me3 were noted upon ablation of MLL binding to the chromatin. Upon DSF treatment we identified 873 peaks characterised by reduced MLL binding and acetylation, the majority of these peaks with reduced H3K27Ac (516, localised around the TSS,  $\pm$  1kb) correlated with gene

expression changes (downregulation in THP-1 cells treated with DSF and copper for 4 hours and 16 hours). The epigenetic changes highlighted by our ChIP-seq were highly correlated with leukaemic and oncogene regulated (PML-RARA and MLL-fusions) transcriptional programs. GSEA analysis showed that genes up-regulated in *MLL* rearranged AML were down regulated in our RNA-seq at 4h and 16h and also that the genes with low H3K27Ac at gene TSS, upon MLL eviction, were negatively enriched in THP-1 cells in which the MLL-AF9 expression was silenced via siRNA. These data suggest that most likely the peaks with reduced H3K27ac might be regulated by the MLL-fusions. This data would also confirm the results from a recent study from Milne's group which showed that the loss of MLL-AF4 cause a reduction in H3K27ac at target loci (Godfrey et al., 2017).

The data illustrated in this chapter supported our initial hypothesis; upon DSF and copper treatment wtMLL and MLL-AF9 fusion proteins lose their ability to bind unmethylated CpG at the promoter regions of MLL-fusion target genes. As consequence of this event the transcription of MLL-fusion target genes is blocked. Conversely in the absence of DSF the MLL-fusion protein is bound to the promoter of target genes causing their continuous transcription (figure 45). Our data showed also that MLL-AF9 ablation caused epigenetic changes which might contribute to reduce the accessibility of the transcriptional machinery to specific loci.

The region allowing the MLL binding to the DNA is the CXXC domain that is localised in the MLL N-terminal region, which is retained in MLL fusion proteins.

The CXXC domain has a Zn finger motif containing two zinc atoms connected, through disulphide bonds, to four cysteine residues each. Studies from Cleary and Warrens laboratories showed the importance of the CXXC domain in recognition of target genes in myeloid transformation and also that the integrity of disulphide bonds connecting the cysteine residues to the zinc ions is essential to preserve the CXXC fold and the DNA binding function (Allen et al., 2006, Ayton et al., 2004). The CXXC domain is also present in other chromatin associated proteins, such as DNMT1. It has been shown that exposure to DSF inhibits DNMT1 catalytic activity (Lin *et al.*, 2011). It is possible that this inhibition is the result of the oxidation of cysteine residues located in the DNMT1 CXXC domain. DSF could interfere also with cysteine residues located in the MLL-fusion CXXC motif. The perturbation of disulphide bonds, connecting cysteine residues and zinc atoms, could cause an unfolding of the MLL-fusion CXXC motif and a consequent detachment from the DNA. The degradation of MLL-fusion proteins would be a secondary consequence of this detachment (figure 46). Our CHIP-seq results clearly show that DSF affects the DNA binding ability of MLL-fusion proteins. We started a collaboration with Professor Alan Warren from the Haematology department of the Cambridge Institute for Medical Research to investigate the potential unfolding of the MLL-fusion CXXC domain by DSF treatment.

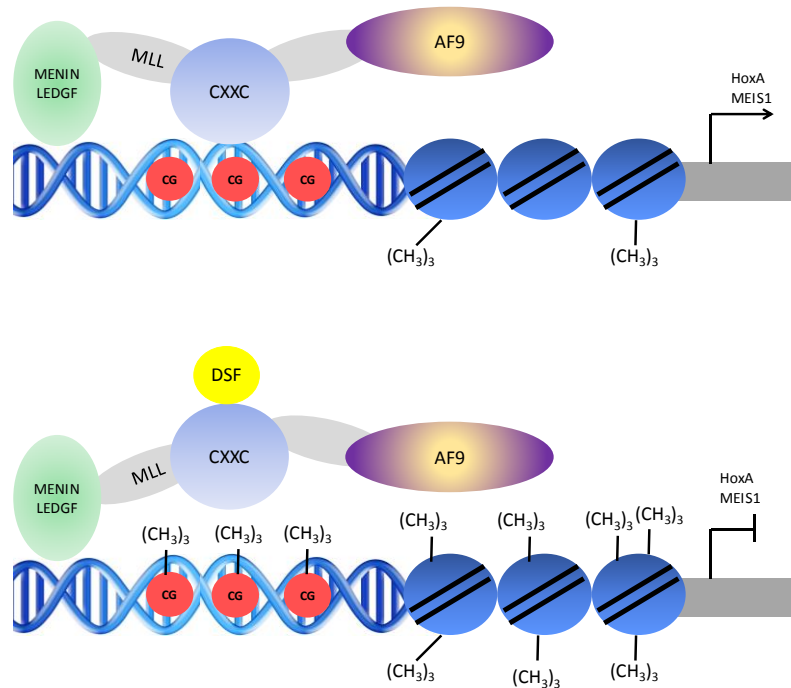


**Figure 45 Disulfiram mechanism of action**

In absence of disulfiram MLL-fusion proteins bind constantly the unmethylated CpGs in the promoter of MLL target genes. In these conditions MLL target genes are constantly transcribed. In presence of disulfiram the MLL-fusion is unable to bind the DNA. In these conditions the transcription of MLL target gene is blocked (adapted from Riesner *et al*, 2013).

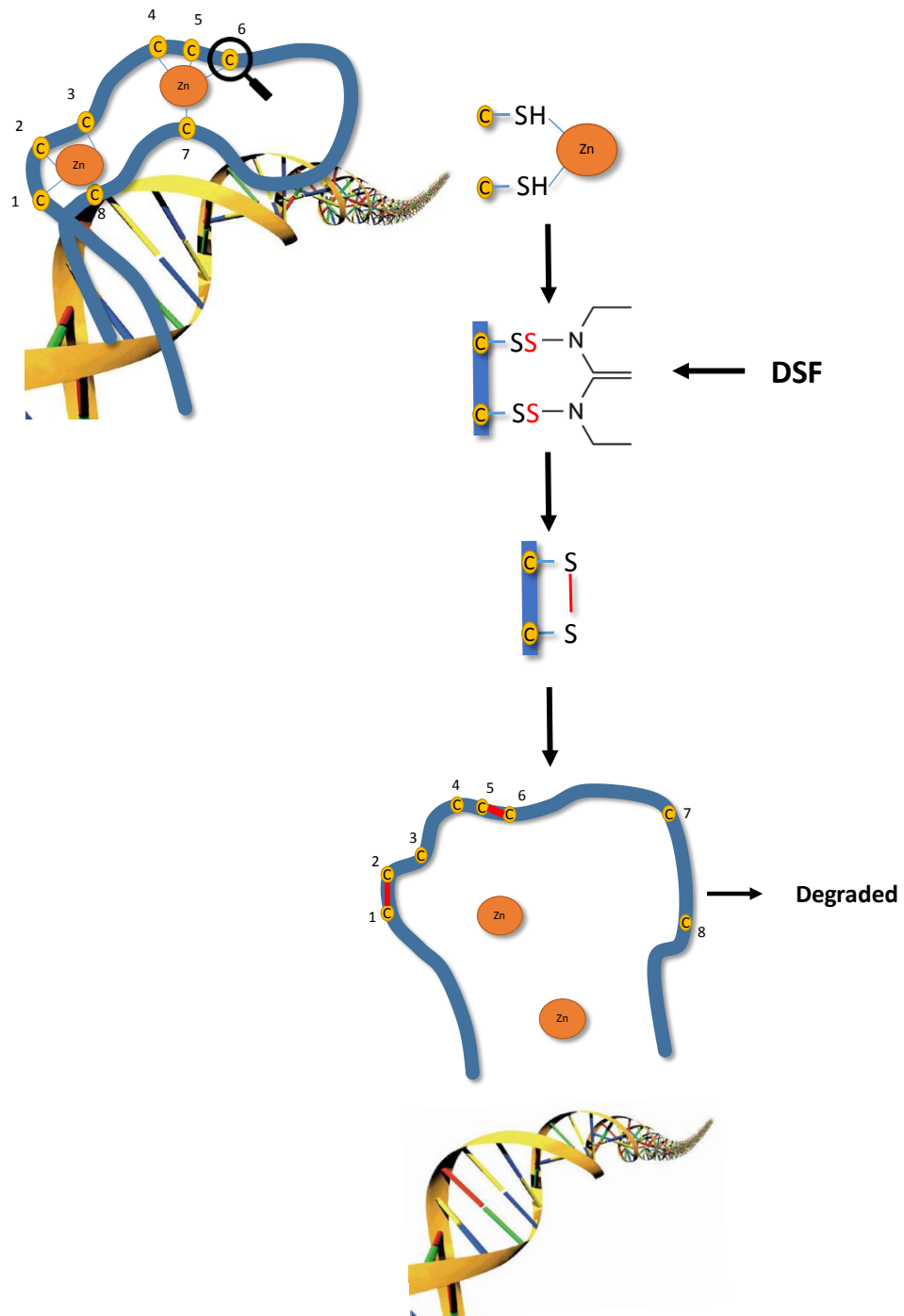


**Figure 46 Potential mechanism of MLL-fusion detachment from DNA**

The figures shows the folding of the MLL-fusion CXXC domain. The treatment with DSF could interfere with the disulphide bonds connecting the CXXC cysteine residues to the zinc atoms. This event would cause the unfolding of the CXXC domain with the consequent loss of its DNA binding ability. The MLL-fusion degradation would be a secondary consequence of this event.

## 7 CHAPTER VII: Investigating the effect of DSF *in vivo* and *in vitro* functional assays

### 7.1 Introduction

Acute Myeloid Leukaemia (AML) is a group of heterogeneous disorders characterised by uncontrolled proliferation and accumulation of progenitor cells in the bloodstream and bone marrow. It is widely accepted the concept that only a small fraction of cells within a tumour (cancer stem cells) have the ability to initiate and maintain the tumour growth. Leukaemic stem cells (LSC) can originate from haematopoietic stem cells (HSC) through accumulation of consecutive mutations. It is believed that LSCs could also originate from more committed progenitors or more differentiated cells that could re-acquire self-renewal ability through consecutive mutations [reviewed in (Bonnet, 2005)]. A possible therapeutic approach to target the LSC compartment could be to target the driver genetic lesion [reviewed in (Horton and Huntly, 2012)]. Rearrangements involving the *MLL* gene are well known driver mutations in AML and the inactivation of MLL-fusions has been proved to be beneficial to induce leukaemia regression (Horton *et al.*, 2009).

In the previous chapter of this thesis we showed that DSF causes MLL-fusion eviction from target loci, reduction in target gene expression and degradation of MLL-fusions. We predicted that DSF will compromise the function of AML cells. In the following chapter we will assess the functional consequences of MLL-fusion inhibition by examining the self-renewal ability of DSF-treated AML cells

using methylcellulose assays. To determine whether a therapeutic window for potential targeted therapy exists we will also examine, by colony forming assays, normal HPC function following DSF treatment. The colony forming assay is an *in vitro* assay widely used to study haematopoietic stem/progenitor function. The assay is based on the ability of isolated haematopoietic progenitor cells to proliferate and differentiate in a semisolid medium.

Disulfiram-copper and diethyldithiocarbamate-copper complexes have previously been shown to elicit a pro-apoptotic effect in glioblastoma (Liu et al., 2012), in breast cancer (Chen et al., 2006) and in other malignancies. In these studies disulfiram treatment resulted also in reduced tumour growth *in vivo*. We decided to evaluate the effects of drug treatment on cell viability of *MLL* rearranged AML cell lines. Cell viability will be assessed by flow cytometry using the viability dye TO-PRO3 while Annexin V-PI double staining will be used to evaluate cell death. Furthermore, we planned to verify the consequences of disulfiram and copper administration in experiments *in vivo*.

## 7.2 Results

### 7.2.1 Studying consequences of drugs administration on cell viability

We analysed cell viability of MLL-r cells in presence or absence of complexes disulfiram-copper and diethyldithiocarbamate-copper. We treated THP-1, SHI-1 and MV4-11 cells for 16, 24, 48 and 72 hours and next we assessed cell viability by flow cytometry using the viability dye TO-PRO3. Membranes of live cells are impermeable to TO-PRO3 that can cross only the compromised membranes of apoptotic and necrotic cells. Once inside the cells the TO-PRO3 binds dsDNA and emits fluorescence in the far red (660-700nm). After 16 hours of treatment the percentage of live cells was comparable to the percentage measured in untreated controls (Figure 47). The fact that at 16 hours the cells were viable excluded the possibility that MLL degradation was a result of induction of cell death. Flow cytometry analysis performed at later time points (24-48 and 72 hours) revealed that percentage of TO-PRO3 positive cells increased in a time-dependent manner and consequently the percentage of live cells was drastically reduced (Figure 47). To-PRO3 analysis at 24, 48 and 72 hours gave us also information on relative cell proliferation rates. While untreated THP-1, SHI-1 and MV4-11 actively proliferated, co-administration of disulfiram-copper or of diethyldithiocarbamate-copper drastically reduced cell proliferation (Figure 48).

The reduction in cell viability suggested induction of cell death in cells subjected to prolonged treatments with copper and DSF or DDC. To discriminate between

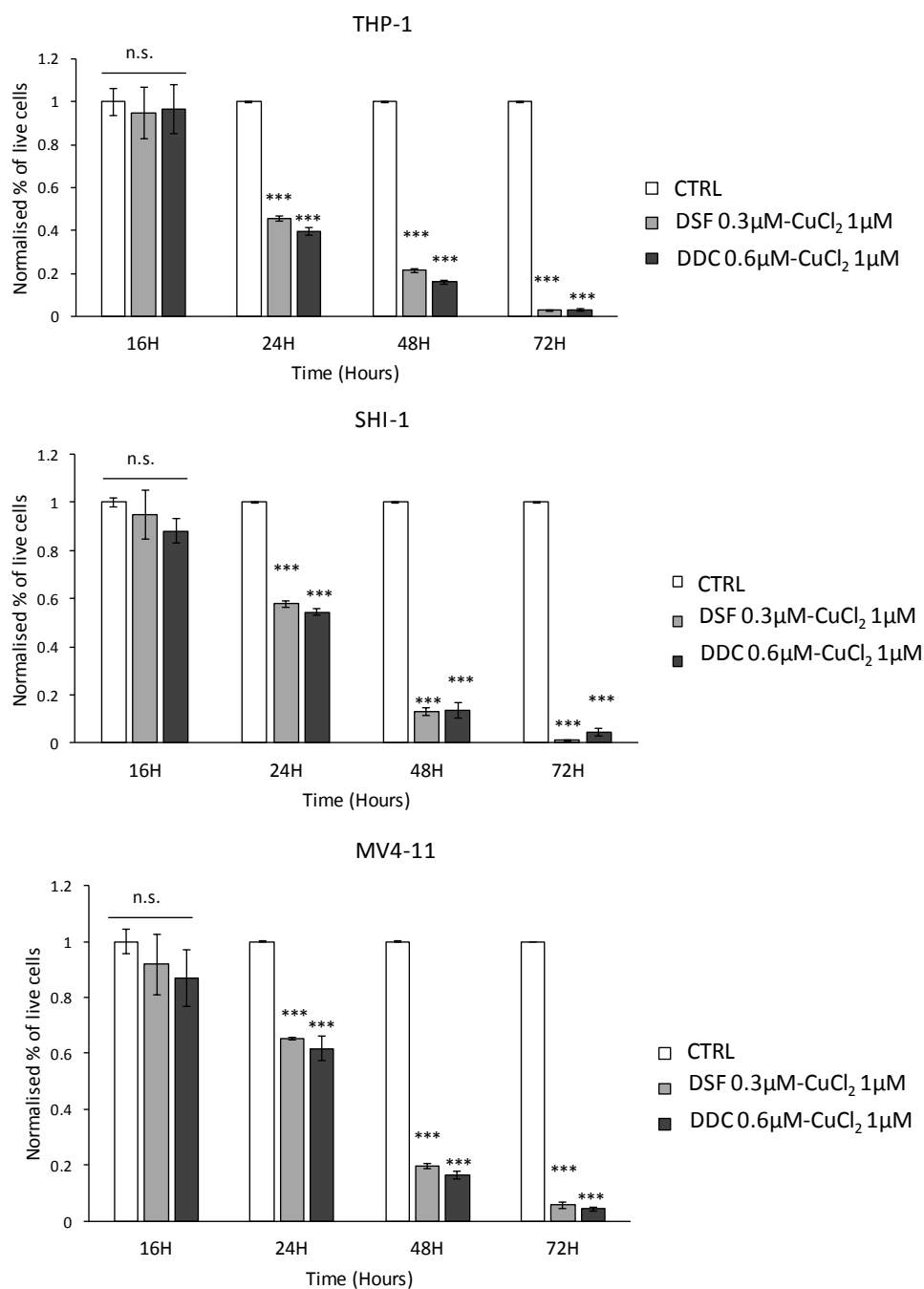


**Figure 47 Disulfiram and diethyldithiocarbamate complexes with copper do not affect cell viability after 16 hours of treatment**

THP-1, SHI-1 and MV4-11 were treated for 16, 24, 48 and 72 hours with 0.3µM DSF -1µM CuCl<sub>2</sub> or with 0.6µM DDC -1µM CuCl<sub>2</sub>. Cells were then collected,

stained with TO-PRO3 and analysed by flow cytometry. The bar chart shows the percentage of live cells in the three MLL rearranged cell lines. The bars represent average of three independent experiments and error bars represent standard deviation (SD). The p-value was obtained comparing untreated to drug treated cells using an unpaired t-test; (n.s.: not significant  $P \geq 0.05$ ; (\*\*\*)  $P \leq 0.001$ )

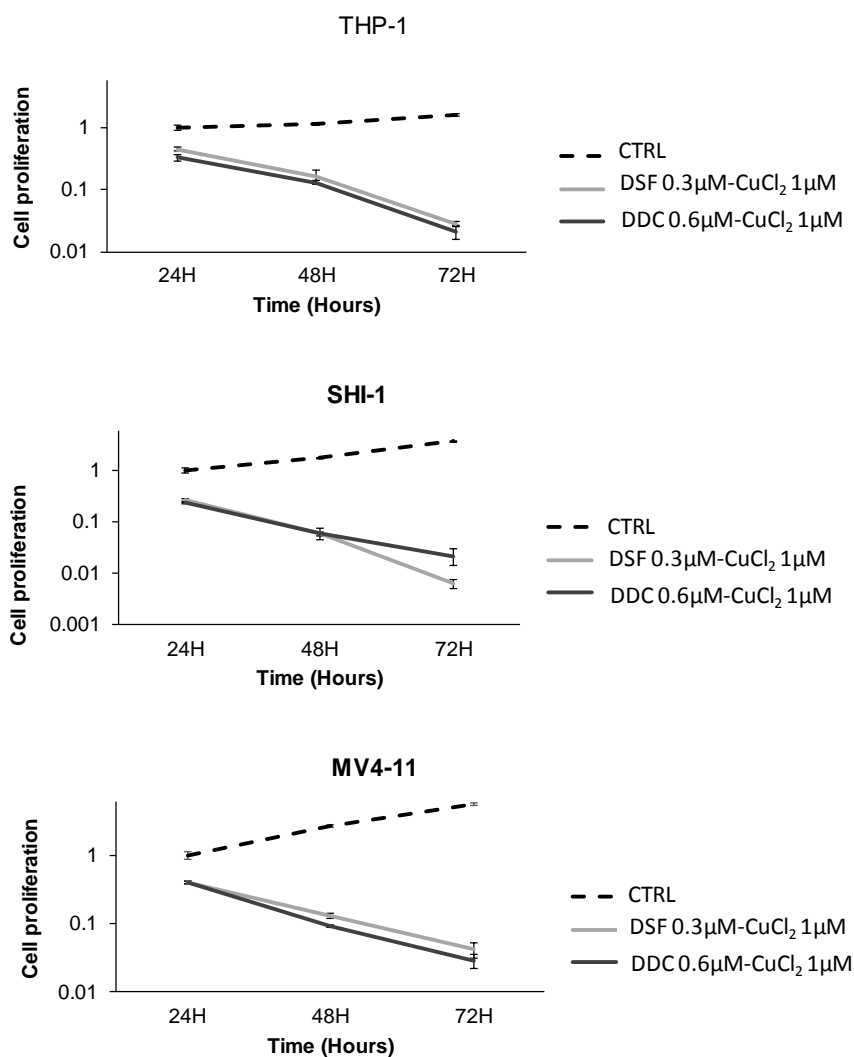


**Figure 48 Disulfiram and diethyldithiocarbamate complexes with copper reduce cell proliferation rates in a time dependent manner**

THP-1, SHI-1 and MV4-11 were treated for 24, 48 and 72 hours with 0.3µM disulfiram -1µM CuCl<sub>2</sub> or with 0.6µM diethyldithiocarbamate -1µM CuCl<sub>2</sub>. Cells were then collected, stained with TO-PRO3 and analysed by flow cytometry. The graph shows the cell proliferation over time in the three MLL rearranged cell lines. Results represent the average of three independent experiments and error bars represent standard deviation (SD).

apoptotic and necrotic cell death mechanisms we combined annexin-V and PI staining. Flow cytometry analysis revealed that after 48 hours of drug treatment 50-60% of the cells were positive to annexin-V and PI while 20-30% showed only annexin-V positivity (Figure 49). This result indicates that DSF induces apoptosis in AML cells.

All together these data confirm that DSF does not affect cell viability after 16 hours of treatment and therefore that MLL degradation is not a secondary consequence of induction of cell death mechanisms. Prolonged drug treatments affected cell viability and proliferation rates in a time-dependent manner. In particular, flow cytometry analysis confirmed that DSF induced AML apoptosis and that a majority of cells were in a late apoptotic/necrotic phase after 48 hours of treatment.

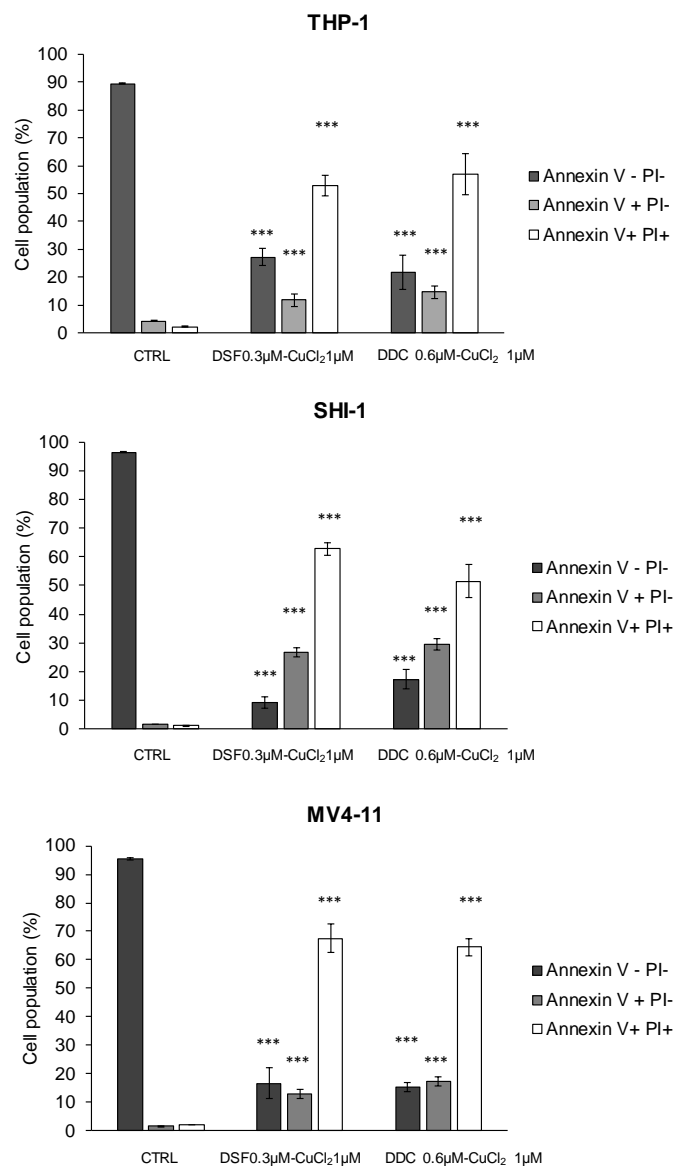


**Figure 49 Disulfiram and diethyldithiocarbamate induced cells death after 48h of treatment**

THP-1, SHI-1 and MV4-11 cells were treated for 48 hours with 0.3µM disulfiram-1µM CuCl<sub>2</sub> or with 0.6µM diethyldithiocarbamate -1µM CuCl<sub>2</sub>. 1x10<sup>6</sup> cells were collected, stained with Annexin-v and PI and analysed by flow cytometry. The graph shows cell percentage in each population. Bars represent average of three independent experiments and error bars are SD. The P-value was obtained comparing cells percentage in untreated controls and in drug treated cells using an unpaired t-test (\*\*\*) P≤0.001.

## 7.2.2 Disulfiram inhibit cell self-renewal ability

Many cases of relapse in AML patients are due to mechanisms of drug resistance. Such resistance could be caused by the presence of leukaemic stem cells (LSC). These cells, able to initiate and maintain leukaemia, have maintained or acquired the ability of self-renew. Current treatment strategies are aiming to target this cell compartment.

In chapter V of this thesis, to evaluate the effect of DSF on gene expression, we generated MLL-AF6 gene expression profiles in cells treated for 16 hours with DSF and copper. Here we compared the MLL-AF6 gene expression changes to a published leukaemic stem cell signature (Somerville *et al.*, 2009). Interestingly GSEA analysis showed negative enrichment of the LSC signature (figure 51). This means that genes usually upregulated in leukaemic stem cells were downregulated by 16 hours of treatment with disulfiram and copper. This negative enrichment suggests a possible inhibition of AML self-renewal compromising AML cells functionality. To clarify the functional consequences of DSF inhibition of MLL-fusions we examined, using colony forming assay, the effect of AML cells self-renewal upon DSF exposure. To evaluate the possibility of a therapeutic window for targeted therapy we examined the effect of DSF also on non *MLL* rearranged AML cell lines and on normal HPC. We plated *MLL* rearranged AML cell lines (SHI-1, THP-1 and MV4-11), normal cord blood HPC and non *MLL* rearranged AML cell lines (OCIAML3 and KASUMI1) in methylcellulose with or without DSF and copper. The co-administration of DSF and copper inhibited the colony formation of *MLL* rearranged cell lines. In

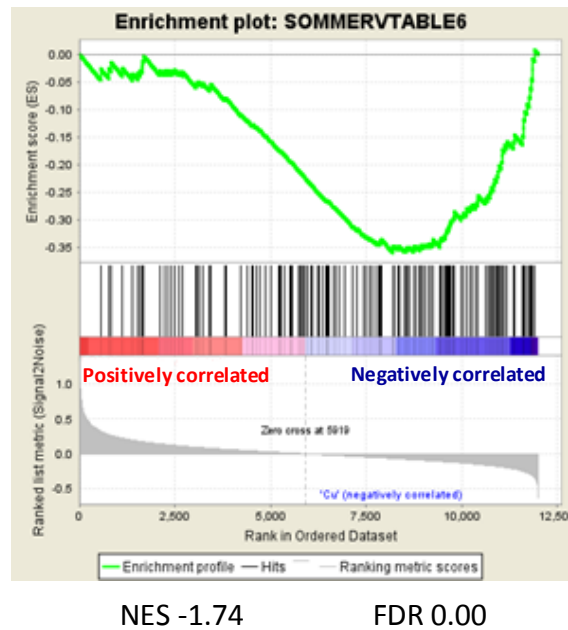


**Figure 50 GSEA plot showing negative correlation with published leukaemic stem cell signature**

THP-1 cells were plated at density of  $0.5 \times 10^6$  cells/ml. Total RNA was extracted using the QIAGEN kit. RNA concentration and quality was determined using the NanoDrop ND-100 and then it was submitted to UCL Genomics for sequencing. Data were analysed using the GSEA software. The plot is showing negative enrichment or correlation between our signature and MLL signature generated by Sommerville et al (Sommerville et al, 2009).

contrast, the colony formation was only marginally affected in non *MLL* rearranged cell line and cord blood cells (Figure 52).

Data illustrated in this chapter shows that the combination DSF-copper is able to inhibit self-renewal of *MLL* rearranged AML cell lines but not that of normal HPC and non *MLL* rearranged AML cells. This result indicates the real possibility to target specifically only *MLL-r* cells in AML patients but not normal haematopoietic cells.

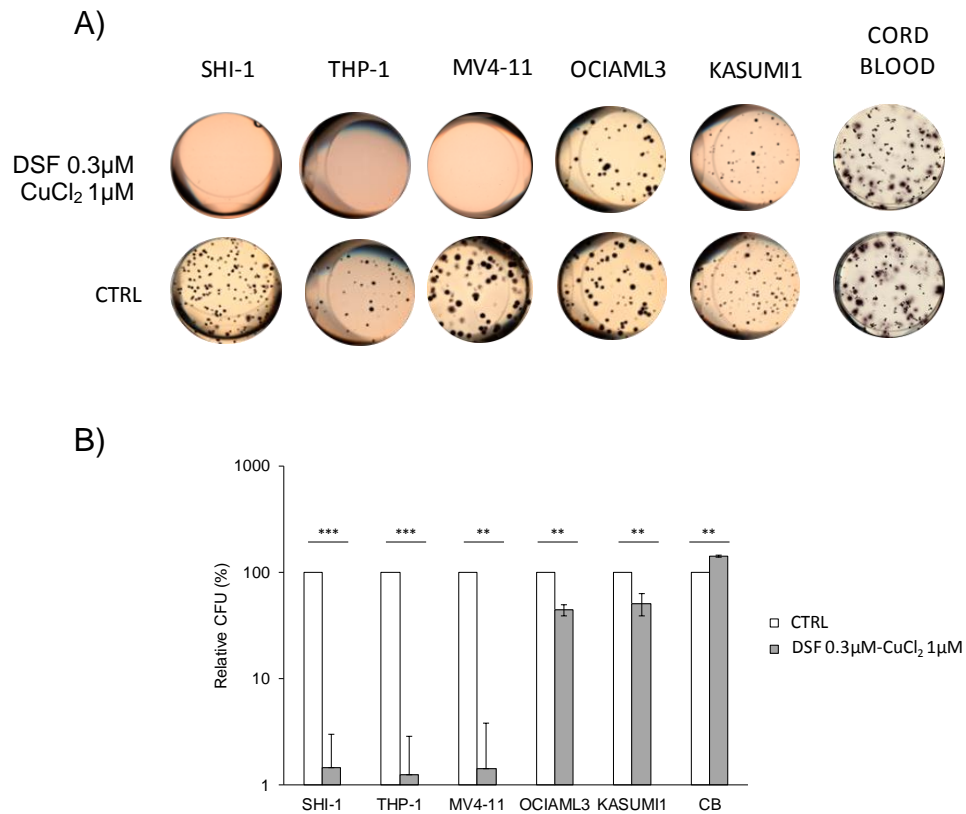


### Figure 51 Disulfiram inhibit leukaemic self-renewal

MLL rearranged cell lines (SHI-1, THP-1 and MV4-11), non MLL rearranged cell lines (OCIAML3 and KASUMI1) and cord blood cells were plated, in quadruplicate wells in each experiment, in serum free methylcellulose with or without 0.3 $\mu$ M DSF and 1 $\mu$ M CuCl<sub>2</sub>. After 15 days in culture cells were stained with INT and scanned with a densitometer (A). Colonies were quantified using the ImageQuant software. The bar charts represent the mean of three independent experiments  $\pm$  the standard deviation. The P-value was determined using a One sample t-test,  $P < 0.01$  (\*\*),  $P \leq 0.001$  (\*\*\*) (B).

### 7.2.3 Investigating the effect of disulfiram on primary ALL

Despite the fact that cell lines maintain the original driver mutation they might not represent entirely the original disease. For this reason we carried out further studies to assess whether the exposure to DSF and copper would target MLL proteins in primary samples. We analysed by western blot protein lysates from patient-derived ALL MLL-AF9 cells after exposure to DSF and copper for 16 hours. The co-treatment resulted in a decrease of the MLL protein levels by 80% (figure 52).

Mesenchymal stem cells (MSCs) have been used as a feeder layer to support growth and stemness of stem cells *in vitro*. Immortalised MSCs can be used also as a support for the expansion of leukaemic blasts. Dr. Pal, from Newcastle Cancer Centre, established a screening platform suitable for preclinical drug testing based on a bioluminescent ALL-MSC co-culture system (Pal *et al.*, 2016). With her collaboration we proved the efficacy of our drug treatment in a system mimicking a patient microenvironment. The plot in figure 53 shows a reduction of luciferase activity in a dose dependent manner.

In conclusion these results demonstrate that the combination disulfiram-copper targets the MLL proteins also in primary ALL *MLL* rearranged cells. The efficacy of DSF in the co-culture system provided an optimistic preliminary data for *in vivo* studies.

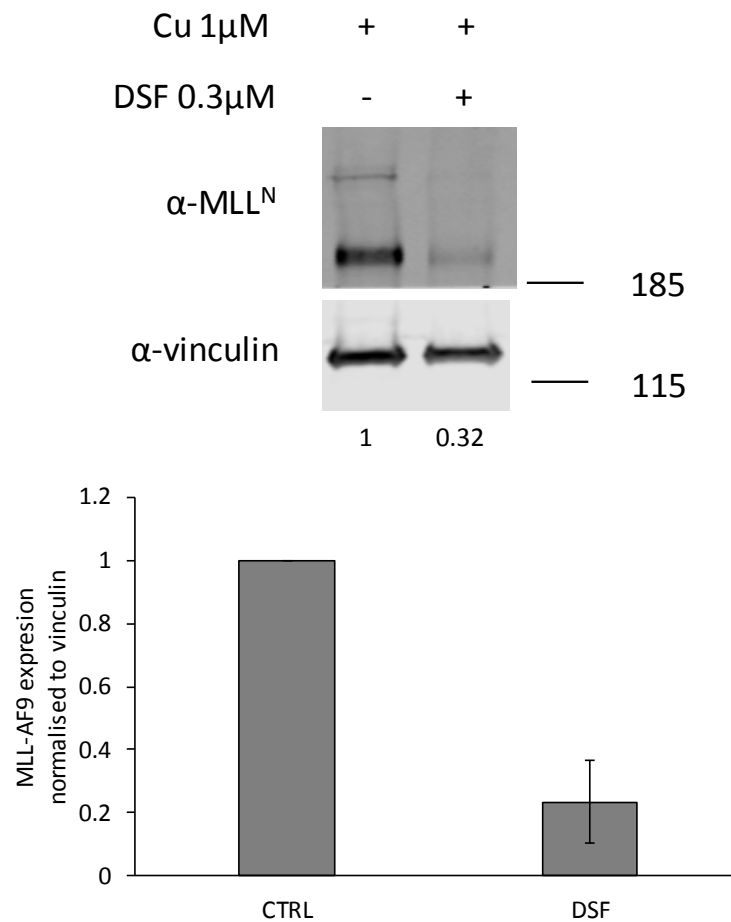
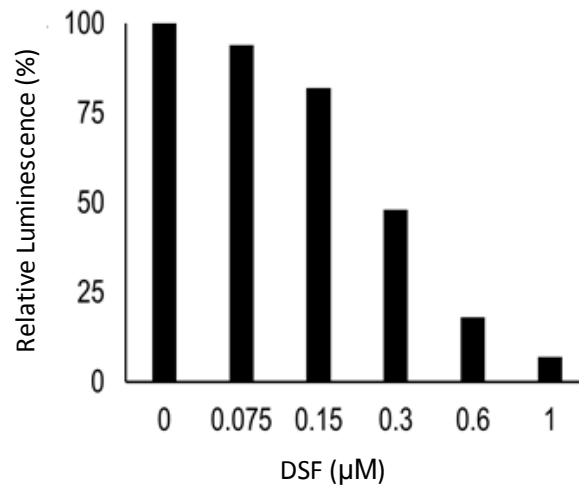


**Figure 52 DSF effect on patient-derived ALL *MLL* rearranged cells**

Western blot analysis of protein extracts from primary ALL samples carrying the MLL-AF9 fusion (A).  $4 \times 10^6$  cells were treated with the mixture DSF-CuCl<sub>2</sub>. Protein lysates were collected after 16 hours of treatment and resolved in a 7% bis-acrylamide gel. Membranes were probed with an anti-MLLN/ HRX (clone N4.4) antibody and with an anti-vinculin antibody, as protein loading control. Membranes were imaged using Odyssey CLX imaging system. Bands were quantified using the software Image Studio, provided by the manufacturer. The intensities of each band was normalised to the intensity of the housekeeping gene. Numbers represent densitometric quantification. (B) The bar chart represents the quantification of total MLL (MLL fusions and wild type) normalised to the loading control vinculin.

A)



B)

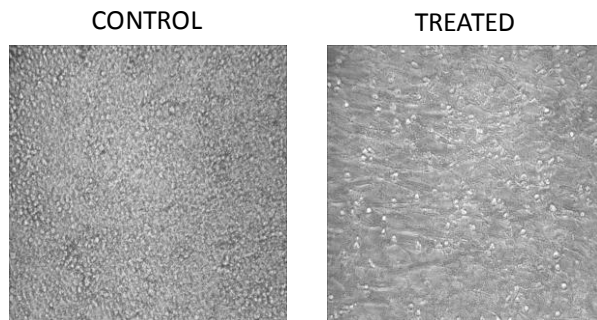


**Figure 53 Bioluminescent ALL-MSC assay**

Patient derived ALL cells were lentivirally transduced to express the firefly luciferase. Then these ALL cells were seeded on MSCs for two weeks in presence of different doses of disulfiram. Bioluminescence was measured using the FLUOstar Omega microplate reader after adding the firefly luciferase substrate. The plot shows the Relative luminescence in treated and untreated cells (A). Phase contrast photographs of patient derived ALL cells in co-cultures with MSCs with or without treatment (B).

## 7.2.4 Studying the consequences of disulfiram *in vivo*

Having shown an anti-leukaemic effect of disulfiram and copper *in vitro*, we tested the response to drug treatment *in vivo*. We transplanted NOD-SCID- $\gamma^{-/-}$  (NSG) mice with murine MLL-AF9 cells (all transplantations were performed by Dr Owen Williams). Peripheral blood was analysed weekly for the presence of leukaemic cells that were identified by simultaneous analysis of mH-2Kb and mCD45 expression. We started the treatment as soon as leukaemic cells were detected in the blood. A group of mice received daily a solution of DSF 5mg/kg in corn oil via intraperitoneally (IP) injection while another group of mice was feed with diet mixed with 0.1% DSF. Copper was resuspended in saline at 0.5mg/kg and injected IP daily in both groups of mice. The animals were sacrificed as soon as they showed the first signs of disease progression. All treated and untreated mice of this preliminary experiment showed signs of disease and large spleens. However, FACS analysis of spleen cells showed increase mean fluorescence intensity (MFI) of the myeloid differentiation marker CD11b in both groups of DSF-treated mice (Figure 54).

Therefore, we decided to repeat the experiment by transplanting primary human patient-derived MLL-AF9-expressing AML cells into NSG mice. In this second experiment, a group of mice was feed with a mixture of DSF 0.05% diet whereas a second group received 0.05% DSF in the food and CuSO<sub>4</sub> at 0.5mg/kg via IP injection. Cell engraftment was monitored weekly for the presence of leukaemic cells and the treatment started at the first signs of engraftment. During this experiment the disease progressed quicker than

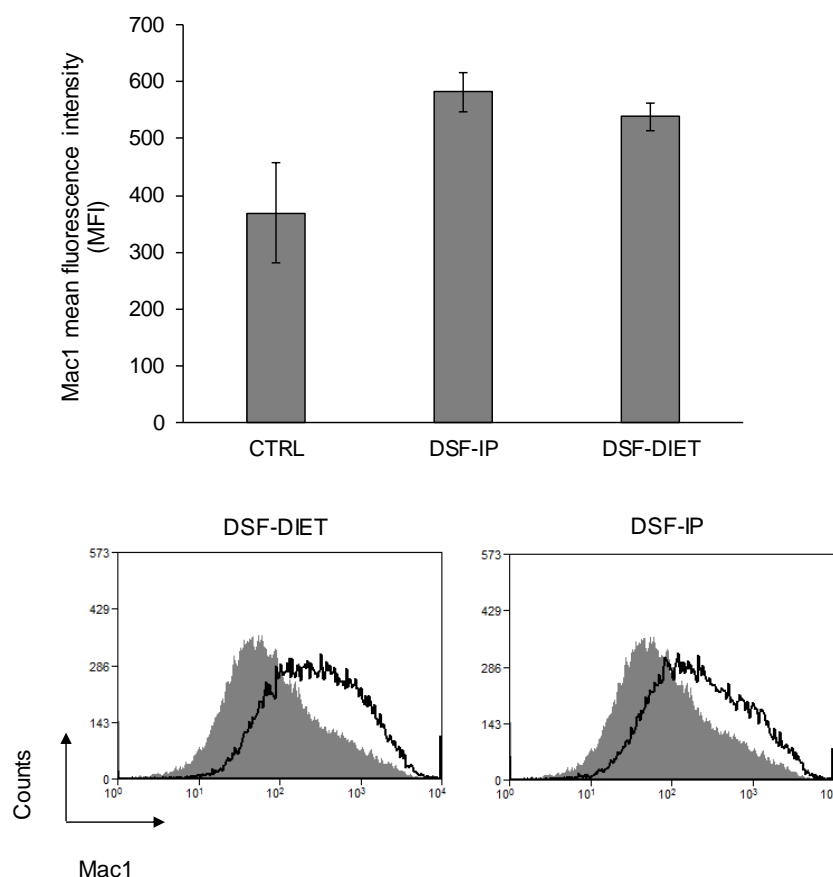


**Figure 54 Disulfiram increase CD11b expression in vivo**

$1 \times 10^6$  murine MLL-AF9 cells were transplanted via intravenous tail injection in NOD-SCID- $\gamma^{-/-}$  (NSG) mice. Peripheral blood was analysed weekly for the presence of leukaemic cells.  $\text{CuSO}_4$  at 0.5 mg/kg was resuspended in saline and IP injected daily to all the mice. DSF at 5mg/kg was dissolved in corn oil and IP injected daily in a first group of mice. In a second group of mice the DSF was administered always daily but mixed to the diet (0.1% DSF). Mice were sacrificed as soon as first signs of leukaemia were visible. Peripheral blood was stained using an  $\alpha$ -Mac-1 antibody APC conjugated. Analysis of the mean fluorescence intensity revealed an increased expression of the differentiation marker in both groups of treated mice. (A) The graph shows the mean fluorescence intensity of Mac1 in the three groups of mice. Bars represent the MFI average in each group of mice. (B) Two FACS plots showing the CD11b expression in the two groups of treated mice. The gray area represent cells from control mice while the white area indicates the DSF-treated mice. This experiment was performed only once.

expected and mice were treated for only 3 days. Despite the relatively short treatment, the group of mice receiving disulfiram and copper presented significantly smaller spleens compared to DSF treated mice and to control group (figure 55). The successful results obtained in this second experiment, after only 3 treatments, were particularly encouraging. Therefore we planned a third experiment using the same treatment conditions used during the second *in vivo* experiment. This *in vivo* experiment is currently ongoing.

In conclusion, the positive results obtained in these preliminary experiments *in vivo* are consistent with the *in vitro* data.

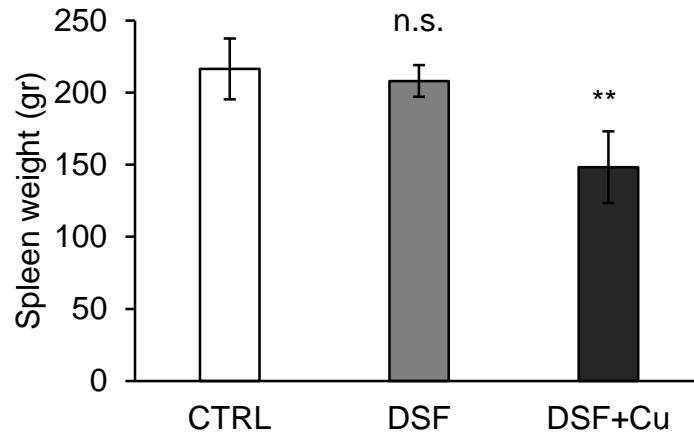


**Figure 55 Disulfiram treatment reduces spleen size of leukaemic mice**

$1 \times 10^6$  primary human AML (MLL-AF9) cells were transplanted via intravenous tail injection in NOD-SCID- $\gamma^{-/-}$  (NSG) mice. Peripheral blood was analysed weekly for the presence of leukaemic cells. A group of mice received 0.05% DSF mixed with diet, a second group of mice was fed with diet containing 0.05% disulfiram and IP injected with  $\text{CuSO}_4$  at 0.5 mg/kg in saline. Mice were sacrificed as soon as first signs of leukaemia were visible. The graph shows the average spleen size in each group of mice.  $n=4$  mice per group. This experiment was performed only once.

## 7.2.5 Discussion

GSEA analysis of MLL-AF6 gene expression changes upon 16 hours DSF treatment showed a negative enrichment for a leukaemic stem cell signature. We confirmed that this resulted in inhibition of cell self-renewal using methylcellulose colony forming assay. DSF inhibited colony formation of AML *MLL-r* cell lines, while the ability to form colonies in non *MLL* rearranged AML cells and normal cord blood HPC was not affected. This finding indicates the clinical relevance of a DSF-based therapy.

We showed that the DSF-copper mix targets MLL-proteins also in primary ALL with MLL rearrangement. Furthermore, the efficacy of disulfiram in an MSC co-culture system, mimicking the microenvironment in patients, provided preliminary data for *in vivo* studies. To study the effect of disulfiram and copper *in vivo* we transplanted murine MLL-AF9 cells and primary human AML (MLL-AF9) cells into different groups of NSG mice. Mice were treated with copper and two different doses of disulfiram but unfortunately all died of leukaemia. However, in mice transplanted with murine MLL-AF9 cells the DSF treatment increased expression of the myeloid differentiation marker CD11b. Mice transplanted with primary human AML and treated with DSF and copper exhibited reduced splenomegaly compared to control mice. To better characterise the effect of DSF *in vivo* we have more experiments ongoing.

## 8 CHAPTER VII: CONCLUSIONS

Rearrangements of the *MLL* gene are associated with acute leukaemias with poor outcome. Acute leukaemia depends on the continuous expression of *MLL*-fusion genes and despite the presence of secondary mutations the *MLL*-fusions are necessary for leukaemia survival (Horton *et al.*, 2009). Previous studies in our and other laboratories showed that the inactivation of driving fusion genes (PML-RAR $\alpha$  , *MLL*-ENL, BCR-ABL) resulted in delayed disease progression and complete eradication *in vivo* (Ablain and de The, 2011, Horton *et al.*, 2009, Shami and Deininger, 2012). All these studies suggested that targeting the driving oncoproteins would be an effective approach to eradicate the associated leukaemia. The aim of this study was to develop an approach of medium throughput screening for destabilisers of leukaemic fusion proteins based on a dual luciferase assay.

To identify compounds destabilising leukaemic fusion proteins we generated a novel screening platform based on the expression of luciferase tagged *MLL* fusion proteins. We screened 1280 clinically approved drugs contained in the Prestwick chemical library and we identified 24 positive hits. A counter screening based on western blot analysis on two human *MLL* rearranged cell lines allowed the validation of 7 drugs. Disulfiram (DSF), one of the seven drugs validated, is currently used to prevent the alcohol abuse. We decided to continue to study the effect of DSF on *MLL*-fusion proteins due to the low toxicity profile and to its high tolerability in patients (Skrott *et al.*, 2017). Furthermore, recent studies suggested a potential anti-tumour effect of DSF

(Chen *et al.*, 2006, Liu *et al.*, 2012). Our data proved that disulfiram and its first metabolite diethyldithiocarbamate (DDC), promoted degradation of wild type MLL and MLL fusion proteins in a panel of MLL rearranged cell lines. Further analysis showed that their effect was enhanced by the co-administration of copper. A recent study from Bartek laboratory showed that the DDC-copper complex is the active metabolite responsible for the DSF effect (Skrott *et al.*, 2017).

To examine the role of disulfiram in the transcription of MLL target genes, we performed RNA-seq on cells untreated or treated with the disulfiram-copper mixture for 16 hours. The GSEA analysis showed negative enrichment of the DSF gene expression profiles in MLL-AF9 (Bernt *et al.*, 2011) and MLL-AF4 (Guenther *et al.*, 2008) gene sets. Validation of these data by qRT-PCR confirmed the downregulation of the most common MLL target genes (*HOXA10*, *MEIS1*, *c-MYB*) upon DSF and copper treatment. Furthermore we discovered that MLL-fusion target genes were already downregulated after 4 hours of treatment while proteins degradation was detectable only after prolonged incubation (12-16 hours). This suggested that the degradation of MLL oncoproteins was most likely a secondary consequence of MLL-fusion inhibition. We hypothesised that all this might be a possible consequence of a reduced ability of MLL-fusions to bind the DNA. The CXXC domain is the region responsible for the wild type MLL and MLL-fusion proteins binding to the DNA. This domain contains a zinc finger like motif in which two zinc atoms are connected, through disulphide bonds, to four cysteine residues. Mutations involving these cysteine residues caused an unfolding of the CXXC domain

(Allen et al., 2006). Mutations in the CXXC motif abolish the MLL-fusion binding to the DNA and abrogate myeloid transformation (Ayton et al., 2004). The MLL CXXC domain has high degree of homology with other chromatin associated proteins, such as DNMT1. A study published by Risner highlighted the similarities between the MLL CXXC and DNMT1 CXXC domains (Risner et al., 2013). It has been shown that DSF is able to inhibit DNMT1 by oxidising cysteine residues located in the DNMT1 CXXC motif (Lin et al., 2011). We hypothesised that DSF might interfere with cysteine residues located in the CXXC motif of MLL-fusions. This event would cause the potential unfolding of the CXXC domain and MLL-fusions detachment from DNA with a consequent block of the transcription of MLL-fusion target genes.

To investigate this possibility we performed a ChIP-seq assay. We immunoprecipitated and sequenced chromatin regions interacting with MLL, in control and in cells treated with disulfiram for 4 hours. It has been shown that common and specific MLL-AF9 and MLL-AF4 target genes are marked by H3K4me3 and H3K27ac (Prange et al., 2017). Considering that the drug treatment might have altered the epigenetic signature we immunoprecipitated also chromatin regions marked by H3K4me3 and H3K27ac, respectively marks of active transcription sites and open chromatin. The expertise of Dr Martens, from Radboud University in Netherland, was essential to analyse the data obtained in MLL, H3K4me3 and H3K27ac ChIP-seq and to correlate them with each other. Our ChIP-seq data showed that DSF impaired the MLL-fusion binding to the promoter regions of MLL target genes and blocked the transcription of target genes, which usually are highly expressed in acute

leukaemia. Ongoing collaboration with Professor Alan Warren from the haematology department of the Cambridge Institute of Medical Research is aimed to analyse the potential unfolding of the MLL-fusion CXXC domain upon DSF treatment. CHIP-seq results showed also that the MLL peaks were marked by H3K4me3 and H3K27ac and that while the 4 hours DSF treatment did not cause changes in H3K4me3 status, it caused a reduction of H3K27ac peaks. Reduction of H3K27ac levels was observed also after MLL-AF4 siRNA knockdown in a study from Konopleva and Milne laboratories (Godfrey et al., 2017). These data suggest that MLL-AF9 depletion caused epigenetic changes which might contribute to reduce the access of the transcriptional machinery to specific loci.

Disulfiram and its derivatives (dithiocarbamates) are known inhibitors of ALDH1, the Nf- $\kappa$ B pathway and proteasome activity. DSF function has been associated with activation of pathways (JNK/c-jun) which could interfere with the mechanism of drug resistance. But despite the fact that DSF has been associated with inhibition/activation of several cellular pathways, our findings indicate that DSF act specifically on MLL-fusions.

The GSEA analysis showed a negative correlation between the DSF gene expression profiles and a published leukaemic stem cell signature. Reduced cell self-renewal upon DSF treatment was confirmed by analysing the colony forming ability of AML *MLL* rearranged, non *MLL* rearranged AML cell lines and cord blood derived cells in methylcellulose assays. Furthermore, our flow cytometry analysis proved that the drug treatment was affecting cell viability and

proliferation only after prolonged exposures. Induction of cell death was detectable after 24 hours of treatment. Preliminary xenotransplantation studies showed an increased expression of the myeloid differentiation marker CD11b and reduced spleen size in treated mice. We have additional *in vivo* experiments ongoing to better clarify the DSF effect *in vivo*.

The novel screening platform, described in this thesis, allowed the identification of a drug with anti-leukaemic properties. I believe that this screening strategy could be used to target driving oncoproteins in other kinds of malignancies and lead to development of new clinical trials. We also showed that DSF cause degradation of MLL-fusions, their eviction from target loci and the reduction in target gene expression. The functional consequence of these events is the specific inhibition of self-renewal ability of AML MLL rearranged cell lines. The self-renewal capacity of non MLL-rearranged AML and normal HPC cells is not inhibited by DSF. The current therapeutic options for AML patients are limited to cytotoxic drugs with anti-proliferative effect. This last finding provides the first real opportunity of targeted therapeutic treatment for AML patients characterised by MLL rearrangements. The MLL oncoproteins give rise to very aggressive acute leukaemia, which depend on continuous expression of the MLL-fusion proteins. Therefore, the discovery of a compound able to target the fusion proteins and to block the dependence of the disease on those fusions has important therapeutic implications. Furthermore, an epidemiological study published in December 2017 in Nature revealed a correlation between the continuous use of disulfiram in cancer patients and favourable prognosis. The mortality rates were lower in patients that were taking disulfiram after a cancer

diagnosis than in patients that stopped the treatment (Skrott et al., 2017). This study suggests that, given the anti-cancer effect, disulfiram should be combined with current cancer therapies. Another study on non-metastatic recurrent prostate cancers shows that DSF induced transient demethylation (DNMT1 inhibition) in 30% of patients indicating that it is possible to target the CXXC domain in patients (Schweizer et al., 2013). I am confident that our discovery will translate soon into clear patients benefit with the development of therapies for paediatric and adult acute leukaemia. Considering that disulfiram was never used before to treat leukaemia patients, we will clearly need to develop clinical trials. However the close partnership between our institute and the Great Ormond Street Hospital (GOSH) will facilitate the development of paediatric clinical trials.

## REFERENCES

- ABLAIN, J. & DE THE, H. 2011. Revisiting the differentiation paradigm in acute promyelocytic leukemia. *Blood*, 117, 5795-802.
- ABLAIN, J., NASR, R., BAZARBACHI, A. & DE THE, H. 2011. The drug-induced degradation of oncoproteins: an unexpected Achilles' heel of cancer cells? *Cancer Discov*, 1, 117-27.
- ADOLFSSON, J., MANSSON, R., BUZA-VIDAS, N., HULTQUIST, A., LIUBA, K., JENSEN, C. T., BRYDER, D., YANG, L., BORGE, O. J., THOREN, L. A., ANDERSON, K., SITNICKA, E., SASAKI, Y., SIGVARDSSON, M. & JACOBSEN, S. E. 2005. Identification of Flt3+ lympho-myeloid stem cells lacking erythro-megakaryocytic potential a revised road map for adult blood lineage commitment. *Cell*, 121, 295-306.
- ALLEN, M. D., GRUMMITT, C. G., HILCENKO, C., MIN, S. Y., TONKIN, L. M., JOHNSON, C. M., FREUND, S. M., BYCROFT, M. & WARREN, A. J. 2006. Solution structure of the nonmethyl-CpG-binding CXXC domain of the leukaemia-associated MLL histone methyltransferase. *Embo j*, 25, 4503-12.
- ANDERSSON, A. K., MA, J., WANG, J., CHEN, X., GEDMAN, A. L., DANG, J., NAKITANDWE, J., HOLMFELDT, L., PARKER, M., EASTON, J., HUETHER, R., KRIWACKI, R., RUSCH, M., WU, G., LI, Y., MULDER, H., RAIMONDI, S., POUNDS, S., KANG, G., SHI, L., BECKSFORT, J., GUPTA, P., PAYNE-TURNER, D., VADODARIA, B., BOGGS, K., YERGEAU, D., MANNE, J., SONG, G., EDMONSON, M., NAGAHAWATTE, P., WEI, L., CHENG, C., PEI, D., SUTTON, R., VENN, N. C., CHETCUTI, A., RUSH, A., CATCHPOOLE, D., HELDRUP, J., FIORETOS, T., LU, C., DING, L., PUI, C. H., SHURTLEFF, S., MULLIGHAN, C. G., MARDIS, E. R., WILSON, R. K., GRUBER, T. A., ZHANG, J. & DOWNING, J. R. 2015. The landscape of somatic mutations in infant MLL-rearranged acute lymphoblastic leukemias. *Nat Genet*, 47, 330-7.
- ANJOS-AFONSO, F., CURRIE, E., PALMER, H. G., FOSTER, K. E., TAUSSIG, D. C. & BONNET, D. 2013. CD34(-) cells at the apex of the human hematopoietic stem cell hierarchy have distinctive cellular and molecular signatures. *Cell Stem Cell*, 13, 161-74.
- ARIGONY, A. L., #XFA, VARGAS, C., DE OLIVEIRA, I. M., MACHADO, M., BORDIN, D. L., BERGTER, L., PR, #XE1, , D., #XEA, GAS HENRIQUES, J., #XE3 & ANTONIO, O. 2013. The Influence of Micronutrients in Cell Culture: A Reflection on Viability and Genomic Stability. *BioMed Research International*, 2013, 22.

- ASHBURN, T. T. & THOR, K. B. 2004. Drug repositioning: identifying and developing new uses for existing drugs. *Nat Rev Drug Discov*, 3, 673-83.
- AYTON, P. M., CHEN, E. H. & CLEARY, M. L. 2004. Binding to nonmethylated CpG DNA is essential for target recognition, transactivation, and myeloid transformation by an MLL oncoprotein. *Mol Cell Biol*, 24, 10470-8.
- AYTON, P. M. & CLEARY, M. L. 2001. Molecular mechanisms of leukemogenesis mediated by MLL fusion proteins. *Oncogene*, 20, 5695-707.
- BANNISTER, A. J. & KOUZARIDES, T. 2011. Regulation of chromatin by histone modifications. *Cell Res*, 21, 381-95.
- BARABE, F., KENNEDY, J. A., HOPE, K. J. & DICK, J. E. 2007. Modeling the initiation and progression of human acute leukemia in mice. *Science*, 316, 600-4.
- BELLONI, E., SHING, D., TAPINASSI, C., VIALE, A., MANCUSO, P., MALAZZI, O., GERBINO, E., DALL'OLIO, V., EGURBIDE, I., ODERO, M. D., BERTOLINI, F. & PELICCI, P. G. 2011. In vivo expression of an aberrant MYB-GATA1 fusion induces leukemia in the presence of GATA1 reduced levels. *Leukemia*, 25, 733-6.
- BERNT, K. M., ZHU, N., SINHA, A. U., VEMPATI, S., FABER, J., KRIVTSOV, A. V., FENG, Z., PUNT, N., DAIGLE, A., BULLINGER, L., POLLOCK, R. M., RICHON, V. M., KUNG, A. L. & ARMSTRONG, S. A. 2011. MLL-rearranged leukemia is dependent on aberrant H3K79 methylation by DOT1L. *Cancer Cell*, 20, 66-78.
- BIONDI, A., CIMINO, G., PIETERS, R. & PUI, C. H. 2000. Biological and therapeutic aspects of infant leukemia. *Blood*, 96, 24-33.
- BITOUN, E., OLIVER, P. L. & DAVIES, K. E. 2007. The mixed-lineage leukemia fusion partner AF4 stimulates RNA polymerase II transcriptional elongation and mediates coordinated chromatin remodeling. *Hum Mol Genet*, 16, 92-106.
- BOISCLAIR, M., EGAN, D., HUBERMAN, K. & INFANTINO, R. 2004. High-Throughput Screening in Industry. In: TEICHER, B. & ANDREWS, P. (eds.) *Anticancer Drug Development Guide*. Humana Press.
- BONNET, D. 2005. Normal and leukaemic stem cells. *Br J Haematol*, 130, 469-79.
- BONNET, D. & DICK, J. E. 1997. Human acute myeloid leukemia is organized as a hierarchy that originates from a primitive hematopoietic cell. *Nature Medicine*, 3, 730.

- BROACH, J. R. & THORNER, J. 1996. High-throughput screening for drug discovery. *Nature*, 384, 14-6.
- CEN, D., BRAYTON, D., SHAHANDEH, B., MEYSKENS, F. L., JR. & FARMER, P. J. 2004. Disulfiram facilitates intracellular Cu uptake and induces apoptosis in human melanoma cells. *J Med Chem*, 47, 6914-20.
- CHEN, D., CUI, Q. C., YANG, H. & DOU, Q. P. 2006. Disulfiram, a clinically used anti-alcoholism drug and copper-binding agent, induces apoptotic cell death in breast cancer cultures and xenografts via inhibition of the proteasome activity. *Cancer Res*, 66, 10425-33.
- COLLINS, C. T. & HESS, J. L. 2016. Deregulation of the HOXA9/MEIS1 Axis in Acute Leukemia. *Current opinion in hematology*, 23, 354-361.
- COLLINS, E. C., PANNELL, R., SIMPSON, E. M., FORSTER, A. & RABBITTS, T. H. 2000. Inter-chromosomal recombination of Mll and Af9 genes mediated by cre-loxP in mouse development. *EMBO Rep*, 1, 127-32.
- CORRAL, J., LAVENIR, I., IMPEY, H., WARREN, A. J., FORSTER, A., LARSON, T. A., BELL, S., MCKENZIE, A. N., KING, G. & RABBITTS, T. H. 1996. An Mll-AF9 fusion gene made by homologous recombination causes acute leukemia in chimeric mice: a method to create fusion oncogenes. *Cell*, 85, 853-61.
- COZZIO, A., PASSEGUE, E., AYTON, P. M., KARSUNKY, H., CLEARY, M. L. & WEISSMAN, I. L. 2003. Similar MLL-associated leukemias arising from self-renewing stem cells and short-lived myeloid progenitors. *Genes Dev*, 17, 3029-35.
- CRAWFORD, B. D. & HESS, J. L. 2006. MLL core components give the green light to histone methylation. *ACS Chem Biol*, 1, 495-8.
- DASER, A. & RABBITTS, T. H. 2005. The versatile mixed lineage leukaemia gene MLL and its many associations in leukaemogenesis. *Semin Cancer Biol*, 15, 175-88.
- DE THE, H. & CHEN, Z. 2010. Acute promyelocytic leukaemia: novel insights into the mechanisms of cure. *Nat Rev Cancer*, 10, 775-83.
- DOBSON, C. L., WARREN, A. J., PANNELL, R., FORSTER, A., LAVENIR, I., CORRAL, J., SMITH, A. J. & RABBITTS, T. H. 1999. The mll-AF9 gene fusion in mice controls myeloproliferation and specifies acute myeloid leukaemogenesis. *Embo j*, 18, 3564-74.
- DOU, Y. & HESS, J. L. 2008. Mechanisms of transcriptional regulation by MLL and its disruption in acute leukemia. *Int J Hematol*, 87, 10-8.
- DOULATOV, S., NOTTA, F., LAURENTI, E. & DICK, J. E. 2012. Hematopoiesis: a human perspective. *Cell Stem Cell*, 10, 120-36.

- DREWS, J. 2000. Drug discovery: a historical perspective. *Science*, 287, 1960-4.
- DREWS, J. & RYSER, S. 1997. The role of innovation in drug development. *Nat Biotechnol*, 15, 1318-9.
- DRYNAN, L. F., PANNELL, R., FORSTER, A., CHAN, N. M., CANO, F., DASER, A. & RABBITTS, T. H. 2005. Mll fusions generated by Cre-loxP-mediated de novo translocations can induce lineage reassignment in tumorigenesis. *Embo j*, 24, 3136-46.
- EGUCHI, M., EGUCHI-ISHIMAE, M. & GREAVES, M. 2003. The role of the MLL gene in infant leukemia. *Int J Hematol*, 78, 390-401.
- EKINS, S., WILLIAMS, A. J., KRASOWSKI, M. D. & FREUNDLICH, J. S. 2011. In silico repositioning of approved drugs for rare and neglected diseases. *Drug Discov Today*, 16, 298-310.
- FELIX, C. A. & LANGE, B. J. 1999. Leukemia in infants. *Oncologist*, 4, 225-40.
- FORD, A. M., RIDGE, S. A., CABRERA, M. E., MAHMOUD, H., STEEL, C. M., CHAN, L. C. & GREAVES, M. 1993. In utero rearrangements in the trithorax-related oncogene in infant leukaemias. *Nature*, 363, 358-60.
- FORSTER, A., PANNELL, R., DRYNAN, L. F., MCCORMACK, M., COLLINS, E. C., DASER, A. & RABBITTS, T. H. 2003. Engineering de novo reciprocal chromosomal translocations associated with Mll to replicate primary events of human cancer. *Cancer Cell*, 3, 449-58.
- FUKA, G., KANTNER, H. P., GRAUSENBURGER, R., INTHAL, A., BAUER, E., KRAPF, G., KAINDL, U., KAUER, M., DWORZAK, M. N., STOIBER, D., HAAS, O. A. & PANZER-GRUMAYER, R. 2012. Silencing of ETV6/RUNX1 abrogates PI3K/AKT/mTOR signaling and impairs reconstitution of leukemia in xenografts. *Leukemia*, 26, 927-33.
- GALE, K. B., FORD, A. M., REPP, R., BORKHARDT, A., KELLER, C., EDEN, O. B. & GREAVES, M. F. 1997. Backtracking leukemia to birth: Identification of clonotypic gene fusion sequences in neonatal blood spots. *Proceedings of the National Academy of Sciences of the United States of America*, 94, 13950-13954.
- GODFREY, L., KERRY, J., THORNE, R., REPAPI, E., DAVIES, J. O., TAPIA, M., BALLABIO, E., HUGHES, J. R., GENG, H., KONOPLEVA, M. & MILNE, T. A. 2017. MLL-AF4 binds directly to a BCL-2 specific enhancer and modulates H3K27 acetylation. *Exp Hematol*, 47, 64-75.
- GORDON, R. M. & SEATON, D. R. 1942. Observations On The Treatment Of Scabies. *The British Medical Journal*, 1, 685-687.

- GREAVES, M. 2006. Infection, immune responses and the aetiology of childhood leukaemia. *Nat Rev Cancer*, 6, 193-203.
- GREAVES, M. 2015. When one mutation is all it takes. *Cancer Cell*, 27, 433-4.
- GREAVES, M. F. & WIEMELS, J. 2003. Origins of chromosome translocations in childhood leukaemia. *Nat Rev Cancer*, 3, 639-49.
- GUENTHER, M. G., JENNER, R. G., CHEVALIER, B., NAKAMURA, T., CROCE, C. M., CANAANI, E. & YOUNG, R. A. 2005. Global and Hox-specific roles for the MLL1 methyltransferase. *Proc Natl Acad Sci U S A*, 102, 8603-8.
- GUENTHER, M. G., LAWTON, L. N., ROZOVSKAIA, T., FRAMPTON, G. M., LEVINE, S. S., VOLKERT, T. L., CROCE, C. M., NAKAMURA, T., CANAANI, E. & YOUNG, R. A. 2008. Aberrant chromatin at genes encoding stem cell regulators in human mixed-lineage leukemia. *Genes Dev*, 22, 3403-8.
- GUTIERREZ, L., TSUKAMOTO, S., SUZUKI, M., YAMAMOTO-MUKAI, H., YAMAMOTO, M., PHILIPSEN, S. & OHNEDA, K. 2008. Ablation of Gata1 in adult mice results in aplastic crisis, revealing its essential role in steady-state and stress erythropoiesis. *Blood*, 111, 4375-85.
- HALD, J. & JACOBSEN, E. 1948. A drug sensitizing the organism to ethyl alcohol. *Lancet*, 2, 1001-4.
- HAN, J., LIU, L., YUE, X., CHANG, J., SHI, W. & HUA, Y. 2013. A binuclear complex constituted by diethyldithiocarbamate and copper(I) functions as a proteasome activity inhibitor in pancreatic cancer cultures and xenografts. *Toxicol Appl Pharmacol*, 273, 477-83.
- HARRIS, N. L., JAFFE, E. S., DIEBOLD, J., FLANDRIN, G., MULLER-HERMELINK, H. K., VARDIMAN, J., LISTER, T. A. & BLOOMFIELD, C. D. 1999. The World Health Organization classification of neoplastic diseases of the hematopoietic and lymphoid tissues. Report of the Clinical Advisory Committee meeting, Airlie House, Virginia, November, 1997. *Ann Oncol*, 10, 1419-32.
- HESS, J. L. 2004. MLL: a histone methyltransferase disrupted in leukemia. *Trends Mol Med*, 10, 500-7.
- HESS, J. L., BITTNER, C. B., ZEISIG, D. T., BACH, C., FUCHS, U., BORKHARDT, A., FRAMPTON, J. & SLANY, R. K. 2006. c-Myb is an essential downstream target for homeobox-mediated transformation of hematopoietic cells. *Blood*, 108, 297-304.
- HESS, J. L., YU, B. D., LI, B., HANSON, R. & KORSMEYER, S. J. 1997. Defects in yolk sac hematopoiesis in Mll-null embryos. *Blood*, 90, 1799-806.

- HORTON, S. J., GRIER, D. G., MCGONIGLE, G. J., THOMPSON, A., MORROW, M., DE SILVA, I., MOULDING, D. A., KIOUSSIS, D., LAPPIN, T. R., BRADY, H. J. & WILLIAMS, O. 2005. Continuous MLL-ENL expression is necessary to establish a "Hox Code" and maintain immortalization of hematopoietic progenitor cells. *Cancer Res*, 65, 9245-52.
- HORTON, S. J. & HUNTLY, B. J. P. 2012. Recent advances in acute myeloid leukemia stem cell biology. *Haematologica*, 97, 966-974.
- HORTON, S. J., WALF-VORDERWULBECKE, V., CHATTERS, S. J., SEBIRE, N. J., DE BOER, J. & WILLIAMS, O. 2009. Acute myeloid leukemia induced by MLL-ENL is cured by oncogene ablation despite acquisition of complex genetic abnormalities. *Blood*, 113, 4922-9.
- HUNTLY, B. J. P. & GILLILAND, D. G. 2005. Leukaemia stem cells and the evolution of cancer-stem-cell research. *Nature Reviews Cancer*, 5, 311.
- IWASAKI, H. & AKASHI, K. 2007. Myeloid lineage commitment from the hematopoietic stem cell. *Immunity*, 26, 726-40.
- IWASAKI, H., SOMOZA, C., SHIGEMATSU, H., DUPREZ, E. A., IWASAKI-ARAI, J., MIZUNO, S., ARINOBU, Y., GEARY, K., ZHANG, P., DAYARAM, T., FENYUS, M. L., ELF, S., CHAN, S., KASTNER, P., HUETTNER, C. S., MURRAY, R., TENEN, D. G. & AKASHI, K. 2005. Distinctive and indispensable roles of PU.1 in maintenance of hematopoietic stem cells and their differentiation. *Blood*, 106, 1590-600.
- JACOBSEN, E. 1952. The metabolism of ethyl alcohol. *Pharmacol Rev*, 4, 107-35.
- JUDE, C. D., CLIMER, L., XU, D., ARTINGER, E., FISHER, J. & ERNST, P. 2007. Unique and independent roles for MLL in adult hematopoietic stem cells and progenitors. *Cell stem cell*, 1, 324-337.
- KAWAJI, H., SEVERIN, J., LIZIO, M., WATERHOUSE, A., KATAYAMA, S., IRVINE, K. M., HUME, D. A., FORREST, A. R. R., SUZUKI, H., CARNINCI, P., HAYASHIZAKI, Y. & DAUB, C. O. 2009. The FANTOM web resource: from mammalian transcriptional landscape to its dynamic regulation. *Genome Biology*, 10, R40-R40.
- KIM, A., STACHURA, D. & TRAVER, D. 2014. Cell Signaling Pathways Involved in Hematopoietic Stem Cell Specification. *Experimental cell research*, 329, 227-233.
- KIMOTO-KINOSHITA, S., NISHIDA, S. & TOMURA, T. T. 2004. Diethyldithiocarbamate can induce two different type of death: apoptosis and necrosis mediating the differential MAP kinase activation and redox regulation in HL60 cells. *Mol Cell Biochem*, 265, 123-32.

- KONO, S. 2013. Chapter Six - Aceruloplasminemia: An Update. *In: BHATIA, K. P. & SCHNEIDER, S. A. (eds.) International Review of Neurobiology.* Academic Press.
- KRAGH, H. 2008. FROM DISULFIRAM TO ANTABUSE: THE INVENTION OF A DRUG. *Bull. Hist. Chem*, 33.
- KRIGE, D., NEEDHAM, L. A., BAWDEN, L. J., FLORES, N., FARMER, H., MILES, L. E., STONE, E., CALLAGHAN, J., CHANDLER, S., CLARK, V. L., KIRWIN-JONES, P., LEGRIS, V., OWEN, J., PATEL, T., WOOD, S., BOX, G., LABER, D., ODEDRA, R., WRIGHT, A., WOOD, L. M., ECCLES, S. A., BONE, E. A., AYSCOUGH, A. & DRUMMOND, A. H. 2008. CHR-2797: an antiproliferative aminopeptidase inhibitor that leads to amino acid deprivation in human leukemic cells. *Cancer Res*, 68, 6669-79.
- KRIVTSOV, A. V. & ARMSTRONG, S. A. 2007. MLL translocations, histone modifications and leukaemia stem-cell development. *Nat Rev Cancer*, 7, 823-33.
- KUMAR, A. R., LI, Q., HUDSON, W. A., CHEN, W., SAM, T., YAO, Q., LUND, E. A., WU, B., KOWAL, B. J. & KERSEY, J. H. 2009. A role for MEIS1 in MLL-fusion gene leukemia. *Blood*, 113, 1756-8.
- LALLEMAND-BREITENBACH, V. & DE THÉ, H. 2010. A new oncoprotein catabolism pathway. *Blood*, 116, 2200.
- LAVAU, C., DU, C., THIRMAN, M. & ZELEZNIK-LE, N. 2000a. Chromatin-related properties of CBP fused to MLL generate a myelodysplastic-like syndrome that evolves into myeloid leukemia. *The EMBO Journal*, 19, 4655-4664.
- LAVAU, C., LUO, R. T., DU, C. & THIRMAN, M. J. 2000b. Retrovirus-mediated gene transfer of MLL-ELL transforms primary myeloid progenitors and causes acute myeloid leukemias in mice. *Proc Natl Acad Sci U S A*, 97, 10984-9.
- LAVAU, C., SZILVASSY, S. J., SLANY, R. & CLEARY, M. L. 1997. Immortalization and leukemic transformation of a myelomonocytic precursor by retrovirally transduced HRX-ENL. *The EMBO Journal*, 16, 4226-4237.
- LAWRENCE, H. J., CHRISTENSEN, J., FONG, S., HU, Y. L., WEISSMAN, I., SAUVAGEAU, G., HUMPHRIES, R. K. & LARGMAN, C. 2005. Loss of expression of the Hoxa-9 homeobox gene impairs the proliferation and repopulating ability of hematopoietic stem cells. *Blood*, 106, 3988-94.
- LIN, J., HAFFNER, M. C., ZHANG, Y., LEE, B. H., BRENNEN, W. N., BRITTON, J., KACHHAP, S. K., SHIM, J. S., LIU, J. O., NELSON, W. G., YEGNASUBRAMANIAN, S. & CARDUCCI, M. A. 2011. Disulfiram is a

- DNA demethylating agent and inhibits prostate cancer cell growth. *Prostate*, 71, 333-43.
- LINGGI, B. E., BRANDT, S. J., SUN, Z. W. & HIEBERT, S. W. 2005. Translating the histone code into leukemia. *J Cell Biochem*, 96, 938-50.
- LIU, F., LEI, W., O'ROURKE, J. P. & NESS, S. A. 2006. Oncogenic mutations cause dramatic, qualitative changes in the transcriptional activity of c-Myb. *Oncogene*, 25, 795-805.
- LIU, P., BROWN, S., GOKTUG, T., CHANNATHODIYIL, P., KANNAPPAN, V., HUGNOT, J. P., GUICHET, P. O., BIAN, X., ARMESILLA, A. L., DARLING, J. L. & WANG, W. 2012. Cytotoxic effect of disulfiram/copper on human glioblastoma cell lines and ALDH-positive cancer-stem-like cells. *Br J Cancer*, 107, 1488-97.
- LOWENBERG, B., DOWNING, J. R. & BURNETT, A. 1999. Acute myeloid leukemia. *N Engl J Med*, 341, 1051-62.
- MACARRON, R., BANKS, M. N., BOJANIC, D., BURNS, D. J., CIROVIC, D. A., GARYANTES, T., GREEN, D. V. S., HERTZBERG, R. P., JANZEN, W. P., PASLAY, J. W., SCHOPFER, U. & SITTAMPALAM, G. S. 2011. Impact of high-throughput screening in biomedical research. *Nat Rev Drug Discov*, 10, 188-195.
- MANGOLINI, M., DE BOER, J., WALF-VORDERWULBECKE, V., PIETERS, R., DEN BOER, M. L. & WILLIAMS, O. 2013. STAT3 mediates oncogenic addiction to TEL-AML1 in t(12;21) acute lymphoblastic leukemia. *Blood*, 122, 542-9.
- MANSOUR, M. R., ABRAHAM, B. J., ANDERS, L., BEREZOVSKAYA, A., GUTIERREZ, A., DURBIN, A. D., ETCHIN, J., LAWTON, L., SALLAN, S. E., SILVERMAN, L. B., LOH, M. L., HUNGER, S. P., SANDA, T., YOUNG, R. A. & LOOK, A. T. 2014. An Oncogenic Super-Enhancer Formed Through Somatic Mutation of a Noncoding Intergenic Element. *Science (New York, N.Y.)*, 346, 1373-1377.
- MANTO, M. 2014. Abnormal Copper Homeostasis: Mechanisms and Roles in Neurodegeneration. *Toxics*, 2, 327.
- MAYR, L. M. & BOJANIC, D. 2009. Novel trends in high-throughput screening. *Current Opinion in Pharmacology*, 9, 580-588.
- MCCMAHON, K. A., HIEW, S. Y., HADJUR, S., VEIGA-FERNANDES, H., MENZEL, U., PRICE, A. J., KIOUSSIS, D., WILLIAMS, O. & BRADY, H. J. 2007. Mll has a critical role in fetal and adult hematopoietic stem cell self-renewal. *Cell Stem Cell*, 1, 338-45.
- MEYER, C., SCHNEIDER, B., JAKOB, S., STREHL, S., ATTARBASCHI, A., SCHNITTGER, S., SCHOCH, C., JANSEN, M. W., VAN DONGEN, J. J.,

- DEN BOER, M. L., PIETERS, R., ENNAS, M. G., ANGELUCCI, E., KOEHL, U., GREIL, J., GRIESINGER, F., ZUR STADT, U., ECKERT, C., SZCZEPANSKI, T., NIGGLI, F. K., SCHAFER, B. W., KEMPSKI, H., BRADY, H. J., ZUNA, J., TRKA, J., NIGRO, L. L., BIONDI, A., DELABESSE, E., MACINTYRE, E., STANULLA, M., SCHRAPPE, M., HAAS, O. A., BURMEISTER, T., DINGERMANN, T., KLINGEBIEL, T. & MARSCHALEK, R. 2006. The MLL recombinome of acute leukemias. *Leukemia*, 20, 777-84.
- MISHRA, B. P., ZAFFUTO, K. M., ARTINGER, E. L., ORG, T., MIKKOLA, H. K., CHENG, C., DJABALI, M. & ERNST, P. 2014. The histone methyltransferase activity of MLL1 is dispensable for hematopoiesis and leukemogenesis. *Cell Rep*, 7, 1239-47.
- MULLIGHAN, C. G., KENNEDY, A., ZHOU, X., RADTKE, I., PHILLIPS, L. A., SHURTLEFF, S. A. & DOWNING, J. R. 2007. Pediatric acute myeloid leukemia with NPM1 mutations is characterized by a gene expression profile with dysregulated HOX gene expression distinct from MLL-rearranged leukemias. *Leukemia*, 21, 2000-9.
- MURATI, A., GERVAIS, C., CARBUCCIA, N., FINETTI, P., CERVERA, N., ADELAIDE, J., STRUSKI, S., LIPPERT, E., MUGNERET, F., TIGAUD, I., PENTHER, D., BASTARD, C., POPPE, B., SPELEMAN, F., BARANGER, L., LUQUET, I., CORNILLET-LEFEBVRE, P., NADAL, N., NGUYEN-KHAC, F., PEROT, C., OLSCHWANG, S., BERTUCCI, F., CHAFFANET, M., LESSARD, M., MOZZICONACCI, M. J. & BIRNBAUM, D. 2009. Genome profiling of acute myelomonocytic leukemia: alteration of the MYB locus in MYST3-linked cases. *Leukemia*, 23, 85-94.
- MUTHYALA, R. 2011. Orphan/rare drug discovery through drug repositioning. *Drug Discovery Today: Therapeutic Strategies*, 8, 71-76.
- NAKAMURA, T., MORI, T., TADA, S., KRAJEWSKI, W., ROZOVSKAIA, T., WASSELL, R., DUBOIS, G., MAZO, A., CROCE, C. M. & CANAANI, E. 2002. ALL-1 is a histone methyltransferase that assembles a supercomplex of proteins involved in transcriptional regulation. *Mol Cell*, 10, 1119-28.
- NECKERS, L. & WORKMAN, P. 2012. Hsp90 molecular chaperone inhibitors: are we there yet? *Clin Cancer Res*, 18, 64-76.
- OKUDA, T., VAN DEURSEN, J., HIEBERT, S. W., GROSVELD, G. & DOWNING, J. R. 1996. AML1, the target of multiple chromosomal translocations in human leukemia, is essential for normal fetal liver hematopoiesis. *Cell*, 84, 321-30.
- ORKIN, S. H. 2000. Diversification of haematopoietic stem cells to specific lineages. *Nat Rev Genet*, 1, 57-64.

- ORKIN, S. H. & ZON, L. I. 2008. Hematopoiesis: an evolving paradigm for stem cell biology. *Cell*, 132, 631-44.
- PAL, D., BLAIR, H. J., ELDER, A., DORMON, K., RENNIE, K. J., COLEMAN, D. J., WEILAND, J., RANKIN, K. S., FILBY, A., HEIDENREICH, O. & VORMOOR, J. 2016. Long-term in vitro maintenance of clonal abundance and leukaemia-initiating potential in acute lymphoblastic leukaemia. *Leukemia*, 30, 1691-700.
- PRADHAN, M., ESTEVE, P. O., CHIN, H. G., SAMARANAYKE, M., KIM, G. D. & PRADHAN, S. 2008. CXXC domain of human DNMT1 is essential for enzymatic activity. *Biochemistry*, 47, 10000-9.
- PRANGE, K. H. M., MANDOLI, A., KUZNETSOVA, T., WANG, S. Y., SOTOCA, A. M., MARNETH, A. E., VAN DER REIJDEN, B. A., STUNNENBERG, H. G. & MARTENS, J. H. A. 2017. MLL-AF9 and MLL-AF4 oncofusion proteins bind a distinct enhancer repertoire and target the RUNX1 program in 11q23 acute myeloid leukemia. *Oncogene*, 36, 3346-3356.
- PUI, C. H., CARROLL, W. L., MESHINCHI, S. & ARCECI, R. J. 2011. Biology, risk stratification, and therapy of pediatric acute leukemias: an update. *J Clin Oncol*, 29, 551-65.
- QUELEN, C., LIPPERT, E., STRUSKI, S., DEMUR, C., SOLER, G., PRADE, N., DELABESSE, E., BROCCARDO, C., DASTUGUE, N., MAHON, F. X. & BROUSSET, P. 2011. Identification of a transforming MYB-GATA1 fusion gene in acute basophilic leukemia: a new entity in male infants. *Blood*, 117, 5719-22.
- RISNER, L. E., KUNTIMADDI, A., LOKKEN, A. A., ACHILLE, N. J., BIRCH, N. W., SCHOENFELT, K., BUSHWELLER, J. H. & ZELEZNIK-LE, N. J. 2013. Functional specificity of CpG DNA-binding CXXC domains in mixed lineage leukemia. *J Biol Chem*, 288, 29901-10.
- RUBNITZ, J. E. & INABA, H. 2012. Childhood Acute Myeloid Leukaemia. *British journal of haematology*, 159, 259-276.
- SALESSE, S. & VERFAILLIE, C. M. 2002. BCR/ABL: from molecular mechanisms of leukemia induction to treatment of chronic myelogenous leukemia. *Oncogene*, 21, 8547-59.
- SANDERS, D. S., MUNTEAN, A. G. & HESS, J. L. 2011. Significance of AF4-MLL reciprocal fusion in t(4;11) leukemias? *Leuk Res*, 35, 299-300.
- SARDANA, D., ZHU, C., ZHANG, M., GUDIVADA, R. C., YANG, L. & JEGGA, A. G. 2011. Drug repositioning for orphan diseases. *Brief Bioinform*, 12, 346-56.
- SAYGIN, C. & CARRAWAY, H. E. 2017. Emerging therapies for acute myeloid leukemia. *J Hematol Oncol*, 10, 93.

- SCHULZE, J. M., WANG, A. Y. & KOBOR, M. S. 2009. YEATS domain proteins: a diverse family with many links to chromatin modification and transcription. *Biochem Cell Biol*, 87, 65-75.
- SCHWEIZER, M. T., LIN, J., BLACKFORD, A., BARDIA, A., KING, S., ARMSTRONG, A. J., RUDEK, M. A., YEGNASUBRAMANIAN, S. & CARDUCCI, M. A. 2013. Pharmacodynamic study of disulfiram in men with non-metastatic recurrent prostate cancer. *Prostate Cancer Prostatic Dis*, 16, 357-61.
- SELL, S. 2005. Leukemia: stem cells, maturation arrest, and differentiation therapy. *Stem Cell Rev*, 1, 197-205.
- SHAMI, P. J. & DEININGER, M. 2012. Evolving treatment strategies for patients newly diagnosed with chronic myeloid leukemia: the role of second-generation BCR-ABL inhibitors as first-line therapy. *Leukemia*, 26, 214-24.
- SKROTT, Z., MISTRİK, M., ANDERSEN, K. K., FRIIS, S., MAJERA, D., GURSKY, J., OZDIAN, T., BARTKOVA, J., TURI, Z., MOUDRY, P., KRAUS, M., MICHALOVA, M., VACLAVKOVA, J., DZUBAK, P., VROBEL, I., POUCKOVA, P., SEDLACEK, J., MIKLOVICOVA, A., KUTT, A., LI, J., MATTOVA, J., DRIESSEN, C., DOU, Q. P., OLSEN, J., HAJDUCH, M., CVEK, B., DESHAIES, R. J. & BARTEK, J. 2017. Alcohol-abuse drug disulfiram targets cancer via p97 segregase adaptor NPL4. *Nature*, 552, 194-199.
- SLANY, R. K. 2009. The molecular biology of mixed lineage leukemia. *Haematologica*, 94, 984-93.
- SLANY, R. K., LAVAU, C. & CLEARY, M. L. 1998. The oncogenic capacity of HRX-ENL requires the transcriptional transactivation activity of ENL and the DNA binding motifs of HRX. *Mol Cell Biol*, 18, 122-9.
- SMITH, E., LIN, C. & SHILATIFARD, A. 2011. The super elongation complex (SEC) and MLL in development and disease. *Genes Dev*, 25, 661-72.
- SOMERVILLE, T. C., MATHENY, C. J., SPENCER, G. J., IWASAKI, M., RINN, J. L., WITTEN, D. M., CHANG, H. Y., SHURTLEFF, S. A., DOWNING, J. R. & CLEARY, M. L. 2009. Hierarchical maintenance of MLL myeloid leukemia stem cells employs a transcriptional program shared with embryonic rather than adult stem cells. *Cell Stem Cell*, 4, 129-40.
- SUBRAMANIAN, A., TAMAYO, P., MOOTHA, V. K., MUKHERJEE, S., EBERT, B. L., GILLETTE, M. A., PAULOVICH, A., POMEROY, S. L., GOLUB, T. R., LANDER, E. S. & MESIROV, J. P. 2005. Gene set enrichment analysis: a knowledge-based approach for interpreting genome-wide expression profiles. *Proc Natl Acad Sci U S A*, 102, 15545-50.

- SUZUKI, H., FORREST, A. R., VAN NIMWEGEN, E., DAUB, C. O., BALWIERZ, P. J., IRVINE, K. M., LASSMANN, T., RAVASI, T., HASEGAWA, Y., DE HOON, M. J., KATAYAMA, S., SCHRODER, K., CARNINCI, P., TOMARU, Y., KANAMORI-KATAYAMA, M., KUBOSAKI, A., AKALIN, A., ANDO, Y., ARNER, E., ASADA, M., ASAHARA, H., BAILEY, T., BAJIC, V. B., BAUER, D., BECKHOUSE, A. G., BERTIN, N., BJORKEGREN, J., BROMBACHER, F., BULGER, E., CHALK, A. M., CHIBA, J., CLOONAN, N., DAWE, A., DOSTIE, J., ENGSTROM, P. G., ESSACK, M., FAULKNER, G. J., FINK, J. L., FREDMAN, D., FUJIMORI, K., FURUNO, M., GOJOBORI, T., GOUGH, J., GRIMMOND, S. M., GUSTAFSSON, M., HASHIMOTO, M., HASHIMOTO, T., HATAKEYAMA, M., HEINZEL, S., HIDE, W., HOFMANN, O., HORNQUIST, M., HUMINIECKI, L., IKEO, K., IMAMOTO, N., INOUE, S., INOUE, Y., ISHIHARA, R., IWAYANAGI, T., JACOBSEN, A., KAUR, M., KAWAJI, H., KERR, M. C., KIMURA, R., KIMURA, S., KIMURA, Y., KITANO, H., KOGA, H., KOJIMA, T., KONDO, S., KONNO, T., KROGH, A., KRUGER, A., KUMAR, A., LENHARD, B., LENNARTSSON, A., LINDOW, M., LIZIO, M., MACPHERSON, C., MAEDA, N., MAHER, C. A., MAQUNGO, M., MAR, J., MATIGIAN, N. A., MATSUDA, H., MATTICK, J. S., MEIER, S., MIYAMOTO, S., MIYAMOTO-SATO, E., NAKABAYASHI, K., NAKACHI, Y., NAKANO, M., NYGAARD, S., OKAYAMA, T., OKAZAKI, Y., OKUDA-YABUKAMI, H., ORLANDO, V., OTOMO, J., PACHKOV, M., PETROVSKY, N., et al. 2009. The transcriptional network that controls growth arrest and differentiation in a human myeloid leukemia cell line. *Nat Genet*, 41, 553-62.
- TARIQ, M., NUSSBAUMER, U., CHEN, Y., BEISEL, C. & PARO, R. 2009. Trithorax requires Hsp90 for maintenance of active chromatin at sites of gene expression. *Proc Natl Acad Sci U S A*, 106, 1157-62.
- TAUSSIG, D. C., MIRAKI-MOUD, F., ANJOS-AFONSO, F., PEARCE, D. J., ALLEN, K., RIDLER, C., LILLINGTON, D., OAKERVEE, H., CAVENAGH, J., AGRAWAL, S. G., LISTER, T. A., GRIBBEN, J. G. & BONNET, D. 2008. Anti-CD38 antibody-mediated clearance of human repopulating cells masks the heterogeneity of leukemia-initiating cells. *Blood*, 112, 568-75.
- THORSTEINSDOTTIR, U., SAUVAGEAU, G. & HUMPHRIES, R. K. 1997. Hox homeobox genes as regulators of normal and leukemic hematopoiesis. *Hematol Oncol Clin North Am*, 11, 1221-37.
- UAUY, R., OLIVARES, M. & GONZALEZ, M. 1998. Essentiality of copper in humans. *Am J Clin Nutr*, 67, 952s-959s.
- VEVERKA, K. A., JOHNSON, K. L., MAYS, D. C., LIPSKY, J. J. & NAYLOR, S. 1997. Inhibition of aldehyde dehydrogenase by disulfiram and its metabolite methyl diethylthiocarbamoyl-sulfoxide. *Biochem Pharmacol*, 53, 511-8.

- WANG, L. C., SWAT, W., FUJIWARA, Y., DAVIDSON, L., VISVADER, J., KUO, F., ALT, F. W., GILLILAND, D. G., GOLUB, T. R. & ORKIN, S. H. 1998. The TEL/ETV6 gene is required specifically for hematopoiesis in the bone marrow. *Genes Dev*, 12, 2392-402.
- WANG, P., LIN, C., SMITH, E. R., GUO, H., SANDERSON, B. W., WU, M., GOGOL, M., ALEXANDER, T., SEIDEL, C., WIEDEMANN, L. M., GE, K., KRUMLAUF, R. & SHILATIFARD, A. 2009. Global analysis of H3K4 methylation defines MLL family member targets and points to a role for MLL1-mediated H3K4 methylation in the regulation of transcriptional initiation by RNA polymerase II. *Mol Cell Biol*, 29, 6074-85.
- WINTERS, A. C. & BERNT, K. M. 2017. MLL-Rearranged Leukemias-An Update on Science and Clinical Approaches. *Front Pediatr*, 5, 4.
- WONG, P., IWASAKI, M., SOMERVILLE, T. C., SO, C. W. & CLEARY, M. L. 2007. Meis1 is an essential and rate-limiting regulator of MLL leukemia stem cell potential. *Genes Dev*, 21, 2762-74.
- XU, K., GUIDEZ, F., GLASOW, A., CHUNG, D., PETRIE, K., STEGMAIER, K., WANG, K. K., ZHANG, J., JING, Y., ZELENT, A. & WAXMAN, S. 2005. Benzodithiophenes potentiate differentiation of acute promyelocytic leukemia cells by lowering the threshold for ligand-mediated corepressor/coactivator exchange with retinoic acid receptor alpha and enhancing changes in all-trans-retinoic acid-regulated gene expression. *Cancer Res*, 65, 7856-65.
- YAGI, H., DEGUCHI, K., AONO, A., TANI, Y., KISHIMOTO, T. & KOMORI, T. 1998. Growth disturbance in fetal liver hematopoiesis of Mll-mutant mice. *Blood*, 92, 108-17.
- YAMAMOTO, R., MORITA, Y., OOEHARA, J., HAMANAKA, S., ONODERA, M., RUDOLPH, K. L., EMA, H. & NAKAUCHI, H. 2013. Clonal analysis unveils self-renewing lineage-restricted progenitors generated directly from hematopoietic stem cells. *Cell*, 154, 1112-26.
- YOKOYAMA, A. & CLEARY, M. L. 2008. Menin critically links MLL proteins with LEDGF on cancer-associated target genes. *Cancer Cell*, 14, 36-46.
- YOKOYAMA, A., KITABAYASHI, I., AYTON, P. M., CLEARY, M. L. & OHKI, M. 2002. Leukemia proto-oncoprotein MLL is proteolytically processed into 2 fragments with opposite transcriptional properties. *Blood*, 100, 3710-8.
- YOKOYAMA, A., LIN, M., NARESH, A., KITABAYASHI, I. & CLEARY, M. L. 2010. A higher-order complex containing AF4 and ENL family proteins with P-TEFb facilitates oncogenic and physiologic MLL-dependent transcription. *Cancer Cell*, 17, 198-212.
- YOKOYAMA, A., SOMERVILLE, T. C., SMITH, K. S., ROZENBLATT-ROSEN, O., MEYERSON, M. & CLEARY, M. L. 2005. The menin tumor

suppressor protein is an essential oncogenic cofactor for MLL-associated leukemogenesis. *Cell*, 123, 207-18.

ZAKHARI, S. 2006. Overview: How Is Alcohol Metabolized by the Body?

ZHENG, Y., THOMAS, P. M. & KELLEHER, N. L. 2013. Measurement of acetylation turnover at distinct lysines in human histones identifies long-lived acetylation sites. *Nature communications*, 4, 2203-2203.

ZHENG, Y., TIPTON, J. D., THOMAS, P. M., KELLEHER, N. L. & SWEET, S. M. M. 2014. Site-specific human histone H3 methylation stability: fast K4me3 turnover. *Proteomics*, 14, 2190-2199.

ZUBER, J., RAPPAPORT, A. R., LUO, W., WANG, E., CHEN, C., VASEVA, A. V., SHI, J., WEISSMUELLER, S., FELLMANN, C., TAYLOR, M. J., WEISSENBOECK, M., GRAEBER, T. G., KOGAN, S. C., VAKOC, C. R. & LOWE, S. W. 2011. An integrated approach to dissecting oncogene addiction implicates a Myb-coordinated self-renewal program as essential for leukemia maintenance. *Genes Dev*, 25, 1628-40.

## APPENDIX

### Appendix 1

PLATE 1: THP-1 MA9-LUC-REN

	1	2	3	4	5	6	7	8	9	10	11	12
A	–	0.97	0.95	1.04	0.98	0.99	0.86	1.21	1.00	1.01	1.00	–
B	–	1.01	1.00	0.98	0.99	0.99	0.90	1.20	0.98	1.00	0.95	–
C	–	1.00	1.02	1.01	0.98	0.99	0.96	1.16	0.95	0.97	0.96	–
D	–	1.06	1.09	1.10	1.15	1.02	1.10	1.32	1.08	1.07	0.01	–
E	–	1.02	0.98	1.01	1.01	1.00	0.99	1.13	0.95	0.97	0.95	–
F	–	1.02	0.99	0.98	1.01	0.98	1.02	1.10	0.94	0.98	0.97	–
G	–	1.00	0.99	1.04	1.00	0.98	1.04	1.16	0.95	0.93	0.91	–
H	–	1.00	1.05	0.97	1.05	1.01	0.99	1.09	0.90	1.02	0.92	–

PLATE 2: THP-1 MA9-LUC-REN

	1	2	3	4	5	6	7	8	9	10	11	12
A	–	0.95	1.18	1.13	1.02	0.97	0.98	0.91	0.97	0.97	0.92	–
B	–	1.00	1.09	1.04	1.05	1.09	1.04	0.73	1.02	1.01	0.92	–
C	–	0.96	1.08	1.09	0.99	1.09	0.95	1.00	0.96	0.93	0.95	–
D	–	0.98	1.01	1.03	1.06	1.06	1.00	1.02	1.02	0.97	0.84	–
E	–	1.00	1.15	1.05	1.04	1.04	0.90	1.09	1.00	0.95	0.78	–
F	–	0.97	1.21	1.06	1.02	1.02	1.01	0.98	0.78	0.97	0.98	–
G	–	1.09	1.35	1.00	1.06	1.05	0.97	0.91	0.98	0.82	0.79	–
H	–	0.99	1.03	0.99	1.08	0.94	0.95	0.96	1.07	0.99	0.98	–

PLATE 3: THP-1 MA9-LUC-REN

	1	2	3	4	5	6	7	8	9	10	11	12
A	–	1.19	1.11	1.08	NA	1.08	1.09	1.06	1.11	0.19	1.08	–
B	–	1.05	1.00	0.97	1.03	0.96	1.00	1.05	0.92	0.97	1.08	–
C	–	1.01	0.99	0.99	0.98	0.92	1.03	0.99	1.04	1.02	1.02	–
D	–	0.93	0.94	0.91	0.99	0.94	0.96	0.92	0.97	0.88	1.55	–
E	–	1.06	1.02	1.00	1.14	1.04	1.08	1.08	1.03	1.05	0.64	–
F	–	1.01	0.85	1.03	1.06	0.99	0.98	1.06	1.10	0.99	0.98	–
G	–	0.98	1.05	1.00	1.06	0.98	1.04	0.94	0.99	1.01	1.01	–
H	–	0.98	1.03	1.07	1.03	1.03	1.03	1.03	0.93	0.93	0.93	–

**PLATE 5: THP-1 MA9-LUC-REN**

	1	2	3	4	5	6	7	8	9	10	11	12
<b>A</b>	—	1.09	1.06	1.02	1.14	0.97	0.98	1.02	0.99	0.85	0.88	—
<b>B</b>	—	1.03	0.98	0.99	1.02	1.03	1.08	0.98	0.97	0.95	0.96	—
<b>C</b>	—	0.98	0.98	0.99	0.80	1.08	0.96	1.07	1.06	1.05	1.02	—
<b>D</b>	—	1.03	1.03	1.04	1.07	1.09	0.90	0.98	0.93	0.99	0.94	—
<b>E</b>	—	0.99	0.88	1.17	1.01	1.04	1.00	0.98	0.99	0.97	0.97	—
<b>F</b>	—	0.90	0.88	0.91	0.97	0.90	2.00	0.85	0.91	0.84	0.82	—
<b>G</b>	—	1.04	1.03	0.94	1.10	0.70	1.07	0.97	1.15	0.89	1.11	—
<b>H</b>	—	1.04	0.95	1.00	1.04	0.97	1.04	1.00	0.97	0.98	1.00	—

**PLATE 6: THP-1 MA9-LUC-REN**

	1	2	3	4	5	6	7	8	9	10	11	12
<b>A</b>	—	0.95	0.92	0.90	0.84	0.86	1.00	0.87	0.75	1.90	NA	—
<b>B</b>	—	0.98	1.01	0.96	1.01	1.02	1.09	0.99	0.96	1.04	0.93	—
<b>C</b>	—	NA	1.03	0.99	1.06	0.82	1.13	0.99	0.98	1.02	0.98	—
<b>D</b>	—	1.12	1.03	1.06	1.09	0.91	NA	NA	0.64	1.07	1.07	—
<b>E</b>	—	1.05	1.04	1.04	1.04	1.03	1.00	0.84	0.99	0.98	0.94	—
<b>F</b>	—	1.00	1.01	0.98	1.03	1.01	0.94	1.10	1.00	1.01	0.93	—
<b>G</b>	—	1.03	1.01	1.00	1.02	1.01	1.06	1.02	0.95	1.00	0.90	—
<b>H</b>	—	0.90	1.02	1.02	1.03	0.98	1.01	1.06	1.01	1.04	0.93	—

**PLATE 7: THP-1 MA9-LUC-REN**

	1	2	3	4	5	6	7	8	9	10	11	12
<b>A</b>	—	1.04	1.04	1.01	1.03	0.98	0.88	1.33	0.98	0.96	0.74	—
<b>B</b>	—	0.99	1.02	0.98	0.99	0.99	1.15	0.97	0.90	0.96	1.04	—
<b>C</b>	—	0.99	0.98	1.01	1.01	1.03	0.99	1.00	1.02	0.96	1.01	—
<b>D</b>	—	0.78	0.79	0.84	0.83	0.86	0.82	1.79	0.75	0.84	1.70	—
<b>E</b>	—	0.98	0.93	0.99	1.11	1.08	1.02	0.99	0.97	0.93	0.99	—
<b>F</b>	—	0.94	0.96	0.99	1.04	1.00	1.00	1.01	1.01	1.02	1.02	—
<b>G</b>	—	0.91	1.00	0.99	1.01	1.02	1.00	1.02	1.01	1.00	1.03	—
<b>H</b>	—	NA	0.96	1.03	1.00	0.88	1.04	1.04	1.01	1.05	NA	—

**PLATE 8: THP-1 MA9-LUC-REN**

	1	2	3	4	5	6	7	8	9	10	11	12
<b>A</b>	—	0.91	1.04	0.99	0.97	0.99	1.29	0.88	1.03	0.96	0.94	—
<b>B</b>	—	NA	1.57	0.82	0.87	0.78	0.76	1.73	0.83	0.81	0.83	—
<b>C</b>	—	1.01	1.03	0.99	1.01	0.94	1.12	1.05	1.02	0.96	0.87	—
<b>D</b>	—	1.01	1.02	1.03	0.99	0.91	1.17	1.00	0.96	0.94	0.96	—
<b>E</b>	—	1.09	1.00	1.01	0.88	0.90	0.96	1.03	1.18	0.98	0.98	—
<b>F</b>	—	1.04	1.06	0.99	0.97	0.97	1.12	1.00	0.95	0.86	1.04	—
<b>G</b>	—	0.98	1.04	1.02	0.98	1.00	1.02	1.05	0.98	0.91	1.03	—
<b>H</b>	—	0.96	1.02	1.07	1.00	0.96	1.01	1.09	1.02	0.89	0.99	—

**PLATE 9: THP-1 MA9-LUC-REN**

	1	3	4	5	6	7	8	9	10	11	12
<b>A</b>	—	1.07	0.81	1.23	0.90	0.89	1.01	0.96	0.94	1.05	—
<b>B</b>	—	1.02	0.99	1.14	0.92	NA	1.00	1.01	1.00	1.08	—
<b>C</b>	—	1.00	1.04	1.00	1.00	1.07	1.01	0.76	1.05	1.00	—
<b>D</b>	—	0.95	1.00	1.02	1.00	1.00	1.00	1.06	1.04	0.96	—
<b>E</b>	—	1.00	1.02	1.03	0.99	NA	0.97	0.98	1.00	0.98	—
<b>F</b>	—	0.99	1.01	0.99	1.02	0.99	1.05	1.08	0.89	1.01	—
<b>G</b>	—	0.98	0.96	1.06	NA	1.04	1.01	0.94	0.96	0.93	—
<b>H</b>	—	1.12	1.02	1.02	0.97	0.99	0.97	0.86	1.13	0.83	—

**PLATE 10: THP-1 MA9-LUC-REN**

	1	2	3	4	5	6	7	8	9	10	11	12
<b>A</b>	—	0.89	0.94	0.92	0.93	1.06	1.01	1.02	1.21	1.11	0.90	—
<b>B</b>	—	1.43	0.84	0.86	0.90	1.06	0.99	1.03	1.04	1.15	0.71	—
<b>C</b>	—	0.93	0.94	0.92	1.08	1.19	0.97	1.09	0.87	1.11	0.90	—
<b>D</b>	—	0.95	0.49	0.95	1.10	1.22	0.93	1.11	1.12	1.16	0.97	—
<b>E</b>	—	0.96	0.97	0.92	0.97	1.19	0.99	1.05	1.00	1.04	0.90	—
<b>F</b>	—	0.90	0.50	1.07	0.99	1.07	1.12	NA	1.22	1.13	1.00	—
<b>G</b>	—	1.10	1.40	1.08	1.01	NA	1.06	0.82	1.22	NA	0.78	—
<b>H</b>	—	0.96	0.75	0.98	0.95	1.23	0.94	1.14	1.13	NA	0.92	—

**PLATE 11: THP-1 MA9-LUC-REN**

	1	2	3	4	5	6	7	8	9	10	11	12
<b>A</b>	—	1.12	1.07	0.96	1.02	0.97	1.09	1.00	0.96	0.99	0.83	—
<b>B</b>	—	0.10	1.10	0.98	1.02	1.00	1.03	0.93	0.95	0.99	0.99	—
<b>C</b>	—	1.02	0.95	0.88	1.14	0.89	1.03	1.26	0.97	0.96	0.91	—
<b>D</b>	—	1.10	1.08	1.04	1.02	1.07	0.36	1.13	1.05	1.09	1.07	—
<b>E</b>	—	1.01	1.00	0.99	0.97	0.98	1.00	1.00	1.03	1.02	1.00	—
<b>F</b>	—	1.00	0.98	0.94	0.98	0.89	1.12	1.02	1.03	1.01	1.03	—
<b>G</b>	—	0.91	1.05	0.92	0.98	0.95	1.14	0.98	0.96	0.91	1.19	—
<b>H</b>	—	0.99	1.01	1.02	1.03	0.89	1.00	1.05	1.04	0.93	1.04	—

**PLATE 12: THP-1 MA9-LUC-REN**

	1	2	3	4	5	6	7	8	9	10	11	12
<b>A</b>	—	1.00	1.05	NA	1.04	1.00	0.96	0.99	0.98	1.00	0.99	—
<b>B</b>	—	0.90	1.01	0.99	1.01	1.01	1.02	1.01	1.00	1.02	1.03	—
<b>C</b>	—	1.06	0.99	1.04	1.07	1.04	1.15	1.03	1.03	0.56	1.03	—
<b>D</b>	—	0.95	1.00	1.01	1.02	1.03	0.93	1.01	1.00	1.02	1.02	—
<b>E</b>	—	1.01	1.02	1.00	NA	NA	0.99	0.94	0.99	1.06	0.99	—
<b>F</b>	—	0.95	1.01	1.01	1.00	1.00	1.01	0.99	1.01	1.01	1.00	—
<b>G</b>	—	1.03	1.00	0.94	1.12	1.07	1.00	1.03	0.97	0.99	0.97	—
<b>H</b>	—	0.97	NA	1.02	0.97	0.98	1.01	1.04	1.01	1.02	0.98	—

**PLATE 13: THP-1 MA9-LUC-REN**

	1	2	3	4	5	6	7	8	9	10	11	12
<b>A</b>	—	0.99	1.07	1.01	1.02	0.96	0.98	1.01	1.00	1.02	0.95	—
<b>B</b>	—	0.97	1.00	0.98	0.99	0.96	1.03	0.99	0.96	1.06	1.05	—
<b>C</b>	—	0.97	1.02	1.04	0.99	1.00	NA	0.97	0.99	0.98	1.04	—
<b>D</b>	—	1.77	0.91	0.96	0.92	0.91	0.92	0.79	0.95	0.94	0.92	—
<b>E</b>	—	1.02	0.95	1.08	1.04	0.92	1.02	1.00	0.96	0.97	1.03	—
<b>F</b>	—	0.95	1.11	1.01	1.08	1.00	0.98	1.01	0.98	0.97	0.92	—
<b>G</b>	—	0.95	1.06	1.01	1.01	1.01	1.00	0.99	0.99	0.98	1.00	—
<b>H</b>	—	1.01	0.98	0.99	1.01	0.99	0.99	1.01	1.01	1.00	NA	—

**PLATE 14: THP-1 MA9-LUC-REN**

	1	2	3	4	5	6	7	8	9	10	11	12
<b>A</b>	—	1.05	1.09	1.01	0.92	0.95	0.98	1.09	1.04	0.94	0.93	—
<b>B</b>	—	1.03	1.00	0.87	1.13	0.91	1.05	1.06	1.04	0.96	0.97	—
<b>C</b>	—	1.03	1.01	0.99	1.04	0.90	1.00	0.98	1.03	0.93	1.07	—
<b>D</b>	—	1.06	0.93	1.06	1.04	1.02	1.07	1.07	0.97	0.95	0.83	—
<b>E</b>	—	1.03	1.00	1.02	1.06	0.93	1.38	0.92	0.93	0.90	0.83	—
<b>F</b>	—	1.06	1.02	0.90	1.09	1.06	1.00	1.07	0.98	0.99	0.83	—
<b>G</b>	—	1.08	1.08	1.07	1.14	NA	1.10	1.03	1.02	0.74	0.75	—
<b>H</b>	—	1.05	1.03	1.00	0.93	1.04	1.12	1.06	1.01	0.81	0.95	—

**PLATE 15: THP-1 MA9-LUC-REN**

	1	2	3	4	5	6	7	8	9	10	11	12
<b>A</b>	—	0.98	1.03	0.95	1.01	0.96	0.98	0.95	0.99	0.95	1.18	—
<b>B</b>	—	0.98	0.89	0.96	1.00	0.80	1.01	0.91	0.96	1.03	1.45	—
<b>C</b>	—	0.96	0.99	1.03	1.03	1.14	0.98	0.96	0.99	0.94	0.99	—
<b>D</b>	—	0.95	0.92	1.05	0.97	1.19	1.00	0.92	0.92	1.08	1.01	—
<b>E</b>	—	1.02	0.98	1.00	1.04	0.89	1.04	1.00	0.93	1.07	1.03	—
<b>F</b>	—	1.91	0.88	0.95	0.84	0.93	0.89	0.89	0.89	0.88	0.94	—
<b>G</b>	—	0.98	0.96	0.96	0.99	1.13	1.03	0.93	1.00	1.02	1.01	—
<b>H</b>	—	0.69	0.96	0.98	1.02	1.07	1.11	1.05	0.96	1.05	1.10	—

**PLATE 16: THP-1 MA9-LUC-REN**

	1	2	3	4	5	6	7	8	9	10	11	12
<b>A</b>	—	1.17	1.21	1.08	1.17	1.12	0.13	1.06	1.06	1.03	0.98	—
<b>B</b>	—	0.06	NA	0.56	NA	0.59	0.58	NA	0.57	0.60	NA	—
<b>C</b>	—	1.15	1.03	1.26	0.06	1.04	0.93	1.06	1.05	1.37	1.04	—
<b>D</b>	—	1.19	0.96	0.99	1.04	1.05	0.92	0.77	1.01	1.07	1.00	—
<b>E</b>	—	1.03	1.03	0.99	1.03	1.05	0.99	0.95	0.98	1.01	0.94	—
<b>F</b>	—	1.00	1.05	0.98	1.01	1.04	0.82	1.04	0.99	1.09	0.99	—
<b>G</b>	—	1.55	0.83	1.01	0.99	0.97	0.90	0.93	0.89	1.02	0.91	—
<b>H</b>	—	1.07	1.01	1.02	0.96	0.96	0.92	1.05	1.12	0.87	1.01	—

## Appendix 2

<b>Prestw number</b>	<b>Plate Nb / Position Nb</b>	<b>Chemical name</b>
Prestw-1	01A02	Azaguanine-8
Prestw-2	01A03	Allantoin
Prestw-3	01A04	Acetazolamide
Prestw-4	01A05	Metformin hydrochloride
Prestw-5	01A06	Atracurium besylate
Prestw-6	01A07	Isoflupredone acetate
Prestw-7	01A08	Amiloride hydrochloride dihydrate
Prestw-8	01A09	Amprolium hydrochloride
Prestw-9	01A10	Hydrochlorothiazide
Prestw-10	01A11	Sulfaguanidine
Prestw-11	01B02	Meticrane
Prestw-12	01B03	Benzonatate
Prestw-13	01B04	Hydroflumethiazide
Prestw-14	01B05	Sulfacetamide sodic hydrate
Prestw-15	01B06	Heptaminol hydrochloride
Prestw-16	01B07	Sulfathiazole
Prestw-17	01B08	Levodopa
Prestw-18	01B09	Idoxuridine
Prestw-19	01B10	Captopril
Prestw-20	01B11	Minoxidil
Prestw-21	01C02	Sulfaphenazole
Prestw-22	01C03	Panthenol (D)
Prestw-23	01C04	Sulfadiazine
Prestw-24	01C05	Norethynodrel
Prestw-25	01C06	Thiamphenicol
Prestw-26	01C07	Cimetidine
Prestw-27	01C08	Doxylamine succinate
Prestw-28	01C09	Ethambutol dihydrochloride
Prestw-29	01C10	Antipyrine
Prestw-30	01C11	Antipyrine, 4-hydroxy
Prestw-31	01D02	Chloramphenicol
Prestw-32	01D03	Epirizole
Prestw-33	01D04	Diprophylline
Prestw-34	01D05	Triamterene
Prestw-35	01D06	Dapsone

Prestw-36	01D07	Troleandomycin
Prestw-37	01D08	Pyrimethamine
Prestw-38	01D09	Hexamethonium dibromide dihydrate
Prestw-39	01D10	Diflunisal
Prestw-40	01D11	Niclosamide
Prestw-41	01E02	Procaine hydrochloride
Prestw-42	01E03	Moxisylyte hydrochloride
Prestw-43	01E04	Betazole hydrochloride
Prestw-44	01E05	Isoxicam
Prestw-45	01E06	Naproxen
Prestw-46	01E07	Naphazoline hydrochloride
Prestw-47	01E08	Ticlopidine hydrochloride
Prestw-48	01E09	Dicyclomine hydrochloride
Prestw-49	01E10	Amyleine hydrochloride
Prestw-50	01E11	Lidocaine hydrochloride
Prestw-51	01F02	Trichlorfon
Prestw-52	01F03	Carbamazepine
Prestw-53	01F04	Triflupromazine hydrochloride
Prestw-54	01F05	Mefenamic acid
Prestw-55	01F06	Acetohexamide
Prestw-56	01F07	Sulpiride
Prestw-57	01F08	Benoxinate hydrochloride
Prestw-58	01F09	Oxethazaine
Prestw-59	01F10	Pheniramine maleate
Prestw-60	01F11	Tolazoline hydrochloride
Prestw-61	01G02	Morantel tartrate
Prestw-62	01G03	Homatropine hydrobromide (R,S)
Prestw-63	01G04	Nifedipine
Prestw-64	01G05	Chlorpromazine hydrochloride
Prestw-65	01G06	Diphenhydramine hydrochloride
Prestw-66	01G07	Minaprine dihydrochloride
Prestw-67	01G08	Miconazole
Prestw-68	01G09	Isoxsuprine hydrochloride
Prestw-69	01G10	Acebutolol hydrochloride
Prestw-70	01G11	Tolnaftate
Prestw-71	01H02	Todralazine hydrochloride
Prestw-72	01H03	Imipramine hydrochloride
Prestw-73	01H04	Sulindac
Prestw-74	01H05	Amitryptiline hydrochloride
Prestw-75	01H06	Adiphenine hydrochloride
Prestw-76	01H07	Dibucaine
Prestw-77	01H08	Prednisone
Prestw-78	01H09	Thioridazine hydrochloride

Prestw-79	01H10	Diphepanil methylsulfate
Prestw-80	01H11	Trimethobenzamide hydrochloride
Prestw-81	02A02	Metronidazole
Prestw-1424	02A03	Fulvestrant
Prestw-83	02A04	Edrophonium chloride
Prestw-84	02A05	Moroxidine hydrochloride
Prestw-85	02A06	Baclofen (R,S)
Prestw-86	02A07	Acyclovir
Prestw-87	02A08	Diazoxide
Prestw-88	02A09	Amidopyrine
Prestw-1179	02A10	Busulfan
Prestw-90	02A11	Pindolol
Prestw-91	02B02	Khellin
Prestw-92	02B03	Zimelidine dihydrochloride monohydrate
Prestw-93	02B04	Azacyclonol
Prestw-94	02B05	Azathioprine
Prestw-95	02B06	Lynestrenol
Prestw-96	02B07	Guanabenz acetate
Prestw-97	02B08	Disulfiram
Prestw-98	02B09	Acetylsalicylsalicylic acid
Prestw-99	02B10	Mianserine hydrochloride
Prestw-100	02B11	Nocodazole
Prestw-101	02C02	R(-) Apomorphine hydrochloride hemihydrate
Prestw-102	02C03	Amoxapine
Prestw-103	02C04	Cyproheptadine hydrochloride
Prestw-104	02C05	Famotidine
Prestw-105	02C06	Danazol
Prestw-106	02C07	Nicorandil
Prestw-1314	02C08	Pioglitazone
Prestw-108	02C09	Nomifensine maleate
Prestw-109	02C10	Dizocilpine maleate
Prestw-1192	02C11	Oxandrolone
Prestw-111	02D02	Naloxone hydrochloride
Prestw-112	02D03	Metolazone
Prestw-113	02D04	Ciprofloxacin hydrochloride monohydrate
Prestw-114	02D05	Ampicillin trihydrate
Prestw-115	02D06	Haloperidol
Prestw-116	02D07	Naltrexone hydrochloride dihydrate
Prestw-117	02D08	Chlorpheniramine maleate
Prestw-118	02D09	Nalbuphine hydrochloride
Prestw-119	02D10	Picotamide monohydrate
Prestw-120	02D11	Triamcinolone

Prestw-121	02E02	Bromocryptine mesylate
Prestw-1471	02E03	Amfepramone hydrochloride
Prestw-123	02E04	Dehydrocholic acid
Prestw-1184	02E05	Tioconazole
Prestw-125	02E06	Perphenazine
Prestw-126	02E07	Mefloquine hydrochloride
Prestw-127	02E08	Isoconazole
Prestw-128	02E09	Spirolactone
Prestw-129	02E10	Pirenzepine dihydrochloride
Prestw-130	02E11	Dexamethasone acetate
Prestw-131	02F02	Glipizide
Prestw-132	02F03	Loxapine succinate
Prestw-133	02F04	Hydroxyzine dihydrochloride
Prestw-134	02F05	Diltiazem hydrochloride
Prestw-135	02F06	Methotrexate
Prestw-136	02F07	Astemizole
Prestw-137	02F08	Clindamycin hydrochloride
Prestw-138	02F09	Terfenadine
Prestw-139	02F10	Cefotaxime sodium salt
Prestw-140	02F11	Tetracycline hydrochloride
Prestw-141	02G02	Verapamil hydrochloride
Prestw-142	02G03	Dipyridamole
Prestw-143	02G04	Chlorhexidine
Prestw-144	02G05	Loperamide hydrochloride
Prestw-145	02G06	Chlortetracycline hydrochloride
Prestw-146	02G07	Tamoxifen citrate
Prestw-147	02G08	Nicergoline
Prestw-148	02G09	Canrenoic acid potassium salt
Prestw-149	02G10	Thiopropazine dimesylate
Prestw-150	02G11	Dihydroergotamine tartrate
Prestw-151	02H02	Erythromycin
Prestw-1474	02H03	Chloroxine
Prestw-153	02H04	Didanosine
Prestw-154	02H05	Josamycin
Prestw-155	02H06	Paclitaxel
Prestw-156	02H07	Ivermectin
Prestw-157	02H08	Gallamine triethiodide
Prestw-158	02H09	Neomycin sulfate
Prestw-159	02H10	Dihydrostreptomycin sulfate
Prestw-160	02H11	Gentamicine sulfate
Prestw-161	03A02	Isoniazid
Prestw-162	03A03	Pentylentetrazole
Prestw-163	03A04	Chlorzoxazone

Prestw-164	03A05	Ornidazole
Prestw-165	03A06	Ethosuximide
Prestw-166	03A07	Mafenide hydrochloride
Prestw-167	03A08	Riluzole hydrochloride
Prestw-168	03A09	Nitrofurantoin
Prestw-169	03A10	Hydralazine hydrochloride
Prestw-170	03A11	Phenelzine sulfate
Prestw-171	03B02	Tranexamic acid
Prestw-172	03B03	Etofylline
Prestw-173	03B04	Tranylcypromine hydrochloride
Prestw-174	03B05	Alverine citrate salt
Prestw-175	03B06	Aceclofenac
Prestw-176	03B07	Iproniazide phosphate
Prestw-177	03B08	Sulfamethoxazole
Prestw-178	03B09	Mephesisin
Prestw-179	03B10	Phenformin hydrochloride
Prestw-180	03B11	Flutamide
Prestw-181	03C02	Ampyrone
Prestw-182	03C03	Levamisole hydrochloride
Prestw-183	03C04	Pargyline hydrochloride
Prestw-184	03C05	Methocarbamol
Prestw-185	03C06	Aztreonam
Prestw-186	03C07	Cloxacillin sodium salt
Prestw-187	03C08	Catharanthine
Prestw-188	03C09	Pentolinium bitartrate
Prestw-189	03C10	Aminopurine, 6-benzyl
Prestw-190	03C11	Tolbutamide
Prestw-191	03D02	Midodrine hydrochloride
Prestw-192	03D03	Thalidomide
Prestw-193	03D04	Oxolinic acid
Prestw-194	03D05	Nimesulide
Prestw-1231	03D06	Asenapine maleate
Prestw-196	03D07	Pentoxifylline
Prestw-197	03D08	Metaraminol bitartrate
Prestw-198	03D09	Salbutamol
Prestw-199	03D10	Prilocaine hydrochloride
Prestw-200	03D11	Camptothecine (S,+)
Prestw-201	03E02	Ranitidine hydrochloride
Prestw-202	03E03	Tiratricol, 3,3',5-triiodothyroacetic acid
Prestw-203	03E04	Flufenamic acid
Prestw-204	03E05	Flumequine
Prestw-205	03E06	Tolfenamic acid

Prestw-206	03E07	Meclofenamic acid sodium salt monohydrate
Prestw-1181	03E08	Tibolone
Prestw-208	03E09	Trimethoprim
Prestw-209	03E10	Metoclopramide monohydrochloride
Prestw-210	03E11	Fenbendazole
Prestw-211	03F02	Piroxicam
Prestw-212	03F03	Pyrantel tartrate
Prestw-213	03F04	Fenspiride hydrochloride
Prestw-214	03F05	Gemfibrozil
Prestw-215	03F06	Mefexamide hydrochloride
Prestw-216	03F07	Tiapride hydrochloride
Prestw-217	03F08	Mebendazole
Prestw-218	03F09	Fenbufen
Prestw-219	03F10	Ketoprofen
Prestw-220	03F11	Indapamide
Prestw-221	03G02	Norfloxacin
Prestw-222	03G03	Antimycin A
Prestw-223	03G04	Xylometazoline hydrochloride
Prestw-224	03G05	Oxymetazoline hydrochloride
Prestw-225	03G06	Nifenazone
Prestw-226	03G07	Griseofulvin
Prestw-227	03G08	Clemizole hydrochloride
Prestw-228	03G09	Tropicamide
Prestw-229	03G10	Nefopam hydrochloride
Prestw-230	03G11	Phentolamine hydrochloride
Prestw-231	03H02	Etodolac
Prestw-232	03H03	Scopolamin-N-oxide hydrobromide
Prestw-233	03H04	Hyoscyamine (L)
Prestw-234	03H05	Chlorphensin carbamate
Prestw-1771	03H06	Carmofur
Prestw-236	03H07	Dilazep dihydrochloride
Prestw-237	03H08	Ofloxacin
Prestw-238	03H09	Lomefloxacin hydrochloride
Prestw-239	03H10	Orphenadrine hydrochloride
Prestw-240	03H11	Proglumide
Prestw-241	04A02	Mexiletine hydrochloride
Prestw-242	04A03	Flavoxate hydrochloride
Prestw-243	04A04	Bufexamac
Prestw-244	04A05	Glutethimide, para-amino
Prestw-245	04A06	Dropropizine (R,S)
Prestw-246	04A07	Pinacidil
Prestw-247	04A08	Albendazole

Prestw-248	04A09	Clonidine hydrochloride
Prestw-249	04A10	Bupropion hydrochloride
Prestw-250	04A11	Alprenolol hydrochloride
Prestw-251	04B02	Chlorothiazide
Prestw-252	04B03	Diphenidol hydrochloride
Prestw-253	04B04	Norethindrone
Prestw-254	04B05	Nortriptyline hydrochloride
Prestw-255	04B06	Niflumic acid
Prestw-256	04B07	Isotretinoin
Prestw-257	04B08	Retinoic acid
Prestw-258	04B09	Antazoline hydrochloride
Prestw-259	04B10	Ethacrynic acid
Prestw-260	04B11	Praziquantel
Prestw-261	04C02	Ethisterone
Prestw-262	04C03	Tripolidine hydrochloride
Prestw-263	04C04	Doxepin hydrochloride
Prestw-264	04C05	Dyclonine hydrochloride
Prestw-265	04C06	Dimenhydrinate
Prestw-266	04C07	Disopyramide
Prestw-267	04C08	Clotrimazole
Prestw-268	04C09	Vinpocetine
Prestw-269	04C10	Clomipramine hydrochloride
Prestw-270	04C11	Fendiline hydrochloride
Prestw-271	04D02	Vincamine
Prestw-272	04D03	Indomethacin
Prestw-273	04D04	Cortisone
Prestw-274	04D05	Prednisolone
Prestw-275	04D06	Fenofibrate
Prestw-276	04D07	Bumetanide
Prestw-277	04D08	Labetalol hydrochloride
Prestw-278	04D09	Cinnarizine
Prestw-279	04D10	Methylprednisolone, 6-alpha
Prestw-280	04D11	Quinidine hydrochloride monohydrate
Prestw-281	04E02	Fludrocortisone acetate
Prestw-282	04E03	Fenoterol hydrobromide
Prestw-283	04E04	Homochlorcyclizine dihydrochloride
Prestw-284	04E05	Diethylcarbamazine citrate
Prestw-285	04E06	Chenodiol
Prestw-286	04E07	Perhexiline maleate
Prestw-287	04E08	Oxybutynin chloride
Prestw-288	04E09	Siperone
Prestw-289	04E10	Pyrilamine maleate
Prestw-290	04E11	Sulfapyrazone

Prestw-291	04F02	Dantrolene sodium salt
Prestw-292	04F03	Trazodone hydrochloride
Prestw-293	04F04	Glafenine hydrochloride
Prestw-294	04F05	Pimethixene maleate
Prestw-295	04F06	Pergolide mesylate
Prestw-296	04F07	Acemetacin
Prestw-297	04F08	Benzydamine hydrochloride
Prestw-298	04F09	Fipexide hydrochloride
Prestw-299	04F10	Mifepristone
Prestw-300	04F11	Diperodon hydrochloride
Prestw-301	04G02	Lisinopril
Prestw-302	04G03	Lincomycin hydrochloride
Prestw-303	04G04	Telenzepine dihydrochloride
Prestw-304	04G05	Econazole nitrate
Prestw-305	04G06	Bupivacaine hydrochloride
Prestw-306	04G07	Clemastine fumarate
Prestw-307	04G08	Oxytetracycline dihydrate
Prestw-308	04G09	Pimozide
Prestw-309	04G10	Amodiaquin dihydrochloride dihydrate
Prestw-310	04G11	Mebeverine hydrochloride
Prestw-311	04H02	Ifenprodil tartrate
Prestw-312	04H03	Flunarizine dihydrochloride
Prestw-313	04H04	Trifluoperazine dihydrochloride
Prestw-314	04H05	Enalapril maleate
Prestw-315	04H06	Minocycline hydrochloride
Prestw-316	04H07	Glibenclamide
Prestw-317	04H08	Guanethidine sulfate
Prestw-318	04H09	Quinacrine dihydrochloride hydrate
Prestw-319	04H10	Clofilium tosylate
Prestw-320	04H11	Fluphenazine dihydrochloride
Prestw-321	05A02	Streptomycin sulfate
Prestw-322	05A03	Alfuzosin hydrochloride
Prestw-323	05A04	Chlorpropamide
Prestw-324	05A05	Phenylpropanolamine hydrochloride
Prestw-325	05A06	Ascorbic acid
Prestw-326	05A07	Methyldopa (L,-)
Prestw-327	05A08	Cefoperazone dihydrate
Prestw-328	05A09	Zoxazolamine
Prestw-329	05A10	Tacrine hydrochloride
Prestw-330	05A11	Bisoprolol fumarate
Prestw-331	05B02	Tremorine dihydrochloride
Prestw-332	05B03	Practolol
Prestw-333	05B04	Zidovudine, AZT

Prestw-334	05B05	Sulfisoxazole
Prestw-335	05B06	Zaprinast
Prestw-336	05B07	Chlormezanone
Prestw-337	05B08	Procainamide hydrochloride
Prestw-338	05B09	N6-methyladenosine
Prestw-339	05B10	Guanfacine hydrochloride
Prestw-340	05B11	Domperidone
Prestw-341	05C02	Furosemide
Prestw-342	05C03	Methapyrilene hydrochloride
Prestw-343	05C04	Desipramine hydrochloride
Prestw-344	05C05	Clorgyline hydrochloride
Prestw-345	05C06	Clenbuterol hydrochloride
Prestw-346	05C07	Maprotiline hydrochloride
Prestw-347	05C08	Thioguanosine
Prestw-348	05C09	Chlorprothixene hydrochloride
Prestw-349	05C10	Ritodrine hydrochloride
Prestw-350	05C11	Clozapine
Prestw-351	05D02	Chlorthalidone
Prestw-352	05D03	Dobutamine hydrochloride
Prestw-353	05D04	Moclobemide
Prestw-354	05D05	Clopamide
Prestw-355	05D06	Hycanthone
Prestw-356	05D07	Adenosine 5'-monophosphate monohydrate
Prestw-357	05D08	Amoxicillin
Prestw-1603	05D09	Pemirolast potassium
Prestw-359	05D10	Dextromethorphan hydrobromide monohydrate
Prestw-360	05D11	Droperidol
Prestw-361	05E02	Bambuterol hydrochloride
Prestw-362	05E03	Betamethasone
Prestw-363	05E04	Colchicine
Prestw-364	05E05	Metergoline
Prestw-365	05E06	Brinzolamide
Prestw-368	05E09	Bepidil hydrochloride
Prestw-369	05E10	Meloxicam
Prestw-370	05E11	Benzbromarone
Prestw-371	05F02	Ketotifen fumarate
Prestw-372	05F03	Debrisoquin sulfate
Prestw-373	05F04	Amethopterin (R,S)
Prestw-374	05F05	Methylethergometrine maleate
Prestw-375	05F06	Methiothepin maleate
Prestw-376	05F07	Clofazimine
Prestw-377	05F08	Nafronyl oxalate

Prestw-378	05F09	Bezafibrate
Prestw-1152	05F10	Nefazodone HCl
Prestw-380	05F11	Clebopride maleate
Prestw-381	05G02	Lidoflazine
Prestw-382	05G03	Betaxolol hydrochloride
Prestw-383	05G04	Nicardipine hydrochloride
Prestw-384	05G05	Probucol
Prestw-385	05G06	Mitoxantrone dihydrochloride
Prestw-386	05G07	GBR 12909 dihydrochloride
Prestw-387	05G08	Carbetapentane citrate
Prestw-388	05G09	Dequalinium dichloride
Prestw-389	05G10	Ketoconazole
Prestw-390	05G11	Fusidic acid sodium salt
Prestw-391	05H02	Terbutaline hemisulfate
Prestw-392	05H03	Ketanserin tartrate hydrate
Prestw-393	05H04	Hemicholinium bromide
Prestw-394	05H05	Kanamycin A sulfate
Prestw-395	05H06	Amikacin hydrate
Prestw-396	05H07	Etoposide
Prestw-397	05H08	Clomiphene citrate (Z,E)
Prestw-398	05H09	Oxantel pamoate
Prestw-399	05H10	Prochlorperazine dimaleate
Prestw-400	05H11	Hesperidin
Prestw-401	06A02	Testosterone propionate
Prestw-1269	06A03	Haloprogin
Prestw-403	06A04	Thyroxine (L)
Prestw-1288	06A05	Idebenone
Prestw-405	06A06	Pepstatin A
Prestw-406	06A07	Morpholinoethylamino-3-benzocyclohepta-(5,6-c)-pyridazine dihydrochloride
Prestw-407	06A08	Adamantamine fumarate
Prestw-408	06A09	Butoconazole nitrate
Prestw-409	06A10	Amiodarone hydrochloride
Prestw-410	06A11	Amphotericin B
Prestw-411	06B02	Androsterone
Prestw-1489	06B03	Amifostine
Prestw-413	06B04	Carbarsone
Prestw-1219	06B05	Amlodipine
Prestw-1147	06B06	Modafinil
Prestw-416	06B07	Bacampicillin hydrochloride
Prestw-1298	06B08	Lamivudine
Prestw-418	06B09	Biotin
Prestw-419	06B10	Bisacodyl

Prestw-1242	06B11	Erlotinib
Prestw-421	06C02	Suloctidil
Prestw-1368	06C03	Zotepine
Prestw-423	06C04	Carisoprodol
Prestw-424	06C05	Cephalosporanic acid, 7-amino
Prestw-425	06C06	Chicago sky blue 6B
Prestw-426	06C07	Buflomedil hydrochloride
Prestw-1393	06C08	Dibenzepine hydrochloride
Prestw-428	06C09	Roxatidine Acetate HCl
Prestw-1505	06C10	Valacyclovir hydrochloride
Prestw-430	06C11	Cisapride
Prestw-1303	06D02	Pefloxacin
Prestw-432	06D03	Corticosterone
Prestw-433	06D04	Cyanocobalamin
Prestw-434	06D05	Cefadroxil
Prestw-435	06D06	Cyclosporin A
Prestw-436	06D07	Digitoxigenin
Prestw-437	06D08	Digoxin
Prestw-438	06D09	Doxorubicin hydrochloride
Prestw-439	06D10	Carbimazole
Prestw-440	06D11	Epiandrosterone
Prestw-441	06E02	Estradiol-17 beta
Prestw-1380	06E03	Clobutinol hydrochloride
Prestw-443	06E04	Gabazine bromide
Prestw-1156	06E05	Oxcarbazepine
Prestw-445	06E06	Cyclobenzaprine hydrochloride
Prestw-446	06E07	Carteolol hydrochloride
Prestw-447	06E08	Hydrocortisone base
Prestw-448	06E09	Hydroxytacrine maleate (R,S)
Prestw-449	06E10	Pilocarpine nitrate
Prestw-450	06E11	Dicloxacillin sodium salt hydrate
Prestw-451	06F02	Alizapride HCl
Prestw-1161	06F03	Stanozolol
Prestw-1257	06F04	Calcipotriene
Prestw-1429	06F05	Linezolid
Prestw-455	06F06	Mebhydroline 1,5-naphtalenedisulfonate
Prestw-456	06F07	Meclocycline sulfosalicylate
Prestw-457	06F08	Meclozine dihydrochloride
Prestw-458	06F09	Melatonin
Prestw-1251	06F10	Butalbital
Prestw-460	06F11	Dinoprost trometamol
Prestw-461	06G02	Tropisetron HCl
Prestw-462	06G03	Cefixime

Prestw-463	06G04	Metrizamide
Prestw-1323	06G05	Quetiapine hemifumarate
Prestw-1464	06G06	Tosufloxacin hydrochloride
Prestw-1400	06G07	Efavirenz
Prestw-1157	06G08	Rifapentine
Prestw-468	06G09	Neostigmine bromide
Prestw-469	06G10	Niridazole
Prestw-470	06G11	Ceforanide
Prestw-1358	06H02	Vatalanib
Prestw-1295	06H03	Itopride
Prestw-473	06H04	Cefotetan
Prestw-1254	06H05	Fentiazac
Prestw-475	06H06	Brompheniramine maleate
Prestw-476	06H07	Primaquine diphosphate
Prestw-477	06H08	Progesterone
Prestw-478	06H09	Felodipine
Prestw-1325	06H10	Raclopride
Prestw-1385	06H11	Closantel
Prestw-481	07A02	Serotonin hydrochloride
Prestw-482	07A03	Cefotiam hydrochloride
Prestw-1336	07A04	Rofecoxib
Prestw-484	07A05	Benperidol
Prestw-485	07A06	Cefaclor hydrate
Prestw-486	07A07	Colistin sulfate
Prestw-487	07A08	Daunorubicin hydrochloride
Prestw-488	07A09	Dosulepin hydrochloride
Prestw-489	07A10	Ceftazidime pentahydrate
Prestw-490	07A11	Iobenguane sulfate
Prestw-491	07B02	Metixene hydrochloride
Prestw-492	07B03	Nitrofurazone
Prestw-493	07B04	Omeprazole
Prestw-494	07B05	Propylthiouracil
Prestw-495	07B06	Terconazole
Prestw-496	07B07	Tiaprofenic acid
Prestw-497	07B08	Vancomycin hydrochloride
Prestw-498	07B09	Artemisinin
Prestw-499	07B10	Propafenone hydrochloride
Prestw-500	07B11	Ethamivan
Prestw-501	07C02	Vigabatrin
Prestw-502	07C03	Biperiden hydrochloride
Prestw-503	07C04	Cetirizine dihydrochloride
Prestw-504	07C05	Etifenin

Prestw-505	07C06	Metaproterenol sulfate, orciprenaline sulfate
Prestw-506	07C07	Sisomicin sulfate
Prestw-1159	07C08	Sibutramine HCl
Prestw-110	07C09	Acenocoumarol
Prestw-509	07C10	Bromperidol
Prestw-510	07C11	Cyclizine hydrochloride
Prestw-511	07D02	Fluoxetine hydrochloride
Prestw-512	07D03	Iohexol
Prestw-513	07D04	Norcyclobenzaprine
Prestw-514	07D05	Pyrazinamide
Prestw-515	07D06	Trimethadione
Prestw-516	07D07	Lovastatin
Prestw-517	07D08	Nystatine
Prestw-518	07D09	Budesonide
Prestw-519	07D10	Imipenem
Prestw-520	07D11	Sulfasalazine
Prestw-1430	07E02	Lofexidine
Prestw-522	07E03	Thiostrepton
Prestw-1169	07E04	Miglitol
Prestw-524	07E05	Tiabendazole
Prestw-525	07E06	Rifampicin
Prestw-526	07E07	Ethionamide
Prestw-527	07E08	Tenoxicam
Prestw-528	07E09	Triflusal
Prestw-529	07E10	Mesoridazine besylate
Prestw-530	07E11	Trolox
Prestw-531	07F02	Pirenperone
Prestw-532	07F03	Isoquinoline, 6,7-dimethoxy-1-methyl-1,2,3,4-tetrahydro, hydrochloride
Prestw-533	07F04	Phenacetin
Prestw-534	07F05	Atovaquone
Prestw-535	07F06	Methoxamine hydrochloride
Prestw-953	07F07	(S)-(-)-Atenolol
Prestw-537	07F08	Piracetam
Prestw-538	07F09	Phenindione
Prestw-539	07F10	Thiocolchicoside
Prestw-540	07F11	Clorsulon
Prestw-541	07G02	Ciclopirox ethanolamine
Prestw-542	07G03	Probenecid
Prestw-543	07G04	Betahistine mesylate
Prestw-544	07G05	Tobramycin
Prestw-545	07G06	Tetramisole hydrochloride
Prestw-546	07G07	Pregnenolone

Prestw-547	07G08	Molsidomine
Prestw-548	07G09	Chloroquine diphosphate
Prestw-549	07G10	Trimetazidine dihydrochloride
Prestw-550	07G11	Parthenolide
Prestw-551	07H02	Hexetidine
Prestw-552	07H03	Selegiline hydrochloride
Prestw-553	07H04	Pentamidine isethionate
Prestw-554	07H05	Tolazamide
Prestw-555	07H06	Nifuroxazide
Prestw-1144	07H07	Mirtazapine
Prestw-557	07H08	Dirithromycin
Prestw-558	07H09	Gliclazide
Prestw-559	07H10	DO 897/99
Prestw-560	07H11	Prenylamine lactate
Prestw-1188	08A02	Ziprasidone Hydrochloride
Prestw-1441	08A03	Mevastatin
Prestw-1322	08A04	Pyridostigmine iodide
Prestw-1491	08A05	Pentobarbital
Prestw-565	08A06	Atropine sulfate monohydrate
Prestw-566	08A07	Eserine hemisulfate salt
Prestw-1139	08A08	Itraconazole
Prestw-1174	08A09	Acarbose
Prestw-1403	08A10	Entacapone
Prestw-1449	08A11	Nicotinamide
Prestw-571	08B02	Tetracaine hydrochloride
Prestw-572	08B03	Mometasone furoate
Prestw-1467	08B04	Troglitazone
Prestw-574	08B05	Dacarbazine
Prestw-1351	08B06	Tenatoprazole
Prestw-576	08B07	Acetopromazine maleate salt
Prestw-1271	08B08	Escitalopram oxalate
Prestw-1158	08B09	Ropinirole HCl
Prestw-1297	08B10	Lacidipine
Prestw-1228	08B11	Argatroban
Prestw-1328	08C02	Reboxetine mesylate
Prestw-1498	08C03	Camylofine chlorhydrate
Prestw-583	08C04	Papaverine hydrochloride
Prestw-584	08C05	Yohimbine hydrochloride
Prestw-1500	08C06	Voriconazole
Prestw-1211	08C07	Alfacalcidol
Prestw-587	08C08	Cilostazol
Prestw-588	08C09	Galanthamine hydrobromide
Prestw-1130	08C10	Azelastine HCl

Prestw-1409	08C11	Etretinate
Prestw-1274	08D02	Emedastine
Prestw-1407	08D03	Etofenamate
Prestw-1369	08D04	Zaleplon
Prestw-594	08D05	Diclofenac sodium
Prestw-1410	08D06	Exemestane
Prestw-1499	08D07	Fomepizole
Prestw-1183	08D08	Temozolomide
Prestw-598	08D09	Xylazine
Prestw-1132	08D10	Celiprolol HCl
Prestw-1367	08D11	Zopiclone
Prestw-1198	08E02	Tranilast
Prestw-1182	08E03	Tizanidine HCl
Prestw-1364	08E04	Zafirlukast
Prestw-1252	08E05	Butenafine Hydrochloride
Prestw-1121	08E06	Carbadox
Prestw-1331	08E07	Rimantadine Hydrochloride
Prestw-607	08E08	Eburnamonine (-)
Prestw-1460	08E09	Oxibendazol
Prestw-1292	08E10	Ipsapirone
Prestw-1284	08E11	Hydroxychloroquine sulfate
Prestw-1431	08F02	Loracarbef
Prestw-1501	08F03	Fenipentol
Prestw-1503	08F04	Diosmin
Prestw-1177	08F05	Carbidopa
Prestw-1604	08F06	(-)-Emtricitabine
Prestw-616	08F07	Demecarium bromide
Prestw-617	08F08	Quipazine dimaleate salt
Prestw-1127	08F09	Acipimox
Prestw-619	08F10	Diflorasone Diacetate
Prestw-1502	08F11	Acamprosate calcium
Prestw-1506	08G02	Mizolastine
Prestw-1217	08G03	Amisulpride
Prestw-623	08G04	Pyridoxine hydrochloride
Prestw-1469	08G05	Mercaptopurine
Prestw-1134	08G06	Cytarabine
Prestw-626	08G07	Racecadotril
Prestw-627	08G08	Folic acid
Prestw-1129	08G09	Benazepril HCl
Prestw-1178	08G10	Aniracetam
Prestw-630	08G11	Dimethisoquin hydrochloride
Prestw-1210	08H02	Alendronate sodium
Prestw-632	08H03	Dipivefrin hydrochloride

Prestw-633	08H04	Thiorphan
Prestw-1463	08H05	Tomoxetine hydrochloride
Prestw-1511	08H06	Aceclidine Hydrochloride
Prestw-1488	08H07	Penciclovir
Prestw-1427	08H08	Levetiracetam
Prestw-1392	08H09	Dexfenfluramine hydrochloride
Prestw-1408	08H10	Etoricoxib
Prestw-1341	08H11	Sertindole
Prestw-641	09A02	Sulmazole
Prestw-1270	09A03	Gefitinib
Prestw-643	09A04	Flunisolide
Prestw-644	09A05	N-Acetyl-DL-homocysteine Thiolactone
Prestw-645	09A06	Flurandrenolide
Prestw-1125	09A07	Oxiconazole Nitrate
Prestw-1166	09A08	Rebamipide
Prestw-1154	09A09	Nilvadipine
Prestw-649	09A10	Etanidazole
Prestw-1601	09A11	Pinaverium bromide
Prestw-651	09B02	Glimepiride
Prestw-652	09B03	Picrotoxinin
Prestw-653	09B04	Mepenzolate bromide
Prestw-654	09B05	Benfotiamine
Prestw-655	09B06	Halcinonide
Prestw-656	09B07	Lanatoside C
Prestw-657	09B08	Benzamil hydrochloride
Prestw-658	09B09	Suxibuzone
Prestw-659	09B10	6-Furfurylaminopurine
Prestw-660	09B11	Avermectin B1a
Prestw-1317	09C02	Pranlukast
Prestw-1477	09C03	D,L-Penicillamine
Prestw-1365	09C04	Zileuton
Prestw-1432	09C05	Loratadine
Prestw-1387	09C06	Tetraethylenepentamine pentahydrochloride
Prestw-666	09C07	Nisoldipine
Prestw-1507	09C08	Acefylline
Prestw-1165	09C09	Acitretin
Prestw-1162	09C10	Zonisamide
Prestw-1173	09C11	Irsogladine maleate
Prestw-671	09D02	Dydrogesterone
Prestw-1346	09D03	Sumatriptan succinate
Prestw-1456	09D04	Opipramol dihydrochloride
Prestw-1447	09D05	Nalidixic acid sodium salt

Prestw-1475	09D06	Oxacillin sodium
Prestw-676	09D07	Beta-Escin
Prestw-631	09D08	Thiamine hydrochloride
Prestw-1349	09D09	Tazobactam
Prestw-1285	09D10	Ibandronate sodium
Prestw-1363	09D11	Warfarin
Prestw-1318	09E02	Pranoprofen
Prestw-1340	09E03	Secnidazole
Prestw-683	09E04	Pempidine tartrate
Prestw-1381	09E05	Clodronate
Prestw-1508	09E06	Ibutilide fumarate
Prestw-1194	09E07	Thimerosal
Prestw-1465	09E08	Tramadol hydrochloride
Prestw-688	09E09	Estropipate
Prestw-1253	09E10	Butylscopolammonium (n-) bromide
Prestw-1494	09E11	Irinotecan hydrochloride trihydrate
Prestw-1353	09F02	Tylosin
Prestw-692	09F03	Citalopram Hydrobromide
Prestw-693	09F04	Promazine hydrochloride
Prestw-694	09F05	Sulfamerazine
Prestw-1170	09F06	Venlafaxine
Prestw-696	09F07	Ethotoin
Prestw-697	09F08	3-alpha-Hydroxy-5-beta-androstan-17-one
Prestw-698	09F09	Tetrahydrozoline hydrochloride
Prestw-699	09F10	Hexestrol
Prestw-700	09F11	Cefmetazole sodium salt
Prestw-701	09G02	Trihexyphenidyl-D,L Hydrochloride
Prestw-702	09G03	Succinylsulfathiazole
Prestw-703	09G04	Famprofazone
Prestw-704	09G05	Bromopride
Prestw-705	09G06	Methyl benzethonium chloride
Prestw-706	09G07	Chlorcyclizine hydrochloride
Prestw-707	09G08	Diphenylpyraline hydrochloride
Prestw-708	09G09	Benzethonium chloride
Prestw-709	09G10	Trioxsalen
Prestw-1136	09G11	Doxofylline
Prestw-711	09H02	Sulfabenzamide
Prestw-712	09H03	Benzocaine
Prestw-713	09H04	Dipyron
Prestw-714	09H05	Isosorbide dinitrate
Prestw-715	09H06	Sulfachloropyridazine
Prestw-716	09H07	Pramoxine hydrochloride

Prestw-717	09H08	Finasteride
Prestw-718	09H09	Fluorometholone
Prestw-719	09H10	Cephalothin sodium salt
Prestw-720	09H11	Cefuroxime sodium salt
Prestw-721	10A02	Althiazide
Prestw-722	10A03	Isopyrin hydrochloride
Prestw-723	10A04	Phenethicillin potassium salt
Prestw-724	10A05	Sulfamethoxypyridazine
Prestw-725	10A06	Deferoxamine mesylate
Prestw-726	10A07	Mephentermine hemisulfate
Prestw-1140	10A08	Liranaftate
Prestw-728	10A09	Sulfadimethoxine
Prestw-729	10A10	Sulfanilamide
Prestw-730	10A11	Balsalazide Sodium
Prestw-731	10B02	Sulfaquinoxaline sodium salt
Prestw-732	10B03	Streptozotocin
Prestw-733	10B04	Metoprolol-(+,-) (+)-tartrate salt
Prestw-734	10B05	Flumethasone
Prestw-735	10B06	Flecainide acetate
Prestw-736	10B07	Cefazolin sodium salt
Prestw-1702	10B08	Trimetozine
Prestw-738	10B09	Folinic acid calcium salt
Prestw-739	10B10	Levonordefrin
Prestw-740	10B11	Ebselen
Prestw-741	10C02	Nadide
Prestw-742	10C03	Sulfamethizole
Prestw-743	10C04	Medrysone
Prestw-744	10C05	Flunixin meglumine
Prestw-745	10C06	Spiramycin
Prestw-746	10C07	Glycopyrrolate
Prestw-1600	10C08	Aprepitant
Prestw-748	10C09	Monensin sodium salt
Prestw-749	10C10	Isoetharine mesylate salt
Prestw-750	10C11	Mevalonic-D, L acid lactone
Prestw-751	10D02	Terazosin hydrochloride
Prestw-752	10D03	Phenazopyridine hydrochloride
Prestw-753	10D04	Demeclocycline hydrochloride
Prestw-754	10D05	Fenoprofen calcium salt dihydrate
Prestw-755	10D06	Piperacillin sodium salt
Prestw-756	10D07	Diethylstilbestrol
Prestw-757	10D08	Chlorotrianisene
Prestw-758	10D09	Ribostamycin sulfate salt
Prestw-759	10D10	Methacholine chloride

Prestw-760	10D11	Pipenzolate bromide
Prestw-761	10E02	Butamben
Prestw-762	10E03	Sulfapyridine
Prestw-763	10E04	Meclofenoxate hydrochloride
Prestw-764	10E05	Furaltadone hydrochloride
Prestw-765	10E06	Ethoxyquin
Prestw-766	10E07	Tinidazole
Prestw-767	10E08	Guanadrel sulfate
Prestw-768	10E09	Vidarabine
Prestw-769	10E10	Sulfameter
Prestw-770	10E11	Isopropamide iodide
Prestw-771	10F02	Alclometasone dipropionate
Prestw-772	10F03	Leflunomide
Prestw-773	10F04	Norgestrel(-)-D
Prestw-774	10F05	Fluocinonide
Prestw-775	10F06	Sulfamethazine sodium salt
Prestw-776	10F07	Guaifenesin
Prestw-777	10F08	Alexidine dihydrochloride
Prestw-778	10F09	Proadifen hydrochloride
Prestw-779	10F10	Zomepirac sodium salt
Prestw-780	10F11	Cinoxacin
Prestw-781	10G02	Clobetasol propionate
Prestw-782	10G03	Podophyllotoxin
Prestw-783	10G04	Clofibric acid
Prestw-784	10G05	Bendroflumethiazide
Prestw-785	10G06	Dicumarol
Prestw-786	10G07	Methimazole
Prestw-787	10G08	Merbromin
Prestw-788	10G09	Hexylcaine hydrochloride
Prestw-789	10G10	Drofenine hydrochloride
Prestw-790	10G11	Cycloheximide
Prestw-791	10H02	(R) -Naproxen sodium salt
Prestw-792	10H03	Propidium iodide
Prestw-793	10H04	Cloperastine hydrochloride
Prestw-794	10H05	Eucatropine hydrochloride
Prestw-795	10H06	Isocarboxazid
Prestw-796	10H07	Lithocholic acid
Prestw-797	10H08	Methotrimeprazine maleat salt
Prestw-798	10H09	Dienestrol
Prestw-799	10H10	Pridinol methanesulfonate salt
Prestw-800	10H11	Amrinone
Prestw-801	11A02	Carbinoxamine maleate salt
Prestw-802	11A03	Methazolamide

Prestw-803	11A04	Pyrithyldione
Prestw-804	11A05	Spectinomycin dihydrochloride
Prestw-805	11A06	Piromidic acid
Prestw-806	11A07	Trimipramine maleate salt
Prestw-807	11A08	Chloropyramine hydrochloride
Prestw-808	11A09	Furazolidone
Prestw-809	11A10	Dichlorphenamide
Prestw-810	11A11	Sulconazole nitrate
Prestw-1233	11B02	Auranofin
Prestw-812	11B03	Cromolyn disodium salt
Prestw-813	11B04	Bucladesine sodium salt
Prestw-814	11B05	Cefsulodin sodium salt
Prestw-815	11B06	Fosfosal
Prestw-816	11B07	Suprofen
Prestw-1509	11B08	Deflazacort
Prestw-818	11B09	Nadolol
Prestw-819	11B10	Moxalactam disodium salt
Prestw-820	11B11	Aminophylline
Prestw-821	11C02	Azlocillin sodium salt
Prestw-822	11C03	Clidinium bromide
Prestw-823	11C04	Sulfamonomethoxine
Prestw-824	11C05	Benzthiazide
Prestw-825	11C06	Trichlormethiazide
Prestw-826	11C07	Oxalamine citrate salt
Prestw-827	11C08	Propantheline bromide
Prestw-1361	11C09	Viloxazine hydrochloride
Prestw-829	11C10	Dimethadione
Prestw-830	11C11	Ethaverine hydrochloride
Prestw-831	11D02	Butacaine
Prestw-832	11D03	Cefoxitin sodium salt
Prestw-833	11D04	Ifosfamide
Prestw-834	11D05	Novobiocin sodium salt
Prestw-835	11D06	Tetrahydroxy-1,4-quinone hydrate
Prestw-836	11D07	Indoprofen
Prestw-837	11D08	Carbenoxolone disodium salt
Prestw-838	11D09	locetamic acid
Prestw-839	11D10	Ganciclovir
Prestw-840	11D11	Ethopropazine hydrochloride
Prestw-1455	11E02	Olanzapine
Prestw-842	11E03	Trimeprazine tartrate
Prestw-843	11E04	Nafcillin sodium salt monohydrate
Prestw-844	11E05	Procyclidine hydrochloride
Prestw-845	11E06	Amiprilose hydrochloride

Prestw-846	11E07	Ethinylestradiol 3-methyl ether
Prestw-847	11E08	(-) -Levobunolol hydrochloride
Prestw-848	11E09	Iodixanol
Prestw-1379	11E10	Clinafloxacin
Prestw-850	11E11	Equilin
Prestw-851	11F02	Paroxetine Hydrochloride
Prestw-1454	11F03	Nylidrin
Prestw-853	11F04	Liothyronine
Prestw-854	11F05	Roxithromycin
Prestw-855	11F06	Beclomethasone dipropionate
Prestw-856	11F07	Tolmetin sodium salt dihydrate
Prestw-857	11F08	(+) -Levobunolol hydrochloride
Prestw-858	11F09	Doxazosin mesylate
Prestw-859	11F10	Fluvastatin sodium salt
Prestw-860	11F11	Methylhydantoin-5-(L)
Prestw-861	11G02	Gabapentin
Prestw-862	11G03	Raloxifene hydrochloride
Prestw-863	11G04	Etidronic acid, disodium salt
Prestw-864	11G05	Methylhydantoin-5-(D)
Prestw-865	11G06	Simvastatin
Prestw-866	11G07	Azacytidine-5
Prestw-867	11G08	Paromomycin sulfate
Prestw-868	11G09	Acetaminophen
Prestw-869	11G10	Phthalylsulfathiazole
Prestw-870	11G11	Luteolin
Prestw-871	11H02	Iopamidol
Prestw-872	11H03	Iopromide
Prestw-873	11H04	Theophylline monohydrate
Prestw-874	11H05	Theobromine
Prestw-875	11H06	Reserpine
Prestw-1239	11H07	Bicalutamide
Prestw-877	11H08	Scopolamine hydrochloride
Prestw-878	11H09	Ioversol
Prestw-1495	11H10	Rabeprazole Sodium salt
Prestw-880	11H11	Carbachol
Prestw-881	12A02	Niacin
Prestw-882	12A03	Bemegride
Prestw-883	12A04	Digoxigenin
Prestw-884	12A05	Meglumine
Prestw-1510	12A06	Dolasetron mesilate
Prestw-886	12A07	Clioquinol
Prestw-887	12A08	Oxybenzone
Prestw-888	12A09	Promethazine hydrochloride

Prestw-1167	12A10	Diacerein
Prestw-1137	12A11	Esmolol hydrochloride
Prestw-1486	12B02	Cortisol acetate
Prestw-1416	12B03	Flubendazol
Prestw-893	12B04	Felbinac
Prestw-894	12B05	Butylparaben
Prestw-895	12B06	Aminohippuric acid
Prestw-896	12B07	N-Acetyl-L-leucine
Prestw-897	12B08	Pipemidic acid
Prestw-898	12B09	Dioxybenzone
Prestw-899	12B10	Adrenosterone
Prestw-900	12B11	Methylatropine nitrate
Prestw-901	12C02	Hymecromone
Prestw-1512	12C03	Abacavir Sulfate
Prestw-903	12C04	Diloxanide furoate
Prestw-904	12C05	Metyrapone
Prestw-905	12C06	Urapidil hydrochloride
Prestw-906	12C07	Fluspirilen
Prestw-907	12C08	S-(+)-ibuprofen
Prestw-908	12C09	Ethinodiol diacetate
Prestw-909	12C10	Nabumetone
Prestw-910	12C11	Nisoxetine hydrochloride
Prestw-911	12D02	(+)-Isoproterenol (+)-bitartrate salt
Prestw-912	12D03	Monobenzone
Prestw-913	12D04	2-Aminobenzenesulfonamide
Prestw-914	12D05	Estrone
Prestw-915	12D06	Lorglumide sodium salt
Prestw-916	12D07	Nitrendipine
Prestw-917	12D08	Flurbiprofen
Prestw-918	12D09	Nimodipine
Prestw-919	12D10	Bacitracin
Prestw-920	12D11	L(-)-vesamicol hydrochloride
Prestw-921	12E02	Nizatidine
Prestw-922	12E03	Thioperamide maleate
Prestw-923	12E04	Xamoterol hemifumarate
Prestw-924	12E05	Rolipram
Prestw-925	12E06	Thonzonium bromide
Prestw-926	12E07	Idazoxan hydrochloride
Prestw-927	12E08	Quinapril HCl
Prestw-928	12E09	Nilutamide
Prestw-929	12E10	Ketorolac tromethamine
Prestw-930	12E11	Protriptyline hydrochloride
Prestw-931	12F02	Propofol

Prestw-932	12F03	S(-)Eticlopride hydrochloride
Prestw-933	12F04	Primidone
Prestw-934	12F05	Flucytosine
Prestw-935	12F06	(-)-MK 801 hydrogen maleate
Prestw-936	12F07	Bephenium hydroxynaphthoate
Prestw-937	12F08	Dehydroisoandosterone 3-acetate
Prestw-938	12F09	Benserazide hydrochloride
Prestw-939	12F10	Iodipamide
Prestw-1213	12F11	Allopurinol
Prestw-941	12G02	Pentetic acid
Prestw-942	12G03	Bretylium tosylate
Prestw-943	12G04	Pralidoxime chloride
Prestw-944	12G05	Phenoxybenzamine hydrochloride
Prestw-945	12G06	Salmeterol
Prestw-946	12G07	Altretamine
Prestw-947	12G08	Prazosin hydrochloride
Prestw-948	12G09	Timolol maleate salt
Prestw-949	12G10	(+,-)-Octopamine hydrochloride
Prestw-1279	12G11	Stavudine
Prestw-951	12H02	Crotamiton
Prestw-1197	12H03	Toremifene
Prestw-536	12H04	(R)-(+)-Atenolol
Prestw-954	12H05	Tyloxapol
Prestw-955	12H06	Florfenicol
Prestw-956	12H07	Megestrol acetate
Prestw-957	12H08	Deoxycorticosterone
Prestw-958	12H09	Urosiol
Prestw-959	12H10	Proparacaine hydrochloride
Prestw-960	12H11	Aminocaproic acid
Prestw-961	13A02	Denatonium benzoate
Prestw-1259	13A03	Canrenone
Prestw-963	13A04	Enilconazole
Prestw-964	13A05	Methacycline hydrochloride
Prestw-1415	13A06	Floxuridine
Prestw-966	13A07	Sotalol hydrochloride
Prestw-1267	13A08	Gestrinone
Prestw-968	13A09	Decamethonium bromide
Prestw-1514	13A10	Darifenacin hydrobromide
Prestw-1602	13A11	Indatraline hydrochloride
Prestw-971	13B02	Remoxipride Hydrochloride
Prestw-972	13B03	THIP Hydrochloride
Prestw-973	13B04	Pirlindole mesylate
Prestw-974	13B05	Pronethalol hydrochloride

Prestw-975	13B06	Naftopidil dihydrochloride
Prestw-976	13B07	Tracazolate hydrochloride
Prestw-977	13B08	Zardaverine
Prestw-978	13B09	Memantine Hydrochloride
Prestw-979	13B10	Ozagrel hydrochloride
Prestw-980	13B11	Piribedil hydrochloride
Prestw-981	13C02	Nitrocaramiphen hydrochloride
Prestw-982	13C03	Nandrolone
Prestw-983	13C04	Dimaprit dihydrochloride
Prestw-1459	13C05	Oxfendazol
Prestw-1268	13C06	Guaiacol
Prestw-986	13C07	Proscillaridin A
Prestw-1316	13C08	Pramipexole dihydrochloride
Prestw-1452	13C09	Norgestimate
Prestw-1374	13C10	Chlormadinone acetate
Prestw-1310	13C11	Phenylbutazone
Prestw-991	13D02	Gliquidone
Prestw-992	13D03	Pizotifen malate
Prestw-993	13D04	Ribavirin
Prestw-994	13D05	Cyclopentiazide
Prestw-995	13D06	Fluvoxamine maleate
Prestw-1321	13D07	Prothionamide
Prestw-997	13D08	Fluticasone propionate
Prestw-998	13D09	Zuclopenthixol dihydrochloride
Prestw-999	13D10	Proguanil hydrochloride
Prestw-1000	13D11	Lymecycline
Prestw-1001	13E02	Alfadolone acetate
Prestw-1002	13E03	Alfaxalone
Prestw-1003	13E04	Azapropazone
Prestw-1004	13E05	Meptazinol hydrochloride
Prestw-1005	13E06	Apramycin
Prestw-1006	13E07	Epitiostanol
Prestw-1007	13E08	Fursultiamine Hydrochloride
Prestw-1008	13E09	Gabexate mesilate
Prestw-1009	13E10	Pivampicillin
Prestw-1746	13E11	Lodoxamide
Prestw-1011	13F02	Flucloxacillin sodium
Prestw-1012	13F03	Trapidil
Prestw-1013	13F04	Deptropine citrate
Prestw-1014	13F05	Sertraline
Prestw-1015	13F06	Ethamsylate
Prestw-1016	13F07	Moxonidine
Prestw-1017	13F08	Etilefrine hydrochloride

Prestw-1018	13F09	Alprostadil
Prestw-1019	13F10	Tribenoside
Prestw-1020	13F11	Rimexolone
Prestw-1021	13G02	Isradipine
Prestw-1774	13G03	Nifekalant
Prestw-1023	13G04	Isometheptene mucate
Prestw-1024	13G05	Nifurtimox
Prestw-1025	13G06	Letrozole
Prestw-1026	13G07	Arbutin
Prestw-1027	13G08	Tocainide hydrochloride
Prestw-1028	13G09	Benzathine benzylpenicillin
Prestw-1029	13G10	Risperidone
Prestw-1030	13G11	Torse mide
Prestw-1031	13H02	Halofantrine hydrochloride
Prestw-1032	13H03	Articaine hydrochloride
Prestw-1033	13H04	Nomegestrol acetate
Prestw-1034	13H05	Pancuronium bromide
Prestw-1035	13H06	Molindone hydrochloride
Prestw-1036	13H07	Alcuronium chloride
Prestw-1037	13H08	Zalcitabine
Prestw-1038	13H09	Methyldopate hydrochloride
Prestw-1039	13H10	Levocabastine hydrochloride
Prestw-1040	13H11	Pyrvinium pamoate
Prestw-1041	14A02	Etomidate
Prestw-1042	14A03	Tridihexethyl chloride
Prestw-1043	14A04	Penbutolol sulfate
Prestw-1044	14A05	Prednicarbate
Prestw-1045	14A06	Sertaconazole nitrate
Prestw-1046	14A07	Repaglinide
Prestw-1047	14A08	Piretanide
Prestw-1048	14A09	Piperacetazine
Prestw-1049	14A10	Oxyphenbutazone
Prestw-1050	14A11	Quinethazone
Prestw-1051	14B02	Moricizine hydrochloride
Prestw-1052	14B03	Iopanoic acid
Prestw-1053	14B04	Pivmecillinam hydrochloride
Prestw-1054	14B05	Levopropoxyphene napsylate
Prestw-1055	14B06	Piperidolate hydrochloride
Prestw-1056	14B07	Trifluridine
Prestw-1057	14B08	Oxprenolol hydrochloride
Prestw-1058	14B09	Ondansetron Hydrochloride
Prestw-1059	14B10	Propoxycaine hydrochloride
Prestw-1060	14B11	Oxaprozin

Prestw-1061	14C02	Phensuximide
Prestw-1062	14C03	Ioxaglic acid
Prestw-1063	14C04	Naftifine hydrochloride
Prestw-1064	14C05	Meprylcaine hydrochloride
Prestw-1065	14C06	Milrinone
Prestw-1066	14C07	Methantheline bromide
Prestw-1067	14C08	Ticarcillin sodium
Prestw-1068	14C09	Thiethylperazine dimalate
Prestw-1069	14C10	Mesalamine
Prestw-1362	14C11	Vorinostat
Prestw-1071	14D02	Imidurea
Prestw-1072	14D03	Lansoprazole
Prestw-1073	14D04	Bethanechol chloride
Prestw-1074	14D05	Cyproterone acetate
Prestw-1075	14D06	(R)-Propranolol hydrochloride
Prestw-1076	14D07	Ciprofibrate
Prestw-1420	14D08	Formestane
Prestw-1078	14D09	Benzylpenicillin sodium
Prestw-1079	14D10	Chlorambucil
Prestw-1080	14D11	Methiazole
Prestw-1081	14E02	(S)-propranolol hydrochloride
Prestw-1082	14E03	(-)-Eseroline fumarate salt
Prestw-1294	14E04	Isosorbide mononitrate
Prestw-1516	14E05	Levalbuterol hydrochloride
Prestw-1493	14E06	Topiramate
Prestw-1086	14E07	D-cycloserine
Prestw-1087	14E08	2-Chloropyrazine
Prestw-1088	14E09	(+,-)-Synephrine
Prestw-1089	14E10	(S)-(-)-Cycloserine
Prestw-1090	14E11	Homosalate
Prestw-1091	14F02	Spaglumic acid
Prestw-1092	14F03	Ranolazine
Prestw-1443	14F04	Misoprostol
Prestw-1094	14F05	Sulfadoxine
Prestw-1095	14F06	Cyclopentolate hydrochloride
Prestw-1096	14F07	Estriol
Prestw-1097	14F08	(-)-Isoproterenol hydrochloride
Prestw-1339	14F09	Sarafloxacin
Prestw-1099	14F10	Nialamide
Prestw-1195	14F11	Toltrazuril
Prestw-1101	14G02	Perindopril
Prestw-1102	14G03	Fexofenadine HCl
Prestw-1202	14G04	4-aminosalicylic acid

Prestw-1104	14G05	Clonixin Lysinate
Prestw-1105	14G06	Verteporfin
Prestw-1106	14G07	Meropenem
Prestw-1107	14G08	Ramipril
Prestw-1108	14G09	Mephenytoin
Prestw-1109	14G10	Rifabutin
Prestw-1110	14G11	Parbendazole
Prestw-1111	14H02	Mecamylamine hydrochloride
Prestw-1112	14H03	Procarbazine hydrochloride
Prestw-1113	14H04	Viomycin sulfate
Prestw-1114	14H05	Saquinavir mesylate
Prestw-1115	14H06	Ronidazole
Prestw-1116	14H07	Dorzolamide hydrochloride
Prestw-1117	14H08	Azaperone
Prestw-1118	14H09	Cefepime hydrochloride
Prestw-1119	14H10	Clocortolone pivalate
Prestw-1120	14H11	Nadifloxacin
Prestw-1283	15A02	Bupirone hydrochloride
Prestw-1222	15A03	Anastrozole
Prestw-1399	15A04	Doxycycline hydrochloride
Prestw-1345	15A05	Sulbactam
Prestw-1414	15A06	Fleroxacin
Prestw-1315	15A07	Clavulanate potassium salt
Prestw-1482	15A08	Valproic acid
Prestw-1280	15A09	Mepivacaine hydrochloride
Prestw-1478	15A10	Rifaximin
Prestw-1473	15A11	Estradiol Valerate
Prestw-1206	15B02	Acetylcysteine
Prestw-1435	15B03	Melengestrol acetate
Prestw-1246	15B04	Bromhexine hydrochloride
Prestw-1223	15B05	Anethole-trithione
Prestw-1476	15B06	Amcinonide
Prestw-1256	15B07	Caffeine
Prestw-1262	15B08	Carvedilol
Prestw-1282	15B09	Methenamine
Prestw-1308	15B10	Phentermine hydrochloride
Prestw-1394	15B11	Diclazuril
Prestw-1249	15C02	Famciclovir
Prestw-1398	15C03	Dopamine hydrochloride
Prestw-1263	15C04	Cefdinir
Prestw-1261	15C05	Carprofen
Prestw-1371	15C06	Celecoxib
Prestw-1258	15C07	Candesartan

Prestw-1483	15C08	Fludarabine
Prestw-1484	15C09	Cladribine
Prestw-1356	15C10	Vardenafil
Prestw-1417	15C11	Fluconazole
Prestw-1203	15D02	5-fluorouracil
Prestw-1487	15D03	Mesna
Prestw-1444	15D04	Mitotane
Prestw-1497	15D05	Ambrisentan
Prestw-1479	15D06	Triclosan
Prestw-1401	15D07	Enoxacin
Prestw-1307	15D08	Olopatadine hydrochloride
Prestw-1187	15D09	Granisetron
Prestw-1224	15D10	Anthralin
Prestw-1492	15D11	Lamotrigine
Prestw-1383	15E02	Clofibrate
Prestw-1481	15E03	Cyclophosphamide
Prestw-1229	15E04	Aripiprazole
Prestw-1405	15E05	Ethinylestradiol
Prestw-1419	15E06	Fluocinolone acetonide
Prestw-1343	15E07	Sparfloxacin
Prestw-1390	15E08	Desloratadine
Prestw-1378	15E09	Clarithromycin
Prestw-1199	15E10	Tripelennamine hydrochloride
Prestw-1352	15E11	Tulobuterol
Prestw-1196	15F02	Topotecan
Prestw-1232	15F03	Atorvastatin
Prestw-1234	15F04	Azithromycin
Prestw-1286	15F05	Ibuprofen
Prestw-1433	15F06	Losartan
Prestw-1236	15F07	Benzotropine mesylate
Prestw-1359	15F08	Vecuronium bromide
Prestw-1350	15F09	Telmisartan
Prestw-1490	15F10	Nalmefene hydrochloride
Prestw-1241	15F11	Bifonazole
Prestw-1265	15G02	Gatifloxacin
Prestw-1244	15G03	Bosentan
Prestw-1266	15G04	Gemcitabine
Prestw-1190	15G05	Olmesartan
Prestw-1480	15G06	Racemephrine HCl
Prestw-1189	15G07	Montelukast
Prestw-1180	15G08	Docetaxel
Prestw-1376	15G09	Cilnidipine
Prestw-1291	15G10	Imiquimod

Prestw-1423	15G11	Fosinopril
Prestw-1290	15H02	Imatinib
Prestw-1446	15H03	Moxifloxacin
Prestw-1421	15H04	Formoterol fumarate
Prestw-1338	15H05	Rufloxacin
Prestw-1319	15H06	Pravastatin
Prestw-1337	15H07	Rosiglitazone Hydrochloride
Prestw-1334	15H08	Rivastigmine
Prestw-1342	15H09	Sildenafil
Prestw-1207	15H10	Acetylsalicylic acid
Prestw-1472	15H11	Hexachlorophene
Prestw-1764	16A02	Nelfinavir mesylate
Prestw-1749	16A03	Sildenafil
Prestw-1777	16A04	Trimebutine
Prestw-1739	16A05	Nevirapine
Prestw-1707	16A06	Doxapram hydrochloride
Prestw-1718	16A07	Amlexanox
Prestw-1719	16A08	Amorolfine hydrochloride
Prestw-1786	16A09	Enrofloxacin
Prestw-1784	16A10	Ubenimex
Prestw-1778	16A11	Troxipide
Prestw-1773	16B02	Ipriflavone
Prestw-1762	16B03	Ezetimibe
Prestw-1761	16B04	Rizatriptan benzoate
Prestw-1760	16B05	Tegaserod maleate
Prestw-1758	16B06	Pantoprazole sodium
Prestw-1753	16B07	Tegafur
Prestw-1732	16B08	Tolcapone
Prestw-1716	16B09	Altrenogest
Prestw-1711	16B10	Felbamate
Prestw-1709	16B11	Estramustine
Prestw-1708	16C02	(R)-Duloxetine hydrochloride
Prestw-1706	16C03	Donepezil hydrochloride
Prestw-1703	16C04	1,8-Dihydroxyanthraquinone
Prestw-1733	16C05	Nitazoxanide
Prestw-1748	16C06	Nateglinide
Prestw-1721	16C07	Avobenzon
Prestw-1715	16C08	Algestone acetophenide
Prestw-1763	16C09	Actarit
Prestw-1710	16C10	Ethoxzolamide
Prestw-1722	16C11	Azatadine maleate
Prestw-1717	16D02	Aminacrine
Prestw-1792	16D03	Pidotimod

Prestw-1766	16D04	Benidipine hydrochloride
Prestw-1770	16D05	Perospirone
Prestw-1726	16D06	Cefpiramide
Prestw-1713	16D07	Fenoldopam
Prestw-1714	16D08	Adapalene
Prestw-1705	16D09	Diatrizoic acid dihydrate
Prestw-1743	16D10	Dofetilide
Prestw-1776	16D11	Phenprobamate
Prestw-1730	16E02	Cefuroxime axetil
Prestw-1720	16E03	Anagrelide
Prestw-1701	16E04	Clopidogrel
Prestw-1723	16E05	Benzoxiquine
Prestw-1785	16E06	Phenothiazine
Prestw-1769	16E07	Enalaprilat dihydrate
Prestw-1791	16E08	Pregabalin
Prestw-1787	16E09	Homoveratrylamine
Prestw-1731	16E10	Zoledronic acid hydrate
Prestw-1727	16E11	Cefpodoxime proxetil
Prestw-1736	16F02	Irbesartan
Prestw-1737	16F03	Indinavir sulfate
Prestw-1750	16F04	Terbinafine
Prestw-1700	16F05	Histamine dihydrochloride
Prestw-1734	16F06	Rasagiline
Prestw-1712	16F07	Flumethasone pivalate
Prestw-1756	16F08	Lofepamine
Prestw-1759	16F09	Valdecocib
Prestw-1740	16F10	Besifloxacin hydrochloride
Prestw-1782	16F11	Ritonavir
Prestw-1752	16G02	Epirubicin hydrochloride
Prestw-1741	16G03	Loteprednol etabonate
Prestw-1744	16G04	Tolterodine tartrate
Prestw-1775	16G05	Lomerizine hydrochloride
Prestw-1772	16G06	Ampiroxicam
Prestw-1781	16G07	Alosetron hydrochloride
Prestw-1738	16G08	Risedronic acid monohydrate
Prestw-1783	16G09	Palonosetron hydrochloride
Prestw-1780	16G10	Oxymetholone
Prestw-1765	16G11	Latanoprost
Prestw-1745	16H02	Cisatracurium besylate
Prestw-1794	16H03	Pemetrexed disodium
Prestw-1793	16H04	Raltitrexed
Prestw-1729	16H05	Ceftibuten
Prestw-1735	16H06	Valsartan

Prestw-1788	16H07	Milnacipran hydrochloride
Prestw-1768	16H08	Triclabendazole
Prestw-1751	16H09	Brimonidine L-Tartrate
Prestw-1704	16H10	Desonide
Prestw-1728	16H11	Cefprozil